GNF RAJ-II
Docket No. 71-9309
Safety Analysis Report
Revision 7
05/04/2009

REVISION 7

Description and Explanation of Changes

Locations in SAR	Description / Explanation
All Chapters	Updated to Revision 7 (Dated 5/4/2009) so SAR can be referenced as a single document

TABLE OF CONTENTS

List of Figures

List of Tables

Glossary of Terms and Acronyms

ASME – American Society of Mechanical Engineers
ASME B&PVC – ASME Boiler and Pressure Vessel Code
ASNT – American Society for Non-destructive Testing
CG – Center of Gravity
CTU – Certification Test Unit
BWR – Boiling Water Reactor
HAC – Hypothetical Accident Condition
IC – Inner Container
IC Inner Thermal Insulator (Aluminum Silicate) – The Alumina Silicate thermal insulation between the inner and outer walls of IC container to provide added margin to criteria set forth for HAC fire condition in 10 CFR 71.73(c)(4)
IC Lid – The lid of the inner container
IC Body – The body of the inner container consisting of the outer wall the thermal insulation, the inner wall, the polyethylene liner and the shock absorbing system along with the fuel securement system
JIS – Japanese Industrial Standards
JSNDI – Japanese Society for Non-destructive Inspection
LDPE – Low Density Polyethylene
NCT – Normal Conditions of Transport
NDIS – Non-destructive Inspection Society
OC – Outer Container
OC Body – The assembly consisting of the OC lower wall, and the internal shock absorbing material
OC Lid – The lid for the outer container.
Packaging – The assembly of components necessary to ensure compliance with packaging requirements as defined in 10 CFR 71.4. Within this SAR, the packaging is denoted as the RAJ-II packaging
Package – The packaging with its radioactive contents, as presented for transportation as defined in 10 CFR 71.4. Within this SAR, the package is denoted as the RAJ-II package.
Payload – Unirradiated fuel assemblies and fuel rods.
RAM – Radioactive Material
SAR – Safety Analysis Report (this document)
TI – Transport Index
USL – Upper Safety Limit

1.0 GENERAL INFORMATION

This chapter of the Safety Analysis Report (SAR) presents a general introduction and description of the RAJ-II package. The major components comprising the RAJ-II package are presented in Figure 1-1 through Figure 1-4. Detailed drawings presenting the RAJ-II packaging design are included in Appendix 1.4.1. Terminology and acronyms used throughout this document are presented in the Glossary of Terms and Acronyms on page 1-1. This package is intended to be used to transport Boiling Water Reactor (BWR) fuel assemblies containing both Type A and Type B fissile material.

1.1 INTRODUCTION

The model RAJ-II package has been developed to transport unirradiated fuel for Boiling Water Reactors. The cladding of the fuel provides the primary containment for the radioactive material. The inner and outer containers provide both thermal protection as well as mechanical protection from drops or accident conditions.

The integrity of the fuel is maintained by the protective outer package, the insulated inner package and the fuel rod cladding through both Normal Conditions of Transport (NCT) and Hypothetical Accident Conditions (HAC) deformations. A variety of full-scale engineering development tests were included as part of the certification process. Ultimately, two full-scale Certification Test Units (CTUs) were subjected to a series of free drops and puncture drops.

The payload within each RAJ-II package consists of a maximum of two unirradiated Boiling Water Reactor (BWR) fuel assemblies or individual rods (BWR, Uranium Carbide, or generic Pressurized Water Reactor (PWR)) contained in a cylinder, protective case or bundled together and positioned in one or both sides of the inner container. See Table 6-1 RAJ-II Fuel Assembly Loading Criteria. See Table 6-2 RAJ-II. The containment is provided by the leak tested cladding making up the fuel rods.

The shielding and criticality assessments provided in Chapter 5.0 and Chapter 6.0. The Criticality Safety Index (CSI) for the RAJ-II package is defined in Chapter 6.0.

The RAJ-II package is designed for shipment by truck, ship, or rail as either a Type B(U) fissile material or Type A fissile material package per the definition in 10 CFR 71.4 and 49 CFR 173.403.

Dimensions of the packaging identified in the text, tables, figures, etc. of this SAR, are intended to be nominal. The drawings provided in Appendix 1.4.1 contain the dimensions and the tolerances.

.

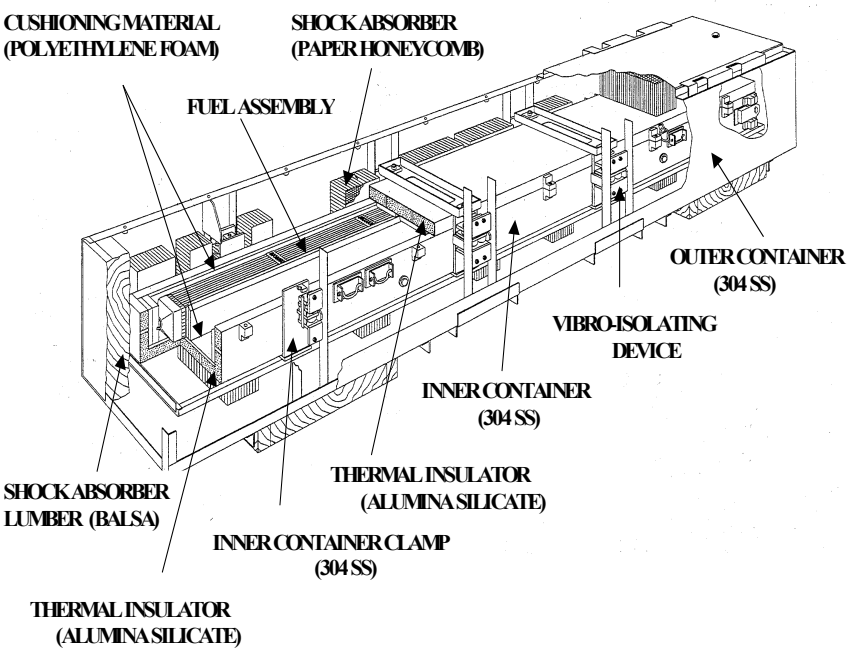

Figure 1-1 RAJ-II Package Assembly

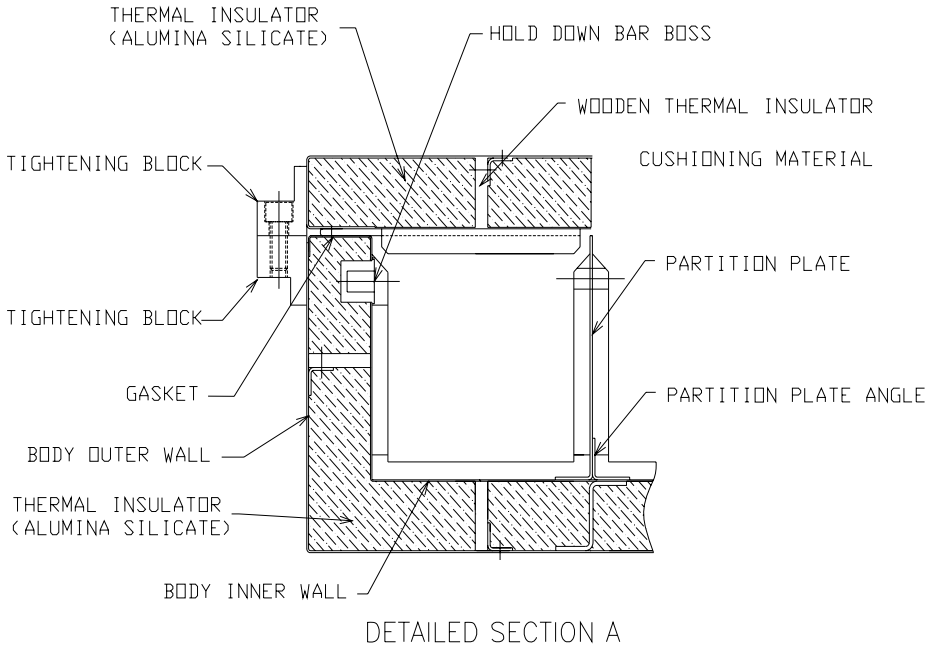

Figure 1-2 Cross-Section of Inner Container

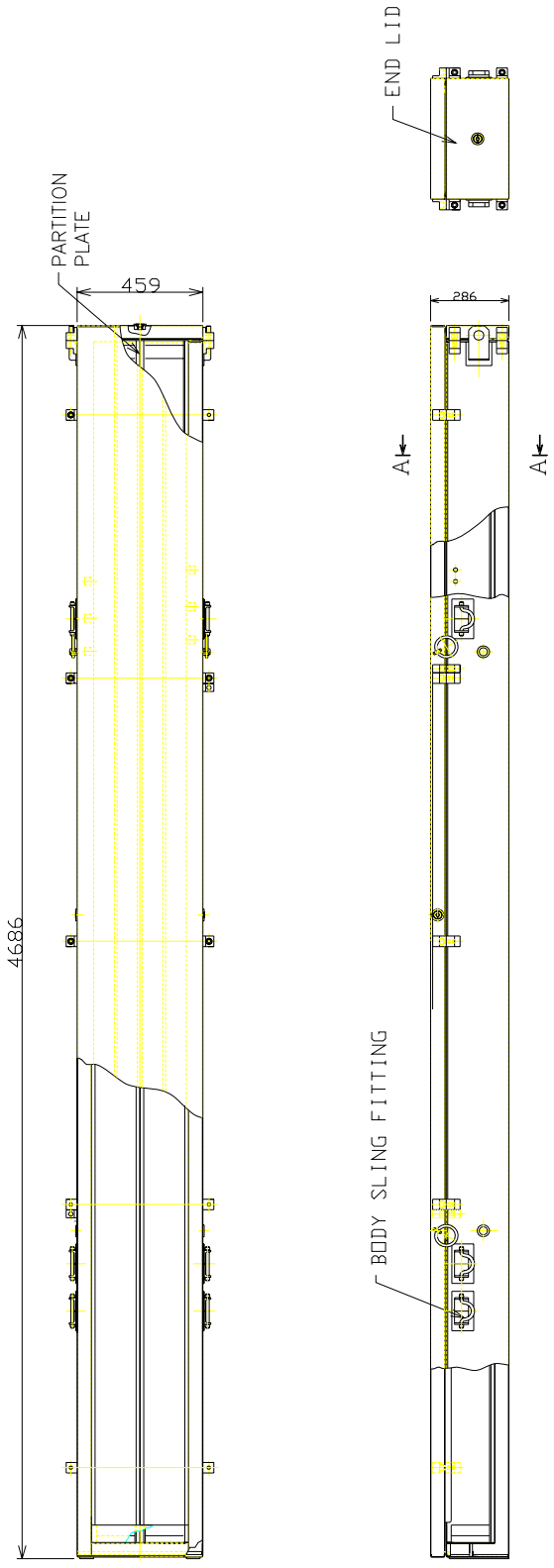

Figure 1-3 Inner Container

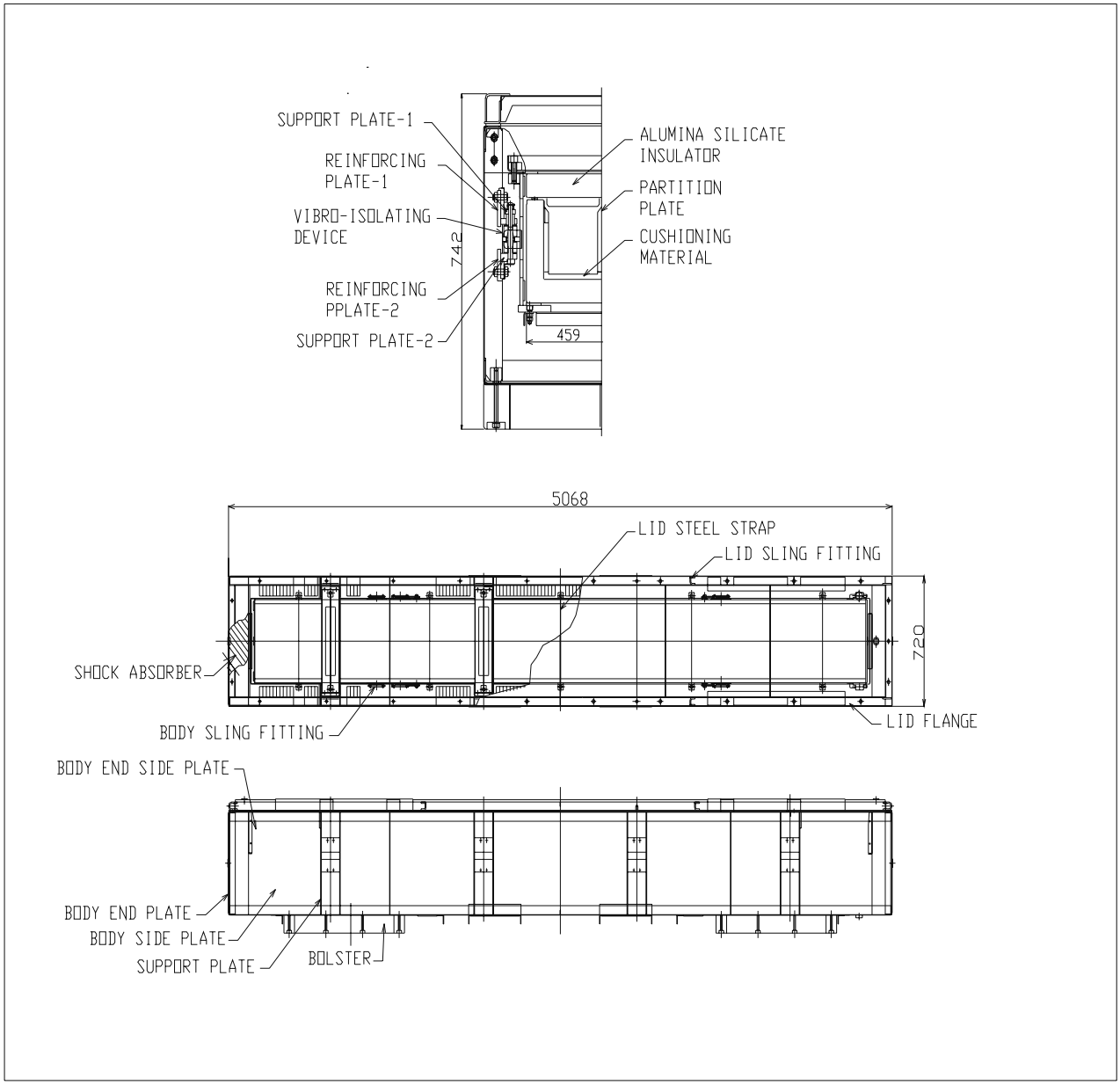

Figure 1-4 Inner and Outer Container

1.2 PACKAGE DESCRIPTION

This section presents a basic description of the model RAJ-II package. General arrangement drawings of the RAJ-II package are presented in Appendix 1.4.1. The Transport Index (TI) for this package is based on shielding and criticality assessments provided in Chapter 5.0 and Chapter 6.0.

1.2.1 Packaging

The packaging is comprised of one inner container and one outer container both made of stainless steel. The inner container is comprised of a double-wall stainless steel sheet structure with alumina silicate thermal insulator filling the gap between the two walls to reduce the flow of heat into the contents in the event of a fire. Foam polyethylene cushioning material is placed on the inside of the inner container for protection of the fuel assembly. The outer container is comprised of a stainless steel angular framework covered with stainless steel plates. Inner container clamps are installed inside the outer container with a vibro-isolating device between to alleviate vibration occurring during transportation. Additionally, wood and a honeycomb resin impregnated kraft paper (hereinafter called "paper honeycomb") are placed as shock absorbers to reduce shock due to a drop of the package. In addition to the packaging described above, the fuel rod clad and ceramic nature of the fuel pellets provide primary containment of the radioactive material.

The design details and overall arrangement of the RAJ-II packaging are shown in Appendix 1.4.1 RAJ-II General Arrangement Drawings.

1.2.1.1 Inner Container (IC)

The structure of the inner container is shown in Figure 1-2 and Figure 1-3. The inner container is comprised of three parts: an inner container body, an inner container end lid (removable), and an inner container top lid (removable). These components are fastened together by bolts made of stainless steel through tightening blocks. The inner container body is fitted with six sling fittings and the inner container lid is fitted with four sling fittings as shown in Figure 2-2 Inner Container Sling Locations. The inner container body has a double wall structure made of stainless steel. Its main components are an outer wall, inner wall and alumina silicate thermal insulator.

The outer wall is made of a 1.5 mm (0.0591 in) thick stainless steel sheet formed to a U-shape that constitutes the bottom and sides of the inner container body. A total of 14 stainless steel tightening blocks are attached on the sides of the outer wall, seven per side, to fasten the inner container lid and the inner container end lid by bolts. Additionally, six stainless steel sling fittings are attached on the sides (three on each side) for handling.

The inner wall of the inner packaging is formed into U-shape with 1.0 mm (0.0391 in) thick stainless steel sheet. The inner packaging is partitioned down the center with 2.0 mm (0.0787 in) thick stainless steel sheet welded to the bottom of the packaging. Foam polyethylene is placed on the inner surface of the inner wall where the fuel assemblies are seated. The void space

between the outer and inner steel sheeting is filled with an alumina silicate thermal insulation 48 mm (1.89 in) thick.

1.2.1.2 Outer Container (OC)

The structure of the outer container is shown in Figure 1-4. The outer container is comprised of three parts: a container body, a container lid and inner container hold clamps made of stainless steel and fastened together using stainless steel bolts.

Two tamper-indicating device attachment locations are provided, one on each end, of the outer container.

1.2.1.2.1 Outer Container Body

The outer container is made from a series of stainless steel angles (50mm x 50mm x 4mm)(1.97 inch x 1.97 inch x 0.157 inches) that make the framework. Welded to the framework are a bottom plate and side plates made of 2 mm (0.079 inch) thick stainless steel.

Sling holding angles for handling with a crane and protective plates for handling with a forklift are welded on the outside of the container body.

A total of eight sets of support plates are welded on the inside of the outer container body for installing the inner container hold clamps. Additionally, shock absorbers made of 146 mm (5.75 in) wood are attached to each end and paper honeycomb shock absorbers are attached to the bottom and sides for absorbing shock due to a drop. The geometry of the shock absorber is shown in Figure 1-5. The shock absorbers are 157 mm (6.18 in) thick and 108 mm (4.25 in) thick.

1.2.1.2.2 Outer Container Lid

The outer container lid is comprised of a lid flange and a lid plate made of stainless steel.

Stainless steel lid sling fittings are welded four places on the top surface of the outer container lid. A paper honeycomb shock absorber, 157 mm (6.18 in) thick by 160 mm (6.30 in) wide and 380 mm (14.96 in) long is attached to the bottom side of the lid similar to the attachment at the bottom of the container.

The outer container lid has holes for bolts in its flange so that it can be fastened to the outer container body by the stainless steel bolts.

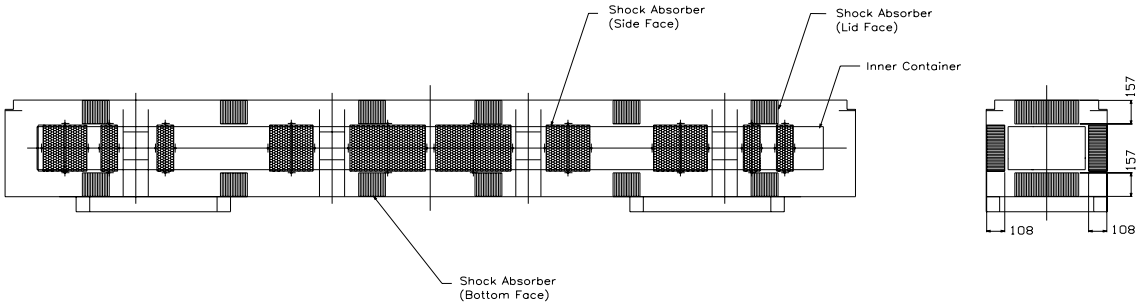

Figure 1-5 Shock Absorber Geometry

1.2.1.2.3 Inner Container Hold Clamp (Located on Outer Container)

The inner container hold clamp consists of an inner container receptacle and a vibro-isolating device.

The inner container receptacle consists of an inner container support plate, a support frame, a bracket and an inner container hold clamp fastener made of stainless steel. The receptacle guides the inner container to the correct position. The inner container receptacle is fitted with the vibro-isolating device through the gusset attached to the bracket.

The vibro-isolating material is attached on the upper and lower side of the gusset. Shock mount fastening bolts go through the center of each piece of vibro-isolating rubber. The bolts at both ends are tightened so that the vibro-isolating rubber pieces press the gusset.

There are four sets (eight pieces) of the vibro-isolating devices mounted on the outer container. Finally, a variety of stainless steel fasteners are used as specified in Appendix 1.4.1.

1.2.1.3 Gross Weight and Dimensions

The maximum gross shipping weight of a RAJ-II package is 1,614 kg (3,558 pounds) maximum. A summary of the major component weights and dimensions are given in Table 1 - 1. A summary of overall component weights is delineated in Table 2 - 1.

Table 1 - 1 Maximum Weights and Outer Dimensions of the Packaging

Item	Weight and outer dimensions
Maximum weight of inner container	308 kg (679 lbs)
Maximum weight of outer container	622 kg (1,371 lbs)
Maximum weight of packaging	930 kg (2,050 lbs)
Dimensions of inner container	Length: 4,686 mm (184.49 in) Width: 459 mm (18.07 in) Height: 286 mm (11.26 in)
Dimensions of outer container	Length: 5,068 mm (199.53 in) Width: 720 mm (28.35 in) Height 742 mm (29.21 in) (including bolsters)

1.2.1.4 Materials and Component Dimensions

1.2.1.4.1 Inner Container

The materials and component dimensions of the inner container are shown in Appendix 1.4.1.

1.2.1.4.2 Outer Container

The materials and component dimensions of the outer container are shown in Appendix 1.4.1.

1.2.1.5 Criticality Control Features

The RAJ-II package does not require specific design features to provide neutron moderation and absorption for criticality control. The contents of the package rely on gadolinia loading for criticality control based on enrichment. Gadolinia loading requirements are provided in Table 6-1 RAJ-II Fuel Assembly Loading Criteria. There are no spacers required for criticality control. Fissile materials in the payload are limited to an amount that ensures safely sub-critical packages for both NCT and HAC. Further discussion of criticality control features is provided in Chapter 6.0.

1.2.1.6 Heat Transfer Features

The unirradiated fuel has negligible decay heat, therefore, the RAJ-II package is not designed for dissipating heat. The packaging is designed to protect the fuel and its containment by providing containment during the Hypothetical Accident Conditions (HAC). A more detailed discussion of the package thermal characteristics is provided in Chapter 3.0

1.2.1.7 Coolants

Due to the passive design of the RAJ-II package with regard to heat transfer, there are no coolants utilized within the RAJ-II package.

1.2.1.8 Protrusions

The only significant protrusions on the RAJ-II packaging exterior are those associated with the lifting features on the outer container exterior. These are the sling holding angles and the bolsters at the bottom of the packaging. The bolsters protrude the furthest at 80 mm (3.15 in).

The only significant protrusions on the inner container exterior are the lifting sling fittings and the tightening blocks that are used for securing the lid. There are lifting sling fittings on the body and the main lid. Each of the sling fittings fold down so they protrude only the thickness of the lifting rod or bail.

1.2.1.9 Lifting and Tie-down Devices

The lifting devices for the RAJ-II consist of the sling holding angles on the outer container which keep the slings from moving when used to sling the container during handling. The loaded container is designed to use four slings that form basket hitches under the container. The empty container is handled with two slings. The package may also be handled by the use of a forklift. The sling hold angles are designed so that even if they failed it would not affect the performance of the package.

The inner container is handled by the use of a series of lifting sling fittings. They are attached in a manner that even if they fail it will not compromise the performance of the inner container. On both the inner and outer containers, the lid lifting devices are marked to ensure proper use. A

detailed discussion of lifting and tie-down designs, with corresponding structural analyses, is provided in Section 2.4.1 and 2.4.2.

1.2.1.10 Shielding

Due to the nature of the unirradiated fuel payload, no biological shielding is necessary or provided by the RAJ-II packaging.

1.2.1.11 Packaging Markings

The packaging will be marked with its model number, serial number, gross weight and also with the package identification number assigned by the NRC.

1.2.2 Containment System

The containment system components are identified above in Section 1.2.1 and accompanying figures. The primary containment boundary of this package is the fuel rod cladding as shown in example Figure 1-6 Example Fuel Rod (Primary Containment). The fuel rod is completed by loading the uranium dioxide pellets into a zirconium alloy cladding tube. The tubes are pressurized with helium and zirconium end plugs are welded to the tube which effectively seals and contains the radioactive material. Welds of the fuel rods are verified for integrity by such means as X-ray inspection, ultrasonic testing, or process control. A representative nominal internal pressure of fuel rods at room temperature conditions is 1.1 MPa (160 psia) (absolute pressure). The RAJ-II package cannot be opened unintentionally. Both the OC and IC lids are attached to their respective bodies with socket-headed cap screws. There are twenty-four bolts holding the outer lid in place. There are no other openings in the outer container. The inner container has ten bolts holding the main lid in place and four bolts holding the end closure in place. Thus, the requirements of 10 CFR 71.43(c) are satisfied.

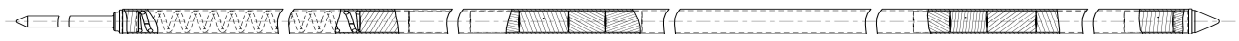

Figure 1-6 Example Fuel Rod (Primary Containment)

1.2.2.1 Pressure Relief System

There are no pressure relief systems included in the RAJ-II package design to relieve pressure from within either the inner or outer containers or the fuel rod. Fire-consumable fusible plugs are used on the exterior surface of both the outer and inner containers to prevent pressure build up from the insulating and shock absorbing material during a fire event. These fusible plugs may be made of plastic. Two plugs are installed in the outer container body and two in the outer container lid. Four are installed in the inner container body, one in the end lid and two in its main lid.

1.2.3 Contents

A maximum of two fuel assemblies are placed in each packaging, see Table 6-1. The packaging is designed and analyzed to ship fuel configured either in 8x8, 9x9 or 10x10 arrays or as loose rods contained in a cylinder, protective case or positioned in one or both sides of the inner container, see Table 6-2. Fuel assemblies may also be shipped in the BWR fuel channel. The nuclear fuel pellets located in rods and contained in the packaging are uranium oxides primarily as UO_2 and U_3O_8. The fuel assembly average enrichment is less than or equal to 5.0% U-235 (the fuel rod maximum enrichment is less than or equal to 5.0% U-235). In addition to the shipment of fuel assemblies, Section 1.2.3.4.2, Section 1.2.3.4.3 and Section 1.2.3.4.4 describe contents configurations for shipping individual fuel rods not contained in a fuel assembly.

Where fuel rods are referenced as being loaded with uranium dioxide mixed with gadolinium oxide (hereinafter gadolinia) the pellets in the gadolinia fuel rods contain a minimum of 2.0% gadolinium.

1.2.3.1 Type A contents

Where the contents of the packaging is commercial grade uranium or other uranium materials where the A_2 value is not exceeded, the packaging may be considered to contain Type A quantities.

1.2.3.2 Type B contents

Where the contents of the packaging is enriched reprocessed uranium or other origin uranium not exceeding the values in Table 1-3, the packaging is considered to contain Type B quantities.

1.2.3.3 Quantity of Radioactive Materials of Main Nuclides

Where the content of the packaging consists of Type B quantities of material, the main nuclides are treated as shown in Tables 1-2 through 1-4 to calculate total activity, activity fractions and A_2 for the mixture.

Table 1 - 2 Quantity of Radioactive Materials (Type A and Type B)

Fuel assembly	**Type 8×8 fuel assembly**	**Type 9×9 fuel assembly**	**Type 10 x10 fuel assembly**
Main nuclides	Low enriched uranium less than or equal to 5% U-235	Low enriched uranium less than or equal to 5% U-235	Low enriched uranium less than or equal to 5% U-235
State of uranium	Uranium oxide ceramic pellet (Solid)	Uranium oxide ceramic pellet (Solid)	Uranium oxide ceramic pellet (Solid)
Fuel assembly average enrichment (Fuel rod maximum enrichment)	5.0% maximum (5.0% maximum)	5.0% maximum (5.0% maximum)	5.0% maximum (5.0% maximum)
Number of fuel rods containing gadolinia	See Table 6-1	See Table 6-1	See Table 6-1
Weight of uranium dioxide pellets (per fuel assembly)	235 kg	240 kg	275 kg

Table 1 - 3 Type B Quantity of Radioactive Material

Isotope	Maximum content[1]	Maximum mass, g	Specific Activity[2],TBq/g	Total Activity, TBq	Total Activity, Ci
U-232	2.00E-09 g/gU	9.68E-04	0.83	8.03E-04	2.17E-02
U-234	2.00E-03 g/gU	9.68E+02	2.30E-04	2.23E-01	6.02E+00
U-235	5.00E-02 g/gU	2.42E+04	8.00E-08	1.94E-03	5.23E-02
U-236	2.50E-02 g/gU	1.21E+04	2.40E-06	2.90E-02	7.85E-01
U-238	9.23E-01 g/gU	4.47E+05	1.20E-08	5.36E-03	1.45E-01
Np-237	1.66E-06 g/gU	8.03E-01	2.61E-05	2.10E-05	5.67E-04
Pu-238	6.20E-11 g/gU	3.00E-05	6.33E-01	1.90E-05	5.13E-04
Pu-239	3.04E-09 g/gU	1.47E-03	2.3E-03	3.38E-06	9.15E-05
Pu-240	3.04E-09 g/gU	1.47E-03	8.40E-03	1.24E-05	3.34E-04
Gamma Emitters	5.18E+05 MeV-Bq/kgU	N/A	N/A	2.51E-02	6.78E-01
			Total	**2.85E-01**	**7.70E+00**

1. Based on a maximum payload of 275 kg UO_2 per assembly, 242 kg U (550 kg UO_2, 484 kg U total)
2. 10CFR71, Appendix A
3. Assuming gamma energy of 0.01 MeV to maximize total content.

Table 1 - 4 Isotopes and A_2 Fractions

Isotope	Maximum Radioactivity content (Ci)	10CFR71 A_2 per isotope (Ci)	Activity Fraction	A_2 Fraction
U-232	2.17E-02	0.0027	2.82E-03	1.04E-01
U-234	6.02E+00	0.1600	7.81E-01	4.88E+00
U-235	5.23E-02	Unlimited	NA	NA
U-236	7.85E-01	0.1600	1.02E-01	6.37E-01
U-238	1.45E-01	Unlimited	NA	NA
Np-237	5.67E-04	0.0540	7.36E-05	1.36E-03
Pu-238	5.13E-04	0.0270	6.67E-05	2.47E-03
Pu-239	9.15E-05	0.0270	1.19E-05	4.40E-04
Pu-240	3.34E-04	0.0270	4.34E-05	1.61E-03
Gamma Emitters	6.78E-01	0.5400	8.80E-02	1.63E-01
Total	**7.70E+00**		**Sum of A_2 fractions**	**5.79E+00**
Mixture A_2				**0.17 Ci**

1.2.3.4 Physical Configuration

1.2.3.4.1 Fuel Assembly

The configuration of typical fuel assemblies is shown in Figure 1-8 Fuel Assembly with Optional Packing Materials. The fuel assemblies may be of various model and type as long as they meet the requirements listed. The dimensions of the main components in the fuel assemblies are listed in Table 1 - 5. The maximum weight of contents including fuel and packing material is 684 kg (1,508 lbs).

1.2.3.4.2 Chemical Properties

Example of structural materials of the fuel assembly is shown in Table 1 - 6. Zirconium alloy, stainless steel and Ni-Cr-Fe alloy are chemically stable materials, and they are excellent in heat resistance and corrosion resistance.

1.2.3.4.3 Density of Materials

The density for the fuel assembly materials is presented in Table 1 - 7.

1.2.3.4.4 Packing Materials

A number of packing materials may be used to guard the fuel assembly (e.g., cluster separators, and polyethylene bags). An example of the packing materials and their use is shown in Figure 1-8.

1.2.3.4.5 Bundled Fuel Rods

In addition to the fuel assembly configuration described above, fuel rods may be shipped bundled together in groups of rods up to 25 total rods. Fuel rods are fixed together using ring clamps. The criticality safety case for loose rods that shows that as many as 25 fuel rods per side can be arranged in any configuration within the volume of the inner container. Based on this criticality safety analysis the ring clamps are not relied on or needed for maintaining the configuration of the fuel rods.

1.2.3.4.6 Fuel Rods In a 5-Inch Pipe

Another physical configuration is the use of a 5-inch diameter schedule 40 stainless steel pipe. The physical configuration of the pipe is shown in drawing 0028B98. The number of fuel rods shipped in this configuration is limited by the quantities in Table 6-2. See Section 6.3.1.3.1 and 6.3.1.3.2 for other descriptions of the pipe.

1.2.3.4.7 Fuel Rods in a Protective Case

Figure 1-7 shows the configuration of the protective case. The protective case is a stainless steel box comprised of a body, lid, wood spacer absorber and end plate. In addition to the figure below, detailed drawings of the protective case are provided in Appendix 1.4.1. The protective case is surrounded by polyurethane foam cushioning material, which provides a snug fit within the inner container. Depending on the rod type, the protective case may be used to transport any number of authorized fuel rods up to a maximum of 30. See Table 6-2.

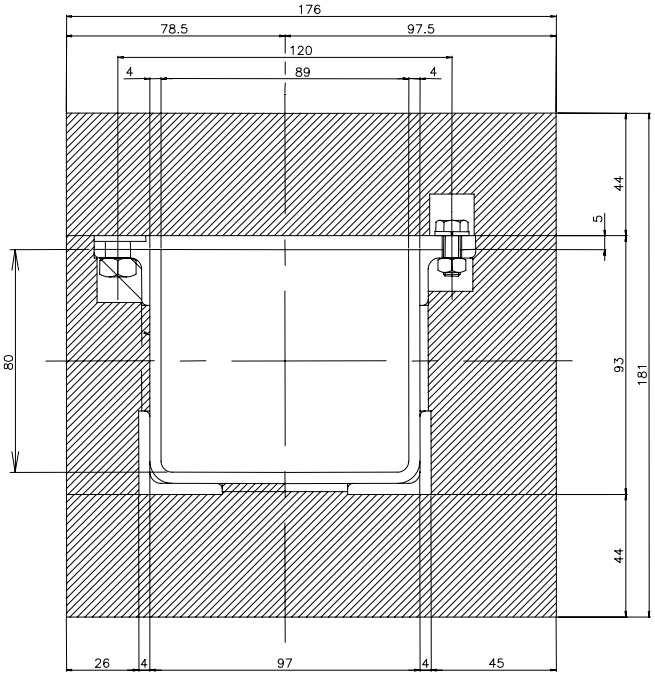

Figure 1-7 Protective Case

Table 1 - 5 Typical Dimensions of the Main Components of Fuel Assembly and Fuel Rod

Item	Dimensions (mm)		
Type of fuel assembly	Boiling Water Reactor		
Fuel assembly full length	Up to 4,480		
Maximum cross-section of fuel assembly	134 x 134		
Fuel rod length	Up to 4,480 and includes partial rods		
Type	**8x8**	**9x9**	**10x10**
Maximum effective fuel length	3,810	3,810	3,850
Wall thickness of cladding tube	0 - 2.06	0 - 1.70	0 - 2.21
Fuel pellet diameter	9.2-10.7	9.2-9.6	8.28-9.2
Fuel Rod OD	10.72-12.50	9.60-11.2	10.0-11.21
Cladding ID	10.44-12.19	9.5-11.1	8.80-10.33

Table 1 - 6 Example of Fuel Structural Materials

Component parts	Structural materials
Pellets	Uranium dioxide sintered (in some cases uranium dioxide blended with gadolinia)
Cladding tube	Zirconium alloy, metallic zirconium
Internal spring	Stainless steel
Getter	Zirconium alloy and stainless steel
Upper and Lower end plug	Zirconium alloy
Water rod	Zirconium alloy
Upper and Lower tie plate	Stainless steel
Spacer	Zirconium alloy and Ni-Cr-Fe alloy (Inconel X-750)
Finger spring	Ni-Cr-Fe alloy
Expansion spring	Ni-Cr-Fe alloy
Nut	Stainless steel
Locking tab washer	Stainless steel

Table 1 - 7 Density of Structural Materials

Main structural materials	Density
Zirconium alloy Metallic zirconium	Approximately 6.5 g/cm³ (0.235lb/in^3)
Uranium dioxide pellet	Approximately 10.4 g/cm³ (0.376 lb/in^3)
Stainless steel	Approximately 7.8 g/cm³ (0.282 lb/in^3)
Ni-Cr-Fe alloy	Approximately 8.5 g/cm³ (0.307 lb/in^3)

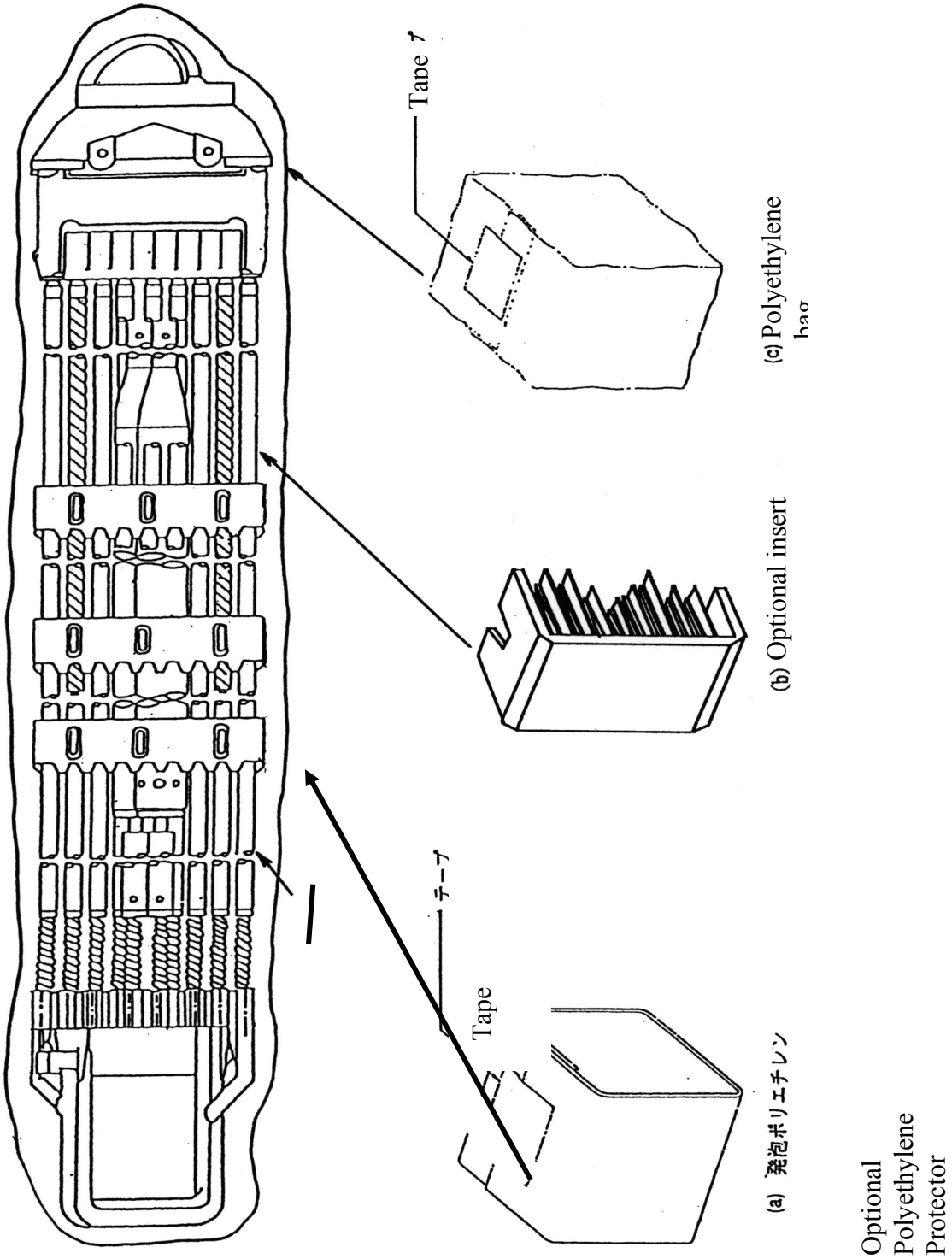

Figure 1-8 Fuel Assembly with Optional Packing Materials

1.2.4 Operational Features

The RAJ-II packaging is not considered operationally complex. Operational features are readily apparent from an inspection of the drawings provided in Appendix 1.4.1 and the previous discussions presented in Section 1.2.1. Operational procedures and instructions for loading, unloading, and preparing empty RAJ-II packages for transport are provided in Chapter 7.0.

1.3 GENERAL REQUIREMENTS FOR ALL PACKAGES

1.3.1 Minimum Package Size

The RAJ-II package is a rectangular box that is 742 mm (29.21 in) high by 720 mm (28.35 in) wide by 5,068 mm (199.53 inches) long. Thus, the requirement of 10 CFR 71.43(a) is satisfied.

1.3.2 Tamper-Indicating Feature

Seal pins are provided at each end of the outer container body and lid for the use of tamper indicating seals. A tamper indicating seal is attached at each end of the loaded outer container by inserting the seal through the holes in the body and lid seal pins and securing the seal. The tamper indicating seal is not readily breakable and would provide evidence of tampering or opening by an unauthorized person. Thus, the requirement of 10 CFR 71.43(b) is satisfied.

1.4 APPENDIX

1.4.1 RAJ-II General Arrangement Drawings

This section presents the RAJ-II packaging general arrangement drawing consisting of 15 drawings entitled, *RAJ-II SAR Drawing,* see drawing list below. Within the packaging general arrangement drawing, dimensions important to the packaging safety are dimensioned and toleranced. Other dimensions are provided as a reference dimension, and are toleranced in accordance with the JIS (Japan Industrial Std.) B 0405. See 2.1.4.1 and 2.1.4.2.

1.4.1.1 Drawing List

Table 1 - 8 Outer Container Drawings

Drawing number	Number of Sheets	Revision #	Name
105E3737	1	6	Outer Container Assembly Licensing Drawings
105E3738	3	7	Outer Container Main Body Assembly Licensing Drawings
105E3739	1	4	Outer Container Fixture Assembly Licensing Drawings
105E3740	1	4	Outer Container Fixture Assembly Installation Licensing Drawings
105E3741	1	1	Outer Container Shock Absorber Assembly Licensing Drawings
105E3742	1	3	Outer Container Bolster Assembly Licensing Drawings
105E3743	1	4	Outer Container Lid Assembly Licensing Drawings
105E3744	1	5	Outer Container Marking Licensing Drawings

Table 1 - 9 Inner Container Drawings

Drawing number	Number of Sheets	Revision #	Name
105E3745	4	8	Inner Container Main Body Assembly Licensing Drawings
105E3746	1	1	Inner Container Parts Assembly Licensing Drawings
105E3747	1	4	Inner Container Lid Assembly Licensing Drawings
105E3748	1	2	Inner Container End Lid Assembly Licensing Drawings
105E3749	1	6	Inner Container Marking Licensing Drawings

Table 1 - 10 Contents Drawings

Drawing number	Number of Sheets	Revision #	Name
105E3773	1	1	Protective Case
0028B98	1	1	Shipping Container Loose Fuel Rods

DRAWINGS WITHHELD UNDER 10 CFR 2.390

2.0 STRUCTURAL EVALUATION

This section presents evaluations demonstrating that the RAJ-II package meets applicable structural criteria. The RAJ-II packaging, consisting of unirradiated fuel assemblies that provide containment, an inner container, and an outer container with paper honeycomb spacers, is evaluated and shown to provide adequate protection for the payload. Normal Conditions of Transport (NCT) and Hypothetical Accident Condition (HAC) evaluations, using analytic and empirical techniques, are performed to address 10 CFR 71 performance requirements.

Numerous tests were successfully performed on the RAJ-II package during its initial qualification in Japan that provided a basis for selecting the certification tests. RAJ-II certification testing involved two full-scale Certification Test Units (CTU) at Oak Ridge, TN. The RAJ-II CTUs were subjected to a series of free drop and puncture drop tests. The RAJ-II CTU protected the simulated fuel assemblies, allowing them to remain undamaged and leak tight throughout certification testing. Details of the certification test program are provided in Appendix 2.12.1.

2.1 DESCRIPTION OF STRUCTURAL DESIGN

2.1.1 Discussion

A comprehensive discussion on the RAJ-II packaging design and configuration is provided in chapter 1.0. Drawings provided in Appendix 1.4.1 show the construction of the RAJ-II and how it protects the fuel assemblies. The containment is provided by the fuel cladding and welded end fittings of the fuel rods. The fuel is protected by an inner container that provides thermal insulations and soft foam that protects the fuel from vibration. The inner container is supported by vibration isolation system inside the outer container that has shock absorbing blocks of balsa and honeycomb made of resin impregnated kraft paper (hereinafter called "paper honeycomb"). Specific discussions relating to the aspects important to demonstrating the structural configuration and performance to design criteria for the RAJ-II packaging are provided in the following sections. Standard fabrication methods are used to fabricate the RAJ-II package.

Detailed drawings showing applicable dimensions and tolerances are provided in Appendix 1.4.1.

Weights for the various components and the assembled packaging are provided in Section 2.1.3.

2.1.1.1 Containment Structures

The primary containment for the radioactive material in the RAJ-II is the fuel rod cladding, which is manufactured to high standards for use in nuclear reactors. The fabrication standards for the fuel are in excess of what is needed to provide containment for shipping of the fuel. The fuel rod cladding is designed to provide containment throughout the life of the fuel, prior to

loading, in transportation, and while used in the reactor where it operates at higher pressures and temperatures, and must contain fission products as well as the fuel itself.

The cladding tubes for the fuel are high quality seamless tubing. The clad fuel is verified leaktight before shipment.

2.1.1.2 Non-Containment Vessel Structures

The RAJ-II is made up of two non-containment structures, the inner container, and the outer container that are designed to protect the fuel assemblies and clad rods which serve as the containment. The inner container design provides some mechanical protection although its primary function is to provide thermal protection. The outer container consists of a metal wall with shock absorbing devices inside and vibration isolation mounts for the inner container. Section 1.2.1 provides a detailed description of the inner and outer container. Non-containment structures are fabricated in accordance with the drawings in Appendix 1.4.1.

Welds for the non-containment vessel walls are subjected to visual inspection as delineated on the drawings in Appendix 1.4.1.

2.1.2 Design Criteria

Proof of performance for the RAJ-II package is achieved by a combination of analytic and empirical evaluations. The acceptance criteria for analytic assessments are in accordance with 10 CFR 71 and the applicable regulatory guides. The acceptance criterion for empirical assessments is a demonstration that both the inner and outer container are not damaged in such a way that their performance in protecting the fuel assemblies during the thermal event is not compromised and the fuel itself is not damaged throughout the NCT and HAC certification testing. Additionally, package deformations obtained from certification testing are considered in subsequent thermal, shielding, and criticality evaluations are validated.

2.1.2.1 Analytic Design Criteria (Allowable Stresses)

The allowable stress values used for analytic assessments of RAJ-II package structural performance come from the regulatory criteria such as yield strength or 1/3 of yield or from the ASME Code for the particular application. Material yield strengths, taken from the ASME Code, used in the analytic acceptance criteria, S_y, and ultimate strengths, S_u, are presented in Table 2 - 2 of Section 2.2.

2.1.2.2 Containment Structures

The fuel cladding provides the primary containment for the nuclear fuel.

2.1.2.3 Non-Containment Structures

For evaluation of lifting devices, the allowable stresses are limited to one-third of the material yield strength, consistent with the requirements of 10 CFR 71.45(a). For evaluation of tie-down devices, the allowable stresses are limited to the material yield strength, consistent with the requirements of 10 CFR 71.45(b).

2.1.2.4 Miscellaneous Structural Failure Modes

2.1.2.4.1 Brittle Fracture

By avoiding the use of ferritic steels in the RAJ-II packaging, brittle fracture concerns are precluded. Specifically, most primary structural components are fabricated of austenitic stainless steel. Since this material does not undergo a ductile-to-brittle transition in the temperature range of interest (above -40 ºF), it is safe from brittle fracture.

The closure bolts used to secure the inner and outer container lids are stainless steel, socket head cap screws ensuring that brittle fracture is not of concern. Other fasteners used in the RAJ-II packaging assembly provide redundancy and are made from stainless steel, again eliminating brittle fracture concerns.

2.1.2.4.2 Extreme Total Stress Intensity Range

Since the response of the RAJ-II package to accident conditions is typically evaluated empirically rather than analytically, the extreme total stress intensity range has not been quantified. Two full-scale certification test units (see Appendix 2.12.1) successfully passed free-drop and puncture testing. The CTUs were also fabricated in accordance with the drawings in Appendix 1.4.1, thus incurring prototypic fabrication induced stresses. Exposure to these conditions has demonstrated leak tight containment of the fuel, geometric configuration stability for criticality safety, and protection for the fuel. Thus the intent of the extreme total stress intensity range requirement has been met.

2.1.2.4.3 Buckling Assessment

Due to the small diameter of the containment boundary (the fuel rod cladding) and the fact that its radial deflection is limited by the internal fuel pellets, radial buckling is not a failure mode of concern for the containment boundary. Axial buckling deflection is also limited by the inner wall of the inner container and lid. The applied axial load to the fuel is also limited by the wood at the end of the packaging. The limited horizontal movement of the fuel during an end drop limits the ability of the fuel to buckle as demonstrated in tests performed on CTU 2 (see Appendix 2.12.1).

It is also noted that 30-foot drop tests performed on full-scale models with the package in various orientations produced no evidence of buckling of any of the fuel (see Appendix 2.12.1). Certification testing does not provide a specific determination of the design margin against buckling, but is considered as evidence that buckling will not occur. In addition buckling is a

potential concern to insure adequate geometric configuration control of the post accident package for criticality control. This involves not only the internal configuration of the package but the potential spacing between packages as well. Deformation of the RAJ-II is limited by its redundant structure. The wall of the package acts to stiffen the support plates that carry the load of the inner container via the vibration isolating mechanism. Part of the redundant system to minimize deformation of the fuel is the paper honeycomb that absorbs shocks that would impart side loading to the fuel. The inner container, consisting of an inner wall separated from an outer wall by thermal insulation, is lined with cushioning material that supports the fuel. Regardless of the specific failure mechanism of the support plates, the total deformation is limited by the shock absorbers (paper honeycomb). These blocks immediately share the load. Hence, even if the support plates would buckle allowing the outer wall to plastically deform, the amount of deformation is limited by the shock absorbing material. This has been demonstrated by test to allow only 118 mm (4.7 inches) of deformation of the shock absorbing blocks. The criticality evaluation takes into consideration this deformation. The redundant support system combined with the vibro-isolation and shock absorption system prevents the deformation of the inner container and the fuel.

The axial deformation resulting from an end drop is controlled in a similar manner. The end of the outer container has a wood shock absorber built in that carries the load from the inner container to the outer wall after the vibro-isolation device deflects. This reduces the load carried by the outer wall and support plates. It prevents large loads and deformations that could contribute to buckling of the fuel. The inner container constrains the fuel from large deformations or buckling.

Therefore, the support system prevents buckling of the packaging or fuel that would affect the criticality control or containment.

2.1.3 Weights and Centers of Gravity

The maximum gross weight of a RAJ-II package, including a maximum payload weight of 684 kg (1,508 pounds) is 1,614 kg (3,558 pounds). The maximum vertical Center of Gravity (CG) is located 421 mm (16.57 inches) above the bottom surface of the package for a fully loaded package. A maximum horizontal shift of the horizontal CG is 92 mm (3.62 inches). This is allowed for in the lifting and tie-down calculations presented in Section 2.5.1. Figure 2-1 shows the locations of the center of gravity for the major components and the location of the center of gravity for the assembled. A detailed breakdown of the RAJ-II package component weights is summarized in Table 2 - 1.

2.1.3.1 Effect of CG Offset

The shift of the CG of the package 92 mm (3.6 inches) has very little effect on the performance of the package due to the length of the package, 5,068 mm (199.53 in). This results in a small shift of the weight and forces from one end of the package to the other. The actual total shift is:

$$3.6\% = 1 - \frac{(2)((5068/2) - 92)}{5068}$$

The offset of the CG is taken into account in the lifting and tie down calculations. The effect of this relatively small offset can be neglected.

2.1.4 Identification of Codes and Standards for Package Design

The radioactive isotopic content of the fuel is primarily U-235 with small amounts of other isotopes that make it Type B. Using the isotopic content limits shown in Section 1.2.3 the package would be considered a Category II. As such the applicable codes that would apply are the ASME Boiler and Pressure Vessel Code Section III, Subsection ND for the containment boundary which is the fuel cladding and Section III, Subsection NG for the criticality control Structure and the Section VIII for the non containment components.

The fuel cladding, due to its service in the reactor and need for high integrity, is designed to and fabricated to standards that exceed those required by ASME Section III Subsection ND. The structure used to maintain criticality control is demonstrated by test. The packaging capabilities are verified by test and the codes used in fabrication are called out on the drawings in Appendix 1.4.1. The sheet metal construction of the packaging requires different joint designs and manufacturing techniques that would normally be covered by the above referenced codes.

2.1.4.1 JIS/ASTM Comparison of Materials

The Certification Test Units (CTUs) were manufactured in Japan using material meeting JIS specifications. The fuel cladding and ceramic pellets were manufactured in the US to US specifications. The future manufacturing of RAJ-II packages may be performed using American standards (ASTM or ASME) that are appropriate substitutes for the Japanese standards (JIS) material comprising the CTUs. In order to assure that the packaging manufactured in the future meets the performance requirements demonstrated for the RAJ-II CTUs a detailed review of the differences between the American and Japanese standards was performed. The scope of the study included the: stainless steel products, wood products, rubber, paper honeycomb, and polyethylene foam. The study concluded that American standards material is available and compatible to the JIS standards. Future manufacturing of these packages for domestic use may be to American or Japanese specifications meeting the tolerances specified in the general arrangement drawings.

2.1.4.2 JIS/ASME Weld Comparison

Based upon an evaluation, it is concluded that the following standards are equivalent for the purposes of fabrication of the RAJ-II container in the United States:

Japanese Specification	American Specification
JIS Z 3821 Standard qualification procedure for welding technique of stainless steel	ASME Section IX
JIS Z 3140 Method of inspection for spot weld	ASME Section IX
JIS Z 3145 Method of bend test for stud weld	ASME Section IX

2.1.4.3 JIS/JSNDI/ASNT Non-destructive Examination Personnel Qualification and Certification Comparison

The following standards are considered equivalent for Non-destructive Examination Personnel Qualification and Certification. Personnel with these qualifications and certifications are authorized to perform examinations of the fabrication inspection requirements for the RAJ-II container in the United States. Although these documents cover other disciplines, this comparison only applies to Liquid Penetrant Examination.

Japanese Specification	American Specification
JIS Z 2305 Qualification and Certification for NDT Personnel	SNT-TC-1A* Recommended Practice
Certification NDIS 0601	SNT-TC-1A Recommended Practice
Certification NDIS J001	SNT-TC-1A Recommended Practice

*Society of Non-destructive Testing – Technical Council

Table 2 - 1 RAJ-II Weight

Contents	Number of assemblies per package	Maximum 2 Assemblies
	Number of fuel rods per package	See **Error! Reference source not found.**.
	Total weight	684 kg (1,508 lb)
Inner container	Body	200 kg (441 lb) (including bolts)
	Lid	101 kg (223 lb)
	End lids	7 kg (15.4 lb)
	Total weight	308 kg (679 lb)
Outer container	Body	485 kg (1,069 lb) (including bolts)
	Lid	137 kg (302 lb)
	Total weight	622 kg (1,371 lb)
Total weight of package		1,614 kg (3,558 lb)

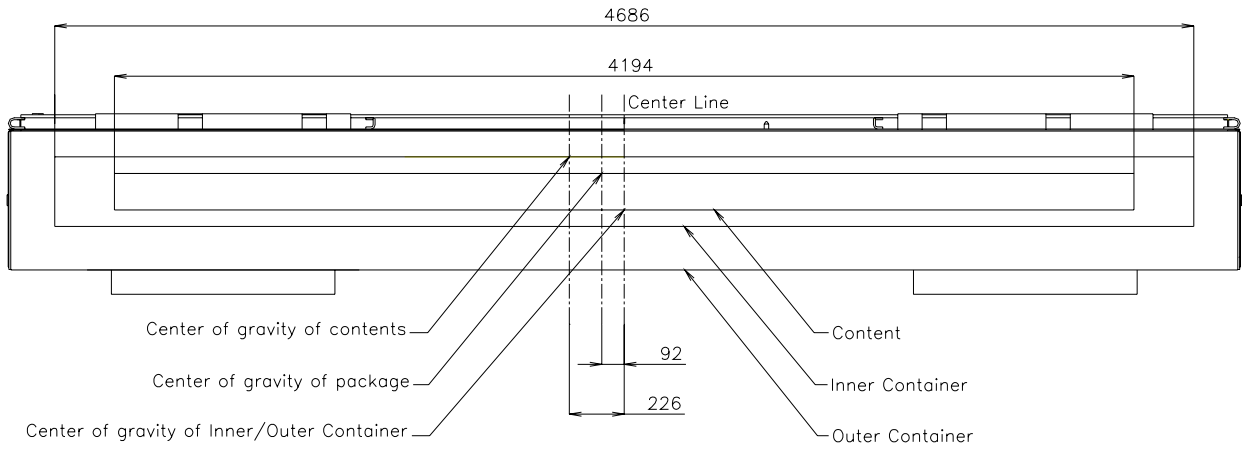

(unit: mm)

Figure 2-1 Center of Gravity of Package Components

2.2 MATERIALS

2.2.1 Material Properties and Specifications

The major structural components, i.e., the Outer Container (OC) and Inner Container (IC) walls, supports, and attachment blocks are fabricated from austenitic stainless steel. Other materials performing a structural function are lumber (bolster), balsa (shock absorber), paper honeycomb (shock absorber), alumina silicate (thermal insulator), polyethylene foam (cushioning material), and zirconium alloy (fuel rod cladding). The drawings presented in Appendix 1.4.1 delineate the specific material(s) used for each RAJ-II packaging.

The remainder of this section presents and discusses pertinent mechanical properties for the materials that perform a structural function. Both the materials that are used in the analytics and those whose function in the package is demonstrated by test such as the shock absorbing material are presented. In general the analytics covering the lifting and tie down capabilities of the package and some normal condition events are limited to the stainless steel structure of the packaging.

Table 2 - 2 presents the bounding mechanical properties for the series 300 stainless steel used in the RAJ-II packaging. Each of the representative mechanical properties is those of Type 304 stainless steel and is taken from Section II, Parts A and D, of the ASME Boiler and Pressure Vessel Code. These properties are applicable to both packages that may have been made in Japan to Japanese specifications, Japanese Industrial Standards (JIS) or using ASME specification material. The density of stainless steel is taken as 0.29 lb/in^3 (8.03E3 kg/m^3), and Poisson's Ratio is 0.3.

Table 2 - 3 presents the mechanical properties of the main non-stainless steel components of the package necessary for the structural analysis.

Table 2 - 2 Representative Mechanical Properties of 300 Series Stainless Steel Components

① Minimum Elongation (%)	Temperature °C (°F)	② Yield Strength, S_y MPa ($\times 10^3$ psi)	③ Ultimate Strength, S_u MPa ($\times 10^3$ psi)	④ Elastic Modulus, E GPa ($\times 10^6$ psi)	⑤ Thermal Expansion Coefficient, α x 10^{-6} mm/mm/°C ($\times 10^{-6}$ in/in/°F)
35	-29 (-20)	206.8 (30.0)	517.1 (75.0)	-----	-----
40	21 (70)	206.8 (30.0)	517.1 (75.0)	195.1 (28.3)	-----
30	38 (100)	206.8 (30.0)	517.1 (75.0)	-----	15.39 (8.55)
25	93 (200)	172.4 (25.0)	489.5 (71.0)	190.3 (27.6)	15.82 (8.79)
30	149 (300)	155.1 (22.5)	455.1 (66.0)	186.2 (27.0)	16.2 (9.00)
40	204 (400)	142.7 (20.7)	444.0 (64.4)	182.7 (26.5)	16.54 (9.19)
40⑥	23°C⑥	205 MPa Min⑥	520 MPa Min⑥	-----	-----
40⑦	21°C⑦	205 MPa Min⑦	515 MPa Min⑦	-----	-----

Notes:
① ASME Code, Section II, Part A

② ASME Code, Section II, Part D, Table Y-1.

③ ASME Code, Section II, Part D, Table U

④ ASME Code, Section II, Part D, Table TM-1, Material Group G.

⑤ ASME Code, Section II, Part D, Table TE-1, 18Cr-8Ni, Coefficient B.

⑥ JIS Handbook Ferrous Materials and Metallurgy I, Sections G4303, G4304, G4305 Material Specifications

⑦ ASTM A240, A666 & A276 Material Specifications

Table 2 - 3 Mechanical Properties of Typical Components

Materials (Usage)	Yield stress or yield strength	Tensile strength	Compressive strength	Bending strength	Static initial peak stress	Modulus of longitudinal elasticity	Density (g/cm^3)
Lumber (bolster)	56.3 MPa Nominal	–	50.5 MPa Nominal	72.0 MPa Nominal	–	7.85 GPa Nominal	0.53 Nominal
Balsa (shock absorber)	–	–	16 MPa Nominal	–	–	–	0.18 Nominal
Paper honeycomb (shock absorber)	–	–	–	–	2.35 MPa Nominal	–	0.06 Nominal
Alumina Silicate (thermal insulator)	–	–	294 kPa Nominal	314 kPa Nominal	–	–	0.25 Nominal
Foam polyethylene (cushioning mat'l)	–	–	Approx. 0.2MPa @ 50% strain	–	0.69 MPa Nominal	–	0.068 Nominal
Zirconium alloy (fuel rods) ASTM B811	241 MPa (35,000psi)	413 MPa (60,000psi)	–	–	–	97.1 GPa Nominal	6.5 Nominal
300 Series Stainless Socket Headed Cap screw	241 MPa (35,000psi) (Min)	379 MPa (75,000psi) (Min)	–	–	–	–	–

2.2.2 Chemical, Galvanic, or Other Reactions

The major materials of construction of the RAJ-II packaging (i.e., austenitic stainless steel, polyurethane foam, alumina thermal insulator, resin impregnated paper honeycomb, lumber

(hemlock and balsa), and natural rubber) will not have significant chemical, galvanic or other reactions in air, inert gas or water environments, thereby satisfying the requirements of 10 CFR 71.43(d). These materials have been previously used, without incident, in radioactive material (RAM) packages for transport of similar payload materials. A successful RAM packaging history combined with successful use of these fabrication materials in similar industrial environments ensures that the integrity of the RAJ-II package will not be compromised by any chemical, galvanic, or other reactions.

The RAJ-II packaging is primarily constructed of series 300 stainless steel. This material is highly corrosion resistant to most environments. The metallic structure of the RAJ-II packaging is composed entirely of this material and compatible 300 series weld material. Since both the base and weld materials are 300 series materials, they have nearly identical electrochemical potential thereby minimizing any galvanic corrosion that could occur.

The stainless steel within the IC cavity between the inner and outer walls is filled with a ceramic alumina silicate thermal insulator. This material is non-reactive with either the wood or the stainless steel, both dry or in water. The alumina silicate is very low in free chlorides to minimize the potential for stress corrosion of the IC structure.

The polyethylene foam that is used in the IC for cushioning material has been used previously and is compatible with stainless steel. The polyethylene foam in is very low in free halogens and chlorides.

Resin impregnated paper honeycomb is used in the RAJ-II packaging as cushioning material. The impregnated paper is resistant to water and break down. It is low in leachable halides.

The natural rubber that is used as a gasket for the lids and in the vibro-isolating system, contains no corrosives that would react adversely affect the RAJ-II packaging. This material is organic in nature and non-corrosive to the stainless steel boundaries of the RAJ-II packaging.

2.2.2.1 Content Interaction with Packaging Materials of Construction

The materials of construction of the RAJ-II packaging are checked for compatibility with the materials that make up the contents or fuel rods that are to be shipped in the RAJ-II. The primary materials of construction of the fuel assembly that could come in contact with the packaging are the stainless steel and the zirconium alloy material that is used for the cladding of the fuel rods. Zirconium alloy (including metal zirconium), stainless steel, and Ni-Cr- Fe alloy, which form a passivated oxide film on the surface under normal atmosphere with slight moisture, are essentially stable. The contact of the above three kinds of metals with polyethylene is chemically stable. These materials are compatible with the stainless steel, polyethylene, and natural rubber that could come in contact with the contents.

2.2.3 Effects of Radiation on Materials

Since this is an unirradiated fuel package, the radiation to the packaging material is insignificant. Also, the primary materials of construction and containment, austenitic stainless steel and the zirconium alloy cladding of the fuel are highly resistant to radiation.

2.3 FABRICATION AND EXAMINATION

2.3.1 Fabrication

The RAJ-II is fabricated using standard fabrication techniques. This includes cutting, bending and welding the stainless steel sheet metal. As shown on the drawing the welding is done to AWS D1.6 Welding of Stainless Steel. The process may also be controlled by ASME Section IX or other international codes. The containment, the cladding of the fuel rods is fabricated to standards that exceed the required Section VIII of the ASME Boiler and Pressure vessel code do to the service requirements of the fuel in reactors.

2.3.2 Examination

The primary means of examination to determine compliance of the RAJ-II to the design requirements is visual examination of each component and the assembled units. This includes dimensional verification as well as material and weld examination. The materials will also be certified to the material specifications. Shock absorbing material such as the paper honeycomb will also have verified material properties.

2.4 LIFTING AND TIE-DOWN STANDARDS FOR ALL PACKAGES

For analysis of the lifting and tie-down components of the RAJ-II packaging, material properties from Section 2.2 are taken at a bounding temperature of 75°C (167 ºF) per Section 2.6.1.1. This is the maximum temperature that the container reaches when in the sun. The primary structural material is 300 series stainless steel that is used in the Outer Container (OC).

A loaded RAJ-II package can be lifted using either a forklift or by slings. The gross weight of the package is a maximum of 1,614 kg (3,558 lbs). Locating/protection plates for the forklift and locating angles for the sling locate the lift points for the package. In both cases the package is lifted from beneath. The failure of these locating/protective features would not cause the package to drop nor compromise its ability to perform its required functions.

The inner container may be lifted empty or filled with the contents using the sling fittings that are attached at the positions shown in Figure 2-2. The details of the sling fittings are as shown in Figure 2-3. Since the center of gravity depends on existence of the contents, the sling fittings for the filled container and the empty container are marked respectively as "Use When Loaded" and

"Use When Empty" to avoid improper operations. Also, the sling fittings on the lid of inner container to lift the lid only are marked as "Use for Lifting Lid" similar to the outer container.

The sling devices are mechanically designed to be able to handle the package and the inner container filled with the fuel assemblies in safety; they can lift three times the gross weight of the package, or three times the gross weight of the filled inner container respectively, so that they can with stand rapid lifting.

Properties of 300 series stainless steel are summarized below.

Table 2 - 4 Properties of 300 Series Stainless Steel

Material Property	Value	Reference
At 75ºC (167 ºF)		
Elastic Modulus, E	191.7 GPa (27.8×10^6 psi)	Table 2 - 2
Yield Strength, σ_y	184.7 MPa (26,788 psi)	
Shear Stress, equal to (0.6) σ_y	110.8 MPa (16,073 psi)	

2.4.1 Lifting Devices

This section demonstrates that the attachments designed to lift the RAJ-II package are designed with a minimum safety factor of three against yielding, per the requirements of 10 CFR71.45 (a).

The lifting devices on the outer container lid are restricted to only lifting the outer container lid, and the lifting devices in the inner lid are restricted to only lifting the inner container lid. Although these lifting devices are designed with a minimum safety factor of three against yielding, detailed analyses are not specifically included herein since these lifting devices are not intended for lifting a RAJ-II package.

The outer container can be handled by either forklift or slings in a basket hitch around the package, requiring no structural component whose failure could affect the performance of the package.

2.4.1.1 Lifting of Inner Container

The inner container is lifted when loaded with fuel from the outer container with sling fittings attached to the body of the inner container. Three pairs (six in total) of the sling fittings are attached to the inner container as shown in Figure 2-2. The center of gravity depends upon whether the container is filled or not. Since the six sling fittings are the same, the stress in the sling fittings are evaluated for the case of at the maximum weight condition that occurs when the inner container is filled with fuel assemblies.

The stress on the sling fitting when lifting the inner container filled with contents is evaluated by determining the maximum load acting on any given fitting.

The maximum load, $P_{v,}$ (see Figure 2-9) acting on one of the sling fitting vertically when lifting is given by the following equation:

$$P_v = \frac{(W_2 + W_3)}{n} \cdot g$$

where

P_v: maximum load acting to sling fitting in vertical direction — N

W_2: mass of inner container — 308 kg (679 lb)

W_3: mass of contents — 684 kg (1,508 lbs)

n: number of sling fittings — 4

g: acceleration of gravity — 9.81 m/s^2

Accordingly, the maximum load acting on the sling fitting vertically is calculated as

$$P_v = \frac{684 + 308}{4} \times 9.81 = 2.433 \times 10^3 \text{ N (546.9 lbf)}$$

The load, P, acting to the sling fitting when the sling is at a minimum angle of 60° is calculated as

$$P = \frac{P_v}{\sin\theta} = \frac{2.433 \times 10^3}{\sin 60^0} = 2.809 \times 10^3 \text{ N (631 lbf)}$$

Also, the maximum load, $P_{H,}$ acting on the sling fitting horizontally is calculated as:

$$P_H = \frac{P_v}{\tan\theta} = \frac{2.433 \times 10^3}{\tan 60^0} = 1.405 \times 10^3 \text{ N (316 lbf)}$$

Each sling fitting is made up of a hooking bar which is a 12mm diameter bent rod and a perforated plate that is made up of two pieces of angle that are welded together. The perforated plate of the sling fitting is welded to a support of that is welded to the body of the inner container.

The shearing stress in the hooking bar (see Figure 2-6) is given by the following equation:

$$\tau_N = \frac{P \times \phi}{A}$$

Where

τ_N: shearing stress on hooking bar of sling fitting MPa

P: maximum load 2.809×10^3 N (631 lbf)

A: cross-section of hooking bar of sling fitting $\pi/4 \times 12^2 = 113$ mm^2 (0.175 in^2)

ϕ: load factor 3

Accordingly, the shearing stress on the hooking bar of the sling fitting at its center is calculated as

$$\tau_N = \frac{2.809 \times 10^3 \times 3}{113} = 74.58 \text{ MPa (10,820 psi)}$$

The yield stress for stainless steel is 184.7 MPa (26,790 psi) and the shear allowable is 0.6 x 184.7 = 110.8 MPa (16,070 psi) at the maximum normal temperature, hence the margin (MS) is

$$MS = \frac{110.8}{74.58} - 1 = 0.48$$

Therefore, the sling fitting can withstand three times the load without yielding in shear.

The strength of the perforated plate of a sling fitting is evaluated for failure by shearing. The shear stress on a perforated plate (see Figure 2-7) of the sling fitting by the total load is given by the following equation.

$$\tau_N = \frac{P \cdot \phi}{A}$$

Where:

τ_N: shearing stress on the perforated plate of a sling fitting MPa

P: maximum load 2.809×10^3 N (631 lbf)

A: cross-section of the upper part of the perforated plate

$$2 \times \frac{50 - 14}{2} \times 6 = 216 \text{ mm}^2 (0.33 \text{ in}^2)$$

ϕ: load factor 3

Accordingly, the shearing stress, τ_N, on the perforated plate of sling fitting is calculated as:

$$\tau_N = \frac{2.809 \times 10^3 \times 3}{216} = 39.01 \text{ MPa (5,658 psi)}$$

The allowable shearing stress for stainless steel is 110.8 MPa (16,073 psi). Then the margin of Safety (MS) is

$$MS = \frac{110.8}{39.01} - 1 = 1.84$$

Therefore, the shear strength of the plate meets the requirement of not yielding under three times the load.

Next, the strength of welds of the sling fittings is evaluated for the torsional loads applied. Torsional loads are applied to the welds of sling fitting per Figure 2-8.

The moment of inertia of area, I_P, to the welds of sling fittings is given by the following equation:

$$I_P = I_X + I_Y$$

$$I_X = I_{X2} - I_{X1}$$

$$I_Y = \Sigma I_{Yi}$$

where

I_P : moment of inertia of area to welds mm^4

I_X : moment of inertia of area to welds for X-axis mm^4

I_Y : moment of inertia of area to welds for Y-axis mm^4

I_{X1} : moment of inertia of area to inside of weld for X-axis mm^4

I_{X2} : moment of inertia of area to outside of weld for X-axis mm^4

I_{Y1} : moment of inertia of area to each weld for Y-axis mm^4

The moment of inertia of area, I, to a cross-sectional area of width, b, and height, h, is given by:

$$I = \frac{1}{12} bh^3$$

Conservatively only the outside welds not including any corner wrap around that attach the sling fitting to the support plate are considered. Thus, the moment of inertia of area, I_X and I_Y to the welds for X-axis and Y-axis are calculated as:

$$I_X = (\frac{1}{12} \times 88 \times 54^3) - (\frac{1}{12} \times 88 \times 50^3) = 2.38 \times 10^5 \text{ mm}^4 (0.57 \text{ in}^4)$$

$$I_Y = 2I_{Y1} = 2 \times \frac{1}{12} \times 2 \times 88^3 = 2.27 \times 10^5 \text{ mm}^4 (0.55 \text{ in}^4)$$

Accordingly, the moment of inertia of area, I_P, to the welds is calculated as

$$I_P = (2.38 \times 10^5) + (2.27 \times 10^5) = 4.65 \times 10^5 \text{ mm}^4 (1.12 \text{ in}^4).$$

The shearing stress, $S_{d,}$ on the weld due to the load acting on the sling fitting is given by the following equation:

$$S_d = \frac{P \cdot \phi}{A}$$

Where:

S_d: shearing stress on welds due to the load to sling fitting — MPa

P: maximum load acting to one of sling fitting — 2.809×10^3 N (631 lbf)

A: overall cross-section of welds — $2 \times 88 = 176$ mm^2 (0.273 in^2)

ϕ: load factor — 3

Accordingly, the shearing stress on welds due to the load acting to the sling fitting is calculated as:

$$S_d = \frac{2.809 \times 10^3 \times 3}{176} = 47.9 \text{ MPa (6,950 psi)}$$

The maximum bending moment acting to the sling fitting is given by the following equation from Figure 2-9

$$M_{max} = P \cdot l$$

Where:

M_{max}: maximum bending moment acting to sling fitting — N · mm

P: maximum load acting to one of sling fitting — 2.809×10^3 N (631 lbf)

l: distance from fulcrum to load point — 17 mm (0.67 in)

Therefore, the maximum bending moment acting to the sling fitting is calculated as:

$$M_{max} = 2.809 \times 10^3 \times 17$$

$$= 4.8 \times 10^4 \text{ N·mm (424.8 in·lbf)}$$

The stress due to this bending moment is given by the following equation:

$$S_m = \frac{M_{max} \cdot r \cdot \phi}{I_P}$$

Where:

S_m: Stress acting to a point at r from center of gravity due to bending moment

MPa

r: distance from center of gravity to end of welds $\sqrt{44^2 + 25^2}$ = 50.6 mm (1.99 in)

M_{max}: maximum bending moment acting to sling fitting

4.8×10^4 N·mm (424.8 in·lbf)

I_P: moment of inertia of area to welds 4.65×10^5 mm^4 (1.12 in^4)

ϕ: load factor 3

From this equation, the maximum bending moment, S_m, acting to the sling fitting is calculated as:

$$S_m = \frac{4.8 \times 10^4 \times 50.6 \times 3}{4.65 \times 10^5} = 15.6\text{MPa (2,260 psi)}$$

In addition, the composite shearing stress, S, on the welds is given by the following equation:

$$S = \sqrt{S_d^2 + S_m^2 + 2S_d S_m \cos\theta}$$

Where:

Cos θ = 25/50.6

From this equation, the composite shearing stress, S, is calculated as

$$S = \sqrt{47.9^2 + 15.6^2 + 2 \times 47.9 \times 15.6 \times 25/50.6}$$

= 57.2 MPa (8,300 psi)

Meanwhile, the allowable shearing stress for 300 series stainless steel is 110.8 MPa (16,073 psi).

Then the margin (MS) is:

$$MS = \frac{110.8}{57.2} - 1 = 0.94$$

The welds are capable of carrying 3 times the expected load without yielding.

Likewise the welds of the support plates for sling fittings are evaluated in the same manner. Since the welds of the support plates (see Figure 2-10) receive the same load as mentioned above in the case of the welds of the sling fittings, it is evaluated by same analytic method as mentioned above. The symbols used here shall have same meaning.

The moment of inertia of area, I_P, to the welds of support plate is given by the following equation:

$$I_P = I_X + I_Y$$

Where:

$$I_X = I_{x2} - I_{x1}$$

$$I_Y = I_{y2} - I_{y1}$$

The moment of inertia of areas I_X and I_Y to the welds for X-axis and Y-axis are calculated as:

$$I_X = \frac{1}{12} \times 153 \times 83^3 - \frac{1}{12} \times 150 \times 80^3$$

$$= 8.903 \times 10^5 \text{ mm}^4 (2.14 \text{ in}^4)$$

$$I_Y = \frac{1}{12} \times 83 \times 153^3 - \frac{1}{12} \times 80 \times 150^3$$

$$= 2.273 \times 10^6 \text{ mm}^4 (5.46 \text{ in}^4)$$

Accordingly, the moments of inertia of areas to the welds for the support plates are calculated as:

$$I_P = 8.903 \times 10^5 + 2.273 \times 10^6$$

$$= 3.163 \times 10^6 \text{ mm}^4 (7.60 \text{ in}^4)$$

The overall cross-section, A, of welds of the support plate is:

$$A = (153 \times 83) - (150 \times 80)$$

$$= 699 \text{ mm}^2 (1.08 \text{ in}^2)$$

The shearing stress, $S_{d,}$ on the welds of the support plate for the sling fitting is calculated by a similar equation as the welds of the sling fitting.

$$S_d = \frac{2.809 \times 10^3 \times 3}{699} = 12.1 \text{ MPa (1,760 psi)}$$

In addition, the stress, $S_{m,}$ on the welds of the support plate due to the bending moment is calculated as:

Where:

$$r = \sqrt{75^2 + 40^2} = 85 \text{ mm (3.35 in)}$$

$$S_m = \frac{5.9 \times 10^4 \times 85 \times 3}{3.163 \times 10^6} = 4.76 \text{ MPa (690 psi)}$$

Accordingly, the composite shearing stress S on the welds of support plate is calculated as:

$$S = \sqrt{S_d^2 + S_m^2 + 2S_d S_m \cos\theta}$$

Where:

$$\text{Cos } \theta = 40/85$$

$$S = \sqrt{12.1^2 + 4.76^2 + \left(2 \times 12.1 \times 4.76 \times (40/85)\right)}$$

$$= 14.9 \text{ MPa (2,160 psi)}$$

Meanwhile, the allowable shearing stress for 300 series stainless steel is 110.8 MPa (16,073 psi). Then the margin of safety (MS) is:

$$MS = \frac{110.8}{14.9} - 1 = 6.4$$

Therefore, the support plate welds are capable of carrying three times the normal load and no yielding.

As indicated by the margins of safety calculated for each component, the hook bar has the lowest margin; therefore in case of an overload the hook bar will fail prior to any other component. This ensures that, at failure, the rest of the packaging is capable of performing its function of protecting the fuel.

2.4.1.2 Package Lifting Using the Outer Container Lid Lifting Lugs

The outer container lid is lifted by four (4) ∅8-mm (∅0.315 in.) Type 304 stainless steel bars that are welded to the 50 × 50 × 4 stainless steel lid flange angle. Under a potential excessive loading condition, such as lifting the entire loaded package, these four lifting lugs are required to fail prior to damaging the outer container lid structure.

The outer container lid is also equipped with the four (4) ∅6-mm (∅0.236 in.) Type 304 stainless steel bar handles, which may be used to manually lift the lid. These bars are welded to the vertical leg of the lid flange angle with single-sided flare-bevel welds for an approximate length of 13 mm, as shown in View G-G on General Arrangement Drawing 105E3743. Since the handles have smaller cross-section (∅6-mm vs. ∅8-mm), and have smaller and shorter attachment welds, the analysis of the lid lifting bars bounds the handles.

The four lifting bars will be used for this analysis with an assumed lifting angle of 45 degrees. From Table 2-1, the RAJ-II package weighs 1,614 kg [15,827 N] (3,558 lbs). For the assumed lifting arrangement, the maximum load on the bar is:

$$F = 1/4\left[\frac{15{,}827}{\sin 45^\circ}\right] = 5{,}596 \text{ N } (1{,}258 \text{ lbs})$$

Assuming that the lift point is centered above the midpoint of the package (located 1,025 mm longitudinally and 318 mm laterally from lifting bar), the resultant forces on the lifting bar will be:

$$F_{horizontal} = F_{vertical} = F\cos 45^\circ = 3{,}957 \text{ N } (890 \text{ lbs})$$

$$F_{//} = F_{horizontal}\sin\left(\tan^{-1}\left(\frac{1{,}025}{318}\right)\right) = 3{,}779 \text{ N } (850 \text{ lbs})$$

$$F_{\perp} = F_{horizontal}\cos\left(\tan^{-1}\left(\frac{1{,}025}{318}\right)\right) = 1{,}173 \text{ N } (264 \text{ lbs})$$

where: $F_{horizontal}$ = Force in horizontal plane
$F_{//}$ = Force parallel to longitudinal axis of package
$F_{\perp}$ = Force perpendicular to longitudinal axis of package

These reaction loads will develop both bending and shear stresses in the bar, shear stresses in the attachment welds, and tensile stresses in the flange angle. Each of these stress components will be analyzed separately.

Bending of Bar

The maximum reaction load on the lifting bar will be bending stresses in the bar. Treating the bar as a fixed-fixed beam, the maximum bending stress, σ_b, will be:

$$\sigma_b = \frac{M_{max}}{Z_{bar}}$$

where: $M_{max} = 1/8[(F_{vertical})^2 + (F_{//})^2]^{1/2}(l) = 1/8(5{,}472)(76) = 51{,}984$ N-mm (460 lb_f-in)
$Z_{bar} = \pi(d^3)/32 = \pi(8^3)/32 = 50.3$ mm^3 (0.003 in^3)
$l = 2(46\text{-}8) = 76$ mm (2.99 in) [assumed equal to bent free length of bar]

Substituting these values results in a maximum bending stress of 1,033 MPa (149,824 psi). The allowable bending stress for the Type 304 material is equal to S_y = 184.7 MPa (26,788 psi). Therefore, the margin of safety against yielding in bending is:

$$MS = \frac{184.7}{1{,}033} - 1.0 = -0.8$$

Shear of Bar

The maximum reaction load on the lifting bar will result in shear stresses in the bar. For the shearing the bar, the maximum shear stress will be:

$$\tau_{bar} = \frac{[(F_{vertical})^2 + (F_{//})^2]^{1/2}}{\text{Area}} = \frac{5{,}472}{(\pi/4)(8)^2} = 108.9 \text{ MPa (15,795 psi)}$$

The allowable shear stress for the Type 304 material is equal to $0.6S_y = 0.6(184.7) = 110.8$ MPa (16,070 psi). Therefore, the margin of safety against yielding in shear is:

$$MS = \frac{110.8}{108.9} - 1.0 = +0.02$$

Tension in Bar

Since the bending stress is well beyond the yield strength, the bar will bend until the reaction load will be reacted as pure tension in the bar. For this condition, the tensile stress, $\sigma_{t\text{-}bar}$, in the bar will be:

$$\sigma_{t\text{-}bar} = \frac{F}{2(\text{Area})} = \frac{5{,}596}{2[(\pi/4)(8^2)]} = 55.7 \text{ MPa (8,079 psi)}$$

The allowable tensile stress for the Type 304 material is equal to the minimum yield strength, 184.7 MPa (26,788 psi). The margin of safety for this condition is then:

$$MS = \frac{184.7}{55.7} - 1.0 = +2.3$$

Attachment Welds

As shown in View F-F on General Arrangement Drawing 105E3743, the lifting bars are welded to the lid flange angle with double-sided flare-bevel welds for an approximate length of 28 mm (1.10 in.) on each leg of the bar. The ends of the bar are welded with a seal fillet weld, which has minimal strength and hence, will be ignored. Since the bar is relatively small, the flare-bevel weld will be treated as an equivalent fillet weld with a 4-mm leg. For this assumption, the maximum primary shear stress, τ_{weld}, in the weld will be:

$$\tau_{weld} = \frac{[(F_{vertical})^2 + (F_{//})^2]^{1/2}}{\text{Shear area of welds}} = \frac{5{,}472}{4(4\cos 45^\circ)(28)} = 17.3 \text{ MPa (2,509 psi)}$$

Due to the off-set, there will also be a secondary (torsion) shear stress, τ'_{weld}, component:

$$\tau'_{weld} = \frac{Mr}{J}$$

where: M = applied moment to weld group
= $[(F_{vertical})^2 + (F_{//})^2]^{1/2}$(distance from centroid + bend radius + ½bar diameter)
= 5,472(14 + 8 + 4) = 142,272 N-mm (1,259 lb_f - in)
r_{max} = distance from centroid of weld group to farthest point in weld
= $[(1/2(46\text{-}8))^2 + (14)^2]^{1/2}$ = 23.6 mm (0.929 in)
J = second polar moment of inertia of weld group, mm^4

Since the four flare-bevel welds are the same size and location, the second polar moment of inertia for the weld group is determined treating the welds as a line[a]. For this case, the second polar moment of inertia is:

$$J = 0.707(h)\frac{d(3b^2 + d^2)}{6}$$

where: h = leg length of weld = 4 mm
d = length of weld = 28 mm
b = distance between weld groups = $(46^2 + 46^2)^{1/2}$ = 65.1 mm

Substituting these values results in a secondary polar moment of inertia of 178,138 mm^4 (0.428 in^4). The secondary shear stress then becomes:

$$\tau'_{weld} = \frac{(142,272)(23.6)}{178,138} = 18.8\text{MPa (2,727 psi)}$$

The total shear stress in the weld is then the square root of the sum of the squares of the primary shear and secondary shear:

$$\tau_{total} = \left[(\tau_{weld})^2 + (\tau'_{weld})^2\right]^{\frac{1}{2}} = 25.5\text{ MPa (3,698 psi)}$$

The allowable shear stress for the Type 304 material is equal to 110.8 MPa (16,070 psi). Therefore, the margin of safety against yielding in shear for the welds is:

$$MS = \frac{110.8}{25.5} - 1.0 = +3.3$$

Shear Tearout of Base Metal

Shear tearout of the 4-mm thick base metal is evaluated by conservatively considering only the area of a section equal to the weld length of the two welds. The 2-mm thick sheet that is attached to the vertical leg of the flange angle is ignored for this calculation. The total tensile area, A_t, will be:

$$A_{shear} = 2[4(28)] = 224\text{ mm}^2\ (0.347\text{ in}^2)$$

For this case, the shear stress of the base metal, $\tau_{base\ metal}$, is:

[a]Shigley, Joseph E., and Mischke, Charles R., *Mechanical Engineering Design, Fifth Edition*, McGraw-Hill, Inc., 1989.

$$\tau_{\text{base metal}} = \frac{F}{A_{\text{shear}}} = \frac{5{,}596}{224} = 25.0 \text{ MPa } (3{,}624 \text{ psi})$$

The allowable shear stress for the Type 304 material is equal to 110.8 MPa (16,070 psi). The margin of safety for this condition is then:

$$MS = \frac{110.8}{25.0} - 1.0 = +3.4$$

Summary

As demonstrated by these calculations, the minimum margin of safety for the outer container lid lifting lugs is -0.8, which results in failure of the bar in bending for lifting the complete loaded package. The largest positive margin of safety (+3.4) occurs in the base metal of the lid flange angle, which demonstrates that the outer container lid structure would not fail in an excessive load condition. All other margins of safety in the load path are positive, but are lower than the base metal. Therefore, potentially lifting the complete package by these lid lifting lugs will fail the lifting bar and have no detrimental affect on the effectiveness of the RAJ-II package.

2.4.2 Tie-Down Devices

There are no tie-down features that are a structural part of the RAJ-II package. The packages are transported either in container vans or on flatbed trucks. When transported in container vans, blocking and bracing is provided that distributes any loads into the packages. This bracing and blocking is customized to address individual shipping configurations and the specific container van being used. When transported on a flatbed trailer, straps going over the package are used to secure it to the trailer. Therefore, the requirements of 10 CFR 71.45(b) are satisfied since no structural part of the package is used as a tie-down device.

An evaluation is performed on the ability of the package to withstand loadings of 2g vertical and 5 g laterally when restrained by strapping. The worst case loading situation for the packages is when they are stacked in groups of 9 on a flatbed trailer and secured with a minimum of 3 straps. Although the packages may be shipped in other configurations such as 2x3 the greatest strap loading that would be applied to the package when secured in a 3x3 configuration. Between each adjacent column of packages 2 × 4 wood shoring may be placed where the straps will be applied. The evaluation below is conservatively performed without the 2 × 4 shoring in place.

As a bounding evaluation, it is assumed that the outside corners of the top outside packages carry all the vertical loads that would result from the vertical acceleration and the vertical load required to resist the over-turning moment from the horizontal acceleration. The corners of all top packages would actually carry the vertical load. See Figure 2-11.

For modeling purposes, the matrix of nine packages is treated as a rigid body. By summing moments, the vertical force required to prevent the over-turning of the stack by the horizontal loads is determined. This load is conservatively applied to one edge of one container

The key dimensions and weights for each package are:

Width	w = 720 mm (28.3in)
Total Height	h = 742 mm (29.2in)

CG height	cgy = 421 mm (16.6 in)
Mass of each package	m = 1,614 kg (3,558 lb)
Gravitational acceleration	g = 9.81 m/sec^2
Vertical acceleration factor	g_v =2
Horizontal acceleration factor	g_h =5

The vertical center of gravity of the 9-package matrix is:

$$CGy = 3mg(2h + cgy)/9mg + 3mg(h + cgy)/9mg + 3mg(cgy)/9mg = 1.163 \times 10^3 \text{ mm (45.8 in)}$$

Summing the forces in the vertical direction due to the 2 g loading, the strap load applied at the two locations can be determined for this load condition.

$$R_{st} = 9\ gv\ m\ g/2 = 1.425 \times 10^5 \text{ N } (3.202 \times 10^4 \text{ lb}_f)$$

Summing moments about one of the bottom corners of the stack will determine the strap force required to resist overturning due to the horizontal loading.

$$R_s = \frac{(gh(CG_y)9mg)}{(3w)} = 3.835 \times 10^5 \text{ N } (8.621 \times 10^4 \text{ lb}_f)$$

Total vertical strap load is:

$$R_t = R_{st} + R_s = 5.260 \times 10^5 \text{ N } (1.182 \times 10^5 \text{ lb}_f)$$

Checking the support plate carrying capability:

There are eight (8) 5mm × 55mm support plates in groups of two (2) that carry the vibro-isolation frame inside the outer container. These are skipped welded to the wall, plus have two thick (10 and 15 mm) by 80 mm and 70 mm wide plates welded between them. These plates are in addition to the body straps and the body struts (angles) in corners that provide vertical stiffening to the side panels. On top of the side panel, there are two angles that make up the flange in both the body and the lid that provide load distribution capability to the side wall and the internal structure. In addition these angles are stiffen at the ends by the bolster support angle that further distributes the end strap loads to the end structure of the package reducing load in the sides of the package.

Since the eight support plates are assembled together in groups of two with the reinforcement plates connecting the plates along with the welding to the wall, each two-plate section is considered as a column that is capable of carrying the tie-down loads. Addressing the support plates as a channel section, which is 140 mm wide and 57 mm deep, its properties can be determined.

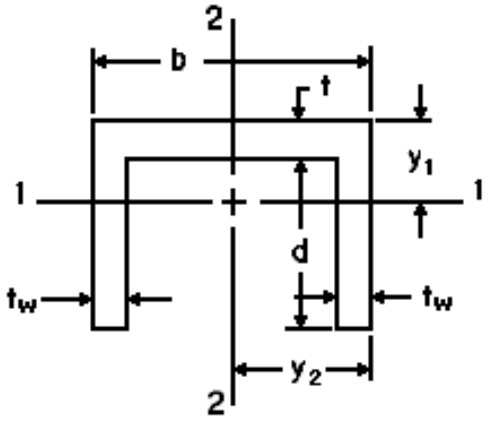

Channel section

Length of web $b = 140$ mm (5.5 in)

Length of flange $d = 55$mm (2.2 in)

Web thickness $t = 2$ mm (0.08 in)

Flange thickness $t_w = 5$ mm (0.2 in)

Area $A = t_b + 2t_w d = 830.3$ mm^2 (1.287 in^2)

Since there are four of these assemblies to a side the total area is:

$$A_{spt} = 4A = 3{,}321 \text{ mm}^2 \ (5.148 \text{ in}^2)$$

The compressive stress is:

$$\sigma_c = R_t/A_{spt} = 158.4 \text{ MPa } (23.0 \text{ ksi})$$

This is less than the yield stress of the Type 304 stainless steel $S_y = 206.8$ MPa (30.0 ksi)

The resistance of the plate to buckling is also evaluated. The equation to obtain the moments of inertia of area of the support plate which are subject to buckling is:

$$y_1 = (bt^2+2t_w d(2t+d))/2(tb+2t_w d) = 19.9 \text{ mm } (0.783 \text{ in})$$

$$y_2 = b/2 = 70 \text{ mm } (2.756 \text{ in})$$

Moments of Inertia

$$I_1 = b(d+t)^3/3 + d^3(b-2t_w)/3 - A(d+t-y_1)^2 = 2.894 \times 10^5 \text{mm}^4 \ (0.695 \text{ in}^4)$$

$$I_2 = (d+t)b^3/12 - d(b-2t_w)^3/12 = 2.110 \times 10^7 \text{ mm}^4 \ (7.122 \text{ in}^4)$$

The radius of gyration can than be calculated for each axis:

$$r_1 = \sqrt{\frac{I_1}{A}} = 18.7 \text{ mm } (0.736 \text{ in}) \qquad r_2 = \sqrt{\frac{I_2}{A}} = 59.7 \text{ mm } (2.35 \text{ in})$$

The minimum radius of gyration indicates the weakest orientation for buckling:

$$k = r_1 = 18.7 \text{ mm } (0.736 \text{ in})$$

ℓ: Length of support plate = 160 mm (6.3 in)

Also, the slenderness ratio, $\frac{l}{k}$, is:

$$\frac{l}{k} = \frac{160}{18.7} = 8.6$$

As the ends are fixed, the coefficient "n" becomes 4, so the limit value of the slenderness ratio becomes:

$$85\sqrt{n} = 85\sqrt{4} = 170$$

Because the slenderness ratio of this material is less than the limit value slenderness ratio, Euler's equation is not applicable, and the secant formula for buckling is used. The equation to obtain the support plate's buckling strength is:

$$\frac{P}{A} = \frac{S_y}{1 + \frac{ec}{k^2}\sec\left[\frac{C\ell}{2k}\sqrt{\frac{P}{AE}}\right]}$$

Where: P: Buckling strength (load) of support column N

A: Area of column = 830.3 mm^2 (1.287 in^2)

S_y: Minimum yield strength of Type 304 stainless steel = 206.8 MPa (30.0 ksi)

C: Coefficient to the long support fixed at both ends = 1.2

E: Elastic modulus of Type 304 stainless steel = 1.95×10^5 MPa (Table 2-2 at 40°C)

e: Eccentricity small since the strap load is centered = 5 mm (0.2 in)

ℓ: Unsupported length of the support column = 160 mm (6.3 in)

c: Shortest distance to an outside side edge from the centroid = 19.9 mm (0.783 in)

Substituting these values in the above equation and solving for P iteratively results in a buckling strength of the support plate column of:

$$P = 1.332 \times 10^5 \text{ N } (29{,}945 \text{ lb}_f)$$

There are four support columns to a side, which results in the sidewall frame having a minimum capacity of:

$$P_t = 4P = 5.328 \times 10^5 \text{ N } (119{,}780 \text{ lb}_f)$$

Since this load capacity is greater than the applied load ($R_t = 5.259 \times 10^5$ N (1.182×10^5 lb_f)), the supports will not buckle when the worst case tie-down loads are applied to a package. This capacity approaches the force required to yield the columns in compression (i.e., $A_{spt}S_y = 6.868 \times 10^5$ N (1.544×10^5 lb_f).

By considering the stiffening of the support plates with the reinforcement plates used to carry the inner support frame, it has been demonstrated that the support plates have sufficient capacity to react the tie-down load if the package experiences a 5 g lateral and a 2g vertical loading

simultaneously. This evaluation does not take into consideration the large carrying capability of the ends of the package where there are corner angles, end plates, and wood overlay plates that further strengthen the package's buckling capability. The use of three or more straps ensures that the load is distributed along the package so that the load can be reacted by the support plates and other internal structure. The stiffness of the OC lid, when the bolster support angles are considered with the reinforced edge of the OC body, ensures that the load is distributed to the internal structure of the package.

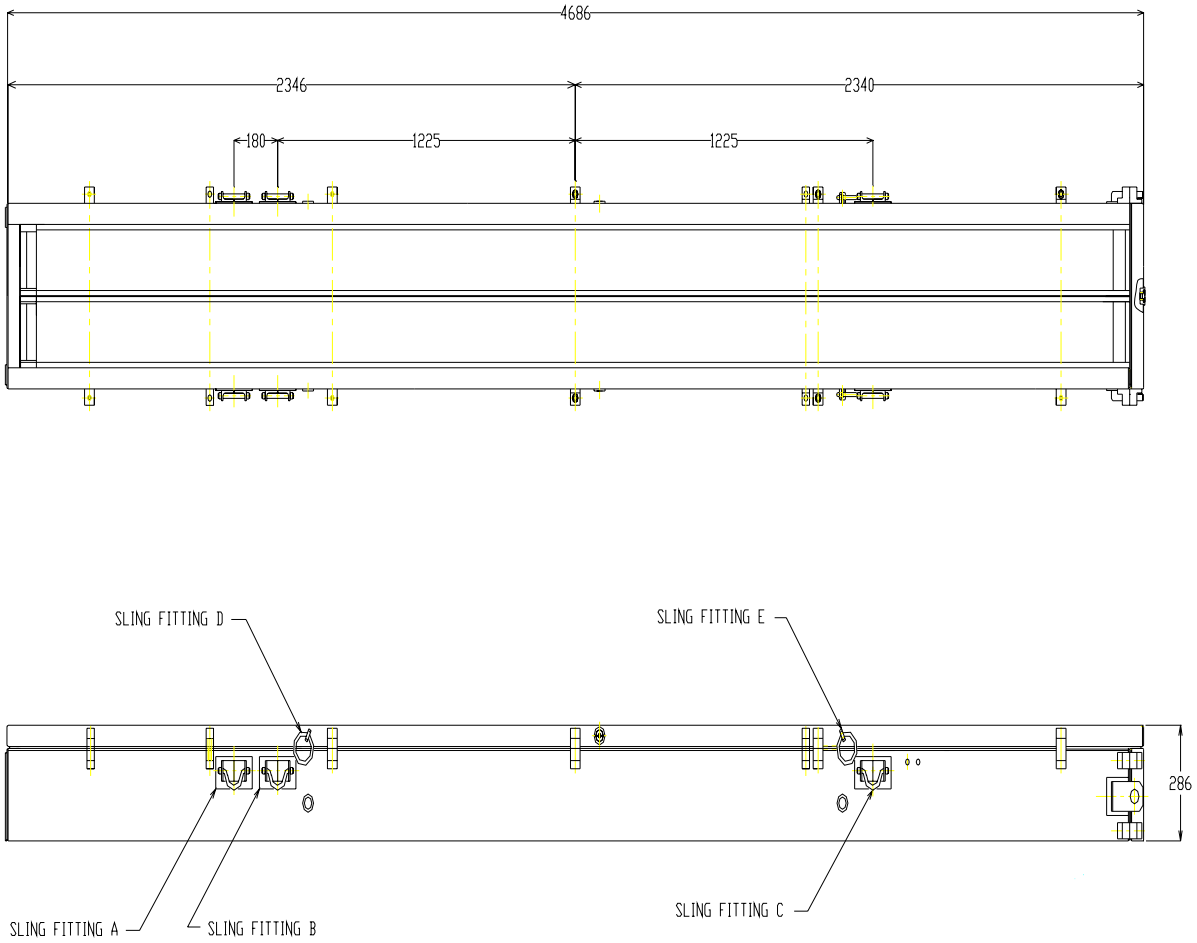

(unit: mm)

Combination of sling fitting	Used for
A and C	Lifting a Loaded Container
B and C	Lifting an Empty Container
D and E	Lifting a Lid

Figure 2-2 Inner Container Sling Locations

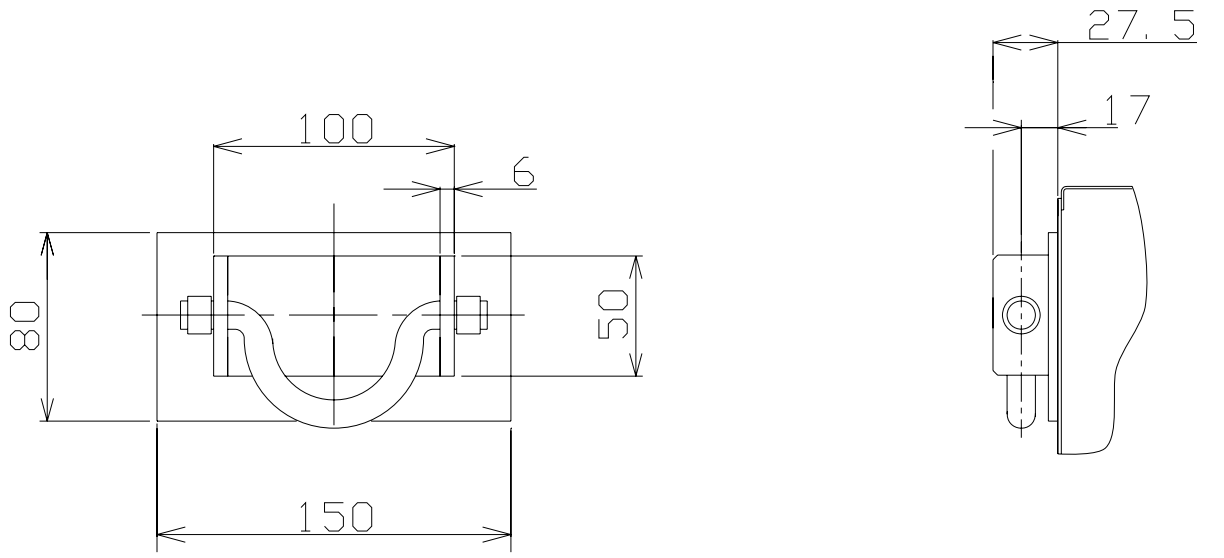

(unit: mm)

Figure 2-3 Sling Attachment Plate Details

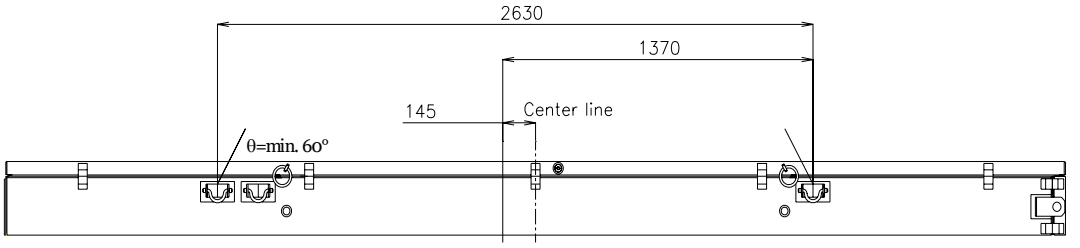

(unit: mm)

Figure 2-4 Lifting Configuration of Inner Container

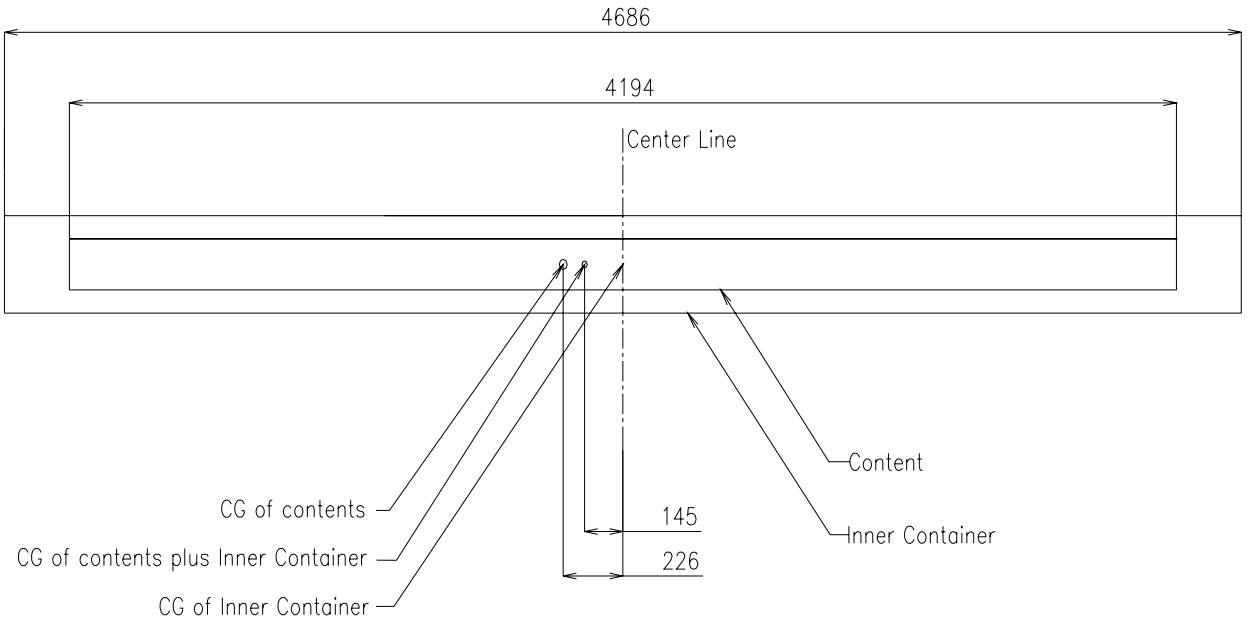

(unit: mm)

Figure 2-5 Center of Gravity of Loaded Inner Container

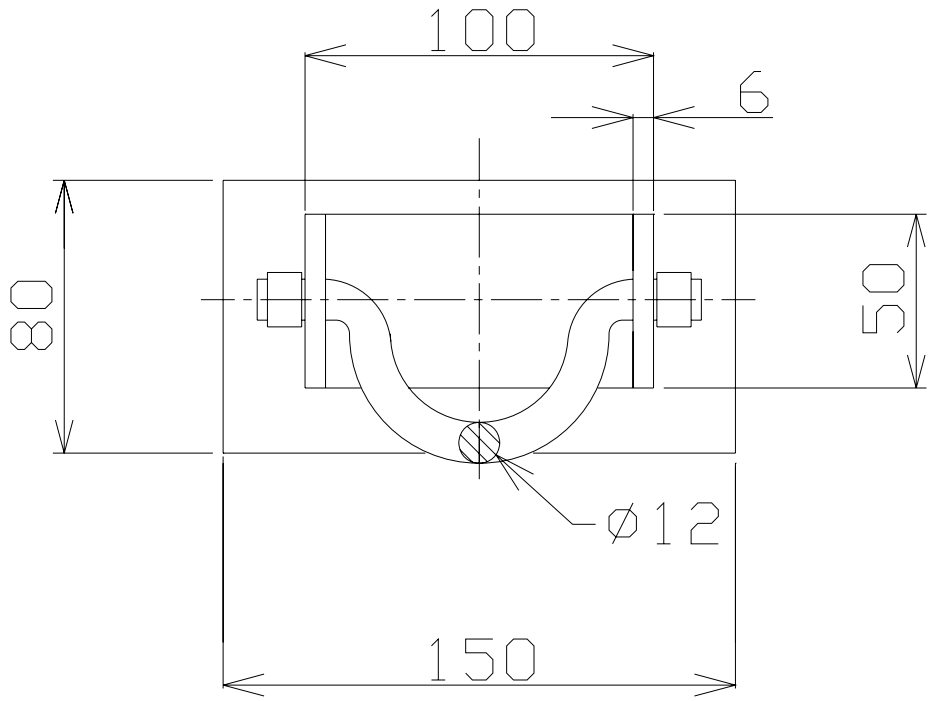

(unit: mm)

Figure 2-6 Hooking Bar of Sling Fitting

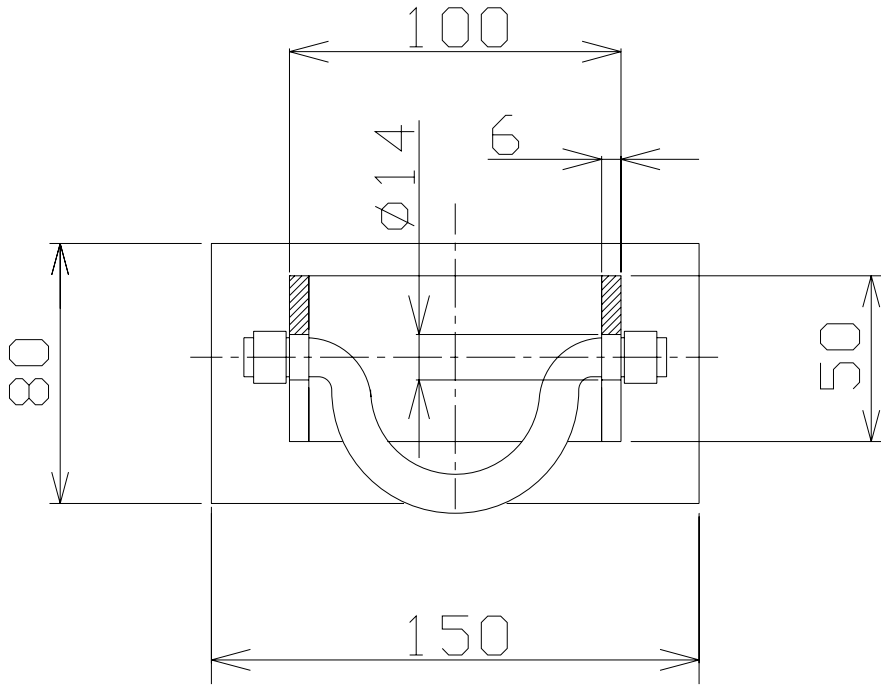

(unit: mm)

Figure 2-7 Perforated Plate of Sling Fitting

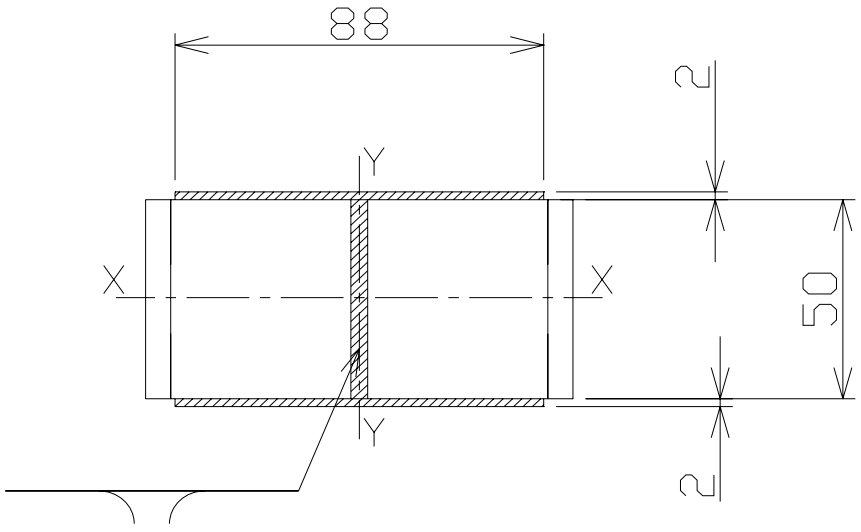

(unit: mm)

Figure 2-8 Sling Fitting Weld Geometry for Attachment to Support Plate

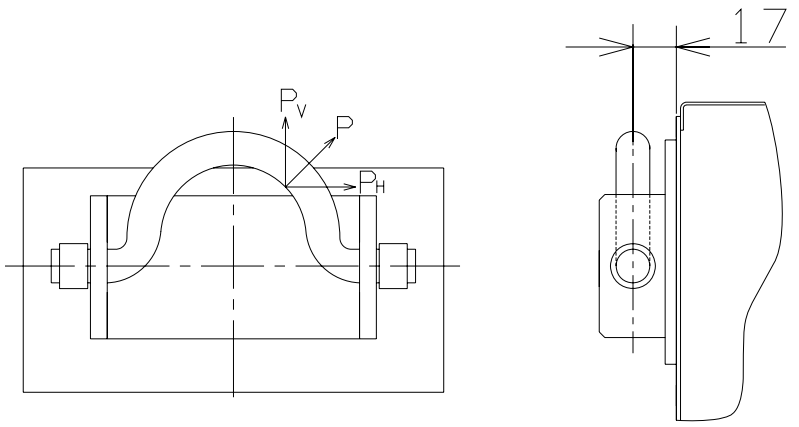

(unit: mm)

Figure 2-9 Loads on Sling Fitting

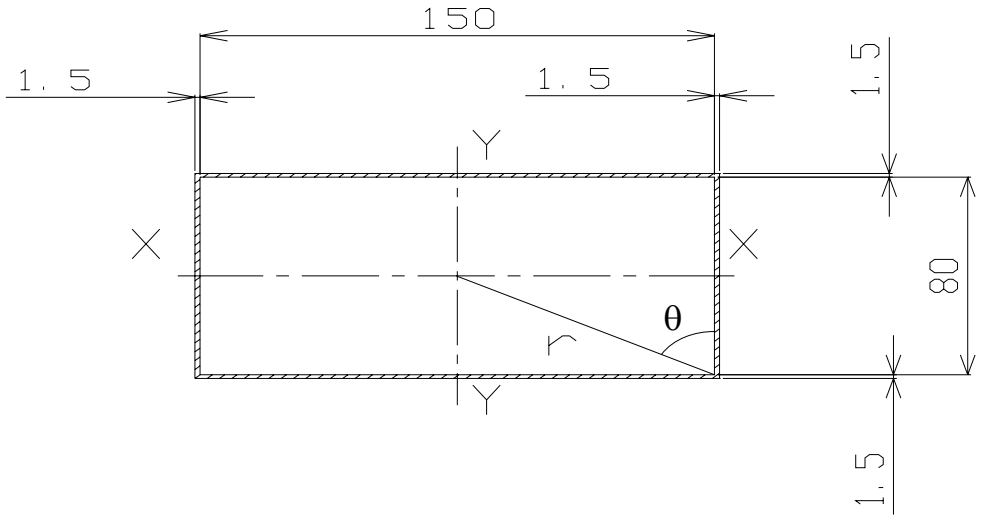

(unit: mm)

Figure 2-10 Welds for Support Plate Attachment to Body

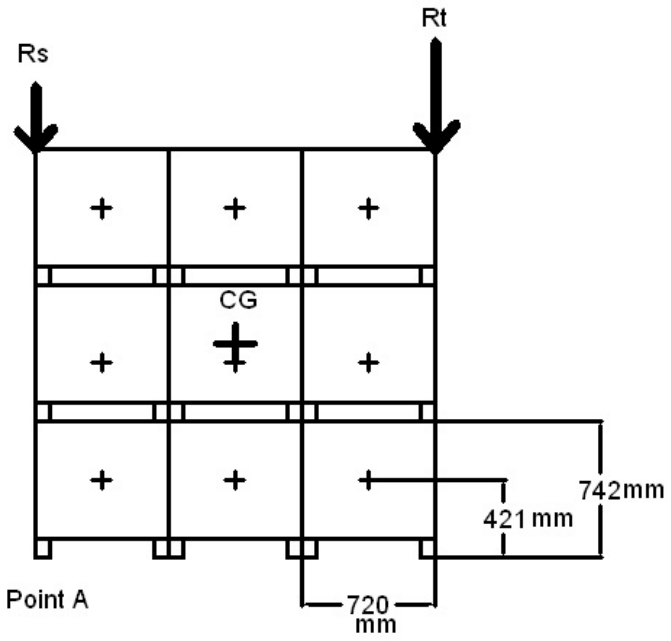

Figure 2-11 Tie-Down Configuration

2.5 GENERAL CONSIDERATIONS

2.5.1 Evaluation by Test

The primary means of demonstrating that the package meets the regulatory accident conditions was by test. The package was tested full-scale by dropping four full-scale certification test units (CTUs) from 9 meters in different orientations. (Two of the test units were dropped as part of the Japanese certification process.) The weight of the units was maximized to provide bounding conditions.

Within the GNF-A CTUs, the fuel was mocked up by a metal boxed section that provided the representative weight in one fuel assembly shipping location. The steel section was segmented to prevent the mockup from adding unrealistic stiffness to the package. In the other fuel assembly shipping position a mock up fuel assembly was used. This had the same cross-sectional properties of the actual fuel. The rods were filled with lead to represent the actual fuel. Weights were added along side of the assembly to provide the correct mass for fuel that may be shipped with channels as well as allowing for the different density between the lead and the uranium oxide pellets.

The units tested in Japan had a simulated 8X8 fuel assembly and weights representing the other fuel assembly in each test unit. The weight and dimensions of the mockup fuel approximated the weight of the fuel to be shipped in the container.

Details of the prototypes used in the drop testing can be found in Section 2.7 and Appendices 2.12.1 and 2.12.2.

The damage caused by the test was evaluated in each of the affected sections, Section 3.0, Section 4.0, and Section 6.0. Both the inner and outer lids stayed in place, although damaged. The inner container holding frame deformed but restrained the inner container. Due to the end drop there was some plastic deformation of the fuel but well within the limits of the criticality evaluation. After the testing, the GNF-A fuel rods passed a helium leakage rate test demonstrating containment.

2.5.2 Evaluation by Analysis

The normal conditions of transport were evaluated by analysis and by comparison to the accident testing. The primary analysis was done for the compression loading. The material properties are taken from Table 2 - 4, which is based on published ASME properties. A static analysis was performed in Section 2.6.9 Compression.

Since the normal condition pressure and temperatures are well below the design conditions for the fuel cladding no separate analysis was performed.

2.6 NORMAL CONDITIONS OF TRANSPORT

The RAJ-II package, when subjected to the Normal Conditions of Transport (NCT) specified in 10 CFR 71.71, is shown to meet the performance requirements specified in Subpart E of 10 CFR 71. As discussed in the introduction to this chapter, with the exception of the NCT free drop, the primary proof of NCT performance is via analytic methods. Regulatory Guide 7.6 criteria are demonstrated as acceptable for NCT analytic evaluations presented in this section. Specific discussions regarding brittle fracture and fatigue are presented in Sections 2.1.2.4 and 2.6.5 and are shown not to be limiting cases for the RAJ-II package design. The ability of the welded containment fuel rod cladding to remain leak-tight is documented in Section 4.0.

Properties of Type 304 stainless steel as representative of those properties for 300 series stainless steel are summarized below.

Table 2 - 5 Material Properties

Material Property	Material Property Value (psi)			Reference
	-40 ºC (-40 ºF)	21ºC (70 ºF)	75ºC (167ºF)	
	Type 304 Stainless Steel			
Elastic Modulus, E	198.6GPa (28.8×10^6psi)	195.1GPa (28.3×10^6psi)	191.7GPa (27.8×10^6psi)	Table 2 - 2
Design Stress Intensity, S_m	137.9MPa (20,000 psi)	137.9MPa (20,000 psi)	137.9MPa (20,000 psi)	
Yield Strength, S_m	206.8MPa (30,000psi)	206.8MPa (30,000psi)	184.7MPa (26,788psi)	
Tensile Strength	517.1MPa (75,000psi)	517.1MPa (75,000psi)	498.6MPa (72,300)	

The RAJ-II package's ability to survive HAC, 30-foot free drop, 40-inch puncture drop, and 30-minute thermal event also demonstrated the packages ability to also survive the NCT. Evaluations are performed, when appropriate, to supplement or expand on the available test results. This combination of analytic and test structural evaluations provides an initial configuration for NCT thermal, shielding and criticality performance. In accordance with 10 CFR 71.43(f), the evaluations performed herein successfully demonstrate that under NCT tests the RAJ-II package experiences "no substantial reduction in the effectiveness of the packaging". Summaries of the more significant aspects of the full-scale free drop testing are included in Section 2.6.7, with details presented in Appendix 2.12.1.

2.6.1 Heat

The NCT thermal analyses presented in Section 3.0, consist of exposing the RAJ -II package to direct sunlight and 100 ºF still air per the requirements of 10 CFR 71.71(b). Since there is negligible decay heat in the unirradiated fuel, the entire heating came from the solar insolation. The maximum temperature of 77°C (171°F) was located on the lid of the outer container.

2.6.1.1 Summary of Pressures and Temperatures

The fuel assembly exhibits negligible decay heat. The RAJ-II package and internal components, when loaded with the required 10 CFR 71.71(c) (1) insulation conditions, develop a maximum temperature of 77 ºC (171 ºF). The resulting pressure at the maximum temperature is 1.33 MPa (192.9 psia).

2.6.1.2 Differential Thermal Expansion

With NCT temperatures throughout the packaging being relatively uniform (i.e. no significant temperature gradients), the concern with differential expansions is limited to regions of the RAJ-II packaging that employ adjacent materials with sufficiently different coefficients of thermal expansion. The IC is a double-walled, composite construction of alumina silicate thermal insulator between inner and outer walls of stainless steel. The alumina silicate thermal insulator is loosely packed between the two walls and does not stress the walls. Differential thermal expansion stresses are negligible in the OC for three reasons: 1) the temperature distribution throughout the entire OC is relatively uniform, 2) the OC is fabricated from only one type of structural material, and 3) the OC is not radially or axially constrained within a tight-fitting structure due to the relatively low temperature differentials and lack of internal restraint within the RAJ-II package.

The cladding of the fuel which serves as containment is not stressed due to differential thermal expansion since a gap remains between the fuel pellet and the cladding at both the cold temperature -40°C and the highest temperature the fuel could see due to the HAC which is 800°C. This is demonstrated as follows:

The nominal fuel pellet and cladding dimensions and the resulting radial gap (0.00335 inches) is shown below based on a temperature of 20°C:

As-Built Dimensions (inches)		
Nominal Clad OD	D_{co}	0.3957
Nominal Clad ID	D_{ci}	0.348
Nominal Pellet OD	D_{fo}	0.3413
Nominal Radial Pellet/Clad Gap	g_n	0.00335

The strain due to thermal expansion or contraction in the Zr cladding is equal to[a]:

$$\left(\frac{\Delta D}{D}\right)_{clad} = 7.4\times10^{-6}(\Delta T)$$

Where ΔT is positive for an increase in temperature and negative for a decrease in temperature.

The strain due to thermal expansion or contraction in the fuel pellet is equal to[b]:

$$\left(\frac{\Delta D}{D}\right)_{fuel} = -3.28\times10^{-3} + 1.179\times10^{-5}T - 2.429\times10^{-9}T^2 + 1.219\times10^{-12}T^3$$

Where T is the absolute final temperature in degrees Kelvin (K).

The following table summarizes the thermal strain and the thermal growth in the cladding and pellets with a temperature change from 20°C to -40°C $(\Delta T = -60^{\circ}C, T = 233K)$. All dimensions are expressed in inches.

Table 2 - 6 Thermal Contraction at -40°C

	Strain at -40°C $\left(\frac{\Delta D}{D}\right)$	**Thermal Expansion at -40°C** $\left(\frac{\Delta D}{D}\right)D$	**Dimension at -40°C** $D+\left(\frac{\Delta D}{D}\right)D$
Pellet OD	-6.49 x 10^{-4}	-2.22 x 10^{-4}	0.3411
Cladding ID	-4.44 x 10^{-4}	-1.55 x 10^{-4}	0.3478

This results in a radial gap at -40°C of:

[a] Framatome ANP MOX Material Properties Manual 51-5010288-03

[b] Framatome ANP MOX Material Properties Manual 51-5010288-02

$$g_{-40} = \frac{0.3478 - 0.3411}{2} = 0.0034 \cdot in$$

The following table summarizes the thermal strain and the thermal growth in the cladding and pellets with a temperature change from 20°C to 800°C $(\Delta T = 780^{\circ} C, T = 1,073K)$. All dimensions are expressed in inches.

Table 2 - 7 Thermal Expansion at 800°C

	Strain at 800°C $\left(\frac{\Delta D}{D}\right)$	**Thermal Expansion at 800°C** $\left(\frac{\Delta D}{D}\right)D$	**Dimension at 800°C** $D+\left(\frac{\Delta D}{D}\right)D$
Pellet OD	8.08 x 10^{-3}	2.76 x 10^{-3}	0.3441
Clading ID	5.77 x 10^{-3}	2.01 x 10^{-3}	0.3500

This results in a radial gap at 800°C of:

$$g_{800} = \frac{0.3500 - 0.3441}{2} = 0.0030 \cdot in$$

2.6.1.3 Stress Calculations

Since the temperatures and pressures generated under normal conditions of transport are well below the design conditions for the boiling water reactor fuel no specific calculations were performed for the fuel containment.

2.6.1.4 Comparison with Allowable Stresses

The normal conditions of transport conditions are well below the operating conditions of the fuel no comparison to allowable stresses was performed.

2.6.2 Cold

The NCT cold condition consists of exposing the RAJ-II packaging to a steady-state ambient temperature of -40 ºF. Insulation and payload internal decay heat are assumed to be zero. These conditions will result in a uniform temperature throughout the package of -40 F. With no internal heat load (i.e., no contents to produce heat), the net pressure differential will only be reduced from the initial conditions at loading.

For the containment, the principal structural concern due to the NCT cold condition is the effect of the differential expansion of the fuel to the zirconium alloy tube. During the cool-down from 20 ºC to -40 ºC, the tube could shrink onto the fuel because of difference in the thermal expansion coefficient. However, the clearance between the fuel and the cladding is such that even if the fuel did not shrink, there would still be clearance. Differential thermal expansion stresses are negligible in the package for three reasons: 1) the temperature distribution

throughout the entire package is relatively uniform, 2) the package is fabricated from only one type of structural material, and 3) the package is not radially or axially constrained.

Brittle fracture at -40 ºF is addressed in Section 2.1.2.4.1.

2.6.3 Reduced External Pressure

The effect of a reduced external pressure of 25 kPa (3.5 psia) per 10 CFR 71.71(c)(3) is negligible for the RAJ-II packaging. The RAJ-II package contains no pressure-tight seal and therefore cannot develop differential pressure. Therefore, the reduced external pressure requirement of 3.5 psia delineated in 10 CFR 71.71(c)(3) will have no effect on the package. Compared with the 1.115 MPa (161.7 psia) internal pressure in the fuel rods, a reduced external pressure of 3.5 psia will have a negligible effect on the fuel rods.

2.6.4 Increased External Pressure

The RAJ-II package contains no pressure-tight seal and, therefore, cannot develop differential pressure. Therefore, the increased external pressure requirement of 140 kPa (20 psia) delineated in 10 CFR 71.71(c)(4) will have no effect on the package. The pressure-tight cladding of the fuel rods is designed for much higher pressures in its normal service in a reactor and is not affected by the slight increase in external pressure.

The containment is provided by the cladding tubes of the fuel. These tubes, designed for the conditions in an operating reactor, have the capability of withstanding the increased external pressure. The failure mode of radial buckling is not a plausible failure mode since the fuel pellets would prevent any significant deformation due to external pressure.

2.6.5 Vibration

The RAJ-II packaging contains an internal shock mount system and, therefore, cannot develop significant vibratory stresses for the package's internal structures. Therefore, vibration normally incident to transportation, as delineated in 10 CFR 71.71(c)(5), will have a negligible effect on the package. Due to concerns of possibly damaging the fuel so it cannot be installed in a reactor after transport, extreme care is taken in packaging the fuel using cushioning material and vibration isolation systems. These systems also ensure that the fuel containment boundary also remains uncompromised. The welded structure of the light weight RAJ-II package is unaffected by vibration. However, after each use the packaging is visually examined for any potential damage.

2.6.6 Water Spray

The materials of construction of the RAJ-II package are such that the water spray test identified in 10 CFR 71.71(c)(6) will have a negligible effect on the package.

2.6.7 Free Drop

Since the maximum gross weight of the RAJ-II package is 1,614 kg (3,558 lb), a 1.2 m or four-foot free drop is required per 10 CFR 71.71(c)(7). The Hypothetical Accident Condition (HAC), 9 m (30 foot) free drop test required in 10 CFR 71.73(c)(1) is substantially more damaging than the 1.2 m (4 foot) NCT free drop test. Section 2.7.1 demonstrates the RAJ-II package's survivability and bounds the free drop requirements of 10 CFR 71.71(c)(7). Due to the relatively fragile nature of the fuel assembly payload in maintaining its configuration for operational use, any event that would come close to approximating the NCT free drop would cause the package to be removed from service and re-examined prior to continued use.

As part of the effort to obtain package certification in Japan by GNF-J, certification testing of the package, which included both an end drop and a lid-down horizontal drop, was performed. In each case a 0.3-meter (1-foot) and a 1.2 meter (4-foot) drop was performed prior to the 9-meter (30-foot) drop. In both cases the RAJ-II was slightly damaged but the damage had no significant effect on the performance of the package in relation to either the containment or the ability of the package to meet the requirements of 10 CFR 71. The GNF-J certification testing is discussed in Appendix 2.12.2.

Therefore, the requirements of 10 CFR 71.71(c)(7) are met.

2.6.8 Corner Drop

This test does not apply, since the package weight is in excess of 100 kg (220 pounds), and the structural materials used in the RAJ-II are not primarily wood or fiberboard, as delineated in 10 CFR 71.71(c)(8).

2.6.9 Compression

Since the package weighs less than 5,000 kg (11,000 pounds), as delineated in 10 CFR 71.71(c)(9), the package must be able to support five times its weight without damage.

The load to be given as the test condition is the load (W_1) times five of the weight of this package or the load (W_2) which is obtained through multiplying the package's vertical projected area by 13 kPa, whichever is heavier. In the case of this package, the equations to obtain each load are:

$$W_1 = 5 \times m \times g$$

$$W_2 = 13 \text{ kPa} \times L \times B$$

Where:

m: Mass of package 1,614 kg (3,558 lb)

g: Gravitational acceleration 9.81 m/s^2

L: Length of package 5,068 mm (199.53 in)

B: Width of package 720 mm (28.35 in)

From this

$W_1 = 5 \times 1{,}614 \times 9.81 = 79.16$ kN (17,800 lbf)

$W_2 = 13 \times 10^{-3} \times 5{,}068 \times 720 = 47.4$ kN (10,660 lbf)

Therefore, as $W_1 > W_2$, the stacking load is assumed as W = 79.16 kN (17,800 lbf)

The stacking of these packages is as shown in Figure 2-12, so the outer container only sustains the stacking load. In this case, it is assumed that loads are carried by a total of eight support plates positioned in the center of the bolster out of sixteen support plates of the outer container body positioned at the lowest layer. This assumption makes the load sustaining area smaller, so the evaluation is conservative. The compressive load given to the support plate is the above-mentioned stacking load plus the weight of the outer container's lid.

The equation to obtain the support plate's compressive load is:

$W_c = W_1 + W_3$

W_c: Compressive load N

W_1: Stacking load 79.16 kN (17,800 lbf)

W_3: Load by the outer container's lid 1.34 kN (301 lbf)

m_F: Mass of outer container lid 137 kg (302 lb)

g: Gravitational acceleration 9.81m/s^2

From this, the 80.5 kN (18,100 lbf)

When the fuel assemblies are packed, the gravity center of the outer container is shifted longitudinally, so the load acting on the support plate, which is closer to the gravity center, becomes larger.

Therefore, the equation to obtain the vertical maximum load given to one support plate, which is closer to the gravity center, is:

$$P = \frac{W \cdot \ell_2}{4 \cdot \ell_0}$$

Where:

P: Maximum load acting on one support plate which is nearer to the gravity center — N

W: Compressive load given to the support plate (18,100 lbf) — 80.5 kN

ℓ_0: Longitudinal support plate space — 3,510 mm (138.2 in)

ℓ_2: Distance from the package's gravity center position to the support

$$\frac{3{,}510}{2} + 92 = 1{,}847 \text{ mm } (73.76 \text{ in})$$

From this, the maximum load P acted to one support plate, which is nearer to the gravity center, is:

$$P = \frac{80.5 \times 10^3 \times 1{,}847}{4 \times 3{,}510}$$
$$= 10.6 \times 10^3 \text{ N } (2{,}380 \text{ lbf})$$

The resistance of the plate to buckling is also evaluated. The equation to obtain the moment of inertia of area of the support plate which is subject to buckling is:

$$I_Z = \frac{1}{12} hb^3$$

Where:

I_Z: Moment of inertia of area of support plate — mm^4

b: Thickness of support plate — 5 mm (0.2 in)

h: Width of support plate — 55 mm (2.2 in)

From this, the moment of inertia of area, I_Z, of the support plate is:

$$I_Z = \frac{1}{12} \times 55 \times 5^3 = 572.9 \text{ mm}^4 (1.376\text{x}10^{-3} \text{ in}^4)$$

Also, the equation to obtain the radius of gyration of the area of the support plate is:

$$k = \sqrt{\frac{I_Z}{A}}$$

Where:

k: Radius of gyration of area of support plate — mm

I_Z: Moment of inertia of area of support plate — $572.9 \text{ mm}^4 (1.376\text{x}10^{-3} \text{ in}^4)$

A: Cross-sectional area of support plate — $5 \times 55 = 275 \text{ mm}^2 (0.426 \text{ in}^2)$

ℓ: Length of support plate — 559 mm (22.4 in)

From this, the radius of gyration of area k of the support plate is:

$$k = \sqrt{\frac{572.9}{275}} = 1.44 \text{ mm } (0.0568 \text{ in})$$

Also, the slenderness ratio $\frac{\ell}{k}$ is:

$$\frac{\ell}{k} = \frac{559}{1.44} = 388$$

As the ends are fixed, the coefficient n becomes 4, so the limit value of the slenderness ratio becomes as below.

$$85\sqrt{n} = 85\sqrt{4} = 170$$

Because the slenderness ratio of this material, 388, exceeds the limit value of slenderness, Euler's equation is used. The equation to obtain the support plate's buckling strength is:

$$P_k = \frac{n\pi^2 E I_Z}{\ell^2}$$

Where:

P_k: Buckling strength (load) of support plate — N

n: Coefficient to the long support fixed at both ends — 4

E: Longitudinal elasticity modulus of Gr304 stainless steel — 1.94×10^5 MPa (at 40°C)

I_Z: Moment of inertia of area of support plate — 572.9 mm^4 (1.376×10^{-3} in^4)

ℓ: Length of the support plate — 559 mm (22.4 in)

From this, the buckling strength P_k of the support plate is:

$$P_k = \frac{4 \times 3.14^2 \times 1.94 \times 10^5 \times 572.9}{559^2} = 14.0 \times 10^3 \text{N } (3{,}050\ )$$

Therefore, $P_k > P$, so the body support plate will not buckle.

2.6.10 Penetration

The one-meter (40-inch) drop of a 6 kg (13-pound), hemispherical-headed, 3.2 cm (1.3-inch) diameter, steel cylinder, as delineated in 10 CFR 71.71(c)(10), is of negligible consequence to the RAJ-II package. This is due to the fact that the RAJ-II package is designed to minimize the consequences associated with the much more limiting case of a 40-inch drop of the entire package onto a puncture bar as discussed in Section 2.7.3. The drop of the 6 kg bar will not damage the outer container.

Table 2 - 8 Temperatures

Location	**Maximum temperature**
Environment (Open air)	38°C
Package's external surface	77°C
Inner container	<77°C

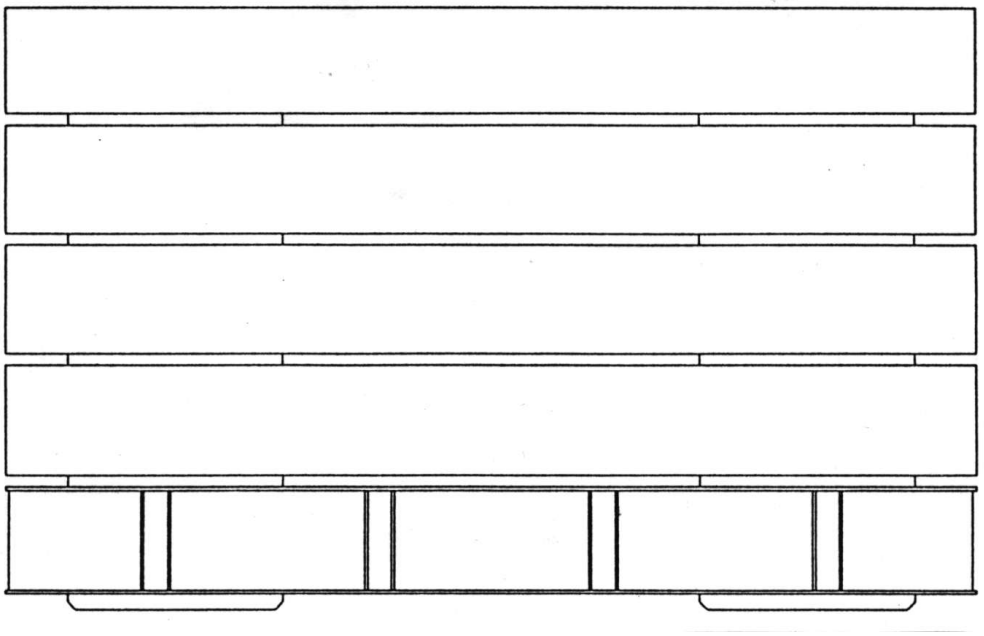

Figure 2-12 Stacking Arrangement

2.7 HYPOTHETICAL ACCIDENT CONDITIONS

The RAJ-II package, when subjected to the sequence of Hypothetical Accident Condition (HAC) tests specified in 10 CFR 71.73 is shown to meet the performance requirements specified in Subpart E of 10 CFR 71. The primary proof of performance for the HAC tests is via the use of full-scale testing. A certification test unit (CTU) was free dropped, and puncture tested to confirm that both the inner and outer containers protected the fuel and allowed containment to be maintained after a worst-case HAC sequence. Another CTU was free dropped from 9 meters on its end with the fuel maintaining containment after the drop. Observations from CTU testing confirm the conservative nature of the deformed geometry assumptions used in the criticality assessment provided in Chapter 6.0. Immersion is addressed by comparison to the design basis for the fuel.

Test results are summarized in Section 2.7.8, with details provided in Appendix 2.12.1.

2.7.1 Free Drop

Subpart F of 10 CFR 71 requires performing a free drop test in accordance with the requirements of 10 CFR 71.73(c)(1). The free drop test involves performing a 30-foot, HAC free drop onto a flat, essentially unyielding, horizontal surface, with the package striking the surface in a position (orientation) for which maximum damage is expected. The ability of the RAJ-II package to adequately withstand this specified free drop condition is demonstrated via testing of four full-scale, certification test units (CTUs).

To properly select a worst-case package orientation for the 30-foot free drop event, items that could potentially compromise containment integrity, shielding integrity, and/or criticality safety of the RAJ-II package must be clearly identified. For the RAJ-II packaging design, there are two primary considerations 1) protect the fuel so that containment is maintained and 2) ensure sufficient structure is around the package to maintain the geometry used in the criticality safety evaluation. Shielding integrity is not a controlling case for the reasons described in Section 5.0. Criticality safety is conservatively evaluated based on measured physical damage to the outer container from certification testing, as described in Section 6.0.

Since the containment is welded closed, the leak-tight capability of the containment may be compromised by two methods: 1) as a result of excessive deformation leading to rupture of the containment boundary, and/or 2) as a result of thermal degradation of the containment material itself in a subsequent fire event and rupture of the weld or the cladding tube by over-pressurization. Importantly, these methods require significant impact damage to the surrounding outer and inner container so that the fuel is either loaded externally or the fuel is directly exposed to the fire.

Additional items for consideration include the possibility of separating the OC lid from the OC body and buckling or deforming of the Outer Container (OC) and/or Inner Container (IC) from an end drop or horizontal drop.

For the above reasons, testing must include impact orientations that affect the lid and stability of the walls of the containers. In general, the energy absorbing capabilities of the RAJ-II are governed by the deformation of the stainless steel and impregnated paper honeycomb that is not significantly affected by temperature.

Appendices 2.12.1 and 2.12.2 provide a comprehensive report of the certification test process and results. Discussions specific to CTU test orientations for free drop and puncture, including initial test conditions, are also provided.

The RAJ-II package has undergone extensive testing during its development. Testing has included 1.2-meter (4-foot) drops on the end in the vertical orientation and the lid in the horizontal orientation. The package has been also dropped from 9 meters in the same orientation demonstrating that the damage from the 1.2-meter (4-foot) drops has little consequence on the performance of the package in 9-meter (30-foot) drop. Based on these preliminary tests it was determined that the worst case orientation for the 9-meter (30-foot) drop test would be slap-down on the lid. The lid down drop demonstrated that the vibration isolation frame bolts would fail allowing the inner container to come in contact with the paper honeycomb in the lid and partially crush the honeycomb. It was expected that the slap-down orientation would maximize the crush of this material minimizing the separation distance between the fuel assemblies in the post accident condition.

A single "worst-case" 9-meter (30-foot) free drop is required by 10 CFR 71.73(c)(1). Based on the above discussion and experience with other long slender packages similar to the RAJ-II, a 15 degree slap-down on the lid was chosen for the 9-meter (30-foot) drop. Following that drop, a 25 degree oblique puncture drop on the damaged lid was performed. See Figure 2-13, Figure 2-14 and Appendix 2.12.1.

Other free drop orientations that were tested include vertical end and bottom corner. These tests demonstrated that the RAJ-II package contains the fuel assemblies without breaching the fuel cladding (containment boundary).

2.7.1.1 End Drop

9-meter (30-foot) end free drops were performed on GNF-J CTU 1J and GNF-A CTU 2. The orientation was selected with the lower end of the fuel down to maximize the damage since the expansion springs in the fuel rods are located in the upper end. This orientation maximized the damage to the energy absorbing wood in the end of the RAJ-II and maximized the axial loading on the fuel assembly. Both tests resulted in deformations of the fuel but were within the limits evaluated in the criticality evaluation in Section 6.0. Following the GNF-A tests, the fuel rods were demonstrated to maintain containment after the free and puncture drops, thus maintaining its containment boundary integrity. Although this orientation caused the most severe damage to the fuel, the damage was well within the structural limits for the fuel and package.

2.7.1.2 Side Drop

No side drop testing was performed in this certification sequence. A side drop test was done in previous testing of the package. That testing resulted in the inner container holding frame top bolts failing and allowing the inner container to come in contact with the outer lid. The inner package showed little damage and the fuel was not deformed. It was judged that the slapdown and the horizontal drop tests bounded the side drop orientation.

2.7.1.3 Corner Drop

A 9-meter (30-foot) free drop on the OC body bottom corner was performed on GNF-J CTU 1J. The impact point previously sustained damage due to 0.3-meter (1-foot) and 1.2-meter (4-foot) free drops. The resultant cumulative deformation was approximately 163 mm (6 inches). There was no loss of contents or significant structural damage to the OC as a result of this free drop. The maximum recorded impact acceleration was 203g. Refer to Appendix 2.12.2 for complete details of the corner free drop.

2.7.1.4 Oblique Drops

An orientation of 15 degrees from horizontal was tested with GNF-A CTU 1. Additional information regarding the selection of this angle is provided in Supplement 1, "Clarifications on the RAJ-II Selection of Slapdown and Puncture Orientations". The IC holding frame was plastically deformed and only a portion of the bolts failed. Neither the fuel nor the IC were not significantly damaged. The damage sustained was bounded by the assumptions utilized in the criticality and thermal evaluations. The fuel was leak tested after the test and was demonstrated to have maintained containment boundary. Refer to Appendix 2.12.1 for complete details of the 15-degree oblique free drop.

2.7.1.5 Horizontal Drop

A 9-meter (30-foot) horizontal free drop on the OC lid was performed on GNF-J CTU 2J. The impact results in a maximum deformation of 19 mm (0.8 inch), which occurred in the OC lid. The side wall of the OC body bulged approximately 19 mm (0.8 inches). Some localized weld failure of OC lid flange/OC lid interface occurred where the bolster angles attach to the lid. None of the OC lid bolts failed as a result of the impact. There was no loss of contents as a result of the free drop. The maximum recorded impact acceleration was 146g. Refer to Appendix 2.12.2 for complete details of the horizontal free drop.

2.7.1.6 Summary of Results

Successful HAC free drop testing of the test units indicates that the various RAJ-II packaging design features are adequately designed to withstand the HAC 30-foot free drop event. The most important result of the testing program was the demonstrated ability of the fuel to remain undamaged and hence maintain its containment capability as defined by ANSI N14.5.

The RAJ-II also maintained its basic geometry required for nuclear criticality safety. Observed permanent deformations of the RAJ-II packaging were less than those assumed for the criticality evaluation.

The GNF-A mock-up fuel assembly rods were leakage rate tested after the conclusion of the testing and were demonstrated to be leaktight, as defined in ANSI N14.5.

A comprehensive summary of free drop test results are provided in Appendices 2.12.1 and 2.12.2.

2.7.2 Crush

Subpart F of 10 CFR 71 requires performing a dynamic crush test in accordance with the requirements of 10 CFR 71.73(c)(2). Since the RAJ-II package weight exceeds 500 kg (1,100 pounds), the dynamic crush test is not required.

2.7.3 Puncture

Subpart F of 10 CFR 71 requires performing a puncture test in accordance with the requirements of 10 CFR 71.73(c)(3). The puncture test involves a 1-meter (40-inch) free drop of a package onto the upper end of a solid, vertical, cylindrical, mild steel bar mounted on an essentially unyielding, horizontal surface. The bar must be 150 mm (6 inches) in diameter, with the top surface horizontal and its edge rounded to a radius of not more than 6 millimeter (0.25 inch). The package is to be oriented in a position for which maximum damage will occur. The length of the bar used was approximately 1.5 meters (60 inches). The ability of the RAJ-II package to adequately withstand this specified puncture drop condition is demonstrated via testing of the full-scale RAJ-II CTUs.

To properly select a worst-case package orientation for the puncture drop event, items that could potentially compromise containment integrity and/or criticality safety of the RAJ-II package must be clearly identified. For the RAJ-II package design, the foremost item to be addressed is the ability of the containment to remain leak-tight. Shielding integrity is not a controlling case for the reasons described in Chapter 5.0. Criticality safety is conservatively evaluated based on measured physical damage to the outer container walls as described in Section 6.0.

Previous testing has shown that the 1-meter drop onto the puncture bar did not penetrate the outer wall or damage the fuel. Based on this previous testing and other experience, an oblique and horizontal puncture drop orientations centered over the fuel were chosen as the most damaging.

Appendices 2.12.1 and 2.12.2 provide a comprehensive report of the certification test process and results. Discussions specific to the configuration and orientation of the test unit are provided.

The "worst-case" puncture drop as required by 10 CFR 71.73(c)(3) was performed on the package with the lid down and 25 degrees from horizontal. The angle was chosen based on experience with other packages and the RAJ-II. Additional information regarding the selection of this angle is provided in Supplement 1, "Clarifications on the RAJ-II Selection of Slapdown and Puncture Orientations". The puncture bar was aimed at the CG of package to maximize the energy imparted to the package.

The puncture pin did not penetrate the outer container. It deformed the lid inward and it contacted the inner container lid and deformed it a small amount. The outer lid total deformation was less than 12 cm (4.7 inches) and the inner container lid deformed less than 5 cm (2.0 inches).

2.7.4 Thermal

Thermal testing of the GNF-J CTU 2J was performed following the free drop and puncture drop tests (refer to Appendix 2.12.2). Although there was no failure of the containment boundary due to the thermal testing, the thermal evaluation of the RAJ-II package for the HAC heat condition as presented in Section 3.0, demonstrates the regulatory compliance to 10 CFR 71.73(c)(4). Because the RAJ-II package does not contain pressure-tight seals, the HAC pressure for the OC and the IC is zero. The fuel assembly exhibits negligible decay heat.

2.7.4.1 Summary of Pressures and Temperatures

The maximum predicted HAC temperature for the fuel assembly is 921 K (1,198 °F) during the fire event. The fuel rods are designed to withstand a minimum temperature of 1,073 K (1,475 °F) without bursting. This has been demonstrated by heating representative fuel rods to this temperature for over 30 minutes. This heating resulted in rupture pressures in the excess of 3.6 MPa (520 psi). The pressure due to the accident conditions does not exceed 3.5 MPa (508 psig). Summary of pressures and related stresses are provided in Section 3.0.

2.7.4.2 Differential Thermal Expansion

The fuel cladding is not restricted by the packaging and hence can not develop any significant differential thermal expansion stresses. The packaging itself is made of the same metal (austenitic stainless steel) eliminating any significant stresses due to differential thermal expansion.

2.7.4.3 Stress Calculations

Stress calculations for the controlling hoop stress for the fuel cladding that provides containment is provided in Section 3.0.

2.7.4.4 Comparison with Allowable Stresses

The allowable stress used in the analysis in Section 3.0 is based on empirical data from burst tests performed on fuel rods when heated to 800 °C and above. The allowed fuel cladding configurations for the RAJ-II have a positive margin of safety based on stresses required to fail the fuel in the test.

2.7.5 Immersion – Fissile Material

Subpart F of 10 CFR 71 requires performing an immersion test for fissile material packages in accordance with the requirements of 10 CFR 71.73(c)(5). The criticality evaluation presented in Chapter 6.0 assumes optimum hydrogenous moderation of the contents, thereby conservatively addressing the effects and consequences of water in-leakage.

2.7.6 Immersion – All Packages

Subpart F of 10 CFR 71 requires performing an immersion test for packages in accordance with the requirements of 10 CFR 71.73(c)(6). Since the RAJ-II package is not sealed against pressure, there will not be any differential pressure with the water immersion loads defined in 10 CFR 71.73(c)(6). The water immersion will have a negligible effect on the container and the payload, consisting of the fuel assemblies that provide the containment. The fuel rods are designed to withstand differential pressures greater than 1,000 psi. Submergence is a normal design condition for the fuel assemblies and the evaluations are performed on that condition.

2.7.7 Deep Water Immersion Test (for Type B Packages Containing More than 10^5 A_2)

Not applicable. The RAJ-II does not contain more than 10^5 A_2.

2.7.8 Summary of Damage

As discussed in the previous sections, the cumulative damaging effects of the free drops and a puncture drop were satisfactorily withstood by the RAJ-II packaging during certification testing. Subsequent helium leak testing confirmed that containment integrity was maintained throughout the test series. The package was also successfully evaluated for maintaining containment during and after the fire event. The deformation of the package in the worst case HAC did not exceed that which is evaluated for in Chapter 6.0. Therefore, the requirements of 10 CFR 71.73 have been satisfied.

Table 2 - 9 Summary of Tests for RAJ-II

Test No.	Test Description	Test Unit Angular Orientation		CTU Temperature	Remarks
		Axial①	Rotational		
1	9 - meter (30-foot) slap down	15°	Lid down	Ambient	Top of package impacted first. Lid crushed over 11 cm (4.3 in).
2	Puncture	25°	Lid down	Ambient	Puncture pin crushed the outer lid down to the inner container lid. It did not rupture the outer lid or significantly deform the inner container lid or fuel.
3	9 - meter (30-foot) end drop	90°	Bottom down	Ambient	Crushed end wood impact absorber. Deformed the fuel assembly but did little damage to the rods

Notes:

① Axial angle,θ, is relative to horizontal (i.e., side drop orientation)

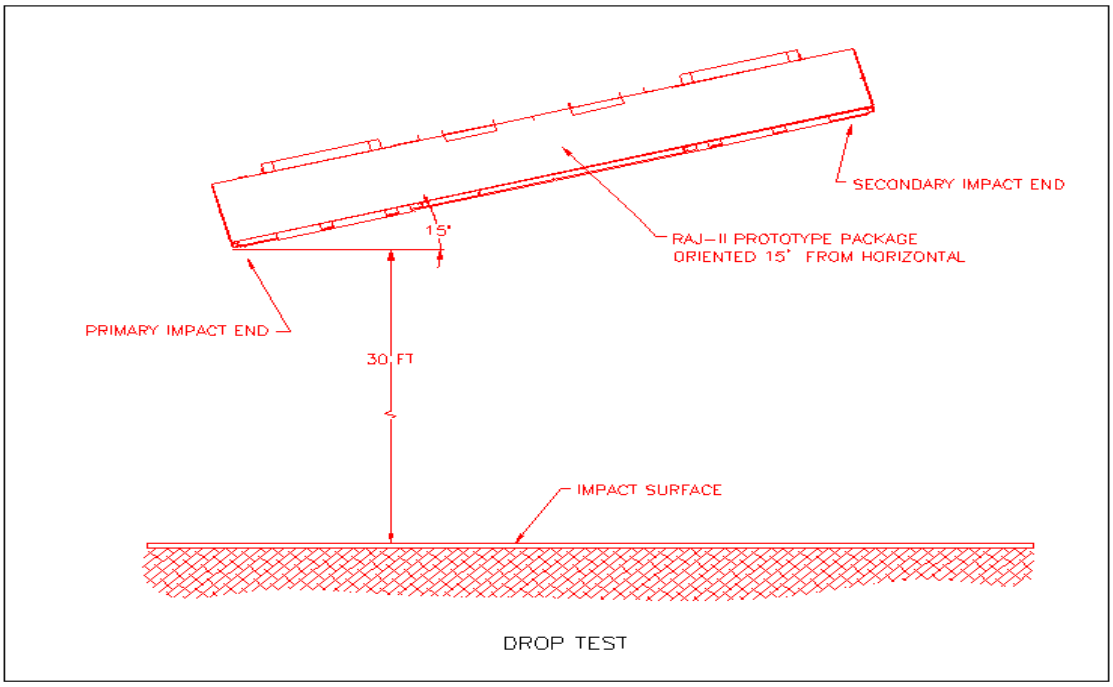

Figure 2-13 Slap-down Orientation

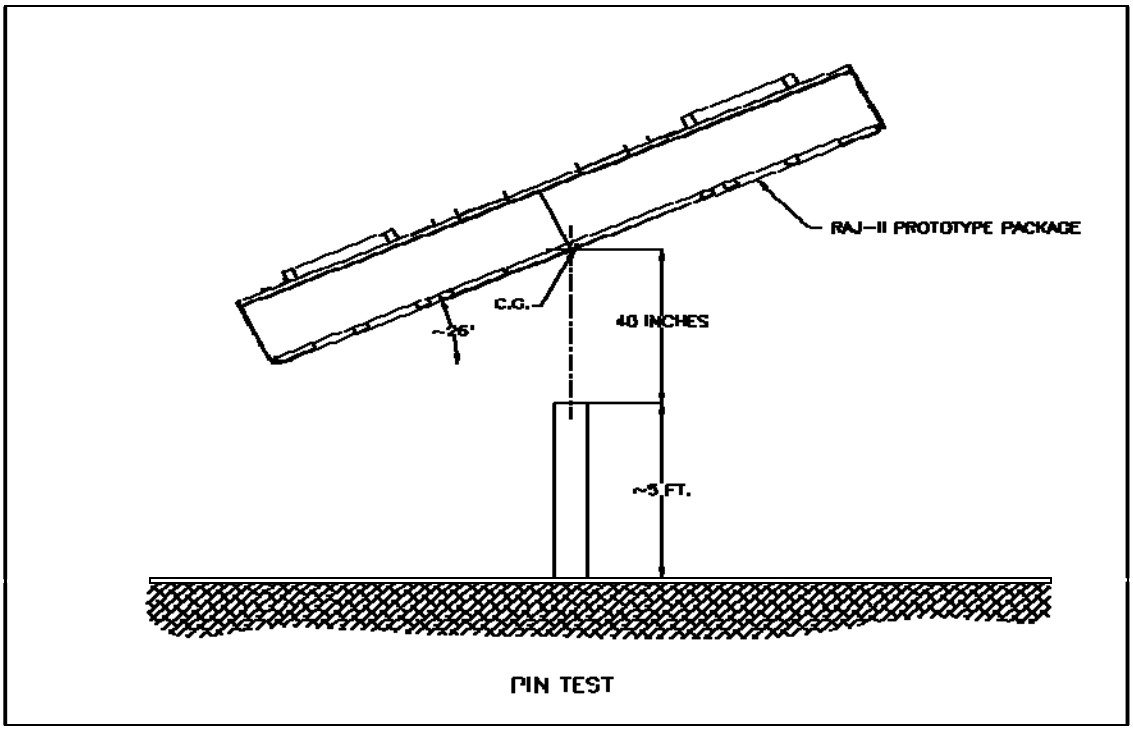

Figure 2-14 Puncture Pin Orientation

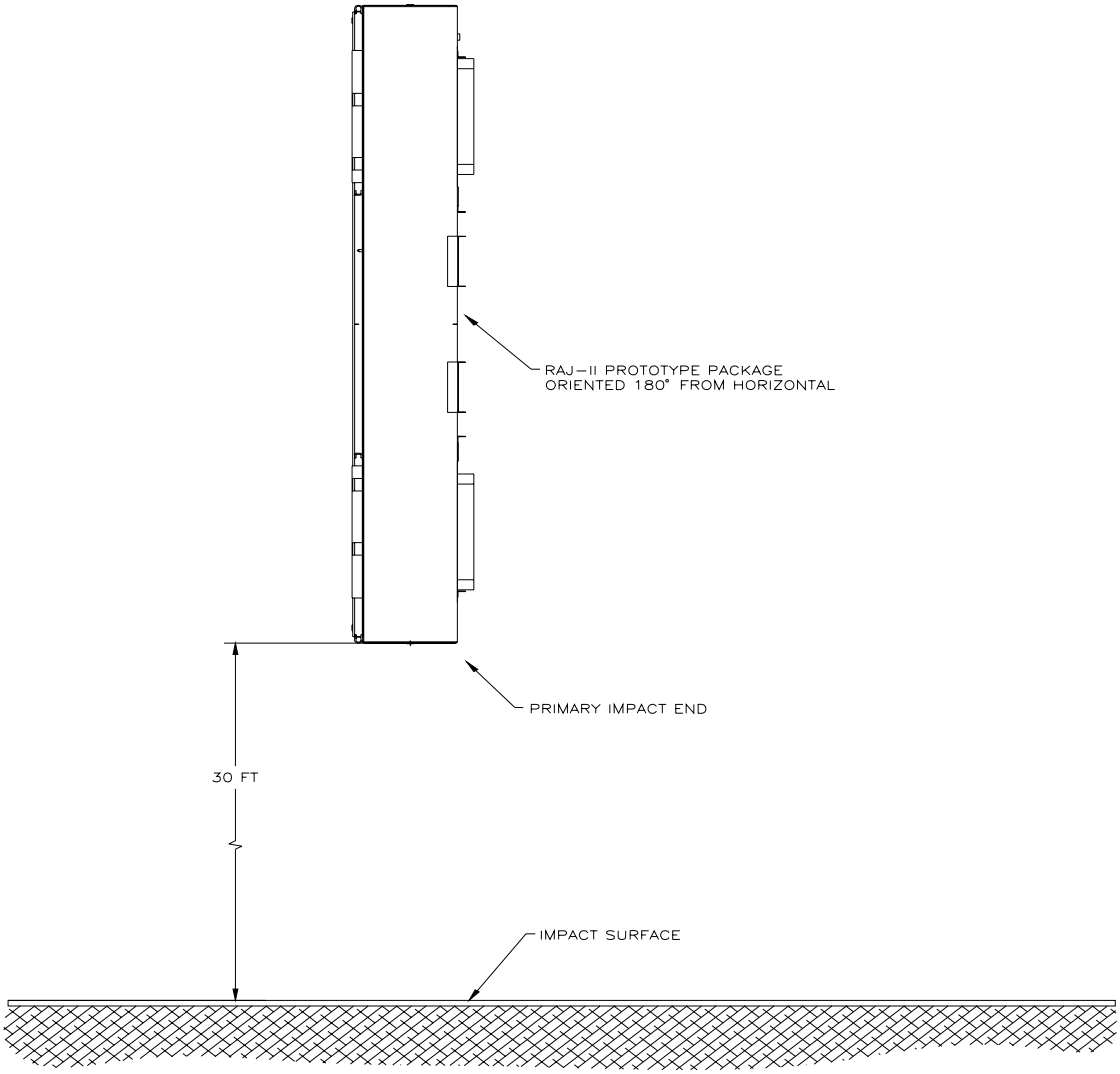

Figure 2-15 End Drop Orientation

2.8 ACCIDENT CONDITIONS FOR AIR TRANSPORT OF PLUTONIUM

Not Applicable. This package will not be used for the air transport of plutonium.

2.9 ACCIDENT CONDITIONS FOR FISSILE MATERIAL PACKAGES FOR AIR TRANSPORT

Not applicable. This package will not be used for the air transport of fissile material.

2.10 SPECIAL FORM

This section does not apply for the RAJ-II package, since special form is not claimed.

2.11 FUEL RODS

In each event evaluated above either by analysis or by test, the unirradiated fuel rods were protected by the RAJ-II package so that they sustained no significant damage. Fuel rod cladding is considered to provide containment of radioactive material under both normal and accident test conditions. Discussion of this cladding and its ability to maintain sufficient mechanical integrity to provide such containment is described in Section 1.2.3 and Chapter 4.0.

2.12 APPENDIX

2.12.1 Certification Tests

2.12.1.1 Certification Test Unit

The RAJ-II test packages were fabricated identically to the configuration depicted in the Packaging General Arrangement Drawing found in Appendix **Error! Reference source not found.**. The certification test unit is identical to the production RAJ-II packages except for some minor differences.

1. For ease in documentation/evaluation, tape and marker were used for reference markings during testing.

2. Minor amounts of the internal foam cushioning material were cut out to accommodate added weight in the fuel cavity.

3. Weight was added to the exterior of the package to allow the test units to be at the maximum allowed package weight.

The fuel assemblies were represented by a mock up fuel assembly (an ATRIUM-10 design). Lead rods inside the cladding replaced the fuel pellets. The fuel rods were seal welded using the same techniques used on the production fuel rods. A composite fuel assembly was used to represent the second fuel assembly. Steel tubes represented the ends with added steel for correct weight. The center section was made up of a mock up fuel assembly similar to the full size mock up fuel assembly. The mock up of the fuel approximated the stiffness of the fuel and added no extra strength to the center section of the package that would potentially be damaged by the puncture test. See Figure 2-16 through Figure 2-22 for container and mock up fuel preparation. Weight was added to the fuel assembly cavity by placing lead sheeting on the side of the fuel where normally there is foam. The lead weighing 143 pounds represented the weight of the water channels that could be shipped with some fuel assemblies. The lead plate was cut into strips that were not over half the height of the fuel assemblies to ensure that there was no support or protection added to the fuel during any of the tests. The total weight of the CTUs is provided in Table 2 - 10. The added weight in the contents represents the maximum payload weight including the fuel, fuel assembly fittings and packing material that could be required in the future.

For CTU 1 that was dropped lid down for a 30-foot slap down event and a 1-meter oblique puncture event, the weight was added between the bolster boards at each end. The added weight representing the difference between the actual tare weights of the package and the maximum allowed tare weight consisted of two ½ inch carbon steel plates. For CTU 1, these were held in place by the bolster and brackets attached to the bolster with lag bolts. See Figure 2-23. These plates were taken off CTU 1 and placed on the opposite end of CTU 2 for the end drop. See Figure 2-24.

Table 2 - 10 Test Unit Weights

Property	**CTU 1**		**CTU 2**	
As fabricated weight	849 kg	1,872 lbs	848 kg	1,869 lbs
Max. fabricated weight	930 kg	2,050 lbs	930 kg	2,050 lbs
Added weight	81.7 kg	180 lbs	81.7 kg	180 lbs
Content weight	684 kg	1,508 lbs	685 kg	1,510 lbs
Measured drop weight	1,614 kg	3,558 lbs	1,611 kg	3,552 lbs
Approximate weight of attaching frame	2.3 kg	5.1 lbs	11.3 kg	24.9 lbs
Approximate drop weight	1,616 kg	3,562 lbs	1,622 kg	3,576 lbs

2.12.1.2 Test Orientations

Three certification tests were performed. Two tests were performed on CTU 1, a 9-meter (30-foot) slap-down on the lid and a 1-meter (40-inch) oblique puncture test on the lid. A 9-meter (30-foot) end drop was performed on CTU 2.

The 9-meter (30-foot) drop on the lid was designed to provide maximum acceleration to the end of the fuel as well as maximize the crush of the package for criticality evaluation purposes. The top down orientation was chosen since the lid contains the least material. The lid down orientation was also chosen since on previous tests horizontal lid down tests had maximized the crush and had resulted in the failure of the retaining bolts on the frame holding the inner container. As discussed in Section 2.7.1.1, the drop orientation was at 15 degrees with the horizontal. See Figure 2-25.

The 1-meter (40-inch) puncture test was performed on CTU 1 with the lid down after the 9-meter (30-foot) slap-down test. The package was oriented at a 25-degree angle to maximize the possibility of the corner of the puncture bar penetrating the outer container and maximizing the damage to the inner container and fuel. The puncture bar was aligned over the center of gravity of the package. See Figure 2-26 and Figure 2-27.

CTU 2 was dropped 9-meters (30-feet) with its bottom end down. The purpose of this orientation was to maximize the damage to the fuel. The bottom end was chosen since it is the most rigid end of the fuel assembly. The expansion springs inside the cladding tubes are on the upper end. See Figure 2-28

2.12.1.3 Test Performance

Testing was performed at the National Transportation Research Center in Oak Ridge, Tennessee. The CTUs were shipped to the facility fully assembled. Only the additional tare weight as described in Section 2.12.1.1 was added at the test facility. Tests were performed on the packages prior to them being transported to the Framatome-ANP facility at Lynchburg, Virginia. At Lynchburg the packages were disassembled and examined and the fuel rods were helium leak tested.

The slapdown test at 15 degrees to horizontal demonstrated the ability of the outer package to protect the fuel and the inner container. The energy absorbing capabilities of the package allowed the package to deform and limited the secondary impact to less than the primary impact. See Figure 2-29 and Figure 2-30. This test resulted in deformation inside the package. See Figure 2-36 and Figure 2-37. The crush of the paper honeycomb was limited by the stiffening plates in the lid. See Figure 2-38. The inner container lid was deformed as well. Neither the lid bolts on either container nor the bolts on the inner container clamping device failed. The frame did bend over 3 cm. The fuel rods, although slightly deformed due to the test and the added weight in the fuel cavity, were not damaged. See Figure 2-39. The added weight placed between the bolster timbers caused a slight deformation of the bottom wall of the outer package in the local area of the weights.

The puncture test was performed with the lid down at a 25 degree angle from horizontal. See Figure 2-25. The puncture pin was bolted with three bolts to the drop pad. The puncture pin struck the lid over the CG of the package after the package had undergone the slapdown test. See Figure 2-26. The pin did not penetrate the outer lid. The outer lid was deformed inward until it came in contact with the inner container. This was confirmed by a slight mark on the inner container lid. The pin appears to have bounced since there are two indentations very close together which could have been caused by the outer lid bottoming out against the inner container lid. See Figure 2-31 and Figure 2-32. No significant internal package or fuel damage appeared to be attributable to the pin puncture test.

The 9-meter (30-foot) end drop test was performed on CTU 2 with the bottom end down. There was little exterior damage to the outer container. See Figure 2-33, Figure 2-34, and Figure 2-35. Extensive damage occurred to the inside of the inner container as the fuel assemblies and the added weight impacted the interior of the inner container. The rigid end fitting of the assembly crushed the wood located at the end of the package. Although some welds broke, the bottom end of the package remained in place. The fuel rods partially came out of the end fitting. The fuel assemblies bent to the side. See Figure 2-40, Figure 2-41, and, Figure 2-42.

The mock up fuel assemblies from both CTU 1 and CTU 2 were helium leak tested. The Assembly form CTU 1 was found to meet the leak tight requirements of having a leak rate less than 1 $x10^{-7}$ atm-cc/s. The assembly from CTU 2 was found to have a He leak rate of $5.5x10^{-6}$ atm-cc/s. This is within the allowable leakage for the fuel as shown in Section 4.0.

2.12.1.4 Test Summaries

Two 9-meter (30-foot) drops and one oblique puncture pin test were performed on two certification test units. The packages retained the fuel assemblies and protected the fuel. Mockup fuel assemblies from both certification units were leak tested after the drop tests and were determined to have maintained containment. The tests are summarized below.

Table 2 - 11 Testing Summary

Test	CTU	Orientation with horizontal	Exterior damage	Interior damage	Fuel
9-meter (30-foot) lid down	1	15º	Minor deformation on both ends.	No bolts broken on the frame or the lids. Significant deformation to inner container and internal clamp frame. Reduction of spacing between outside of package and fuel to about 4 inches.	Minimal damage to the fuel assemblies. Some twist to the assembly. No real damage to the fuel rods. The fuel was demonstrated to have a leak rate of less than 1 $x10^{-7}$ atm-cc/s after the testing.
1-meter (40 in) lid down over cg	1	25º	Did not penetrate outer wall	Outer wall contacted inner container. Section 2.12 Figure 2-39 through 2-42 show some damage to the inner container, however, this damage is conservatively modeled in the HAC criticality analyses in Section 6.0 and is not sufficient to allow fuel to leak from the container.	The fuel appeared not to be affected by this test. Passed helium leak test.
9-meter (30-foot) lower end	2	90º	Localized damage on impact end.	Major crushing of the wood at the end of the inner package and breaking of the inner wall of the inner container on the impacted end. The outer wall was damaged but did not fail completely.	Fuel was bent and separated from end fittings. Fuel spacers were damaged. Fuel rods had no significant damage. Fuel bending was influenced by the movement of the weight added to the fuel cavity. Post drop leak test giving a He leak rate of 5.5 x 10^{-6} atm-cc/s demonstrated that containment had been maintained.

Figure 2-16 Inner Container Being Prepared to Receive Mockup Fuel and Added Weight

Figure 2-17 Partial Fuel Assemblies in CTU 1

Figure 2-18 Top End Fittings on Fuel in CTU 1

Figure 2-19 Contents of CTU 2

Figure 2-20 Outer Container without Inner Container

Figure 2-21 Inner Container Secured in Outer Container

Figure 2-22 CTU 2 Prior to Testing

Figure 2-23 Addition of Tare Weight to CTU 1

Figure 2-24 Addition of Tare Weight to CTU 2

Figure 2-25 CTU 1 Positioned for 15° 9-m (30-foot) Slap-down Drop

Figure 2-26 Alignment for Oblique Puncture

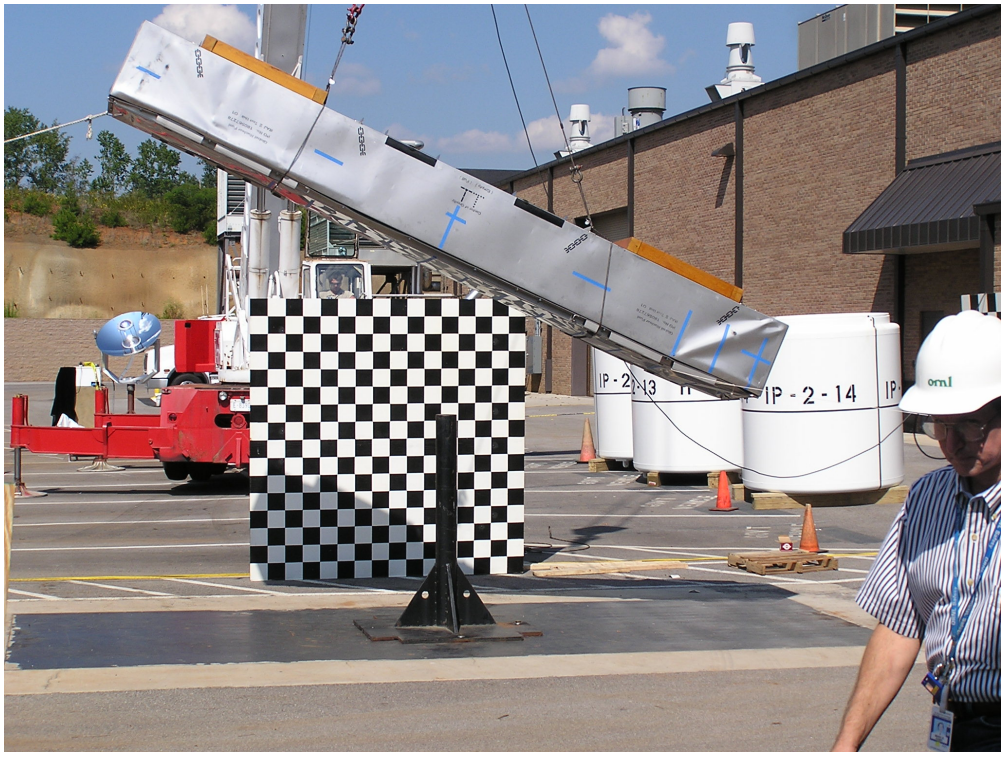

Figure 2-27 Position for Puncture Test

Figure 2-28 Position for End Drop

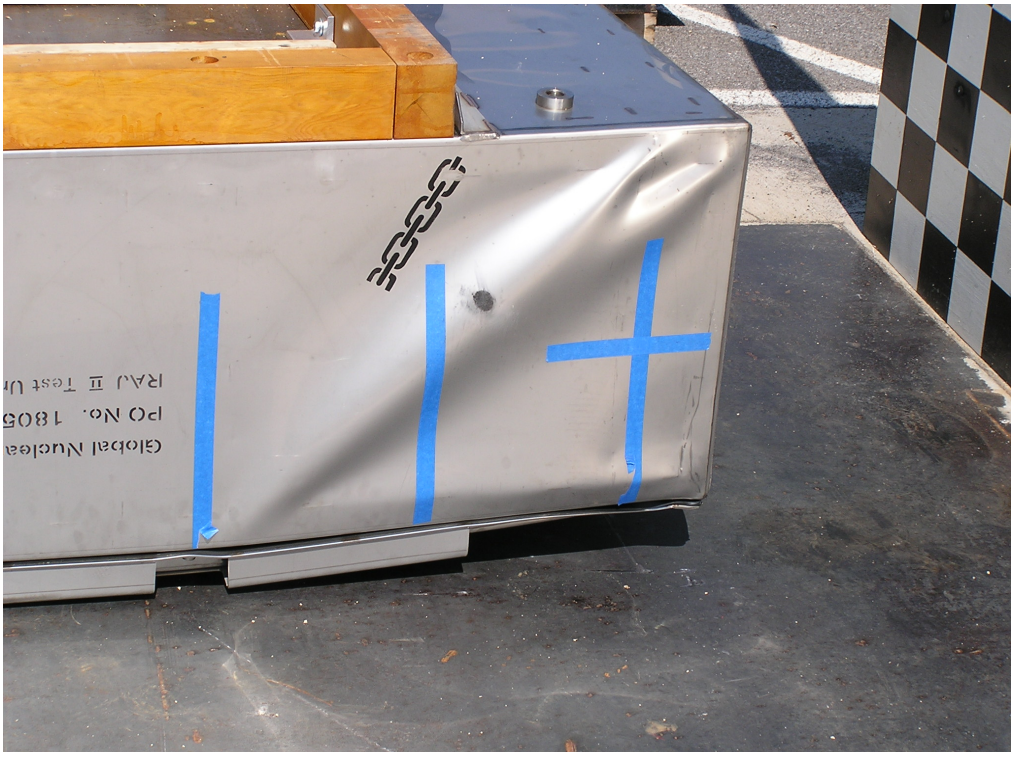

Figure 2-29 Primary Impact End Slap-down Damage

Figure 2-30 Secondary Impact End Damage

Figure 2-31 Puncture Damage

Figure 2-32 Close Up of Puncture Damage

Figure 2-33 End Impact

Figure 2-34 Damage from End Impact (Bottom and Side)

Figure 2-35 End Impact Damage (Top and Side)

Figure 2-36 Damage Inside Outer Container to CTU 1

Figure 2-37 Internal Damage to Outer Container CTU 1

Figure 2-38 Lid Crush on CTU 1

Figure 2-39 Damage to Fuel in CTU 1

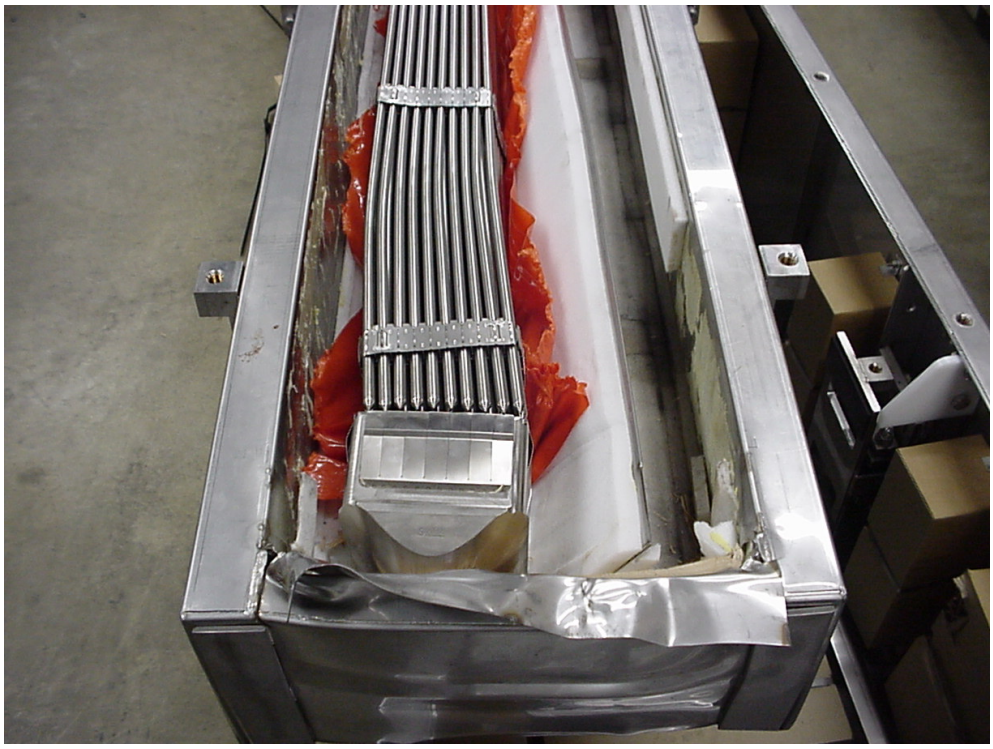

Figure 2-40 Internal Damage to CTU 2

Figure 2-41 Fuel Damage CTU 2

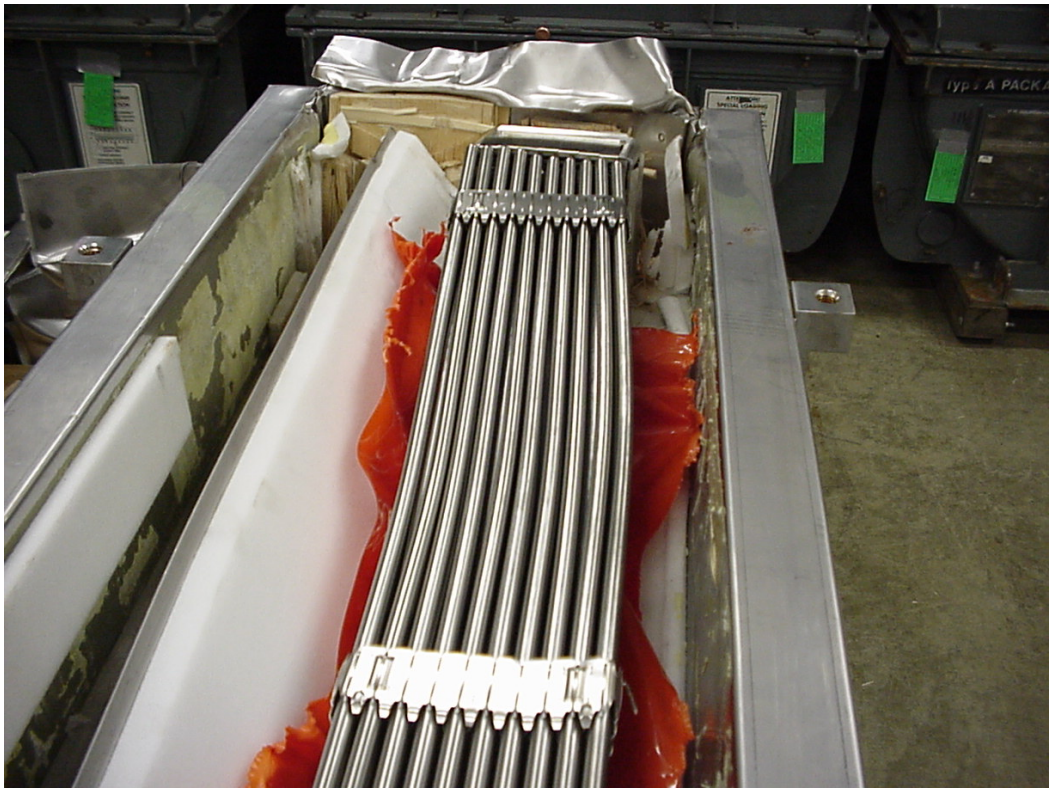

Figure 2-42 Fuel Prior to Leak Testing CTU 2

2.12.2 GNF-J Certification Tests

Normal conditions of transport (NCT) and hypothetical accident conditions (HAC) certification testing of the RAJ-II package was also performed by GNF-J as part of obtaining a Type AF certificate of compliance[a] in Japan. For the U.S. testing, the GNF-J certification tests were utilized to determine the worst-case test orientations for the certification tests identified in Appendix 2.12.1. This appendix summarizes the GNF-J RAJ-II certification tests.

2.12.2.1 Certification Test Units

Two certification test units (CTUs) were utilized for the GNF-J RAJ-II tests. Each CTU was fabricated in accordance with the Packaging General Arrangement Drawings found in Appendix 1.4.1, with the following exceptions:

1. The lateral wood bolsters on each end were not installed. Elimination of these wood bolsters is conservative for the free drops.
2. Maximum content weight was 560 kg (1,235 lbs), which results in a maximum package weight of 1,490 kg (3,285 lbs). This weight reduction is less than 8% lower than the maximum gross weight of the RAJ-II package, and will result in higher impact forces. The small difference in weight will have an insignificant effect on the free drop response of the package and/or fuel assembly.

One simulated fuel assembly and one dummy weight were utilized in each CTU to simulate the payload contents. Accelerometers were installed on the CTUs to measure and record each free drop impact. No accelerometers were used for the puncture drop tests.

2.12.2.2 Test Orientations

Since the RAJ-II package relies on the fuel cladding as the containment boundary, free drop and puncture drop orientations that could damage the fuel cladding and potentially breach the containment boundary should be included in the test series. In addition, orientations that could damage the package and/or the fuel assemblies such that an unsafe criticality geometry would exist should be included in the test series.
Free drop orientations that could result in this type of damage include:

1. Vertical drop on the package end – maximizes axial impact acceleration to a fuel assembly, potentially buckling and failing the fuel cladding (containment boundary).
2. Horizontal drop of the package – maximizes lateral impact acceleration on a fuel assembly, potentially bending and failing the fuel cladding (containment boundary).
3. CG-over-corner of the package – maximizes deformation of outer container (OC).

All of these orientations were included in the free drop test series of the package.
Puncture drop orientations that could potentially breach the containment boundary (cladding) include:

1. Horizontal puncture drop on the center of the package – maximizes puncture impact onto fuel pins and potentially shearing and failure of the fuel cladding (containment boundary).

---

[a] Global Nuclear Fuel - Japan (fka Japan Nuclear Fuel Co., Ltd), *Application for Approval of Packaging, Type RAJ-II*, STO-M00-034, dated September 26, 2000.

2. Vertical puncture drop on the end of the package – maximizes puncture impact onto the fuel assembly

Because of the end internal structure and wood dunnage in the outer container, the puncture drop on the end will not result in any significant deformation of the fuel assembly or the inner container. Therefore, this puncture drop orientation is bounded by the horizontal puncture drop on the center of the package.
The free drop tests included NCT drops of 0.3 meters (1 foot) and 1.2 meters (4 feet) prior to performing the 9-meter (30-foot) HAC free drop on each CTU. The horizontal puncture drop test was only performed on CTU 2J.
Two certification test series were performed. Three free drop tests were performed on CTU 1J, and three free drop and one puncture drop tests were performed on CTU 2J. The test series for each CTU is summarized in Table 2-10. All drop tests were performed at ambient temperature.

2.12.2.3 Test Performance

Free drop and puncture testing was performed at two test facilities in Japan. At one facility, the drop pad consisted of a 32-mm (1.26-inch) thick steel plate that was embedded in a 1-meter (40-inch) thick concrete and steel support structure, with an overall length of 8 meters (26 feet). The other drop pad consisted of a 50-mm (1.97-inch) thick × 5-meter (16.4-feet) × 5-meter (16.4-feet) steel plate that was embedded in a 450-mm (12-inch) thick × 8.5-meter (27.9-feet) wide concrete and steel structure. The mass of each drop pad constituted an essentially unyielding surface for the CTUs, which weighed approximately 1,490 kg (3,285 lbs).

2.12.2.3.1 CTU 1J

CTU 1J was tested for a total of six free drop tests at heights of 0.3 meters (1 foot), 1.2 meters (4 feet), and 9 meters (30 feet). Figures 2-43 through 2-48 sequentially photo-document the CTU 1J tests.
The maximum resultant accumulated deformation, ~163 mm (~6 inches) occurred in the OC body corner. This orientation resulted in the maximum impact acceleration of 203g. No failure of the cladding (containment boundary) occurred from this test series.

2.12.2.3.2 CTU 2J

The testing of CTU 2J focused on free drop orientations not addressed by the CTU 1J tests. In addition, a HAC puncture drop test and HAC thermal test were performed. A total of three free drop tests at heights of 0.3 meters (1 foot), 1.2 meters (4 feet), and 9 meters (30 feet) were performed. Figures 2-49 and 2-50 sequentially photo-document the CTU 2J tests.
The maximum resultant accumulated deformation, ~163 mm (~6 inches) occurred in the OC body corner. This orientation resulted in the maximum impact acceleration of 146g. No failure of the cladding (containment boundary) occurred from this test series.

2.12.2.4 Test Summaries

Two 0.3-meter (1-foot), four 1.2-meter (4-foot), three 9-meter (30-foot) free drops, one 1-meter (40-inch) puncture drop, and one HAC thermal test were performed on two CTUs. The packages retained the fuel assemblies and protected the fuel. There was no visual damage or loss of fuel pellets from the simulated fuel assemblies from both CTUs. A summary of the test results is provided in Table 2 - 11.

Table 2-10 GNF-J CTU Test Series Summary

CTU	Drop Height, m (ft)	Test Description	Purpose
1J	0.3 (1)	Free drop, CG-over-bottom end lower corner	Normal operation impact on OC body corner.
	1.2 (4)	NCT free drop, CG-over-bottom end lower corner	Impart initial deformation in same orientation as subsequent HAC free drop
		NCT free drop, horizontal on OC lid	Impart initial deformation in same orientation as planned HAC free drop
		NCT free drop, vertical, bottom end	Impart initial deformation in same orientation as subsequent HAC free drop
	9 (30)	HAC free drop, CG-over-bottom end lower corner	Maximize OC body deformation; potentially fail fuel rod and breach cladding.
		HAC free drop, vertical, bottom end	Maximize axial impact loads on fuel assemblies, potentially buckle fuel rod and breach cladding.
2J	0.3 (1)	Free drop, CG-over-lid corner	Normal operation impact on OC lid/body corner interface.
	1.2 (4)	NCT free drop, horizontal on lid	Impart initial deformation in same orientation as subsequent HAC free drop
	9 (30)	HAC free drop, horizontal on lid	Maximize lateral impact loads on fuel assemblies, potentially breaching cladding.
	1 (3.3)	HAC puncture drop, horizontal on OC lid	Impact directly on HAC free drop damage; attempt to rupture fuel cladding.
	N/A	HAC thermal test	Demonstrate thermal performance of package.

Table 2-11 GNF-J CTU Test Series Results

CTU	Drop Height, m (ft)	Test Description	Result
1J	0.3 (1)	Free drop, CG-over-bottom end lower corner	Combined deformation of ~40 mm (~1.6 inches) of bottom corner.
	1.2 (4)	NCT free drop, CG-over-bottom end lower corner	
		NCT free drop, horizontal on OC lid	No significant deformation.
		NCT free drop, vertical, bottom end	Impacted end deformed ~3.9 mm (~0.2 inches)
	9 (30)	HAC free drop, CG-over-bottom end lower corner	Impacted OC bottom corner deformed ~163 mm (~6 inches), OC lid corner ~101 mm (~4 inches). Maximum acceleration of 203g.
		HAC free drop, vertical, bottom end	IC body/lid deformed ~2 - 81 mm (~0.08 - 3 inches) in length, U-shaped lifting bar on fuel assembly bent due to contact with wood end dunnage. Maximum acceleration of 58g.
2J	0.3 (1)	Free drop, CG-over-lid corner	Combined deformation of ~2.9 mm (~0.1 inches) of lid corner.
	1.2 (4)	NCT free drop, horizontal on lid	
	9 (30)	HAC free drop, horizontal on lid	Impacted side deformed ~2 - 19 mm (~0.08 -0.8 inches), localized weld failure of OC lid flange/OC lid sheet interface, no failure of OC lid bolts. Maximum acceleration of 146g.
	1 (3.3)	HAC puncture drop, horizontal on OC lid	~100 mm deep × ~2,000 mm (~4 inches × ~79 inches) wide indention in OC lid, no breach of OC lid sheet.
	N/A	HAC thermal test	No failure of simulated fuel assembly cladding.

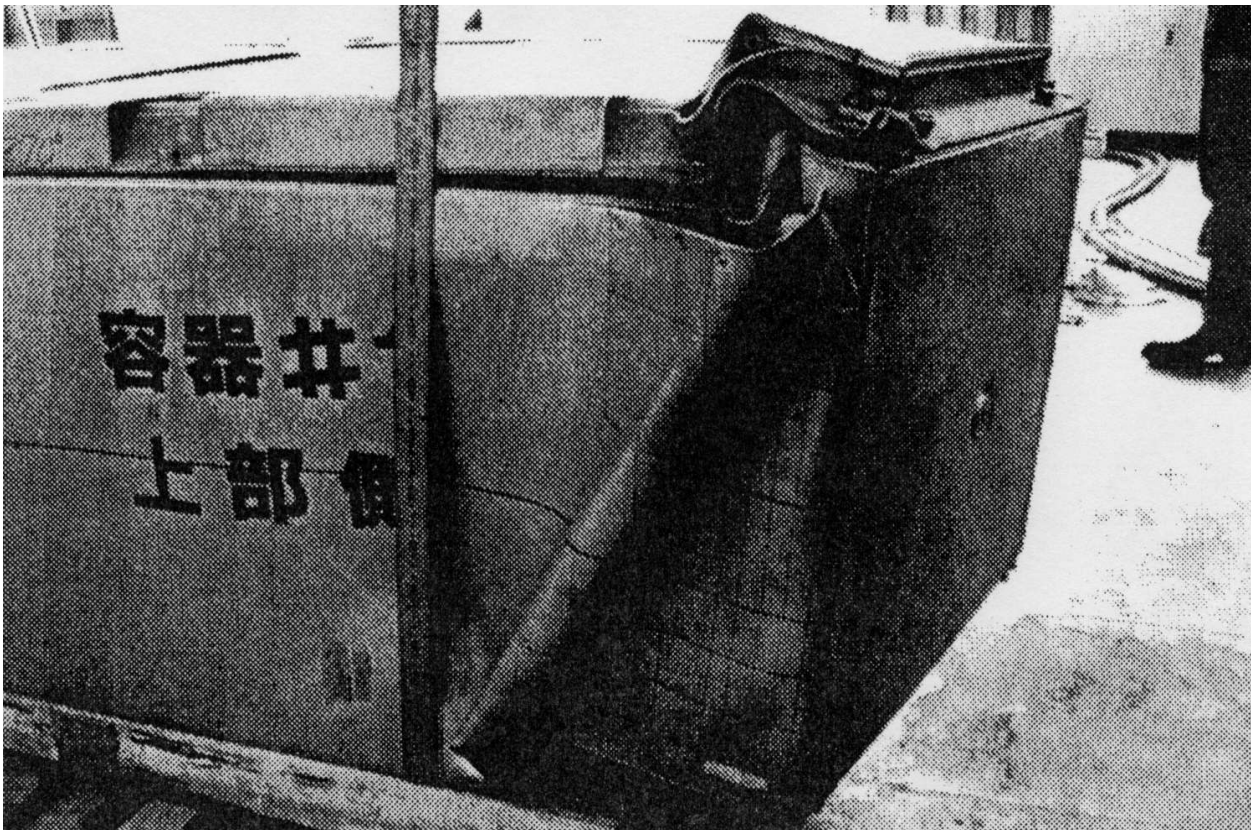

Figure 2-43 CTU 1J 9 m CG-Over-Bottom Corner Free Drop: View of Impacted Corner

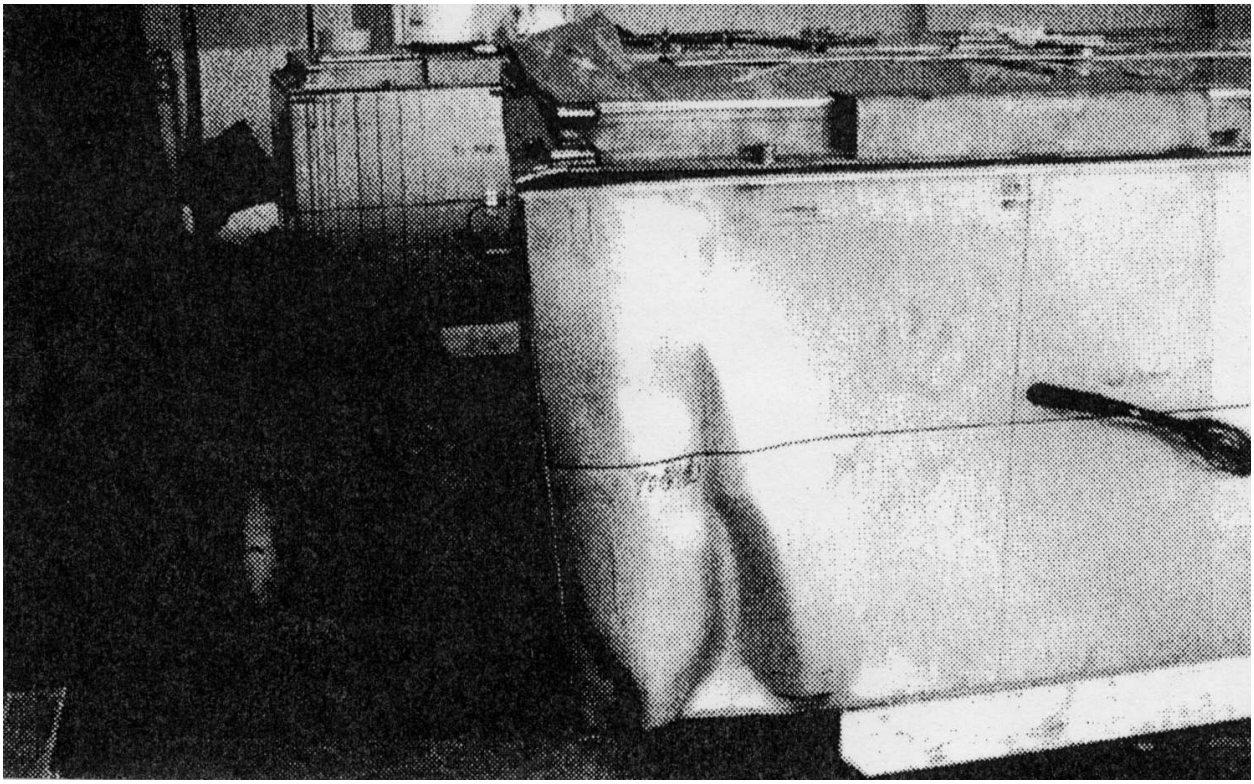

Figure 2-44 CTU 1J 9 m CG-Over-Bottom Corner Free Drop: View of Opposite Corner

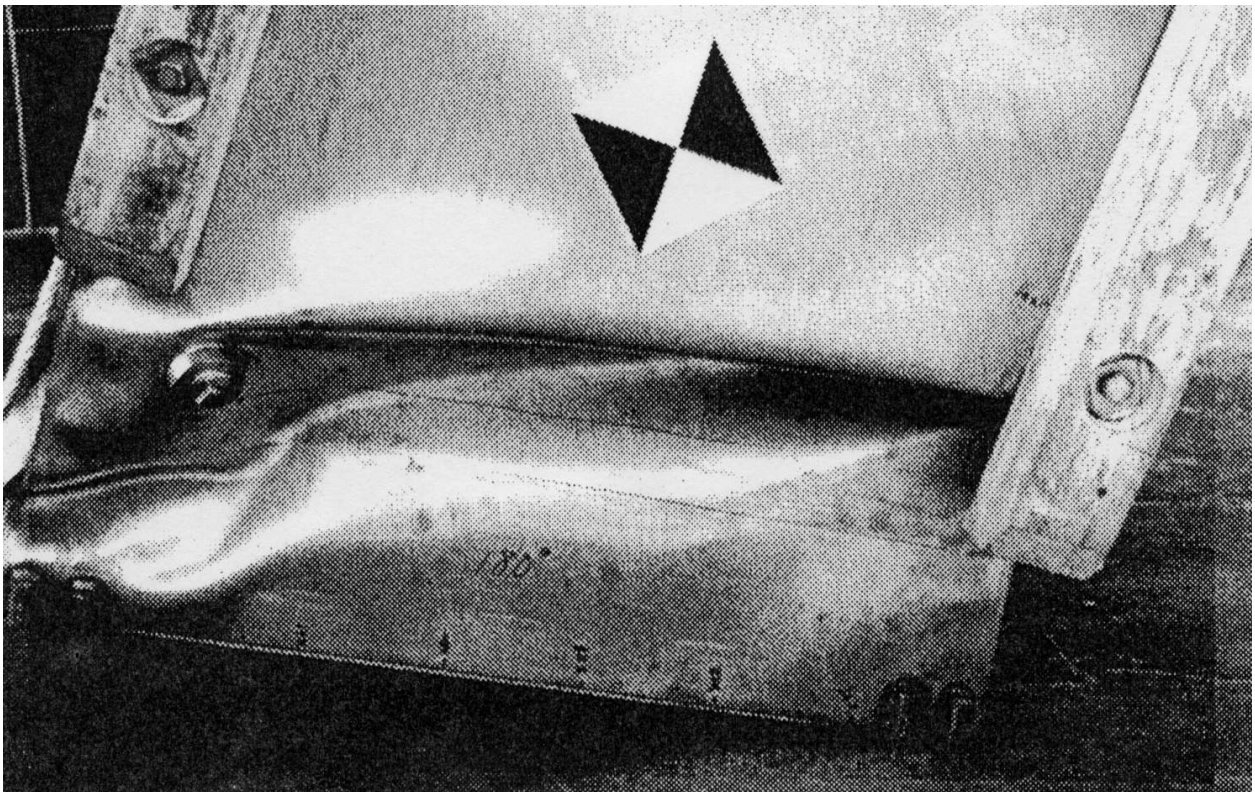

Figure 2-45 CTU 1J 9 m CG-Over-Bottom Corner Free Drop: View of Bottom

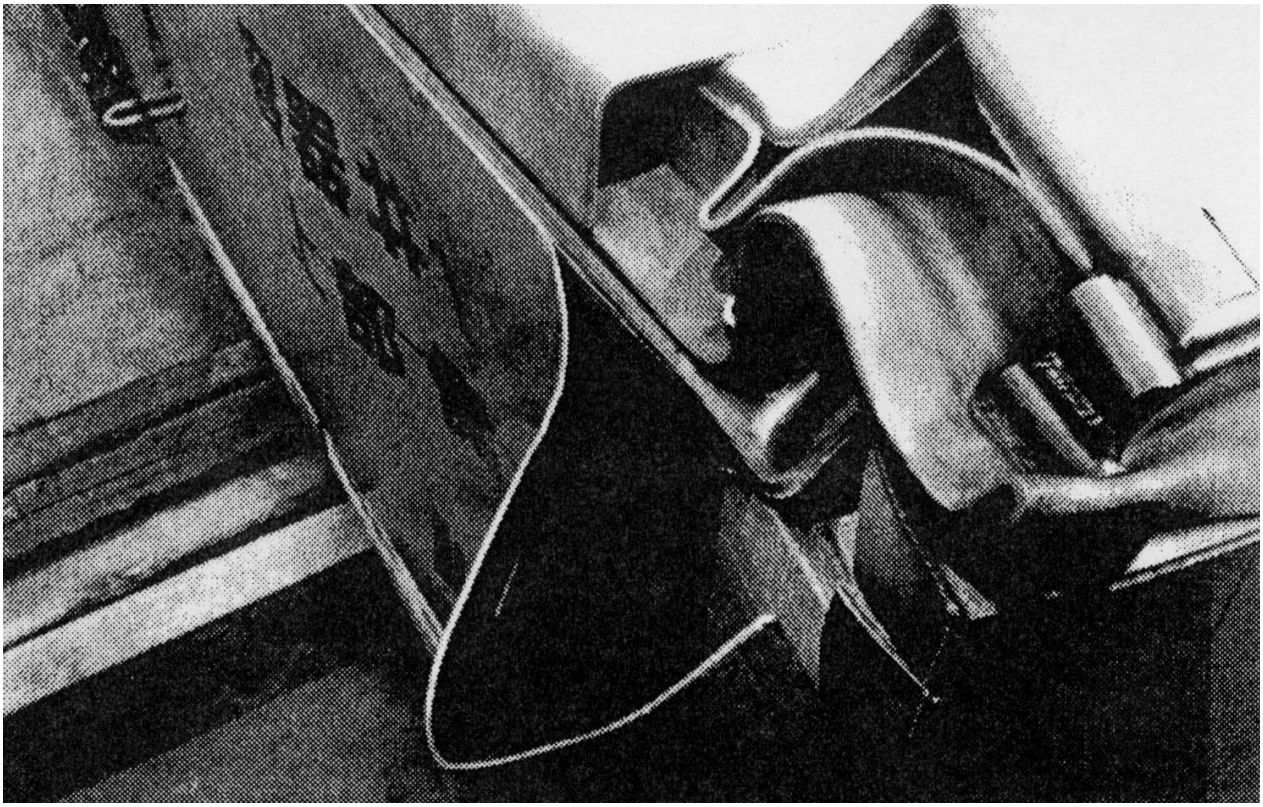

Figure 2-46 CTU 1J 9 m CG-Over-Bottom Corner Free Drop: Close-up View of Top Corner

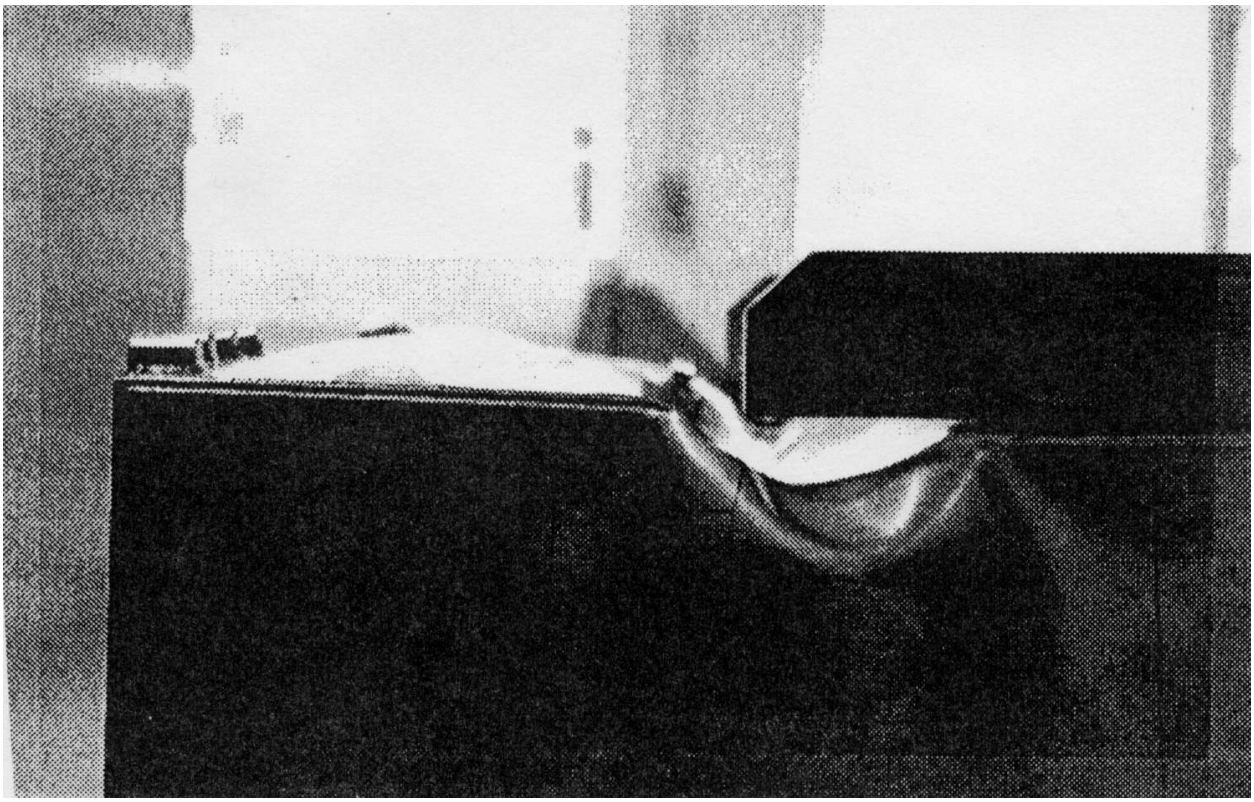

Figure 2-47 CTU 1J 9-m Vertical End Drop: Close-up Side View of Bottom Damage

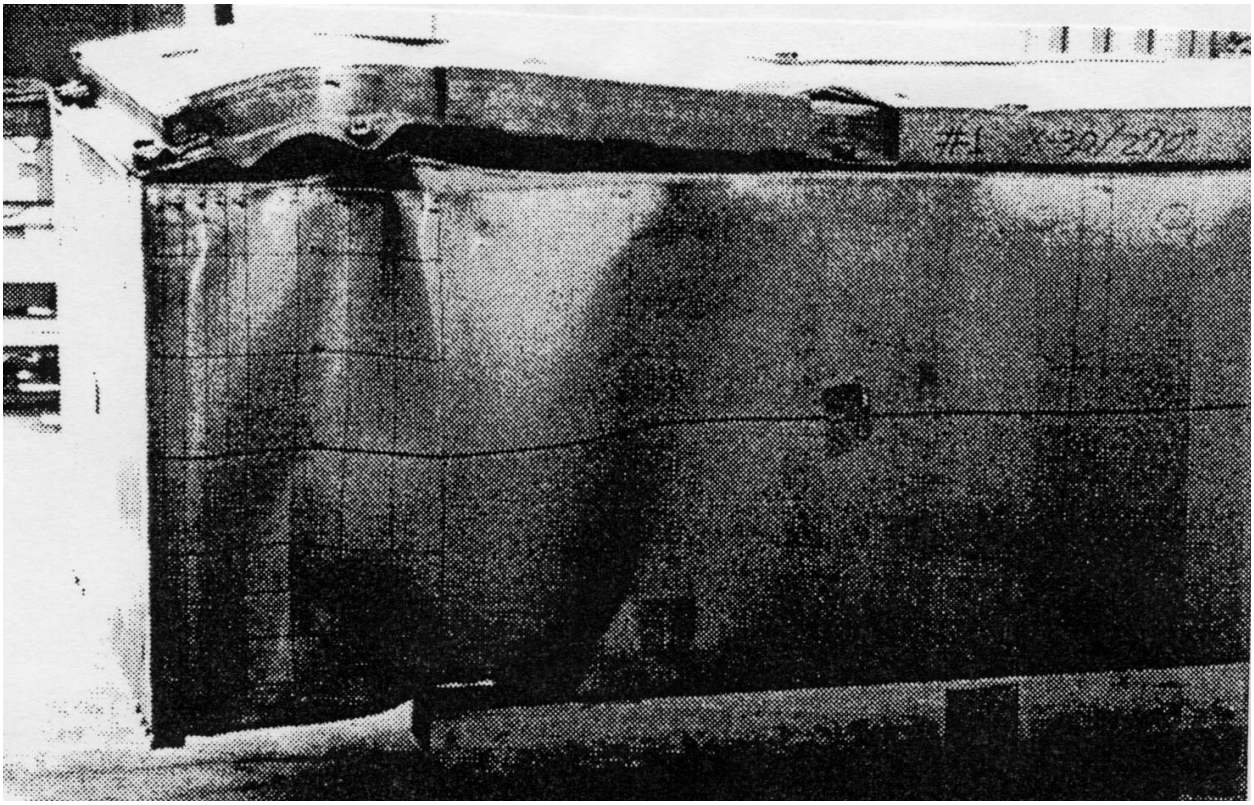

Figure 2-48 CTU 1J 9-m Vertical End Drop: Overall View of Damage

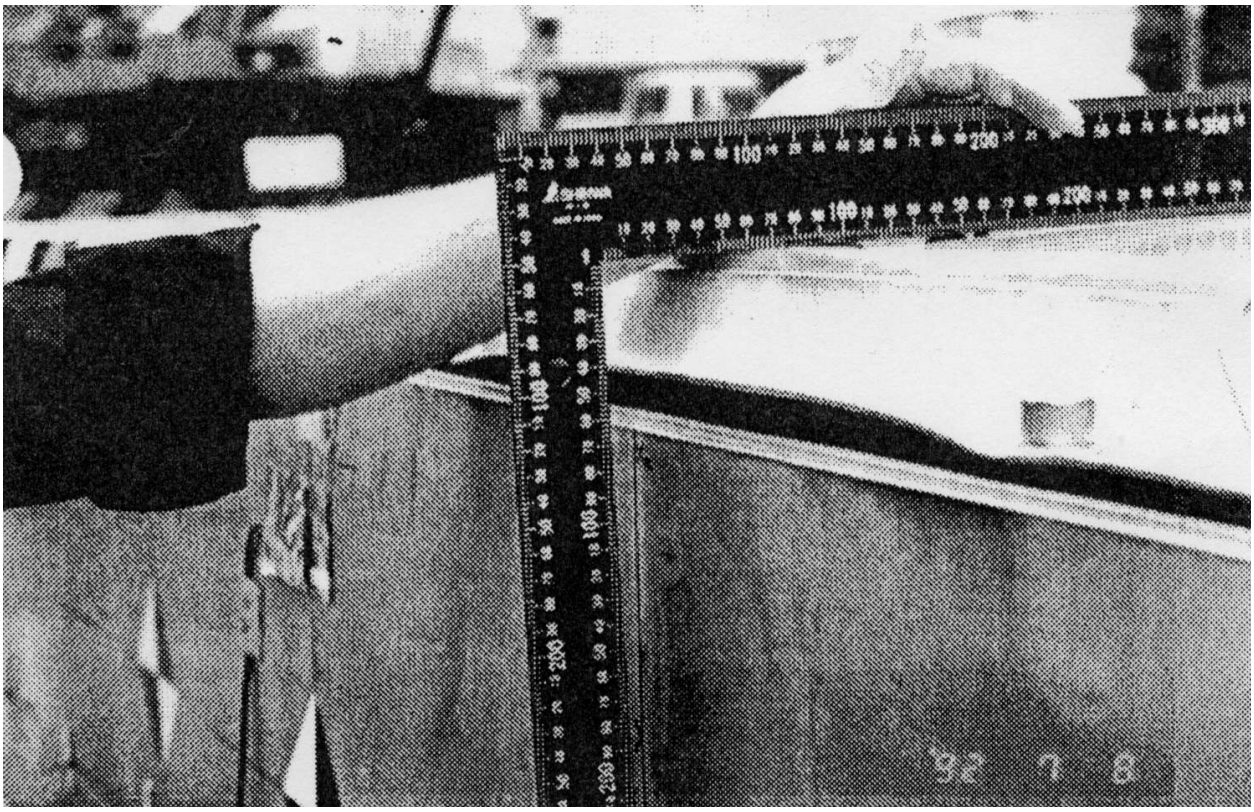

Figure 2-49 CTU 2J 9-m Horizontal Free Drop: Close-up Side View of Damage

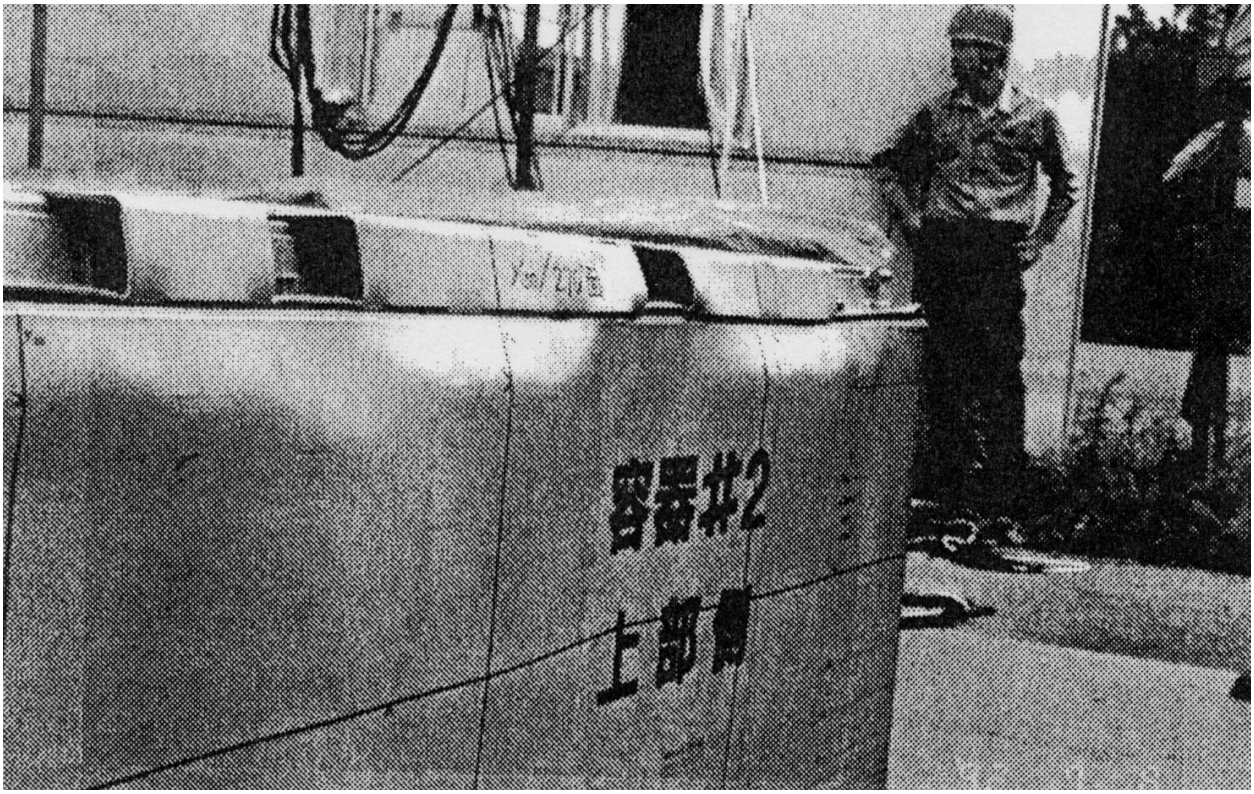

Figure 2-50 CTU 2J 9-m Horizontal Free Drop: Overall Side View of Damage

2.12.3 Outer Container Gasket Sealing Capability

The outer container for the RAJ-II packaging utilizes a 5 mm thick × 40 mm wide × 11,360 mm long, 50 shore durometer, solid natural rubber gasket. As shown in Appendix 1.4.1, Packaging General Arrangement Drawings, the gasket is attached to the flange of the outer container lid. The outer container lid is secured to the outer container body by twenty-four (24) M14 × 2, Type 304 stainless steel bolts, which are tightened to "wrench tight or as defined in user procedures". Since a specific tightening torque is not specified, the maximum bolt tension will be based on the minimum yield strength of the stainless steel.

The maximum force, F_b, in each lid bolt will be:

$$F_b = S_y(A_t)$$

where: S_y = Minimum yield strength = 206.8 MPa (30.0 ksi) (Ref. Table 2-2)

A_t = Tensile area for M14 × 2 bolt = 115 mm^2 (0.1783 in^2)

Substituting these values into the above equation yields a bolt force of 23,782 N (5,349 lb_f). The total compressive force applied to the gasket, F_{gasket}, is then:

$$F_{gasket} = (24)F_b = (24)(23{,}782) = 570{,}768\ \text{N}\ (128{,}376\ \text{lb}_f)$$

For the applied bolt force, the gasket compressive area, A_{gasket}, is 40 × 11,360 = 454,400 mm^2 (704.3 in^2). Conservatively neglecting any deflection of the 4-mm thick lid flange between the lid bolts, the resultant compressive stress on the gasket is then:

$$\sigma_{gasket} = \frac{570{,}768}{454{,}400} = 1.256\ \text{MPa}\ (182\ \text{psi})$$

The shape factor, s, for the 5 × 40 gasket is:

$$s = \frac{\text{One Load Area}}{\text{Total Free Area}} = \frac{\text{Width}}{2(\text{thickness})} = \frac{40}{10} = 4.0$$

From Figure 5-12 of Handbook of Molded and Extruded Rubber[a], the percent compressive deflection of the 50-durometer gasket with s = 4.0 at 182 psi compressive stress is approximately 3%, or 0.15 mm (0.006 in), which is minimal.

To determine whether the gasket is compressed with the applied bolt force, the compression modulus and the linear spring rate for the gasket is computed. Equation 3-7 of Handbook of Molded and Extruded Rubber, the linear spring rate, K_L, for the rubber gasket is:

$$K_L = \frac{E_c(A)}{h}$$

where: E_c = Compression modulus

A = Compression area of gasket = 454,400 mm^2 (704.3 in^2)

h = height of gasket = 5 mm (0.197 in)

The compression modulus is extracted from Figure 5-20 of the Handbook of Molded and Extruded Rubber for a shape factor "s" of 4.0 and an approximate compression of 3% for the 50 durometer gasket. From this figure, the compression modulus is interpolated to be 6,912 psi (47.7 MPa). The linear spring rate of the gasket is then:

[a] *Handbook of Molded and Extruded Rubber, Third Edition*, Goodyear Tire & Rubber Company.

$$K_L = \frac{6{,}912(704)}{0.197} = 24.7\times10^6 \text{ lb}_f\text{/in } (4.33\times10^6 \text{ N/mm})$$

To compress the gasket 0.15 mm (0.006 in), the required force in the bolts is:

$$24F_{bolt} = K_L\Delta = 24.7\times10^6(0.006) = 148{,}200 \text{ lb}_f \text{ } (659{,}266 \text{ N})$$

$$\Rightarrow F_{bolt} = 6{,}175 \text{ lb}_f \text{ } (27{,}648 \text{ N})$$

Since the resultant bolt force required to compress the gasket 3% is greater than the yield strength of the lid bolts, the gasket will not be compressed to the estimated 3% compression. To determine the estimated gasket compression with the maximum lid bolt force at yield strength (23,782 N [5,349 lb_f]), the linear spring rate will be computed for zero compression and then compared to the applied maximum force. From Figure 5-20 of the Handbook of Molded and Extruded Rubber for a shape factor "s" of 4.0, the compression modulus at zero compression will be:

$$E_c = 9{,}000(0.75) = 6{,}750 \text{ psi } (46.5 \text{ MPa})$$

For zero compression and this compression modulus, the linear spring rate is:

$$K_L = \frac{6{,}750(704)}{0.197} = 24.1\times10^6 \text{ lb}_f\text{/in } (4.23\times10^6 \text{ N/mm})$$

The resultant deformation of the gasket for this spring rate with the maximum bolt force is:

$$\Delta_{gasket} = \frac{24(F_{bolt})}{K_L} = \frac{24(23{,}782)}{4.23\times10^6} = 0.135 \text{ mm } (0.005 \text{ in})$$

This deformation is approximately 2.7% compression of the gasket. Prototypic seal testing in support of the TRUPACT-II package[b] has demonstrated that a pressure seal requires a minimum of 10% – 12% compression. Section 3.6, *Squeeze*, of the Parker O-ring Handbook[c] states that "*The minimum squeeze for all seals, regardless of cross-section should be about 0.2 mm (0.007 inches). The reason is that with a very light squeeze almost all elastomers quickly take 100% compression set.*" Based on these test results and the recommendations of Parker, the outer lid gasket will not form a pressure retaining seal.

---

[b] U. S. Department of Energy (DOE), *Safety Analysis Report for the TRUPACT-II Shipping Package*, USNRC Certificate of Compliance 71-9218, U.S Department of Energy, Carlsbad Field Office, Carlsbad, New Mexico.

[c] ORD 5700A/US, *Parker O-ring Handbook*, 2001, Parker Hannifin Corporation, Lexington, KY.

3.0 THERMAL EVALUATION

Provides an evaluation of the package to protect the fuel during varying thermal conditions.

3.1 DESCRIPTION OF THERMAL DESIGN

The RAJ-II package is designed to provide thermal protection as described in Subpart F of 10 CFR 71 for transport of two BWR fuel assemblies with negligible decay heat. Compliance is demonstrated with 10 CFR 71 subpart F in the following subsections. The RAJ-II protects the fuel through the use of an inner and outer container that restricts the exposure of the fuel to external heat loads. The insulated inner container further restricts the heat input to the fuel through its insulation. The fuel requires very little thermal protection since similar fuel has been tested to the 800ºC temperature without rupture.

Given negligible decay heat, the thermal loads on the package come solely from the environment in the form of solar radiation for Normal Conditions of Transport (NCT), as described in Section 3.4 or a half-hour, 800ºC (1,475°F) fire for Hypothetical Accident Conditions (HAC), described in Section 3.5.

Specific ambient temperatures and solar heat loads are considered in the package thermal evaluations. Ambient temperatures ranging from -40ºC to 38ºC (-40ºF to 100ºF) are considered for NCT. The HAC fire event considers an ambient temperature of 38ºC (100 F), with solar heat loading (insulation) before and after the HAC half-hour fire event.

Details and assumptions used in the analytical thermal models are described with the thermal evaluations.

3.1.1 Design Features

The primary features that affect the thermal performance of the package are 1) the materials of construction, 2) the inner and outer containers and 3) the thermal insulation of the inner container. The stainless sheet metal construction of the structural components of the inner and outer containers influences the maximum temperatures under normal conditions. The material also ensures structural stability under the hypothetical accident conditions as well as provides some protection to the fuel. Likewise the zirconium alloy cladding has also been proven to be stabile at the high temperatures potentially seen during the Hypothetical Accident Conditions (HAC).

The multi walled construction of the single walled outer container and the double walled inner container reduces the heat transfer as well as provides additional stability. The multi walled construction also reduces the opportunity for the fire in the accident conditions to impinge directly on the fuel.

The thermal insulation also greatly reduces the heat transfer to the fuel from external sources. The insulation consists of alumina silicate around most of the package plus the use of wood on the ends that both provide some insulation as well as shock absorbing capabilities.

3.1.2 Content's Decay Heat

Since the contents are unirradiated fuel, the decay heat is insignificant.

3.1.3 Summary Tables of Temperatures

Since the decay heat load is negligible, the maximum NCT temperature of 171ºF (77ºC, 350 K) occurs on the package exterior, and the maximum HAC temperature of 1198ºF (648ºC, 921 K) occurs at the inner surface of the inner container at the end of the fire. These analyses demonstrate that the RAJ-II package provides adequate thermal protection for the fuel assembly and will maintain the maximum fuel rod temperature well below the fuel rod rupture temperature of 800+°C under all transportation conditions.

3.1.4 Summary Tables of Maximum Pressures

The maximum pressure within the containment, the fuel rods during normal conditions of transport is 1.33 MPa (192.9 psia).

The maximum pressure during the hypothetical accident conditions is 3.50 MPa (508 psia).

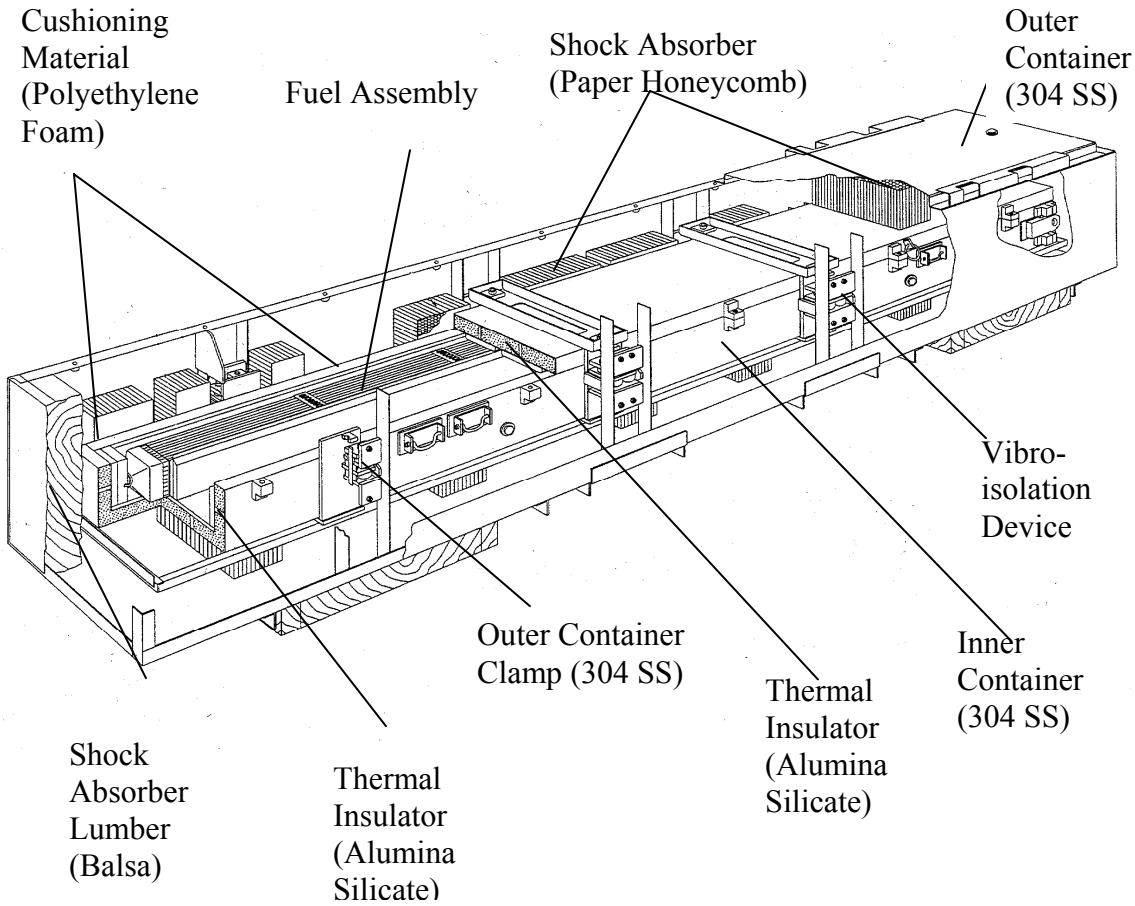

Figure 3-1 Overall View of RAJ-II Package

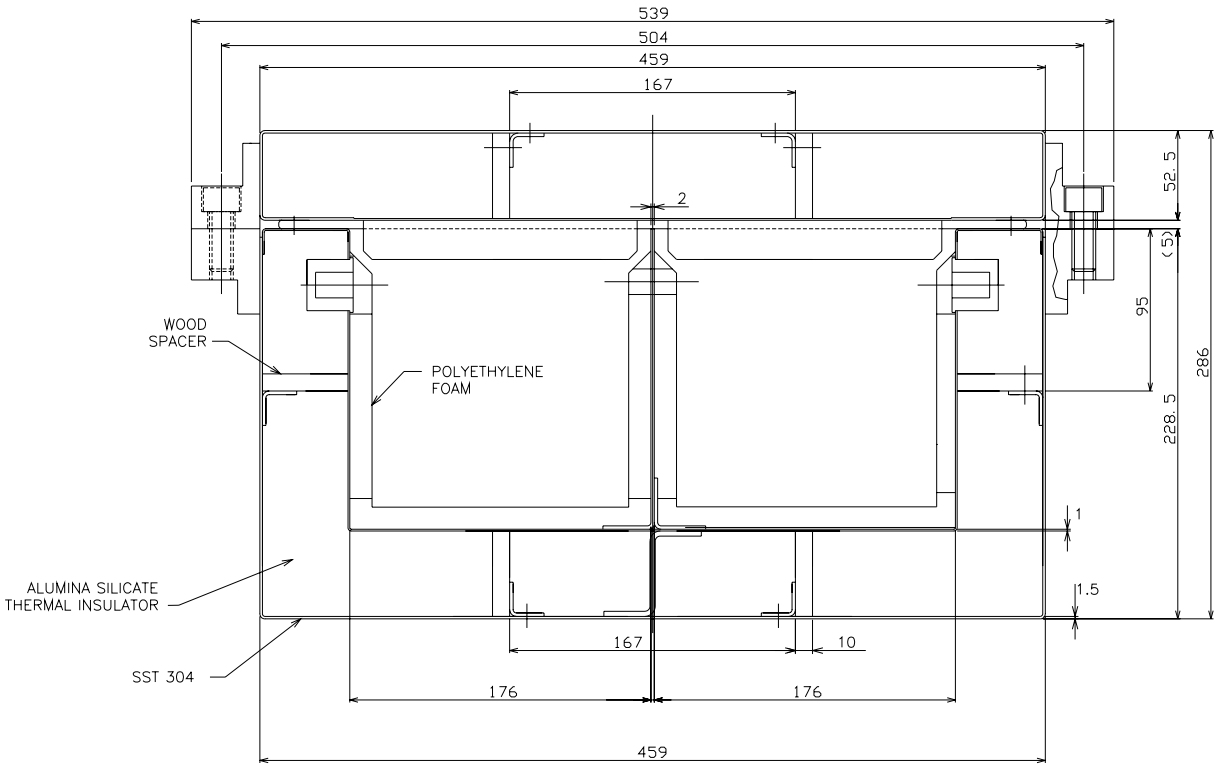

Figure 3-2 Transverse Cross-Sectional View of the Inner Container

3.2 MATERIAL PROPERTIES AND COMPONENT SPECIFICATIONS

3.2.1 Material Properties

The RAJ-II inner container is constructed primarily of Series 300 stainless steel, wood, and alumina silicate insulation. The void spaces within the inner container are filled with air at atmospheric pressure. The outer container is constructed of series 300 stainless steel, wood, and resin impregnated paper honeycomb. The thermal properties of the principal materials used in the thermal evaluations are presented in Table 3 - 1 and Table 3 - 2. Where necessary, the properties are presented as functions of temperature. Note that only properties for materials that constitute a significant heat transfer path are defined. A general view of the package is depicted in Figure 3-1. A sketch of the inner container transversal cross-section with the dimensions used in the calculation is presented in Figure 3-2.

For the Alumina Silicate**,** maximum values are specified because the maximum conductivity is the controlling parameter. This is because there is no decay heat in the payload and the only consideration is the material's ability to block of heat transfer to the fuel during the fire event.

Table 3 - 1 Material Properties for Principal Structural/Thermal Components

Material	Temperature, K	Thermal Conductivity, W/m-K	Specific Heat, J/kg-K	Density, kg/m^3	Notes
Wood	300	0.240	2,800	500	①
Series 300 Stainless Steel	300	15	477	7,900	②
	400	17	515		
	500	18	539		
	600	20	557		
	800	23	582		
	1,000	25	611		
Alumina Silicate Insulation	673	≤0.105	1,046 (Nominal)	250 (Nominal)	③
	873	≤0.151			
	1,073	≤0.198			④
	1,273	≤0.267			④

Notes:

① The material specified for the wood spacers. The properties have been placed with typical values for generic softwood.

② [Reference. 3.6.1.2. p.809, 811, 812, and 820]

③ The values shown are based on published data for Unifrax Duraboard LD [Reference 3.6.1.11] and include compensation for the possible variation in test data (see discussion in Section 3.2.1).

④ Values at higher temperatures than 1,000 K are linearly extrapolated.

Table 3 - 2 Material Properties for Air

Temperature (K)	Thermal Conductivity (W/m·K)	Density (kg/m^3)	Specific Heat (J/kg·K)	Coefficient of Kinematic Viscosity ν (m^2/s)	Prandtl Pr
300	0.0267	1.177	1005	15.66 E-06	0.69
310	0.0274	1.141	1005	16.54 E-06	0.69
320	0.0281	1.106	1006	17.44 E-06	0.69
330	0.0287	1.073	1006	18.37 E-06	0.69
340	0.0294	1.042	1007	19.32 E-06	0.69
350	0.030	1.012	1007	20.30 E-06	0.69
360	0.0306	0.983	1007	21.30 E-06	0.69
370	0.0313	0.956	1008	22.32 E-06	0.69
380	0.0319	0.931	1008	23.36 E-06	0.69
390	0.0325	0.906	1009	24.42 E-06	0.69
400	0.0331	0.883	1009	25.50 E-06	0.69
500	0.0389	0.706	1017	37.30 E-06	0.69
600	0.0447	0.589	1038	50.50 E-06	0.69
700	0.0503	0.507	1065	65.15 E-06	0.70
800	0.0559	0.442	1089	81.20 E-06	0.70
900	0.0616	0.392	1111	98.60 E-06	0.70
1000	0.0672	0.354	1130	117.3 E-06	0.70

Source: Reference 3.6.1.2, p.824

3.2.2 Component Specifications

None of the materials used in the construction of RAJ-II package, such as series 300 stainless steel and alumina silicate insulation, are sensitive to temperatures within the range of -40ºC to 800ºC (-40°F to 1,475 F) that spans the NCT and HAC environment. Stainless steel has a melting point above 1,400°C (2,550 F), and maximum service temperature of 427°C (800 F). Similarly, the ceramic fiber insulation has a maximum operating temperature of 1,300°C (2,372 °F). Wood is used as dunnage and as part of the inner package wall in the RAJ-II package. Before being consumed in the HAC fire, the wood would insulate portions of the inner container from exposure to the flames. However, the HAC transient thermal analyses presented herein conservatively neglects the wood's insulating effect, and assumes that all of the wood is consumed in the fire generating heat for all of its total mass.

The temperature limit for the fuel assembly's rods is greater than 800°C (1,472°F), based on the pressure evaluation provided in Section 3.5.3.2.

3.3 GENERAL CONSIDERATIONS

3.3.1 Evaluation by Analysis

The normal conditions of transport thermal conditions are evaluated by closed form calculations. The details of this analysis and supporting assumptions are found in that evaluation. The evaluation finds the maximum temperature for the outside of the package due to the insulation and uses that temperature for the contents of the package.

The transient hypothetical accident conditions are evaluated using an ANSYS finite element model. The model does not take credit for the outer container or the wood used in the inner container. Details of the model and the supporting assumptions maybe found in Section 3.5.

3.3.2 Evaluation by Test

Thermal testing was performed on fuel rods to determine the ability of the cladding (primary containment) to withstand temperatures greater than 800°C. The testing was performed for a range of fuel rods of different diameters, clad thickness and internal pressure. Since some of the current fuel designs for use in the RAJ-II are outside the range of parameters tested, additional thermal analyses have been performed to demonstrate the fuel rod's ability to withstand the HAC fire. In these tests, the fuel rods were heated to various temperatures from 700°C to 900°C for periods over one hour to determine the rupture temperature and pressure of the fuel. It was found that the fuel cladding did not fail at 800°C the temperature of the hypothetical accident conditions. This temperature associated pressure and resulting stress were used to provide the allowable conditions of the fuel which is used for containment.

3.3.3 Margins of Safety

For the normal condition evaluation the margins of safety are qualitative, based on comparisons to the much higher temperatures the fuel is designed for when it is in service in the reactors. There is no thermal deterioration of the packaging components at normal condition temperatures therefore no margins for the package components are calculated.

The margins of safety for the accident conditions are evaluated in Section 3.5 and are based on the testing discussed in Section 3.3.2.

3.4 THERMAL EVALUATION UNDER NORMAL CONDITIONS OF TRANSPORT

This section presents the results of thermal analysis of the RAJ-II package for the Normal Conditions of Transport (NCT) specified in 10 CFR 71.71. The maximum temperature for the normal conditions of transport is used as input (initial conditions) in the Hypothetical Accident Condition (fire event) analysis.

3.4.1 Heat and Cold

Per 10 CFR 71.71(c)(1), the maximum environmental temperature is 100°F (311 K), and per 10 CFR 71.71(c)(2), the minimum environmental temperature is -40°F (233 K).

Given the negligible decay heat of the fuel assembly, the thermal loads on the RAJ-II package come solely from the environment in the form of solar radiation for NCT as prescribed by 10 CFR 71.71(c)(1). As such, the solar heat input into the package is 800 g·cal/cm^2 for horizontal surfaces and 200 g·cal/cm^2 for vertical surfaces for a varying insolation over a 24-hour period).

3.4.1.1 Maximum Temperatures

For the analysis, the applied insolation is modeled transiently as sinusoidal over a 24-hour period, except when the sine function is negative (the insolation level is set to zero). The timing of the sine wave is set to achieve its peak at 12:00 PM and peak value of the curve is adjusted to ensure that the total energy delivered matched the regulatory values (800 g·cal/cm^2 for horizontal surfaces, 200 g·cal/cm^2 for vertical surfaces). As such, the total energy delivered in one day by the sine wave model is given by:

$$\int_{6\cdot hr}^{18\cdot hr} Q_{peak} \cdot \sin\left(\frac{\pi t}{12\cdot hr} - \frac{\pi}{2}\right) dt = \left(\frac{24\cdot hr}{\pi}\right) \times Q_{peak}$$

Using the expression above for the peak rate of insolation, the peak rates for top and side insolation may be calculated as follows:

-

Based on these inputs, the maximum NCT temperature on the inside surface of the inner container, as calculated in Appendix 3.6.3, is 350 K (77ºC, 171ºF).

Given negligible decay heat, the maximum accessible surface temperature of the RAJ-II package in the shade is the maximum environment temperature of 38°C (100°F), which is less than the 50°C (122°F) limit established in 10 CFR 71.43(g) for a non-exclusive use shipment.

3.4.1.2 Minimum Temperatures

The minimum environmental temperature that the RAJ-II package will be subjected to is -40°F, per 10 CFR 71.71(c)(2). Given the negligible decay heat load, the minimum temperature of the RAJ-II package is -40°F.

3.4.2 Maximum Normal Operating Pressure

The fuel rods are pressurized with helium to a maximum pressure of 1.145 MPa (absolute pressure (161.7 psia) helium at ambient temperature prior to sealing. Hence, the Maximum Normal Operating Pressure (MNOP) at the maximum normal temperature is:

$$MNOP = (P_1)\frac{T_{\max}}{T_{ambient}} = 1.1145 * \frac{350}{293} = 1.33 MPa = 192.9 psia$$

Since there is no significant decay heat and the fuel composition is stable, MNOP calculated above would not be expected to change over a one year time period.

3.4.3 Maximum Thermal Stresses

Due to the construction of the RAJ-II, light sheet metal constructed primarily of the same material, 304 SS, there are no significant thermal stresses. The package is constructed so that there is no significant constraint on any component as it heats up and cools down. The fuel cladding which provides containment is likewise designed for thermal transients, greater than what is found in the normal conditions of transport. The fuel rod is allowed to expand in the package. The fuel within the cladding is also designed to expand without interfering with the cladding.

3.5 THERMAL EVALUATION UNDER HYPOTHETICAL ACCIDENT CONDITIONS

This section presents the results of the thermal analysis of the RAJ-II package for the Hypothetical Accident Condition (HAC) specified in 10 CFR 71.73(c) (4).

For the purposes of the Hypothetical Accident Conditions fire analysis, the outer container of the RAJ-II package is conservatively assumed to be not present during the fire. This allows the outer surface of the inner container to be fully exposed to the fire event. The wood used in the inner container is conservatively assumed to combust completely. By ignoring the outer container and applying the fire environment directly to the inner container, the predicted temperature of the fuel rods is bounded. To provide a conservative estimate of the worst-case fuel rod temperature, the fuel assembly and its corresponding thermal mass are not explicitly modeled as well as the polyethylene foam shock absorber. The maximum fuel rod temperature is conservatively derived from the maximum temperature of the inside surface of the inner stainless steel wall. The analysis considering the insulation and multi-layers of packaging is very conservative because as discussed in Section 3.3.2 the bare fuel has been demonstrated to maintain integrity when exposed to temperatures that equal those found in the hypothetical accident conditions.

Thermal performance of the RAJ-II package is evaluated analytically using a 2-D model that represents a transversal cross-section of the inner container (Figure 3-2) in the region containing the metallic and wood spacers. The 2-D inner container finite element model was developed using the ANSYS computer code [Reference 3.6.1.3]. ANSYS is a comprehensive thermal, structural and fluid flow analysis package. It is a finite element analysis code capable of solving steady state and transient thermal analysis problems in one, two or three dimensions. Heat transfer via a combination of conduction, radiation and convection can be modeled.

The solid entities were modeled in the present analysis with PLANE55 two-dimensional elements and the radiation was modeled using the AUX12 Radiation Matrix method. The developed ANSYS input file is included as Appendix 3.6.2.

The initial temperature distribution in the inner container prior to the HAC fire event is a uniform 375 K conservatively corresponding to the outer surface temperature of the inner container per the normal condition calculations presented in Appendix 3.6.3.

3.5.1 Initial Conditions

The environmental conditions preceding and succeeding the fire consist of an ambient temperature of 38 ºC (311 K) and insulation per the normal condition thermal analysis. The solar absorptivity coefficient of the outer surface has been increased for the post-fire period to 1 to include changes due to charring of the surfaces during the fire event.

3.5.2 Fire Test Conditions

The Hypothetical Accident Condition fire event is specified per 10 CFR 71.73(c) (4) as a half-hour, 800ºC (1,073 K) fire with forced convection. For the purpose of calculation, the value of the package surface absorptivity coefficient (0.8) is selected as the highest value between the actual value of the surface (0.42) and a value of 0.8 as specified in 10 CFR 71.73(c) (4).

A value of 1.0 for the emissivity of the flame for the fire condition is used in the calculation. The rationale for this is that 1.0 maximizes the heating of the package. This value exceeds the minimum value of 0.9 specified in 10 CFR 71.73(c) (4). The Hypothetical Accident Condition (HAC) fire event is specified per 10 CFR 71.73(c)(3) as a half-hour, 800°C (1,475°F) fire with forced convection and an emissivity of 0.9. The environmental conditions preceding and succeeding the fire consist of an ambient temperature of 100 °F and insulation per the NCT thermal analyses.

To model the combustion of the wood, the wood elements of the model are given a heat generation rate based on the high heat value of Western Hemlock of 3630 Btu/lb (8.442×10^6 J/kg) from Reference 3.6.1.8, Section 7, Table 9. It is conservatively assumed that the entire mass of the wood will burn. Moreoever, the wood will burn across its thinnest section from opposite faces. Using data burn rate data for redwood which has approximately the same density as hemlock [3.6.1.8], each face will burn 5 mm at a minimum rate of 0.543 mm/min [Reference 3.6.1.10] resulting in a 9.2 minute time of combustion. This conservatively results in the longest burn time for the hemlock, and the greatest effect on temperature. The resulting heat generation rate in the wood spacers is equal to:

$$\dot{Q} = (8.42\times10^6) \times (500 \text{ kg} / \text{m}^3) / (9.2 \text{ sec} \times 60) = 7.63\times10^6 \text{ W/m}^3\text{/sec.}$$

3.5.2.1 Heat Transfer Coefficient during the Fire Event

During a HAC hydrocarbon fire, the heating gases surrounding the package will achieve velocities sufficient to induce forced convection on the surface of the package. Peak velocities measured in the vicinity of the surfaces were under 10 m/s [Reference 3.6.1.4].

The heat transfer coefficient takes the form [Reference 3.6.1.4, p. 369]:

$$h=k/D\cdot C\cdot(u\cdot D/\upsilon)^m\cdot Pr^{1/3} \qquad (8)$$

Where:

D: average width of the cross-section of the inner container (0.373 m)

k: thermal conductivity of the fluid

υ: kinematic viscosity of the fluid

u: free stream velocity

C, m: constants that depend on the Reynolds number ($Re=u\cdot D/\upsilon$)

Pr: Prandtl number for the fluid

The property values of k, υ and Pr are evaluated at the film temperature, which is defined as the mean of the wall and free stream fluid temperatures. At the start of the fire the wall temperature is 375 K (101.7ºC, 215ºF) and the stream fluid temperature is 1,073 K (1,475ºF). The film temperature is therefore 710.5 K, and the property values for air at this temperature (interpolated from Table 3 - 2) are k=0.0509 W/m·K, υ=66.84E-06 m^2/s and Pr= 0.70. Assuming a maximum stream velocity of 10 m/s this yields a Reynolds number of 55.8E03. At this value of Re, the constants C and n are 0.102 and 0.675 respectively [Reference 3.6.1.4, Table 7.3].

$$h = \frac{0.0509 \cdot 0.102 \cdot (10 \cdot 0.373 / 66.84 \cdot 10^{-6})^{0.675} \cdot (0.70)^{1/3}}{0.373}$$

h=19.8 $W/m^2 \cdot K$

A value of 19.8 $W/m^2 \cdot K$ was conservatively used in the analysis of the regulatory fire.

3.5.2.2 Heat Transfer Coefficient during Post-Fire Period

During the post-fire period of the HAC, it is conservatively assumed that there is negligible wind and that heat is transferred from the inner container to the environment via natural convection. Natural heat transfer coefficients from the outer surface of the square inner container are calculated as follows.

Reference 3.6.1.4 recommends the following correlations for the Nusselt number (Nu) describing natural convection heat transfer to air from heated vertical and horizontal surfaces:

Vertical heated surfaces [Reference 3.6.1.4, p. 493]:

$$Nu = (0.825 + \frac{0.387 \cdot (Gr \cdot \mathrm{Pr})^{1/6}}{(1 + (0.492 / \mathrm{Pr})^{9/16})^{8/27}})^2 \quad \text{For entire range of Ra=Gr·Pr} \qquad (9)$$

Where:

Nu: Nusselt number

Gr: Grashof number

Pr: Prandtl number

Horizontal heated surfaces facing upward [Reference 3.6.1.4, p.498]:

$$Nu = 0.54 \cdot (Gr \cdot \Pr)^{1/4} \text{ for } (10^4 < Gr \cdot Pr < 10^7) \quad (10)$$

$$Nu = 0.15 \cdot (Gr \cdot \Pr)^{1/3} \text{ for } (10^7 < Gr \cdot Pr < 10^{11}) \quad (11)$$

and, for horizontal heated surfaces facing downward:

$$Nu = 0.27 \cdot (Gr \cdot \Pr)^{1/4} \text{ for } (10^5 < Gr \cdot Pr < 10^{10}) \quad (12)$$

The correlations for the horizontal surfaces are calculated using a characteristic length defined by the relation L=A/P, where A is the horizontal surface area and P is the perimeter [Reference 3.6.1.4, p. 498]. The calculated characteristic length for the horizontal surfaces of the inner container is L=0.209 m (A=2.14812 m^2 and P=10.278 m).

The following convective heat transfer coefficients (Table 3 - 1) have been calculated using Eq. (5), (6), (9), (10), (11) and (12). The corresponding characteristic length used in calculating the Nusselt number for each surface is also used in Eq. 5 for calculating the heat transfer coefficient. The thermal properties of air have been evaluated at the mean film temperature ($=(T_s+T_{ambient})/2$).

The effects of solar radiation are included during the post-fire period by specifying the equivalent heat flow for each node of the surfaces exposed to fire for an additional 3.5 hours, i.e. the fire starts at at the time of the peak temperature in the inner container (8 hours after sunrise) and is 0.5 hours in duration. This results in an additional 3.5 hours of solar insolation. Using the peak rates calculated in section 3.4.1.1, the nodal heat flows at 2:30 PM are equal to:

$$\dot{q}_{top} = \frac{1{,}218 \frac{W}{m^2}\left(Sin\left(\frac{\pi \times (6+8.5)}{12} - \frac{\pi}{2} \right)\right)(0.459 m)}{(155-1)} = 2.88\, W/m$$

$$\dot{q}_{side} = \frac{305 \frac{W}{m^2}\left(Sin\left(\frac{\pi \times 14.5}{12} - \frac{\pi}{2} \right)\right)(0.281 m)}{99-1} = 0.69\, W/m$$

where 0.459 m is the width of the inner container, 0.281 m is its height, and the model is 155 nodes in width by 99 nodes in height. For the remaining 3.5 hours of solar insolation, these heat fluxes are conservatively applied as bounding constant values rather than varying with time.

The solar absorptivity coefficient of the outer surface is conservatively assumed to be 1. The duration of the post-fire period has been extended to 12.5 hr to investigate the cool-down of the inner container.

3.5.3 Maximum Temperatures and Pressure

3.5.3.1 Maximum Temperatures

The peak fuel rod temperature, which is conservatively assumed to be the same as the inner wall temperature of the package, response over the course of the HAC fire scenario is illustrated in Figure 3-3. The temperature reaches its maximum point of 921 K or 648°C (1198 F) at the end of the fire or 1,800 seconds after the start of the fire. This peak temperature occurs at top corners of the inner wall.

The maximum temperature even when applied to the fuel directly is well below the maximum temperature the fuel can withstand. Similar fuel with no thermal protection has been tested in fire conditions at over 800°C (1,475°F) for more than 60 minutes without failures.

3.5.3.2 Maximum Internal Pressure

The maximum pressure for the fuel can be determined by considering that the fuel is pressurized initially with helium. As the fuel is heated, the internal pressure in the cladding increases. By applying the perfect gas law the pressure can be determined and the resulting stresses in the cladding can be determined. Since the temperatures can be well above the normal operating range of the fuel the cladding performance can best be determined by comparison to test data.

Similar fuel with similar initial pressures has been heated in an oven to over 800ºC for over an hour without failures (Reference 3.6.1.6). The fuel that was tested in the oven was pressurized with 10 atmospheres of helium. When heated to the 800°C it had an equivalent pressure of:

$$P_{\max} = (P_1)\frac{T_{\max}}{T_{ambient}} = 1.1145 MPa * \frac{1073}{293} = 4.08 MPa = 592 psia$$

This results in an applied load to the cladding of 3.98 MPa or 577.3 psig. The fuel that was tested had an outer diameter of 0.4054 inch (10.30 mm). Since the fuel when tested to 850°C had some ruptures but did not rupture at 800°C when held at those temperatures for 1 hour, the stresses at 800°C are used as the conservative allowable stress. Both the tested fuel and the fuels to be shipped in the RAJ-II have similar zirconium cladding. The stress generated in the cladding of the test fuel is:

$$\sigma = \frac{pr}{t} = \frac{3.98 MPa x 4.56 mm}{0.584 mm} = 31.1 MPa = 4510 psi$$

Recognizing that the properties of the fuel cladding degrade as the temperature increases the above calculated stress is conservatively used as the allowable stress for the fuel cladding for the various fuels to be shipped. The fuel is evaluated at the maximum temperature the inner wall of the inner container sees during the Hypothetical Accident Condition thermal event evaluated above. Table 3 - 5 shows the maximum pressure for each type of fuel and the resulting stress and margin. The limiting design properties of the fuel, maximum cladding internal diameter, minimum cladding wall thickness and initial pressurization for each type of fuel are considered in determining the margin of safety. Positive margins are conservatively determined for each type of fuel demonstrating that containment would be maintained during the Hypothetical Accident events. The minimum cladding thickness does not include the thickness of the liner if used.

The results of the transient analysis are summarized in Table 3 - 4. The temperature evolution during the transient in three representative locations on the inner wall and one on the outer wall is included. The maximum temperature on the inner wall is 921 K (648°C, 1198°F) and is reached at the upper inner corners of the container, 1,800 seconds after the beginning of the fire. The graphic evolution of the temperatures listed in Table 3 - 4 is represented in Figure 3-3. Representative plots of the isotherms at various points in time are depicted in Figure 3-4 through Figure 3-7.

The temperatures and resulting pressures are within the capabilities of the fuel cladding as shown by test. Therefore the fuel cladding and closure welds maintain containment during the Hypothetical Accident Conditions.

The temperatures and resulting pressures are within the capabilities of the fuel cladding as shown by test. Therefore the fuel cladding and closure welds maintain containment during the Hypothetical Accident Conditions.

3.5.4 Accident Conditions for Fissile Material Packages for Air Transport

Approval for air transport is not requested for the RAJ-II.

Table 3 - 3 Convection Coefficients for Post-fire Analysis

T_s (surface temperature)		**$T_{ambient}$**		**H (vertical surface)**	**h (horizontal surface facing upward)**	**h (horizontal surface facing downward)**
ºF	K	ºF	K	($W/m^2 \cdot K$)	($W/m^2 \cdot K$)	($W/m^2 \cdot K$)
150	338.71	100	311	4.68	5.19	2.34
200	366.48	100	311	5.61	6.34	2.74
250	394.26	100	311	6.18	7.05	2.99
300	422.04	100	311	6.60	7.55	3.17
350	449.82	100	311	6.90	7.92	3.30
400	477.59	100	311	7.13	8.18	3.41
600	588.71	100	311	7.64	8.74	3.67
900	755.37	100	311	8.00	9.07	3.89
1,375	1,019.26	100	311	8.25	9.17	4.09

Table 3 - 4 Calculated Temperatures for Different Positions on the Walls of the Inner Container Walls

Time (s)	Inner Wall Temperature (top right corner) (K)	Inner Wall Temperature (bottom) (K)	Inner Wall Temperature (top) (K)	Outer Wall Temperature (K)
0.1	375	375	375	377
911	750	667	546	1,062
1,800	921	821	696	1,067
1,900	918	823	710	807
2,000	905	817	723	686
2,200	868	797	742	583
2,600	803	761	760	509
3,268	723	715	758	463
4,280	639	662	727	437
27,973	354	335	369	378
45,000	349	324	358	377

Table 3 - 5 Maximum Pressure

Parameter	Units	8 X 8 Fuel	9 X 9 Fuel	10 X10 Fuel
Initial Pressure	MPa absolute	0.608	1.1145	1.1145
Fill temperature	°C	20	20	20
Temperature during HAC	°C	648	648	648
Outside Diameter Maximum	mm	12.5	11.46	10.52
	inches	.492	.4512	.4142
Minimum Allowable Cladding Thickness	inches	0.0268	0.0224	0.0205
	mm	.68	0.570	0.520
Cladding Inside Diameter Maximum	mm	11.14	10.32	9.48
	inches	.439	.406	.373
Pressure @ HAC	MPa(absolute)	1.91	3.50	3.50
	Psia	277	508	508
Applied Pressure @ HAC	MPa	1.81	3.40	3.40
	Psig	262	493	493
Stress Pr/t	MPa	14.82	30.8	31.0
	Psi	2,149	4,467	4,498
Margin	(allowed stress/actual stress)-1	1.10	0.01	0.003
Max allowed cladding	Inside Radius/Thickness	20.20	9.14	9.14

Note: Table values for cladding thickness and diameters are for example purposes and represent current limiting fuel designs. However, all fuel to be shipped must have a maximum pre-pressure times the maximum Inside Radius/Thickness product of 9.14 x 1.1145 MPa = 10.18653 MPa or less. Thus, all products must meet the maximum product of allowed pressure multiplied by Inside Radius/Thickness of 10.18653 MPa.

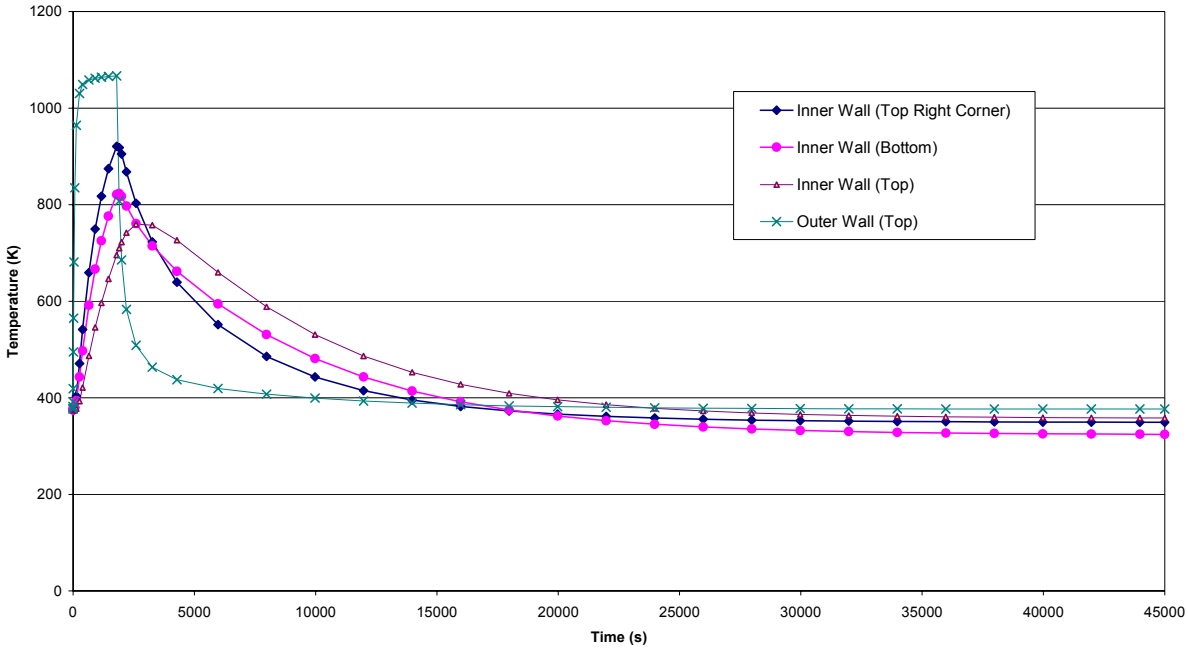

Figure 3-3 Calculated Temperature Evolution During Transient

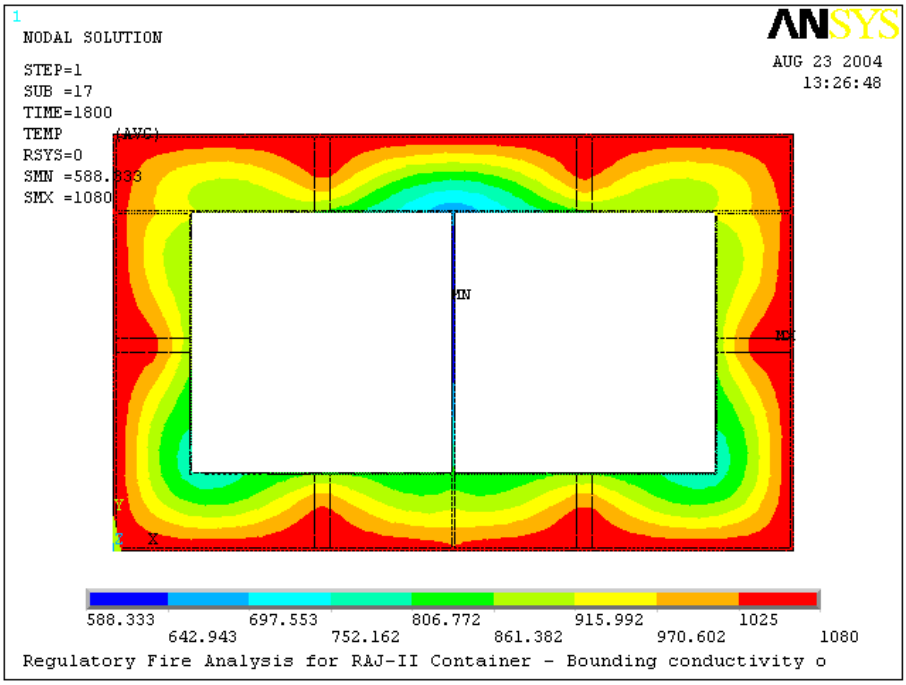

Figure 3-4 Calculated Isotherms at the End of Fire Phase (1,800 s)

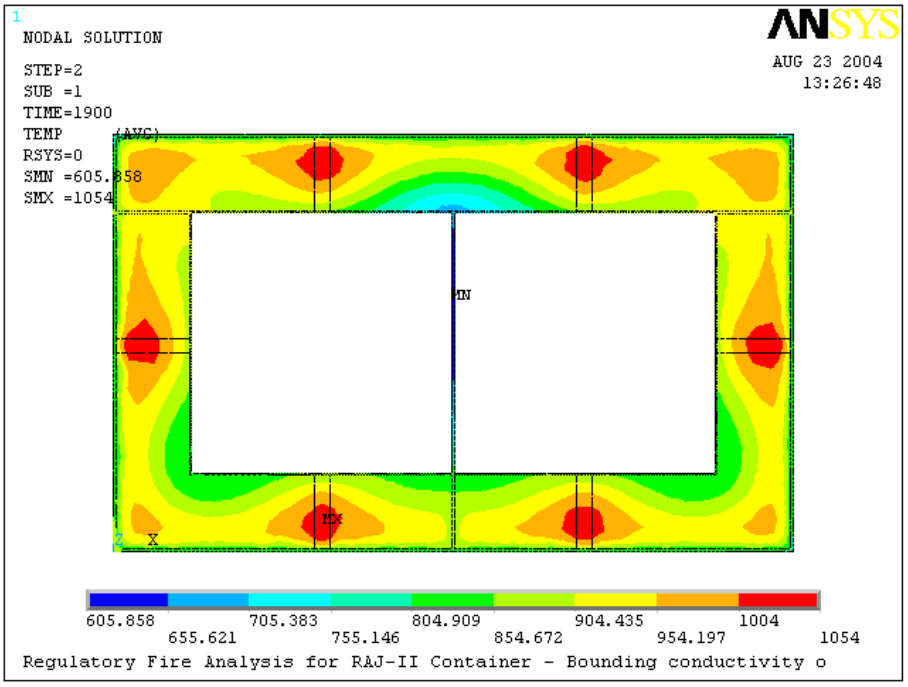

Figure 3-5 Calculated Isotherms at 100s After the End of Fire

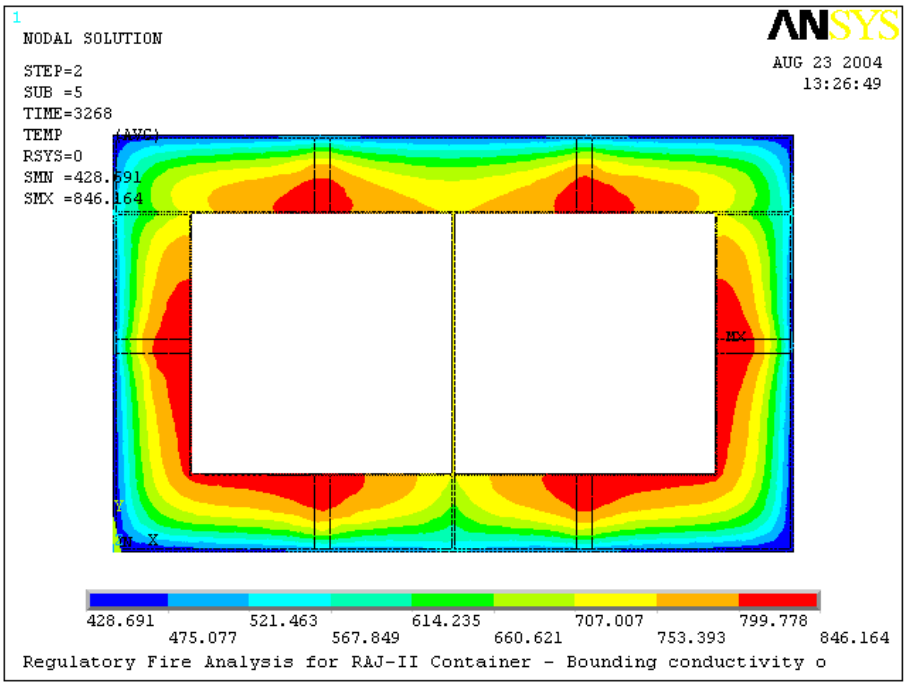

Figure 3-6 Calculated Isotherms at 1,468 s After the End of Fire

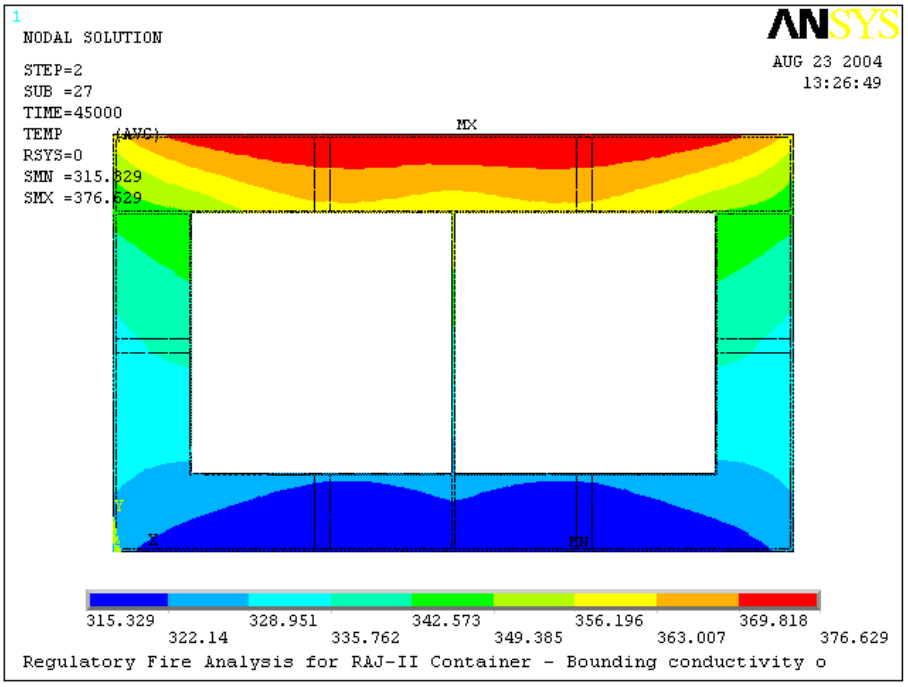

Figure 3-7 Calculated Isotherms at 12 hr After the End of Fire

3.6 APPENDIX

3.6.1 References

3.6.1.1 10 CFR 71, Packaging and Transportation of Radioactive Material

3.6.1.2 Mills, A.F., Heat Transfer, Irwin, Inc., Homewood, Illinois, 1992

3.6.1.3 ANSYS Finite Element Computer Code, Version 5.6, ANSYS, Inc., 2000

3.6.1.4 McCaffery, B.J., Purely Buoyant Diffusion Flames – Some Experimental Results, Report PB80-112113, U.S. National Bureau of Standards, Washington, D.C., 1979

3.6.1.5 Incropera, F.P., Dewitt, D.P., Fundamentals of Heat and Mass Transfer, John Wiley and Sons, Inc., New York, New York, 19966

3.6.1.6 GNF-2 Fuel Rod Response to An Abnormal Transportation Event (proprietary)(30 Minute Fire)

3.6.1.7 Handbook of Heat Transfer, Warren M. Rohsenow, James P. Hartnett, McGraw Hill book company.

3.6.1.8 Standard Handbook for Mechanical Engineers, Baumeister , Marks, McGraw Hill book company, Seventh edition.

3.6.1.9 Thermal Properties of Paper, PTN149, Charles Green, Webster New York, 2002 (http://www.frontiernet.net/~charmar/**).**

3.6.1.10 Tran, H.C., and White, R. H., Burning Rate of Solid Wood Measured in a Heat Release Calrimeter, Fire and Materials, Vol. 16, pp 197-206,1992.

3.6.1.11 "Pactec Specification: Regarding Global Nuclear Fuel Specification for Alumina Silicate for use in the RAJ-II Shipping container," Unifrax Corporation, 6/3/04.

3.6.2 ANSYS Input File Listing

Listing of the ANSYS input file (file: model_fl_heat.inp)

```
fini

/clear

/filnam,model_f1_heat,

/outp,model_f1_heatout,out

/PREP7

/TITLE, Regulatory Fire Analysis for RAJ-II Container -
Bounding conductivity of Alumina

/UNITS,SI

/SHOW,JPEG

!*

!*set element types

!*

ET,1,PLANE55,1

ET,2,LINK32

ET,3,MATRIX50,1

!*

!*  define keypoints

!*

K,1,0,0,0,

K,2,0.459,0,0,

K,3,0,0.0015,0,

K,4,0.0015,0.0015,0,

K,5,0.136,0.0015,0,

K,6,0.146,0.0015,0,

K,7,0.2285,0.0015,0,

K,8,0.2305,0.0015,0,

K,9,0.313,0.0015,0,

K,10,0.323,0.0015,0,

K,11,0.4575,0.0015,0,

K,12,0.459,0.0015,0,

K,13,0.0015,0.0515,0,

K,14,0.0515,0.0515,0,

K,15,0.136,0.0515,0,

K,16,0.146,0.0515,0,

K,17,0.2285,0.0515,0,

K,18,0.2305,0.0515,0,

K,19,0.313,0.0515,0,

K,20,0.323,0.0515,0,

K,21,0.4075,0.0515,0,

K,22,0.4575,0.0515,0,

K,23,0.0515,0.0525,0,

K,24,0.0525,0.0525,0,
```

K,25,0.2285,0.0525,0,

K,26,0.2305,0.0525,0,

K,27,0.4065,0.0525,0,

K,28,0.4075,0.0525,0,

K,29,0.0525,0.0705,0,

K,30,0.0705,0.0705,0,

K,31,0.2105,0.0705,0,

K,32,0.2285,0.0705,0,

K,33,0.2305,0.0705,0,

K,34,0.2485,0.0705,0,

K,35,0.3885,0.0705,0,

K,36,0.4065,0.0705,0,

K,37,0.0015,0.1335,0,

K,38,0.0515,0.1335,0,

K,39,0.4075,0.1335,0,

K,40,0.4575,0.1335,0,

K,41,0.0015,0.1435,0,

K,42,0.0515,0.1435,0,

K,43,0.4075,0.1435,0,

K,44,0.4575,0.1435,0,

K,45,0.0705,0.1975,0,

K,46,0.2105,0.1975,0,

K,47,0.2485,0.1975,0,

K,48,0.3885,0.1975,0,

K,49,0.0525,0.2155,0,

K,50,0.060,0.2115,0,

K,51,0.066,0.2055,0,

K,52,0.2175,0.2055,0,

K,53,0.2235,0.2115,0,

K,54,0.2285,0.2155,0,

K,55,0.2305,0.2155,0,

K,56,0.2355,0.2115,0,

K,57,0.2415,0.2055,0,

K,58,0.393,0.2055,0,

K,59,0.399,0.2115,0,

K,60,0.4065,0.2155,0,

K,61,0.,0.2275,0,

K,62,0.0015,0.2275,0,

K,63,0.0515,0.2275,0,

K,64,0.0525,0.2275,0,

K,65,0.4065,0.2275,0,

K,66,0.4075,0.2275,0,

K,67,0.4575,0.2275,0,

K,68,0.459,0.2275,0,

K,69,0.,0.2285,0,

K,70,0.0525,0.2285,0,

K,71,0.06,0.2285,0,

K,72,0.2235,0.2285,0,

```
K,73,0.2285,0.2285,0,
K,74,0.2305,0.2285,0,
K,75,0.2355,0.2285,0,
K,76,0.399,0.2285,0,
K,77,0.4065,0.2285,0,
K,78,0.459,0.2285,0,
K,79,0.,0.2295,0,
K,80,0.0015,0.2295,0,
K,81,0.136,0.2295,0,
K,82,0.146,0.2295,0,
K,83,0.313,0.2295,0,
K,84,0.323,0.2295,0,
K,85,0.4575,0.2295,0,
K,86,0.459,0.2295,0,
K,87,0.,0.2795,0,
K,88,0.0015,0.2795,0,
K,89,0.136,0.2795,0,
K,90,0.146,0.2795,0,
K,91,0.313,0.2795,0,
K,92,0.323,0.2795,0,
K,93,0.4575,0.2795,0,
K,94,0.459,0.2795,0,
K,95,0.,0.281,0,
K,96,0.459,0.281,0,
SAVE
!*
!* define material properties
!*
!*
!* STAINLESS STEEL (SS304)
!*
MP,DENS,1,7900
MPTEMP,1,300,400,500,600,800,1000
MPDATA,kxx,1,1,15,17,18,20,23,25
MPDATA,c,1,1,477,515,539,557,582,611
!*
!* THERMAL INSULATOR
!*
MP,DENS,2,260
MP,C,2,1046
MPTEMP
MPTEMP,1,673,873,1073,1273
MPDATA,KXX,2,1,0.105,0.151,0.198,0.267 !MAX
VALUES
!*
!*
!*  WOOD (generic softwood)
!*
UIMP,3,EX, , , ,
```

```
UIMP,3,NUXY, , , ,
UIMP,3,ALPX, , , ,
UIMP,3,REFT, , , ,
UIMP,3,MU, , , ,
UIMP,3,DAMP, , , ,
UIMP,3,DENS, , ,500,
UIMP,3,KXX, , ,0.24,
UIMP,3,C, , ,2800,
UIMP,3,ENTH, , , ,
UIMP,3,HF, , , ,
UIMP,3,EMIS, , , ,
UIMP,3,QRATE, , , ,
UIMP,3,VISC, , , ,
UIMP,3,SONC, , , ,
UIMP,3,MURX, , , ,
UIMP,3,MGXX, , , ,
UIMP,3,RSVX, , , ,
UIMP,3,PERX, , , ,
!*
!* define areas
!*
FLST,2,12,3
FITEM,2,1
FITEM,2,2
FITEM,2,12
FITEM,2,11
FITEM,2,10
FITEM,2,9
FITEM,2,8
FITEM,2,7
FITEM,2,6
FITEM,2,5
FITEM,2,4
FITEM,2,3
A,P51X
FLST,2,7,3
FITEM,2,3
FITEM,2,4
FITEM,2,13
FITEM,2,37
FITEM,2,41
FITEM,2,62
FITEM,2,61
A,P51X
FLST,2,5,3
FITEM,2,4
FITEM,2,5
FITEM,2,15
```

```
FITEM,2,14
FITEM,2,13
A,P51X
FLST,2,4,3
FITEM,2,5
FITEM,2,6
FITEM,2,16
FITEM,2,15
A,P51X
FLST,2,4,3
FITEM,2,6
FITEM,2,7
FITEM,2,17
FITEM,2,16
A,P51X
FLST,2,4,3
FITEM,2,7
FITEM,2,8
FITEM,2,18
FITEM,2,17
A,P51X
FLST,2,4,3
FITEM,2,8
FITEM,2,9
```

```
FITEM,2,19
FITEM,2,18
A,P51X
FLST,2,4,3
FITEM,2,9
FITEM,2,10
FITEM,2,20
FITEM,2,19
A,P51X
FLST,2,5,3
FITEM,2,10
FITEM,2,11
FITEM,2,22
FITEM,2,21
FITEM,2,20
A,P51X
FLST,2,7,3
FITEM,2,11
FITEM,2,12
FITEM,2,68
FITEM,2,67
FITEM,2,44
FITEM,2,40
FITEM,2,22
```

```
A,P51X
FLST,2,5,3
FITEM,2,13
FITEM,2,14
FITEM,2,23
FITEM,2,38
FITEM,2,37
A,P51X
FLST,2,8,3
FITEM,2,23
FITEM,2,24
FITEM,2,29
FITEM,2,49
FITEM,2,64
FITEM,2,63
FITEM,2,42
FITEM,2,38
A,P51X
FLST,2,14,3
FITEM,2,14
FITEM,2,15
FITEM,2,16
FITEM,2,17
FITEM,2,18
FITEM,2,19
FITEM,2,20
FITEM,2,21
FITEM,2,28
FITEM,2,27
FITEM,2,26
FITEM,2,25
FITEM,2,24
FITEM,2,23
A,P51X
FLST,2,8,3
FITEM,2,25
FITEM,2,26
FITEM,2,33
FITEM,2,55
FITEM,2,74
FITEM,2,73
FITEM,2,54
FITEM,2,32
A,P51X
FLST,2,8,3
FITEM,2,27
FITEM,2,28
FITEM,2,39
```

```
FITEM,2,43
FITEM,2,66
FITEM,2,65
FITEM,2,60
FITEM,2,36
A,P51X
FLST,2,5,3
FITEM,2,21
FITEM,2,22
FITEM,2,40
FITEM,2,39
FITEM,2,28
A,P51X
FLST,2,4,3
FITEM,2,37
FITEM,2,38
FITEM,2,42
FITEM,2,41
A,P51X
FLST,2,4,3
FITEM,2,39
FITEM,2,40
FITEM,2,44
FITEM,2,43
A,P51X
FLST,2,4,3
FITEM,2,41
FITEM,2,42
FITEM,2,63
FITEM,2,62
A,P51X
FLST,2,4,3
FITEM,2,43
FITEM,2,44
FITEM,2,67
FITEM,2,66
A,P51X
SAVE
FLST,2,6,3
FITEM,2,61
FITEM,2,62
FITEM,2,63
FITEM,2,64
FITEM,2,70
FITEM,2,69
A,P51X
FLST,2,6,3
FITEM,2,65
```

```
FITEM,2,66
FITEM,2,67
FITEM,2,68
FITEM,2,78
FITEM,2,77
A,P51X
FLST,2,18,3
FITEM,2,69
FITEM,2,70
FITEM,2,71
FITEM,2,72
FITEM,2,73
FITEM,2,74
FITEM,2,75
FITEM,2,76
FITEM,2,77
FITEM,2,78
FITEM,2,86
FITEM,2,85
FITEM,2,84
FITEM,2,83
FITEM,2,82
FITEM,2,81
FITEM,2,80
FITEM,2,79
A,P51X
FLST,2,4,3
FITEM,2,79
FITEM,2,80
FITEM,2,88
FITEM,2,87
A,P51X
FLST,2,4,3
FITEM,2,80
FITEM,2,81
FITEM,2,89
FITEM,2,88
A,P51X
FLST,2,4,3
FITEM,2,81
FITEM,2,82
FITEM,2,90
FITEM,2,89
A,P51X
FLST,2,4,3
FITEM,2,82
FITEM,2,83
FITEM,2,91
```

```
FITEM,2,90
A,P51X
FLST,2,4,3
FITEM,2,83
FITEM,2,84
FITEM,2,92
FITEM,2,91
A,P51X
FLST,2,4,3
FITEM,2,84
FITEM,2,85
FITEM,2,93
FITEM,2,92
A,P51X
FLST,2,4,3
FITEM,2,85
FITEM,2,86
FITEM,2,94
FITEM,2,93
A,P51X
SAVE
FLST,2,10,3
FITEM,2,87
FITEM,2,88
FITEM,2,89
FITEM,2,90
FITEM,2,91
FITEM,2,92
FITEM,2,93
FITEM,2,94
FITEM,2,96
FITEM,2,95
A,P51X
SAVE
!*
!* glue all areas
!*
FLST,2,31,5,ORDE,2
FITEM,2,1
FITEM,2,-31
AGLUE,P51X
!*
/PNUM,KP,0
/PNUM,LINE,0
/PNUM,AREA,1
/PNUM,VOLU,0
/PNUM,NODE,0
/PNUM,TABN,0
```

```
/PNUM,SVAL,0
/NUMBER,0
!*
/PNUM,ELEM,0
/REPLOT
!*
APLOT
FLST,5,14,5,ORDE,10
FITEM,5,1
FITEM,5,-2
FITEM,5,6
FITEM,5,10
FITEM,5,12
FITEM,5,-15
FITEM,5,21
FITEM,5,-24
FITEM,5,30
FITEM,5,-31
ASEL,S, , ,P51X
/REPLOT
FLST,5,14,5,ORDE,10
FITEM,5,1
FITEM,5,-2
FITEM,5,6
FITEM,5,10
FITEM,5,12
FITEM,5,-15
FITEM,5,21
FITEM,5,-24
FITEM,5,30
FITEM,5,-31
CM,_Y,AREA
ASEL, , , ,P51X
CM,_Y1,AREA
CMSEL,S,_Y
!*
CMSEL,S,_Y1
AATT,      1, ,   1,      0
CMSEL,S,_Y
CMDELE,_Y
CMDELE,_Y1
!*
ALLSEL,ALL
FLST,5,11,5,ORDE,11
FITEM,5,3
FITEM,5,5
FITEM,5,7
FITEM,5,9
```

```
FITEM,5,11
FITEM,5,16
FITEM,5,19
FITEM,5,-20
FITEM,5,25
FITEM,5,27
FITEM,5,29
ASEL,S, , ,P51X
FLST,5,11,5,ORDE,11
FITEM,5,3
FITEM,5,5
FITEM,5,7
FITEM,5,9
FITEM,5,11
FITEM,5,16
FITEM,5,19
FITEM,5,-20
FITEM,5,25
FITEM,5,27
FITEM,5,29
CM,_Y,AREA
ASEL, , , ,P51X
CM,_Y1,AREA
CMSEL,S,_Y
!*
CMSEL,S,_Y1
AATT,      2, ,   1,      0
CMSEL,S,_Y
CMDELE,_Y
CMDELE,_Y1
!*
ALLSEL,ALL
FLST,5,6,5,ORDE,6
FITEM,5,4
FITEM,5,8
FITEM,5,17
FITEM,5,-18
FITEM,5,26
FITEM,5,28
ASEL,S, , ,P51X
FLST,5,6,5,ORDE,6
FITEM,5,4
FITEM,5,8
FITEM,5,17
FITEM,5,-18
FITEM,5,26
FITEM,5,28
CM,_Y,AREA
```

```
ASEL, , , ,P51X
CM,_Y1,AREA
CMSEL,S,_Y
!*
CMSEL,S,_Y1
AATT,      3, ,   1,      0
CMSEL,S,_Y
CMDELE,_Y
CMDELE,_Y1
!*
ALLSEL,ALL
SAVE
!*
!* mesh the areas
!*
ALLSEL,ALL
APLOT
SMRT,10
FLST,5,31,5,ORDE,2
FITEM,5,1
FITEM,5,-31
CM,_Y,AREA
ASEL, , , ,P51X
CM,_Y1,AREA
CHKMSH,'AREA'
CMSEL,S,_Y
!*
AMESH,_Y1
!*
CMDELE,_Y
CMDELE,_Y1
CMDELE,_Y2
!*
/PNUM,KP,0
/PNUM,LINE,0
/PNUM,AREA,0
/PNUM,VOLU,0
/PNUM,NODE,0
/PNUM,TABN,0
/PNUM,SVAL,0
/NUMBER,0
!*
/PNUM,MAT,1
/REPLOT
ALLSEL,ALL
!* select nodes on the outer sufaces
NSEL,S,LOC,X,0.,0.0001
NSEL,A,LOC,X,0.4589,0.459
```

```
NSEL,A,LOC,Y,0.,0.0001

NSEL,A,LOC,Y,0.2809,0.281

!* define element for outer surface

!*

TYPE,   2

MAT,      1

NPLOT

esurf

!*

!* create space node

N,50000,0.3,0.5,0,,,,

!* select the nodes and elements that

!* make up the radiation surfaces

ESEL,S,TYPE,,2

NSLE,R

NSEL,S,LOC,X,0.,0.0001

NSEL,A,LOC,X,0.4589,0.459

NSEL,A,LOC,Y,0.,0.0001

NSEL,A,LOC,Y,0.2809,0.281

ESLN,R

NSEL,a,node,,50000

FINISH

!* define radiation matrix

/AUX12

EMIS,1,0.8,

STEF,5.67e-08,

GEOM,1,0,

SPACE,50000,

!*

VTYPE,0,20,

MPRINT,0

WRITE,rad

!*

ALLSEL,ALL

FINISH

/PREP7

!*

!*

TYPE,   3

MAT,      1

REAL,

ESYS,      0

SECNUM,

TSHAP,LINE

!*

SE,rad, , ,0.0001,

ESEL,S,TYPE,,2

EDELE,ALL
```

```
SAVE

!* Define effective heat transfer coeficients for

!*  post-fire (vert-20,horiz-up-25, horiz-down-35)

MPTEMP

MPTEMP,1,338.71,366.48,394.26,422.04,449.82,477.59,

MPTEMP,7,588.71,755.37,1019.26,

MPDATA,HF,20,1,4.68,5.61,6.18,6.60,6.90,7.13,

MPDATA,HF,20,7,7.64,8.00,8.25,

MPDATA,HF,25,1,5.19,6.34,7.05,7.55,7.92,8.18,

MPDATA,HF,25,7,8.74,9.07,9.17,

MPDATA,HF,35,1,2.34,2.74,2.99,3.17,3.30,3.41,

MPDATA,HF,35,7,3.67,3.89,4.09,

MPLIST

SAVE

FINISH

/SOLU

!* setup convection coefficients for fire case

ALLSEL,ALL

NSEL,S,LOC,X,0.,0.0001

NSEL,A,LOC,X,0.4589,0.459

NSEL,A,LOC,Y,0.,0.0001

NSEL,A,LOC,Y,0.2809,0.281

SF,ALL,CONV,19.8,1073

NSEL,ALL

!*****************************************************************
******

!* Test Heat Generation modelling wood burning

ASEL,S,MAT,,3

ESLA,S

/GO

!*

*DIM,burning,TABLE,5,1,0,TIME

!*

BFE,ALL,HGEN, , %burning%

!*

!*********BFA,ALL,HGEN, %burning%

*SET,BURNING(1,0,1) , 0.0

*SET,BURNING(2,0,1) , 0.1

*SET,BURNING(3,0,1) , 0.2

*SET,BURNING(4,0,1) , 552.2

*SET,BURNING(5,0,1) , 552.3

*SET,BURNING(1,1,1) , 0.0

*SET,BURNING(2,1,1) , 0.0

*SET,BURNING(3,1,1) , 7.63e6

*SET,BURNING(4,1,1) , 7.63e6

*SET,BURNING(5,1,1) , 0.0

ALLSEL,ALL

SAVE
```

```
!*****************************************************************
******

D,50000,TEMP, 1073

!*****************************************************************
******

TUNIF,375,                    !REVISED FOR NEW NCT
NUMBER (IC OUTER SHELL)

!*****************************************************************
******

SAVE

!*

!* set up run parameters for fire case

!*

ANTYPE,4

!*

TRNOPT,FULL

LUMPM,0

!*

TIME,1800

AUTOTS,-1

DELTIM,0.1,0.1,600,1

KBC,1

!*

TSRES,ERASE

!*

OUTRES,ALL,ALL,

!*

LSWRITE,2,

!*

!* change boundary conditions for post fire case

!*

ALLSEL,ALL

NSEL,S,LOC,X,0.000,0.0001

NSEL,A,LOC,X,0.4589,0.459

SF,ALL,CONV,-20, 311

ALLSEL,ALL

NSEL,S,LOC,Y,0.0,0.0001

SF,ALL,CONV,-35, 311

ALLSEL,ALL

NSEL,S,LOC,Y,0.2809,0.281

SF,ALL,CONV,-25, 311

ALLSEL,ALL

D,50000,TEMP,311

!*

!* apply solar heat flux

!*

ALLSEL,ALL

!* select vertical lines and nodes on the left side

nsel,s,loc,x,0

!FLST,5,4,4,ORDE,4
```

```
!FITEM,5,18
!FITEM,5,76
!FITEM,5,94
!FITEM,5,97
!LSEL,S, , ,P51X
!NSLL,S,1
!FLST,2,97,1,ORDE,9
!FITEM,2,12
!FITEM,2,17
!FITEM,2,56
!FITEM,2,70
!FITEM,2,72
!FITEM,2,447
!FITEM,2,-521
!FITEM,2,2039
!FITEM,2,-2055
/GO
!*
F,all,HEAT,0.69


ALLSEL,ALL
!* select lines and nodes on the right side
nsel,s,loc,x,.459,.460
!FLST,5,4,4,ORDE,4
```

```
!FITEM,5,35
!FITEM,5,77
!FITEM,5,86
!FITEM,5,108
!LSEL,S, , ,P51X
!NSLL,S,1
!FLST,2,97,1,ORDE,9
!FITEM,2,3
!FITEM,2,27
!FITEM,2,57
!FITEM,2,63
!FITEM,2,78
!FITEM,2,795
!FITEM,2,-869
!FITEM,2,2240
!FITEM,2,-2256
!/GO
!*
F,all,HEAT,0.69


!* select nodes on upper surface
ALLSEL,ALL
NSEL,S,LOC,Y,0.2809,0.281
!FLST,2,155,1,ORDE,4
```

```
!FITEM,2,79
!FITEM,2,-80
!FITEM,2,2257
!FITEM,2,-2409
!/GO
!*
F,all,HEAT,2.88
ALLSEL,ALL
!* set up run parameters for post fire
TIME,14400   !was 9000
AUTOTS,-1
DELTIM,0.5,0.1,2000,1
KBC,1
!*
TSRE S,ERASE
!*
TINTP,0.005, , ,-1,0.5,-1
!*
OUTRES,ALL,ALL,
TIME,45000
DELTIM,100,10,2000,1
LSWRITE,3,
SAVE
FINISH
/SOLU
/STATUS,SOLU
LSSOLVE,2,3,1
FINISH
SAVE
/POST26
!*
!* plot temperature evolution at specified nodes
!*
!*
!* inner wall, top right corner
NSOL,2,58,TEMP, ,inn_wtr
!*
!*
!*  inner wall, bottom mid position
NSOL,3,1185,TEMP, ,inn_wbm
!*
!*
!*  inner wall, top mid position
NSOL,4,1720,TEMP, ,inn_wtm
!*
!*
!*  outer wall, top mid position
NSOL,5,2333,TEMP, ,out_wtm
```

```
!*

!*

PLVAR,2,3,4,5,,, , , , ,

PRVAR,2,3,4,5,,,

FINISH

!* plot isothermes at certain moments in time

/POST1

SET,LIST,2

SET, , ,1, , , ,17,

/EFACE,1

!*

PLNSOL,TEMP, ,0,

FINISH

/POST1

SET, , ,1, , , ,18,

/EFACE,1

!*

PLNSOL,TEMP, ,0,

SET, , ,1, , , ,20,

/EFACE,1

!*

PLNSOL,TEMP, ,0,

SET, , ,1, , , ,22,

/EFACE,1

!*

PLNSOL,TEMP, ,0,

SET, , ,1, , , ,30,

/EFACE,1

!*

PLNSOL,TEMP, ,0,

SET, , ,1, , , ,43,

/EFACE,1

!*

PLNSOL,TEMP, ,0,

SET,PREVIOUS

FINISH


!*********************************NEW

allsel

/post1


Tmax=0

TimeMAX=0

nmax=0


nsel,s,loc,x,0.0525,.4065,

nsel,r,loc,y,0.0525,.2285,

!nsel,u,loc,y,0.053,.2280
```

```
nplot
*GET, ncount, NODE, 0, count
cm,icnodes,node

set,1,1

*do,t,1,46
tmaxn=0
cmsel,s,icnodes

*do,i,1,ncount
nodei=node(0,0,0)
*get,tempi,node,nodei,temp
*if,tempi,gt,tmaxn,then
tmaxn=tempi
nmaxn=nodei
*endif
nsel,u,,,nodei
*enddo
*if,tmaxn,gt,tmax,then
tmax=tmaxn
nmax=nmaxn
*GET,timemax, ACTIVE, 0, set, time
*endif
set,next
*enddo

tmax=tmax
nmax=nmax
timemax=timemax

allsel

/show,term
/post1,
! Reverse Video
/rgb,index,100,100,100,0
/rgb,index,80,80,80,13
/rgb,index,60,60,60,14
/rgb,index,0,0,0,15
set,1,17
plnsol,temp
/image,save,fig3-4(1800),wmf
set,2,1
/replot
/image,save,fig3-5(1900),wmf
set,2,5
```

```
/replot

/image,save,fig3-6(3268),wmf

set,last

/replot

/image,save,fig3-7(45000),wmf

!*********************************NEW

! /EXIT,ALL
```

3.6.3 NCT Transient Analysis

The transient analysis uses a one dimensional model of the vertical face of the packaging (thinner part of the packaging) as described in the figure below:

Figure 3-8 Vertical Face Model

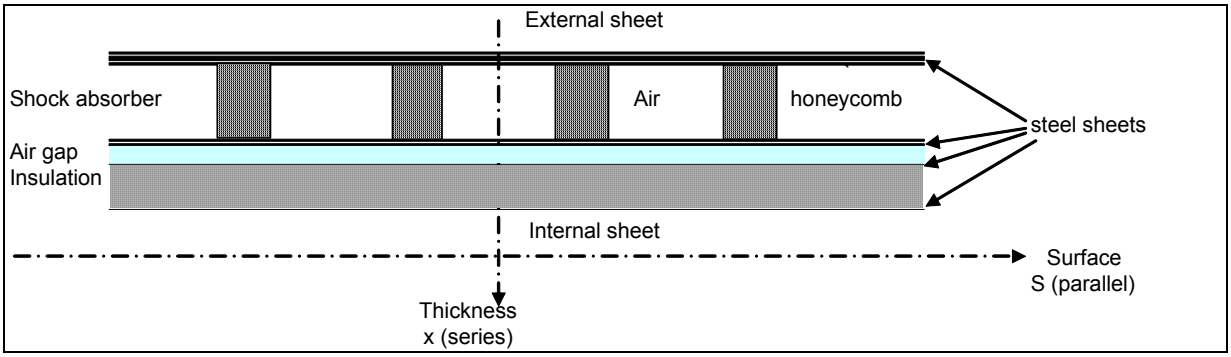

The heat flux is set as a sine wave function:

$$Q = \pi/2 \times 800 \sin(\omega\,\theta) \qquad 0 < (\omega\,\theta) < \pi$$
$$Q = 0 \qquad \pi < (\omega\,\theta) < 2\pi$$

With: Q = heat energy in g-cal/cm^2
$\omega = 2\pi / 24$ pulsation
θ = time in hour

Note that the peak value of ($\pi/2 \times 800$) complies with 10CFR 71.71(c)(1), conservatively assuming the highest value of 800 g-cal/cm^2 for the insolation.

$$\int_0^{24\text{hours}} Q\, d\theta = 800 \text{ g-cal/cm}^2$$

Assuming that at each time step, the external surface of the package achieves steady state conditions, the energy balance between the solar heat load, and the convection and radiation exchanges (see section 3.4.1.1), results time dependant solution for the external surface temperature.

The result is plotted on the Figure 3.6.3-1 (blue curve) and is close to a sine wave function. Indeed, when calculating the energy balance equation, it appears that the convention term represents 65% of the exchange, and the radiation term 35%. As the convection term is linearly proportional to the external temperature, this curve is nearly proportional to the solar heat load.

Assume that the external temperature is a sine function with respect to time as follows (and as plotted on Figure 3.6.3-1):

$Ts = T_{avg} + T^{+} \sin(\omega\ \theta)$

With: $T_{avg} = 420$ K (maximum value of the blue curve)
$T^{+} = (420\text{-}311) = 109$ K

The system is thus modeled as a one dimensional model of conduction, with a sinusoidal wave temperature on the external surface as a boundary condition.

Using equation 4-22 of the "Handbook of Heat Transfer", Reference 3.6.1.7, the heat equation through a layer of material leads to a temperature of:

$T(x,\theta) = T_{avg} + T^{+} \exp(-L\ x/d) \sin[L(2\ L\ Fo - x/d)]$

Using the reference's notation, it becomes:

$T(x,\theta) = T_{avg} + T^{+} \exp[-(\omega/2\alpha)^{1/2}\ x] \sin[\omega\ \theta - (\omega/2\alpha)^{1/2} x]$

With : $\alpha = K / \rho\ C$ = thermal diffusivity,
K = conductivity if material,
ρ = density of material,
C = specific heat of the material,
x = thickness thru the material.

Through each layer of material "i" in the RAJ-II packaging, the temperature of the external surface is so decreased by a factor η and lagged by a factor ϕ:

$\eta_i = \exp[-(\omega/2\alpha_i)^{1/2}\ x_i]$
$\phi_i = (\omega/2\alpha_i)^{1/2} x_i$

Table 3.6.3-1 summarizes the material properties for each component layer through the thickness of the model.

Equivalent properties of material

The thermal properties (K, ρ, C) of a material equivalent to materials of a system are following the rules:

Materials in series $K = \dfrac{e_T}{\sum_i \dfrac{e_i}{K_i}}$ Materials in parallel $K = \dfrac{1}{S_T} \sum_i S_i K_i$

Materials in series $\rho\ C = \dfrac{\sum_i \rho_i C_i e_i}{e_T}$ Materials in parallel $\rho\ C = \dfrac{\sum_i \rho_i C_i S_i}{S_T}$

The maximum temperature of the cavity surface of the packaging resulting from solving the one dimensional model occurs at ten hours into the cycle and is equal to 350 K. The

maximum temperature on the outer surface of the inner container occurs at 8 hours and is equal to 375K. Temperatures are summarized on Table 3.6.3-2.

Table 3 - 6 Material properties

Component	Material	Thickness x (m)	Surface S (m)	Conductivity K (W/m-K)	Density r (kg/m3)	Specific heat C (J/kg-K)	Diffusivity a (m2/s)
OC outer sheet	steel	0.004	-	15	7900	477	3.981E-06
honeycomb①	paper	-	0.084①	0.13595	700①	1531①	3.932E-07
	air	-	0.916①	0.0267	1.177	1005	
Shock absorbers	honeycomb	0.108	0.64	0.0359	60	1522	1.737E-06
	air		3.186	0.0267	1.177	1005	
OC inner sheet	steel	0.001	-	15	7900	477	3.981E-06
Air gap	air	0.01	-	0.0267	1.177	1005	2.257E-05
IC outer sheet	steel	0.0015	-	15	7900	477	3.981E-06
IC insulation	Alumina	0.048	-	0.09	250	1046	3.442E-07
IC inner sheet	steel	0.001	-	15	7900	477	3.981E-06

① The honeycomb is assumed to be a combination of paper and air in a parallel system (see below). The proportion of paper and air is determined by the ratio of the densities:

Honeycomb density = 60 kg/m^3
Paper density = 700 kg/m^3 8.4%
Air density = 1.177 kg/m^3 91.6%

Thermal properties of resin impregnated kraft paper (density, conductivity, specific heat) are conservatively assumed to correspond to that of ordinary paper according to Reference 3.6.1.9.

Table 3 - 7 NCT Temperatures Through the Package Thickness

Time (hour)	Surface temp sin wave Ts (K)	T thru OC Outer Shell	T thru Honeycomb and Air	T thru OC Inner Steel	T thru Air Gap	T thru IC Inner Shell	T thru Alumina Slilicate
0	311	311	311	311	311	311	311
0.5	325	324	311	311	311	311	311
1	339	338	311	311	311	311	311
1.5	353	351	311	311	311	311	311
2	366	364	312	312	311	311	311
2.5	377	376	321	320	320	319	311
3	388	386	329	329	328	327	311
3.5	397	396	337	337	336	335	311
4	405	404	345	345	343	343	312
4.5	412	410	352	352	350	350	317
5	416	415	358	358	357	356	322
5.5	419	418	364	364	362	362	327
6	420	419	368	368	367	367	332
6.5	419	418	372	372	371	370	336
7	416	415	375	375	373	373	340
7.5	412	411	376	376	375	375	343
8	405	405	377	376	376	**375**	346
8.5	397	397	376	376	375	375	348
9	388	388	374	374	373	373	349
9.5	377	378	371	371	371	371	**350**
10	366	366	367	367	367	367	350
10.5	353	353	362	362	362	362	350
11	339	340	357	357	357	357	349
11.5	325	326	350	350	350	350	347
12	311	312	343	343	343	343	344
12.5	311	311	335	335	336	336	342
13	311	311	327	327	328	328	338
13.5	311	311	318	319	319	320	334
14	311	311	311	311	311	311	330
14.5	311	311	311	311	311	311	325
15	311	311	311	311	311	311	320
15.5	311	311	311	311	311	311	315
16	311	311	311	311	311	311	311
16.5	311	311	311	311	311	311	311

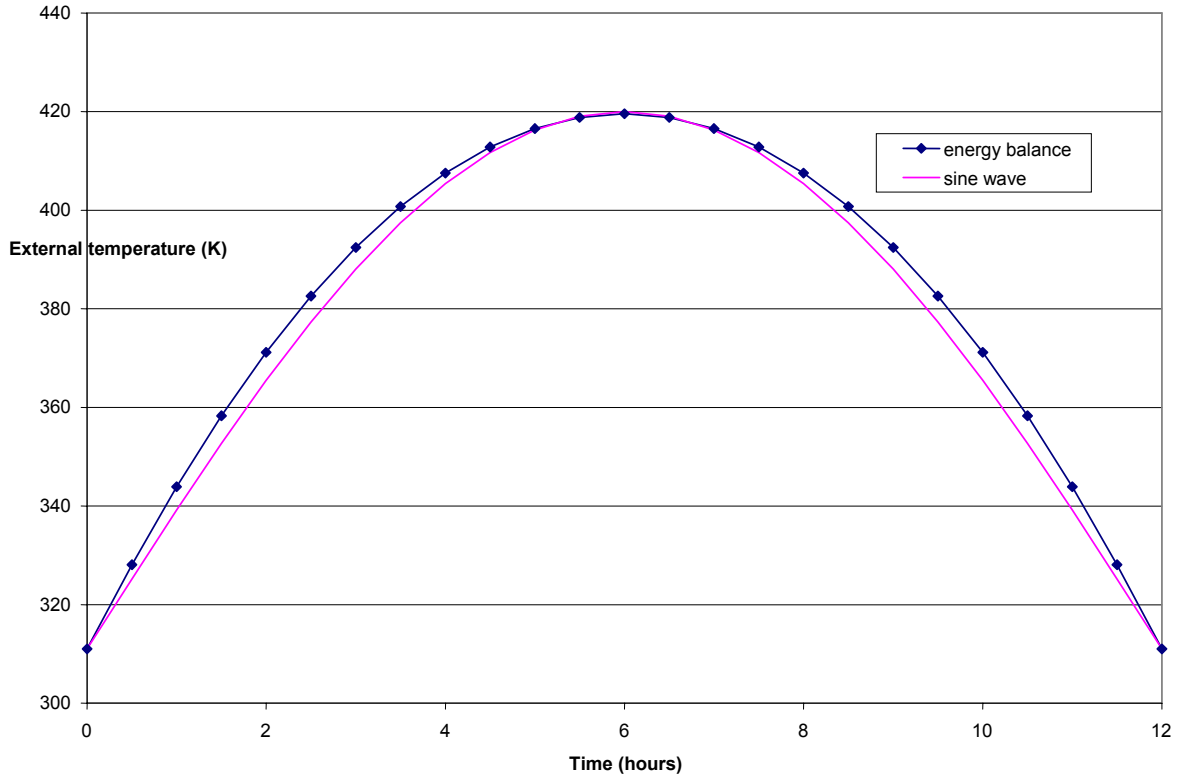

Figure 3-9 Comparison Between Energy Equation Solution with a Sine Wave Equation

4.0 CONTAINMENT

4.1 DESCRIPTION OF THE CONTAINMENT SYSTEM

4.1.1 Containment Boundary

RAJ-II container is limited to use for transporting low enriched uranium, nuclear reactor fuel assemblies and rods. The radioactive material is bound in sintered ceramic pellets having very limited solubility and has minimal propensity to suspend in air. The pellets are sintered at temperatures greater than 1,600°C. These pellets are further sealed into zirconium alloy cladding to form the fuel rod portion of each assembly. The primary containment boundary for the RAJ-II package is the fuel cladding. Design and fabrication details for this cladding are provided in Section 1.2.3. The containment system includes the ceramic sintered pellet, clad in zirconium tubes which are contained in a stainless steel box which is contained in another stainless steel box.

There are no penetrations in the fuel cladding when shipped. The fuel cladding after loading with the pellets is pressurized with helium and end plugs are welded on to close the rod. These welds are designed to withstand the rigorous operating environment of a nuclear reactor. The fuel is leak tested to demonstrate that it is leak tight ($<1x\ 10^{-7}$ atm-cc/s).

4.1.2 Special Requirements for Plutonium

This section is not applicable since the package is not being used for plutonium shipments.

4.2 GENERAL CONSIDERATIONS

4.2.1 Type A Fissile Packages

The Type A fissile package is constructed, and prepared for shipment so that there is no loss or dispersal of the radioactive contents and no significant increase in external surface radiation levels and no substantial reduction in the effectiveness of the packaging during normal conditions of transport. The fissile material is bound as a ceramic pellet and contained in a zirconium fuel rod. These rods are leak tested prior to shipment to assure their integrity. Chapter 6.0 demonstrates that the package remains subcritical under normal and hypothetical accident conditions.

4.2.2 Type B Packages

The Type B fissile package is constructed, and prepared for shipment so that there is no loss or dispersal of the radioactive contents and no significant increase in external surface radiation levels and no substantial reduction in the effectiveness of the packaging during normal conditions of transport.

The package satisfies the quantified release rate of 10 CFR 71.51 by having a release rate less than 10^{-6} A_2/hr as demonstrated below.

A_2 = 0.17 Ci, therefore$10^{-6}A_2$ = 1.7 x 10^{-} Ci/hr

The mass density of UO_2 in an aerosol from NUREG/CR-6487, page 17 is 9 x 10^{-6} g /cm^3. Specific Activity of fuel material is 1.4 x 10^{-5} Ci/g UO_2 (550kg UO_2/7.7 Ci).

Leak rate at 1 x 10^{-7} atm-cm^3/s (3.6 x 10^{-4} cm^3/hr) is equal to 1 x 10^{-6} atm-cm^3/s (3.6 x 10^{-3} cm^3/h) when pressurized to 10 atm. Assuming that the pressure is further increased due to temperature the leak rate is assumed to increase by an additional factor of 10 so that it is equal to 3.6 x 10^{-2} cm^3/h.

Release rate = 3.6 x 10^{-2} cm^3/hr x 1.4 x 10^{-5} Ci/g UO_2 x 9 x 10^{-6} g /cm^3
= 4.5 x 10^{-12} Ci/h

Much less than the 1.7 x 10^{-}Ci/hr limit.

4.3 CONTAINMENT UNDER NORMAL CONDITIONS OF TRANSPORT (TYPE B PACKAGES)

The nature of the contained radioactive material and the structural integrity of the fuel rod cladding including the closure welds are such that there will be no release of radioactivity under normal conditions of transport. The welded close containment boundary is not affected by any of the normal conditions of transport as demonstrated in the previous chapters. The pressurization that could be seen by the containment boundary is far below the normal conditions the fuel experiences while in service.

4.4 CONTAINMENT UNDER FOR HYPOTHETICAL ACCIDENT CONDITIONS (TYPE B PACKAGES)

The sintered pellet form of the radioactive material and the integrity of the fuel rod cladding are such that there will be no substantial release of radioactivity under the Hypothetical Accident Conditions. Before and after the accident condition testing the rods were helium leak tested demonstrating leak tightness. Similar fuel rods have been tested at temperatures and resulting pressures that will be seen by fuel shipped in the RAJ-II.

10 CFR 71.51 requires that no escape of other radioactive material exceeding a total amount A_2 in 1 week, and no external radiation dose rate exceeding 10 mSv/h (1 rem/h) at 1 m (40 in) from the external surface of the package. The following qualitative assessment demonstrates that the performance requirement of 10 CFR 71.51(a)(2) will be satisfied.

Table 1-4 shows the calculated A_2 for the mixture of the maximum radionuclide content in the package is 0.17 Ci. The total radioactivity in the package using the maximum isotopic values is 7.7 Ci. The mass of UO_2 equivalent to an activity of 7.7 Ci is 550 kg (275 kg UO_2/assembly x 2 assemblies) which yields a mass to activity ratio of 71.4kg UO_2/Ci. The mass equivalent A_2 is therefore 2.1 kg UO_2.

Following the drop test, fuel rods were leak tested and shown to have a very low leak rate of He at a rate of 5.5 x 10^{-6} cm^3/s. Over one week this is equal to 3.3 cm^3 (5.5E-6 cm^3/s x 6.05E5 s/wk = 3.3 cm^3). Conservatively assuming that the density of the radioactive material is 10g/cm^3 and using the A_2 mass above of 2,100 g of UO_2, the UO_2 would have a volume of 210 cm^3. This is much greater than the volume leaked. This calculation is extremely conservative since the UO_2 would predominantly stay in a ceramic form and not be available for dispersion.

Test fuel rods as described in Section 2.0 have been baked at 800°C for over 30 minutes and did not leak.

Additionally, the large mass, 2,100 g, of material required to exceed the A_2 would require a catastrophic failure of the rod, significant leak of the inner and outer container.

Dose rates are less than the 10mSv/hr under any condition because of the low specific activity and low abundance of gamma emitters in the fuel.

Based on this evaluation, it is demonstrated that the package meets the containment requirements of 10 CFR 71.51

4.5 LEAKAGE RATE TESTS FOR TYPE B PACKAGES

During manufacturing each fuel rod is He leak tested to demonstrate that it is leak tight (<1x 10^{-7}atm-cc/s). There are no leak rate requirements for the inner and outer packaging.

4.6 APPENDIX

None

5.0 SHIELDING EVALUATION

The contents of the RAJ-II require no shielding since unirradiated fuel gives off no significant radiation either gamma or neutron. Hence the RAJ-II provides no shielding. The minimal shielding provided by the stainless steel sheet is not required. The dose rate limits established by 10 CFR 71.47(a) for normal conditions of transport (NCT) are verified prior to shipping by direct measurement.

Since there is no shielding provided by the package, there is no shielding change during the Hypothetical Accident Conditions (HAC). Therefore, the higher dose rate allowed by 10 CFR 71.51(a)(2) will be met.

6.0 CRITICALITY EVALUATION

6.1 DESCRIPTION OF CRITICALITY DESIGN

A criticality safety analysis is performed to demonstrate the RAJ-II shipping container safety. The RAJ-II meets applicable IAEA and 10 CFR 71 requirements for a Type B fissile material-shipping container, transporting heterogeneous UO_2 enriched to a maximum of 5.00 wt. percent U-235.

The RAJ-II shipping container design features a stainless steel inner container positioned inside an outer stainless steel container by four evenly spaced stainless steel fixture assemblies. The fixture assemblies cradle the inner container and prevent horizontal or vertical movement. The inner container has two fuel assembly transport compartments, aligned side-by-side and separated by a stainless steel divider. Each transport compartment is lined with polyethylene foam in which the fuel assemblies rest. Additional container details are described in Section 1.2, Package Description. Material manufacturing tolerances are presented in the general arrangement drawings in Section 1.4.1.

The uranium transported in the RAJ-II container is UO_2 pellets enclosed in zirconium alloy cladding. The fuel rods are arranged in 8x8, 9x9, or 10x10 square lattice arrays at fixed center-to-center spacing. Fuel rods may also be transported loose with no fixed center-to-center spacing, bundled together in a close packed configuration, or inside a 5-inch diameter stainless steel pipe or protective case.

Water exclusion from the inner container is not required for this package design. The inner container is analyzed in both undamaged and damaged package arrays under optimal moderation conditions and is demonstrated to be safe under Normal Conditions of Transport (NCT) and Hypothetical Accident Condition (HAC) testing.

The criticality analysis for the RAJ-II container is performed at a maximum enrichment of 5.00 wt. percent U-235 for UO_2 or Uranium-Carbide fuel pellets contained in zirconium alloy or stainless steel clad cylindrical rods. The cylindrical fuel rods are arranged in 8x8, 9x9, or 10x10 square lattice arrays at fixed center-to-center spacing. Sensitivity analyses are performed by varying fuel parameters (rod pitch, clad ID, clad OD, pellet OD, fuel orientation, polyethylene spacer quantity, and moderator density) to obtain the most reactive configuration. The most reactive configuration is modeled for each authorized payload to demonstrate safety and to validate the fuel parameter ranges specified as loading criteria.

Table 6-1 RAJ-II Fuel Assembly Loading Criteria summarizes the fuel loading criteria for the RAJ-II shipping container.

Table 6-1 RAJ-II Fuel Assembly Loading Criteria

Parameter	Units	Type	Type	Type	Type
Fuel Assembly Type	Rods	8x8	9x9	FANP 10x10	GNF 10x10
UO_2 Density		≤ 98% Theoretical	≤ 98% Theoretical	≤ 98% Theoretical	≤ 98% Theoretical
Number of water rods	#	0, 2x2	0, 2-2x2 off-center diagonal, 3x3	0, 2-2x2 off-center diagonal, 3x3	0, 2-2x2 off-center diagonal, 3x3
Number of fuel rods	#	60 - 64	72 - 81	91 - 100	91 - 100
Fuel Rod OD	cm	≥ 1.176	≥ 1.093	≥ 1.000	≥ 1.010
Fuel Pellet OD	cm	≤ 1.05	≤ 0.96	≤ 0.895	≤ 0.895
Cladding Type		Zirconium Alloy	Zirconium Alloy	Zirconium Alloy	Zirconium Alloy
Cladding ID	cm	≤ 1.10	≤ 1.02	≤ 0.933	≤ 0.934
Cladding Thickness	cm	≥ 0.038	≥ 0.036	≥ 0.033	≥ 0.038
Active fuel length	cm	≤ 381	≤ 381	≤ 385	≤ 385
Fuel Rod Pitch	cm	≤ 1.692	≤ 1.51	≤ 1.350	≤ 1.350
U-235 Pellet Enrichment	wt%	≤ 5.0	≤ 5.0	≤ 5.0	≤ 5.0
Maximum Lattice Average Enrichment	wt%	≤ 5.0	≤ 5.0	≤ 5.0	≤ 5.0
Channel Thickness[a]	cm	0.17 – 0.3048	0.17 – 0.3048	0.17 – 0.3048	0.17 – 0.3048
Part Length Fuel Rods (1/3 through 2/3 normal length)	Max #	None	12	14	14
Gadolinia Requirements Lattice Average Enrichment[b]	#				
≤ 5.0 wt % U-235	@	7 @ 2 wt %	10 @ 2 wt %	12 @ 2 wt %	12 @ 2 wt %
≤ 4.7 wt % U-235	wt%	6 @ 2 wt %	8 @ 2 wt %	12 @ 2 wt %	12 @ 2 wt %
≤ 4.6 wt % U-235	Gd_2O_3	6 @ 2 wt %	8 @ 2 wt %	10 @ 2 wt %	10 @ 2 wt %
≤ 4.3 wt % U-235		6 @ 2 wt %	8 @ 2 wt %	9 @ 2 wt %	9 @ 2 wt %
≤ 4.2 wt % U-235		6 @ 2 wt %	6 @ 2 wt %	8 @ 2 wt %	8 @ 2 wt %
≤ 4.1 wt % U-235		4 @ 2 wt %	6 @ 2 wt %	8 @ 2 wt %	8 @ 2 wt %
≤ 3.9 wt % U-235		4 @ 2 wt %	6 @ 2 wt %	6 @ 2 wt %	6 @ 2 wt %
≤ 3.8 wt % U-235		4 @ 2 wt %	4 @ 2 wt %	6 @ 2 wt %	6 @ 2 wt %
≤ 3.7 wt % U-235		2 @ 2 wt %	4 @ 2 wt %	6 @ 2 wt %	6 @ 2 wt %
≤ 3.6 wt % U-235		2 @ 2 wt %	4 @ 2 wt %	4 @ 2 wt %	4 @ 2 wt %
≤ 3.5 wt % U-235		2 @ 2 wt %	2 @ 2 wt %	4 @ 2 wt %	4 @ 2 wt %
≤ 3.3 wt % U-235		2 @ 2 wt %	2 @ 2 wt %	2 @ 2 wt %	2 @ 2 wt %
≤ 3.1 wt % U-235		None	2 @ 2 wt %	2 @ 2 wt %	2 @ 2 wt %
≤ 3.0 wt % U-235		None	None	2 @ 2 wt %	2 @ 2 wt %
≤ 2.9 wt % U-235		None	None	None	None
Polyethylene Equivalent Mass (Maximum per Assembly)[c]	kg	11	11	10.2	10.2

a. Transport with or without channels is acceptable
b. Required gadolinia rods must be distributed symmetrically about the major diagonal
c. Polyethylene equivalent mass (refer to 6.3.2.2)

Cylindrical fuel rods containing UO_2, enriched to 5 wt. percent U-235, are analyzed within the RAJ-II inner container in a 5-inch stainless steel pipe, loose, in a protective case, or bundled together. The fuel rod loading criteria, determined from the criticality evaluation for the RAJ-II shipping container, are shown in Table 6-2 RAJ-II Fuel Rod Loading Criteria.

Table 6-2 RAJ-II Fuel Rod Loading Criteria

Parameter	Units	Type					
Fuel Assembly Type		8x8 (UO_2)	9x9 (UO_2)	10x10 (UO_2)	CANDU-14 (UC)	CANDU-25 (UC)	Generic PWR (UO_2)
UO_2 or UC Fuel Density		<98% theoretical	<98% theoretical	<98% theoretical	<98% theoretical	<98% theoretical	<98% theoretical
Fuel rod OD	cm	≥1.10	≥1.02	≥1.00	≥1.340	≥0.996	≥1.118
Fuel Pellet OD	cm	≤1.05	≤0.96	≤0.90	≤1.254	≤0.950	≤0.98
Cladding Type		Zirc. Alloy	Zirc. Alloy	Zirc. Alloy	Zirc. Alloy or SS	Zirc. Alloy or SS	Zirc. Alloy or SS
Cladding ID	cm	≤1.10	≤1.02	≤1.00	≤1.267	≤0.951	≤1.004
Cladding Thickness	cm	≥0.00	≥0.00	≥0.00	≥0.00	≥0.00	≥0.00
Active fuel Length	cm	≤381	≤381	≤385	≤47.752	≤40.013	≤450
Maximum U-235 Pellet Enrichment	wt.%	≤5.0	≤5.0	≤5.0	≤5.0	≤5.0	≤5.0
Maximum Average fuel rod Enrichment	wt.%	≤5.0	≤5.0	≤5.0	≤5.0	≤5.0	≤5.0

6.1.1 Design Features

6.1.1.1 Packaging

A general discussion of the RAJ-II container design is provided in Section 1.2, Package Description. A detailed set of licensing drawings for the RAJ-II container is provided in Appendix 1.4.1 RAJ-II General Arrangement Drawings. Components important to criticality safety are described below.

The RAJ-II is comprised of two primary components: 1) an inner stainless steel container, and 2) an outer stainless steel container.

The inner stainless steel container is 468.6 cm (184.49 in) in length, 45.9 cm (18.07 in) in width, and 28.6 cm (11.26 in) in height, and provides containment for the uranium inside the cylindrical zirconium alloy tubes. The fuel rods are located inside one of two compartments within the inner container. The compartments are fabricated from 18-gauge (0.122 cm thick) stainless steel, 456.7 cm (179.8 in) in length, 17.6 cm (6.93in) in width and height. Each compartment is lined with 1.8 cm (0.71 in) thick polyethylene foam and separated from each other by the compartment walls. A 5 cm (1.97 in) thick Alumina Silicate fiber surrounds the compartments to provide thermal insulation, and a 16-gauge (0.15 cm thick) stainless steel sheet surrounds the insulator. The inner container lid consists of an Alumina Silicate layer encased in a 16-gauge (0.15 cm

thick) stainless steel sheet. The lid width and length are consistent with the inner container and the overall height is 5.25 cm (2.07 in).

The outer container is 506.8 cm (199.53 in) in length, 72.0 cm (28.35 in) in width, and 64.2 cm (25.28 in) in height (with the skids attached the height is 74.2 cm (29.21 in)). The inner container is held rigidly within the outer stainless steel container by four evenly spaced stainless steel fixture assemblies. Shock absorbers, fabricated from a phenol impregnated cardboard material, are placed at six locations above and below the inner container, and twelve locations on either side of the inner container. The wall for the outer container is fabricated from 14-gauge (0.2 cm thick) stainless steel.

6.1.2 Summary Table of Criticality Evaluation

Table 6-3 Criticality Evaluation Summary, lists the bounding cases evaluated for a given set of conditions. The cases include: fuel assembly transport single package normal and Hypothetical Accident Conditions (HAC), fuel assembly transport package array normal conditions of transport, fuel assembly transport package array HAC, fuel rod transport single package normal and hypothetical accident conditions, fuel rod transport package array normal conditions of transport, and fuel rod transport package array HAC.

Table 6-3 Criticality Evaluation Summary

Case	Bounding Fuel Type	k_{eff}	σ	$k_{eff} + 2\sigma$	USL
Fuel Assembly Single Package Normal	GNF 10x10 with worst case fuel parameters, 12, 2.0 wt % Gd_2O_3 fuel rods, and 12 part length fuel rods	0.6673	0.0008	0.6689	0.94254
Fuel Assembly Single Package HAC	GNF 10x10 with worst case fuel parameters, 12, 2.0 wt % Gd_2O_3 fuel rods, and 12 part length fuel rods	0.6931	0.0010	0.6951	0.94254
Fuel Assembly Package Array Normal	GNF 10x10 with worst case fuel parameters, 12, 2.0 wt % Gd_2O_3 fuel rods, and 12 part length fuel rods	0.8519	0.0008	0.8535	0.94254
Fuel Assembly Package Array HAC	GNF 10x10 with worst case fuel parameters, 12, 2.0 wt % Gd_2O_3 fuel rods, and 12 part length fuel rods	0.9378	0.0009	0.9396	0.94254
Fuel Rod Single Package Normal	25 GNF 8x8 fuel rods per container with worst case fuel parameters	0.6365	0.0008	0.6381	0.94254
Fuel Rod Single Package HAC	25 GNF 8x8 fuel rods per container with worst case fuel parameters	0.6532	0.0008	0.6548	0.94254
Fuel Rod Package Array Normal	25 GNF 8x8 fuel rods per container with worst case fuel parameters	0.6365	0.0008	0.6381	0.94254
Fuel Rod Package Array HAC	25 GNF 8x8 fuel rods per container with worst case fuel parameters	0.8731	0.0007	0.8745	0.94254

A comparison between the nominal fuel parameters and the worst case fuel parameters used in the criticality evaluation is shown in Table 6-4 Nominal vs. Worst Case Fuel Parameters for the RAJ-II Criticality Analysis.

Table 6-4 Nominal vs. Worst Case Fuel Parameters for the RAJ-II Criticality Analysis

Case	Fuel Rod Pitch (cm)	Clad Outer Diameter (cm)	Clad Inner Diameter (cm)	Pellet Outer Diameter (cm)	Pellet Theoretical Density
FANP 10x10					
Nominal	1.284, 1.2954	1.010, 1.033	0.9020, 0.9217	0.8682, 0.8882	< 98%
Worst Case Modeled for Fuel Assembly Transport	1.350	1.000	0.9330	0.895	98%
Worst Case Modeled for Fuel Rod Transport	1.350	1.000	1.000	0.900	98%
GNF 10x10					
Nominal	1.2954	1.019	0.9322	0.8941	< 98%
Worst Case Modeled for Fuel Assembly Transport	1.350	1.010	0.9338	0.895	98%
Worst Case Modeled for Fuel Rod Transport	1.350	1.000	1.000	0.900	98%
FANP 9x9					
Nominal	1.4478	1.095, 1.0998	0.968, 0.9601	0.94, 0.9398	< 98%
Worst Case Modeled for Fuel Assembly Transport	1.510	1.093	1.020	0.960	98%
Worst Case Modeled for Fuel Rod Transport	1.510	1.020	1.020	0.960	98%
GNF 9x9					
Nominal	1.438	1.110	0.983	0.955	< 98%
Worst Case Modeled for Fuel Assembly Transport	1.510	1.093	1.020	0.960	98%
Worst Case Modeled for Fuel Rod Transport	1.510	1.020	1.020	0.960	98%
GNF 8x8					
Nominal	1.6256	1.2192	1.072	1.044	< 98%
Worst Case Modeled for Fuel Assembly Transport	1.6923	1.176	1.100	1.050	98%
Worst Case Modeled for Fuel Rod Transport	1.6923	1.100	1.100	1.050	98%

6.1.3 Criticality Safety Index

For the RAJ-II, undamaged packages have been analyzed in 21x3x24 arrays and damaged packages have been analyzed in 10x1x10 arrays. Pursuant to 10 CFR 71.59, the number of

packages "N" in a 2N array that are subjected to the tests specified in 10 CFR 71.73, or in a 5N array for undamaged packages is used to determine the Criticality Safety Index (CSI). The CSI is determined by dividing the number 50 by the most limiting value of "N" as specified in 10 CFR 71.59.

The RAJ-II criticality analysis demonstrates safety for 5N=1,512 (undamaged) and 2N=100 (damaged) packages. The corresponding Criticality Safety Index (CSI) for criticality control is given by CSI = 50/N. Since 5N=1,512 and 2N = 100, it follows that the more restrictive N = 50 and CSI = 50/50 = 1.0. Therefore the maximum allowable number of packages per shipment is 50/1.0 = 50.

Under hypothetical accident conditions, the contents of 2N=64 (8x1x8 array), 48 (4x1x6 array) RAJ-II damaged packages are demonstrated to remain subcritical. Therefore, the CSI for criticality control purposes is 1.6 for an 8x1x8 array and 2.1 for a 4x2x6 array (Ref. 13).

6.2 FISSILE MATERIAL CONTENTS

The RAJ-II shall be used to transport UO_2 conforming to the requirements stated in Section 6.1, Table 6-1 and Table 6-3. The uranium isotopic distribution considered in the models used for the criticality safety demonstration is shown in Table 6-5 Uranium Isotopic Distribution.

Table 6-5 Uranium Isotopic Distribution

Isotope	Modeled wt. %
U-235	5.00
U-238	95.00

The criticality analysis conservatively demonstrates safety for UO_2 pellets within cylindrical zirconium alloy tubes, arranged in 8x8, 9x9, or 10x10 square assembly lattices. Cylindrical fuel rods containing UO_2, enriched up to 5 wt. percent U-235, are also conservatively demonstrated safe within the RAJ-II container in a 5-inch stainless steel pipe, loose, in a protective case, or bundled together. The fuel loadings demonstrated safe in the RAJ-II are specified in Table 6-1 and Table 6-3.

6.3 GENERAL CONSIDERATIONS

Models are generated for single package and package arrays under normal conditions and Hypothetical Accident Conditions (HAC).

6.3.1 Model Configuration

6.3.1.1 RAJ-II Shipping Container Single Package Model

The RAJ-II single package models are constructed for both normal conditions of transport and hypothetical accident conditions. The single package models are enveloped with a 30.48 cm layer of full density water for reflection.

6.3.1.1.1 Single Package Normal Conditions of Transport Model

The RAJ-II is comprised of an inner and outer container fabricated from Stainless Steel. The inner container dimensions are shown in Figure 6-4 RAJ-II Inner Container Normal Conditions of Transport Model and Figure 6-5 RAJ-II Container Cross-Section Normal Conditions of Transport Model. It is lined with polyethylene foam having a density of up to 0.080 g/cm^3. The fuel assemblies rest against the polyethylene foam in a fixed position, and the inner container is positioned within the outer container as shown in Figure 6-5. The inner container has Alumina Silicate thermal insulation between the inner and outer walls. The Alumina Silicate density is approximately 0.25 g/cm^3. The outer container dimensions are contained in Figure 6-3 and Figure 6-5. The outer container provides protection for the inner container and additional separation between fuel assemblies in adjacent containers. No credit is taken for any of the structural steel between the inner and outer containers. The honeycomb shock absorbers, located between the inner and outer containers, are not explicitly modeled. Instead, water is placed in the space between the inner and outer containers, and its density is varied from 0.0 – 1.0 g/cm^3. The honeycomb shock absorbers have a density between 0.04 and 0.08 g/cm^3. The hydrogen number densities for water (1.0 g/cm^3) and for the honeycomb shock absorber (0.08 g/cm^3) are 6.677×10^{-2} and 2.973×10^{-3} atoms/b*cm, respectively. As a result, water is more effective at thermalizing neutrons than the honeycomb shock absorbers. Therefore, the use of water at 1.0 g/cm^3 between the inner and outer containers is considered a conservative replacement for the honeycomb shock absorbers.

The fuel assemblies are modeled inside the inner container, flush with the polyethylene foam. No fuel assembly structures outside the active length of the rod are represented in the models, with the exception of the fuel assembly channel. The fuel assembly structures outside the active fuel length, other than the fuel assembly channel, are composed of materials that absorb neutrons by radiative capture, therefore, neglecting them is conservative. In addition, no grids within the rod active length are represented. The internal grid structure displaces water from between the fuel rods, decreasing the H/X ratio. Since the fuel assemblies are undermoderated, decreasing the H/X ratio decreases system reactivity. Therefore, it is conservative to neglect the internal grid structure in modeling the RAJ-II container. The maximum pellet enrichment and maximum fuel lattice average enrichment is 5.0 wt% U-235. Only 75% credit is taken for gadolinia present in the fuel rods.

Calculations performed with the package array HAC model determine the fuel assembly modeling for the single package Normal Conditions of Transport (NCT) model. A fuel parameter sensitivity study is conducted and a worst case fuel assembly is developed for each fuel design. The sensitivity study results determine the fuel parameter ranges for the fuel assembly loading criteria shown in Table 6-1 and Table 6-2. The ranges are broad enough to accommodate future fuel assembly design changes. The fuel rod pitch, fuel pellet outer diameter, fuel rod clad inner and outer diameters, fuel rod number, and part length fuel rod number are varied independently in the package array HAC calculations. Reactivity effects are investigated, and the worst case is identified for each parameter perturbation. To validate the ranges for worst case fuel parameter combinations (e.g., worst case pellet OD, clad OD, clad ID, etc.) within the same assembly, a worst case fuel assembly is created for each fuel design considered for transport in the RAJ-II container, by choosing each parameter value that provides the highest system reactivity. Calculations performed with the worst case fuel assemblies validate the parameter ranges to be used as fuel acceptance criteria. Both un-channeled (Figure

6-9 through Figure 6-15) and channeled fuel assemblies, Figure 6-16, are considered in the worst case orientation, subjected to the worst case fuel damage, and the most reactive configuration is chosen for subsequent calculations.

The GNF 10x10 worst case fuel assembly is used for the RAJ-II single package NCT model since it is determined to be the most reactive assembly type in the package array HAC fuel parameter studies. The worst case fuel parameters for the GNF 10x10 assembly are presented in Table 6-11.

Polyethylene inserts or cluster separators are positioned between fuel rods at various locations along the axis of the fuel assembly to avoid stressing the axial grids during transportation. Two types of inserts, shown in Figure 6-1 and Figure 6-2, are considered for use with the RAJ-II container. Since the polyethylene cluster separators provide a higher volume average density polyethylene inventory, they are chosen for the RAJ-II criticality analysis. Other types of inserts are acceptable provided that their polyethylene inventory is within the limits established using the cluster separators.

The normal condition model utilizes the maximum allowable polyethylene mass and applies it over the full axial length of the fuel. The polyethylene is smeared into the water region surrounding the fuel rods as well as the water region surrounding the fuel assembly normally occupied by the cluster holder.

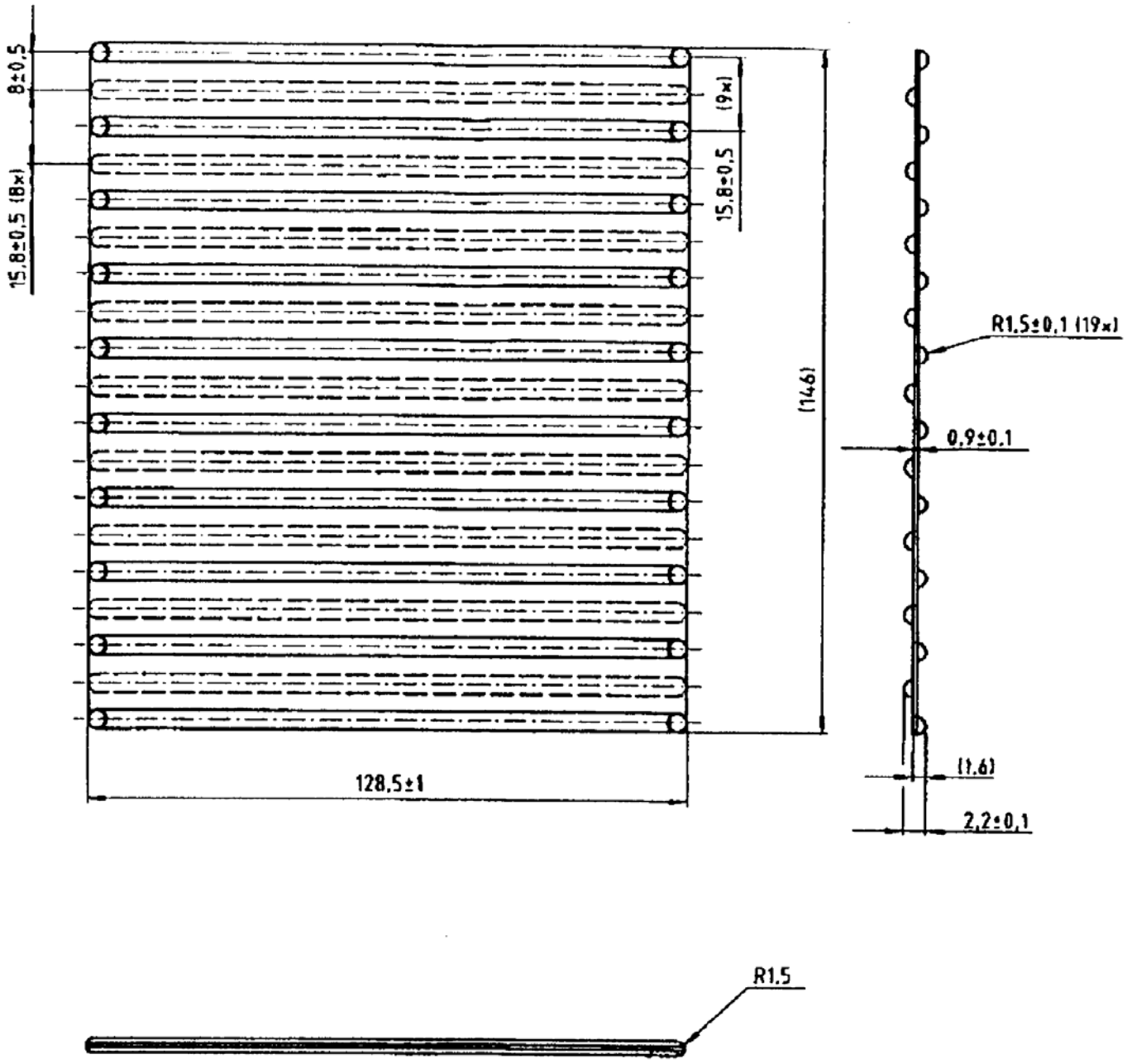

Figure 6-1 Polyethylene Insert (FANP Design)

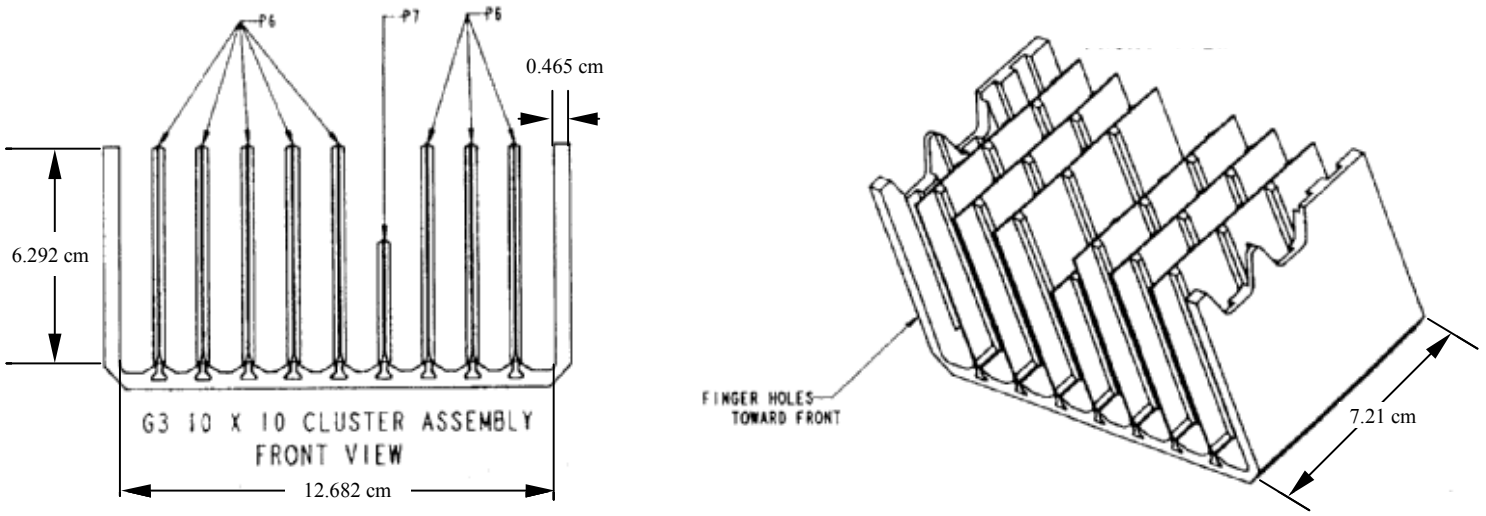

Figure 6-2 Polyethylene Cluster Separator Assembly (GNF Design)

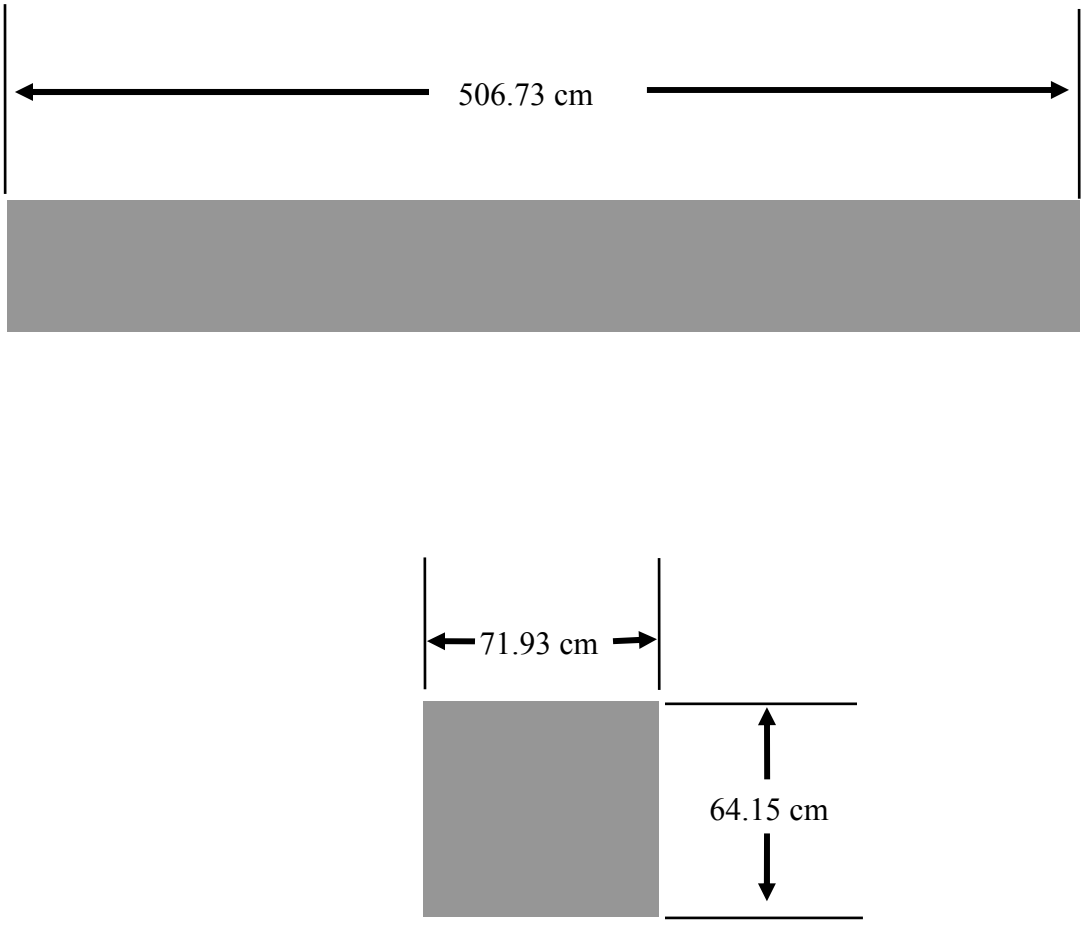

Figure 6-3 RAJ-II Outer Container Normal Conditions of Transport Model

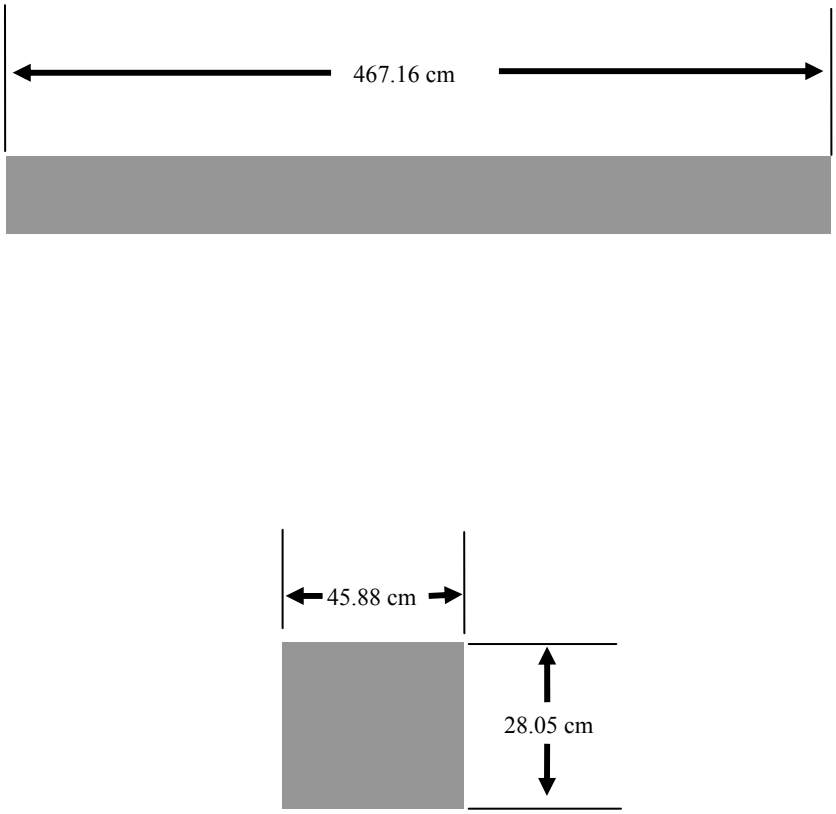

Figure 6-4 RAJ-II Inner Container Normal Conditions of Transport Model

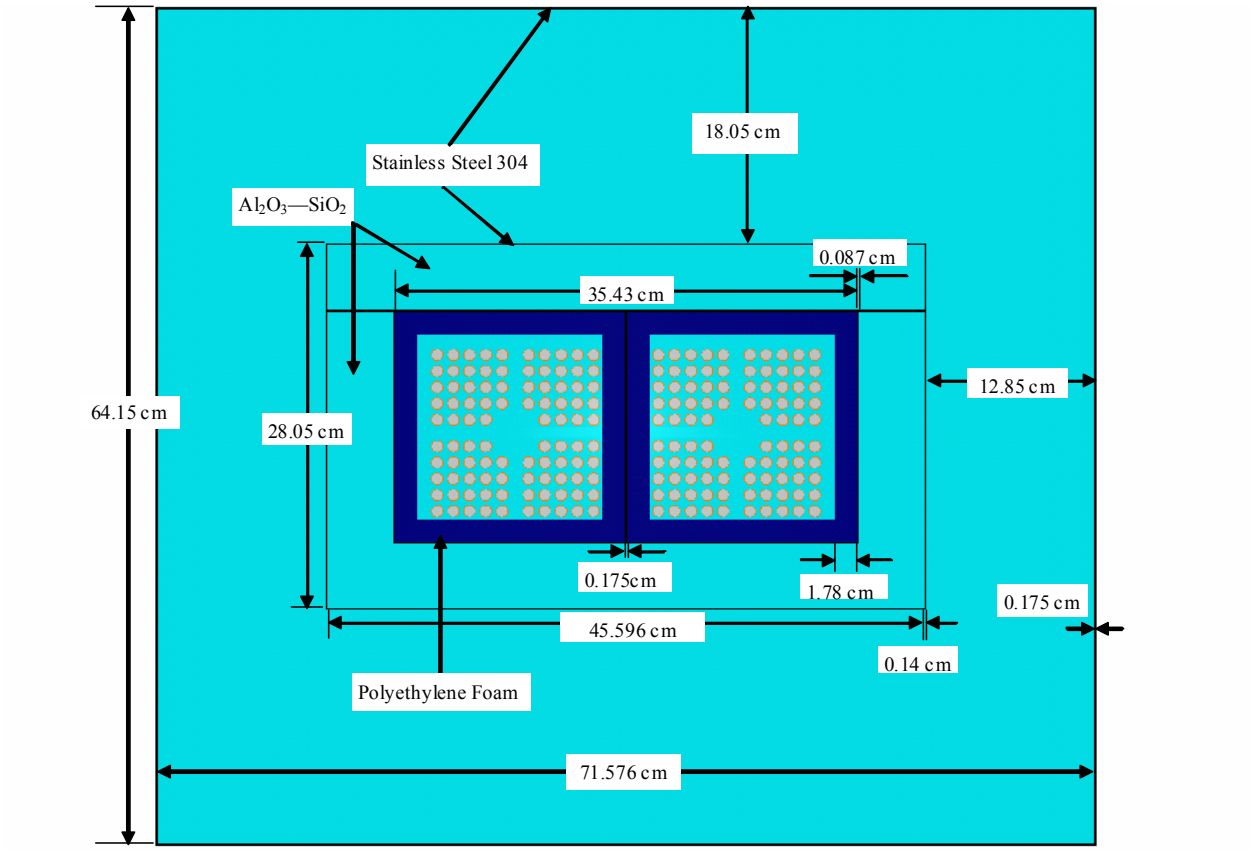

Figure 6-5 RAJ-II Container Cross-Section Normal Conditions of Transport Model

6.3.1.1.2 Single Package Hypothetical Accident Condition Model

The RAJ-II HAC model inner container dimensions are shown in Figure 6-7 and Figure 6-8. The container deformation modeled for the RAJ-II HAC model includes the damage incurred from the 9-meter drop onto an unyielding surface as well as conservative factors. The RAJ-II inner container length is conservatively reduced by 8.1 cm to bound the damage incurred from the 9-meter drop onto an unyielding surface. The polyethylene foam is assumed to burn away for the HAC single package model. Full density water that provides more reflection capability is assumed to flood the RAJ-II inner container fuel compartment. The Alumina Silicate insulation is assumed to remain in place, since scoping calculations proved it to provide a more reactive configuration. The fuel assemblies are assumed to freely move within the respective compartment resulting in a worst case orientation. The rubber vibro-isolating devices are also assumed to melt when exposed to an external fire, allowing the inner container to shift downward about 2.54 cm. However, scoping calculations reveal no increase in reactivity by moving the inner container; therefore, the inner container is positioned within the outer container as shown in Figure 6-8. The inner container horizontal position within the outer container remains the same as the normal condition model, since the stainless steel fixture assemblies remained intact following the 9-meter drop. The outer container dimensions are shown in Figure 6-6 RAJ-II Outer Container Hypothetical Accident Condition Model and Figure 6-8. The outer

container length is reduced by 4.7 cm to bound the damage sustained from a 9-meter drop onto an unyielding surface. In addition, the outer container height is reduced by 2.4 cm to bound the damage sustained during the 9-meter drop (Reference 1). No credit is taken for the structural steel between the inner and outer containers. The honeycomb shock absorbers, located between the inner and outer containers, are not explicitly modeled. Instead, water is placed in the space between the inner and outer containers, and its density is varied from 0.0 – 1.0 g/cm^3. The honeycomb shock absorbers have a density between 0.04 and 0.08 g/cm^3. The hydrogen number densities for water (1.0 g/cm^3) and for the honeycomb shock absorber (0.08 g/cm^3) are $6.677x10^{-2}$ and $2.973x10^{-3}$ atoms/b*cm, respectively. As a result, water is more effective at thermalizing neutrons than the honeycomb shock absorbers. Therefore, the use of water at 1.0 g/cm^3 between the inner and outer containers is considered a conservative replacement for the honeycomb shock absorbers. The reduction in length for the inner and outer containers, the reduction in height for the outer container, the absence of polyethylene foam, the presence of the insulation, and the fuel assembly freedom of movement are consistent with the physical condition of the RAJ-II shipping container after being subjected to the tests specified in 10 CFR Part 71.

Calculations performed with the package array HAC model determine the fuel assembly modeling for the single package HAC model. No fuel assembly structures outside the active length of the rod are represented in the models, with the exception of the fuel assembly channel. The fuel assembly structures outside the active fuel length, other than the fuel assembly channel, are composed of materials that absorb neutrons by radiative capture, therefore, neglecting them is conservative. In addition, no grids within the rod active length are represented. The internal grid structure displaces water from between the fuel rods, decreasing the H/X ratio. Since the fuel assemblies are undermoderated, decreasing the H/X ratio decreases system reactivity. Therefore, it is conservative to neglect the internal grid structure in modeling the RAJ-II container. The maximum pellet enrichment and maximum fuel lattice average enrichment is 5.0 wt% U-235. The gadolinia content of any gadolinia-urania fuel rods is taken to be 75% of the minimum value specified in Table 6-1. The fuel assemblies are modeled inside the inner container, in one of seven orientations shown in Figure 6-9 RAJ-II Hypothetical Accident Condition Model with Fuel Assembly Orientation 1 through Figure 6-15 RAJ-II Hypothetical Accident Condition Model with Fuel Assembly Orientation 7. The worst case orientation is chosen for each fuel assembly design considered for transport and used in subsequent calculations. Fuel damage sustained during the 9-meter (30 foot) drop test is simulated as a change in fuel rod pitch along the full axial length of each fuel assembly considered for transport. Based on the fuel damage sustained in the RAJ-II shipping container drop test (Reference 1), a 10% reduction in fuel rod pitch over the full length of each fuel assembly, or a 4.1% increase in fuel rod pitch over the full length of each fuel assembly, is determined to be conservative. Both un-channeled (Figure 6-9 through Figure 6-15) and channeled fuel assemblies (Figure 6-16) are considered in the worst case orientation, subjected to the worst case fuel damage, and the most reactive configuration is chosen for subsequent calculations.

The fuel damage sustained during the 9-meter drop test is bounded by performing a fuel parameter sensitivity study and creating a worst case fuel assembly for each fuel design. The sensitivity study results determine the fuel parameter ranges for the fuel assembly loading criteria shown in Table 6-1. The ranges are broad enough to accommodate future fuel assembly design changes. The fuel rod pitch, fuel pellet outer diameter, fuel rod clad inner and outer

diameters, fuel rod number, and part length fuel rod number are varied independently in the package array HAC calculations. Reactivity effects are investigated, and the worst case is identified for each parameter perturbation. To validate the ranges for worst case fuel parameter combinations (e.g. worst case pellet OD, clad OD, clad ID, etc.) within the same assembly, a worst case fuel assembly is created for each fuel design considered for transport in the RAJ-II container, by choosing each parameter value that provides the highest system reactivity. Calculations performed with the worst case fuel assemblies validate the parameter ranges to be used as fuel acceptance criteria.

The GNF 10x10 worst case fuel assembly at a 5.0 wt% U-235 enrichment, containing twelve 2 wt % gadolinia-urania fuel rods, and twelve part length fuel rods is used for the RAJ-II single package HAC model since it is determined to be the most reactive assembly in the package array HAC fuel parameter studies. The worst case fuel parameters for the 10x10 assembly are presented in Table 6-11.

Polyethylene inserts (cluster separators) are positioned between fuel rods at various locations along the axis of the fuel assembly to avoid stressing the axial grids during transportation. Two types of inserts, shown in Figure 6-1 and Figure 6-2, are considered for use with the RAJ-II container. Since the polyethylene cluster separators provide a higher volume averaged density polyethylene inventory, they are chosen for the RAJ-II criticality analysis. Other types of inserts are acceptable provided that their polyethylene inventory is within the limits established using the cluster separators.

In the hypothetical accident condition model, the polyethylene inserts are assumed to melt when subjected to the tests specified in 10 CFR Part 71. The polyethylene is assumed to uniformly coat the fuel rods in each fuel assembly forming a cylindrical layer of polyethylene around each fuel rod. Different coating thicknesses are investigated in the package array HAC calculations, and a polyethylene mass limit is developed for each fuel assembly type considered for transport. The RAJ-II single package model contains 10x10 worst case fuel assemblies with 10.2 kg of polyethylene per assembly. The polyethylene is smeared into the fuel rod cladding to accommodate the limitations in the lattice cell modeling for cross-section processing in SCALE. A visual representation of the smeared clad/polyethylene mixture compared to a discrete treatment is shown in Figure 6-21 Visual Representation of the Clad/Polyethylene Smeared Mixture versus Discrete Modeling. The polyethylene mass and the volume fractions of polyethylene and zirconium clad for each fuel assembly analyzed are shown in Table 6-13 Polyethylene Mass and Volume Fraction Calculations. The volume fractions in Table 6-13 are entered into the model input standard composition specification area. Mixtures representing the polyethylene inserts between fuel rods are created using the compositions specified, and used in the KENO V.a calculation. The mixtures are also used in the lattice cell description to provide the lump shape and dimensions for resonance cross-section processing, the lattice corrections for cross-section processing, and the information necessary to create flux-weighted cross-sections based on the lattice cell geometry.

6.3.1.2 Package Array Models

6.3.1.2.1 Package Array Normal Condition Model

The RAJ-II container package array normal condition model consists of a 21x3x24 array of containers, surrounded by a 30.48 cm layer of full density water for reflection. The container array is fully flooded with water at a density sufficient for optimum moderation. The container and fuel model in the array are those discussed in Section 6.3.1.1.1.

6.3.1.2.2 Package Array Hypothetical Accident Condition (HAC) Model

The RAJ-II package array HAC model consists of either a 14x2x16 or 10x1x10 array of containers, surrounded by a 30.48 cm layer of full density water for reflection. The 14x2x16 array (Sections 6.4.1 – 6.4.10) is initially used under the assumption that the polyethylene foam, on which the fuel assemblies rest, completely burns away during a fire. The 10x1x10 array (Sections 6.4.11 – 6.4.13) assumes the polyethylene foam remains intact following a fire. The container array has no interspersed water between packages in the array and no water in the outer container. These moderator conditions optimize the interaction between packages in the array. Unlike the HAC single package model, the HAC package array model assumes the polyethylene foam remains in place following the tests specified in 10 CFR 71. The presence of polyethylene foam allows increased neutron leakage from the inner container fuel compartment and promotes increased neutron interaction among containers in the array. The inner container fuel compartment space not occupied by the polyethylene foam is fully flooded with water at a density sufficient for optimum moderation. The remaining HAC model container and fuel details are those discussed in Section 6.3.1.1.2.

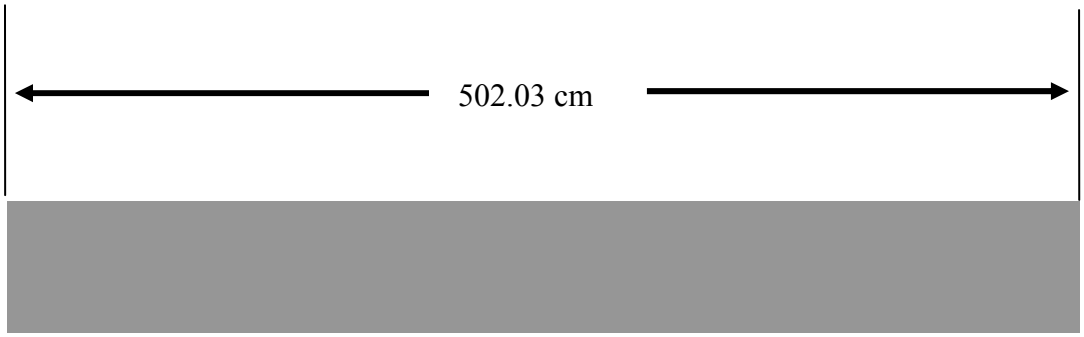

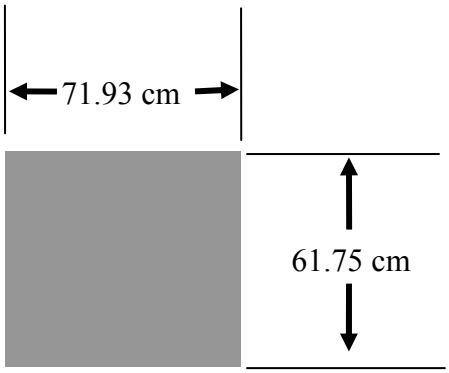

Figure 6-6 RAJ-II Outer Container Hypothetical Accident Condition Model

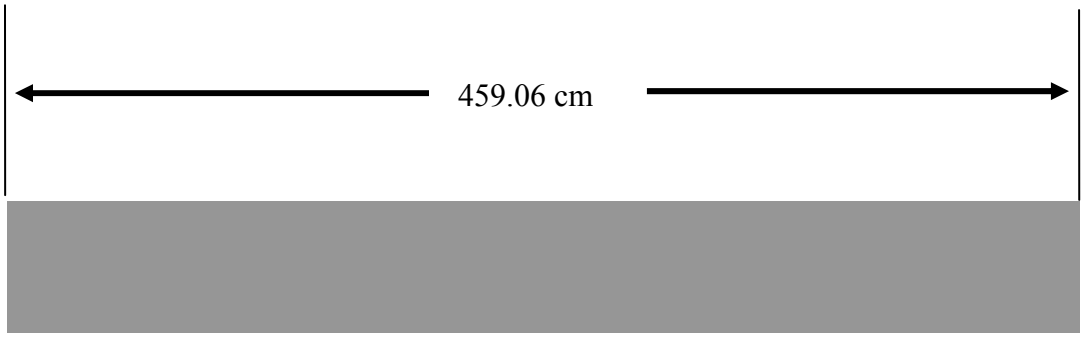

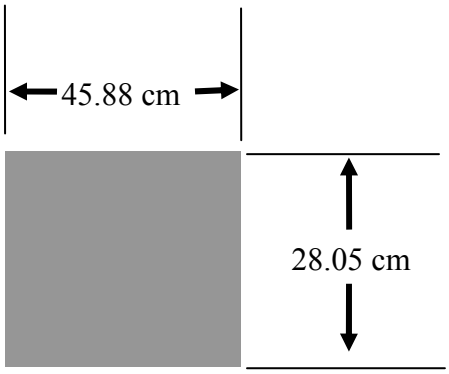

Figure 6-7 RAJ-II Inner Container Hypothetical Accident Condition Model

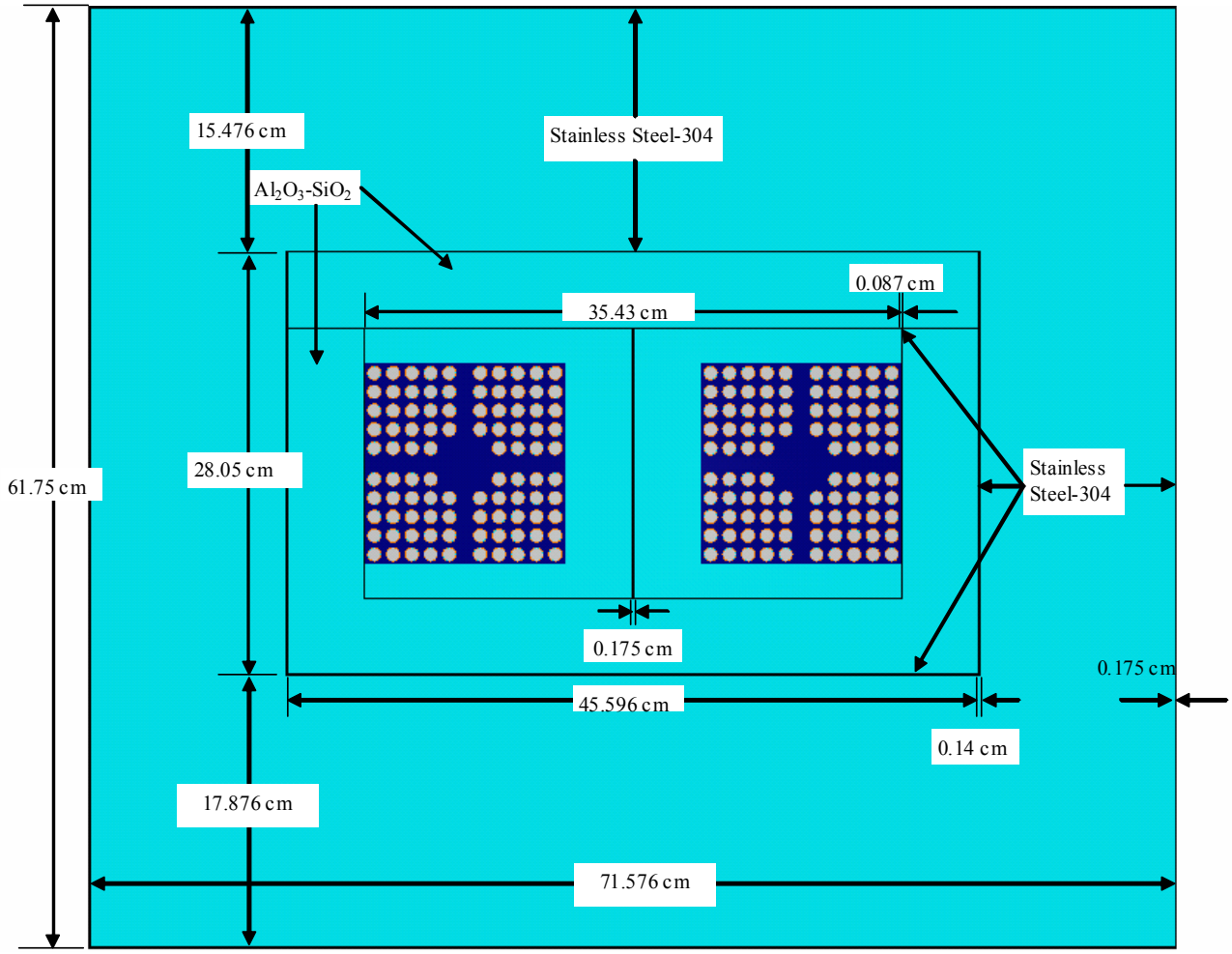

Figure 6-8 RAJ-II Cross-Section Hypothetical Accident Condition Model

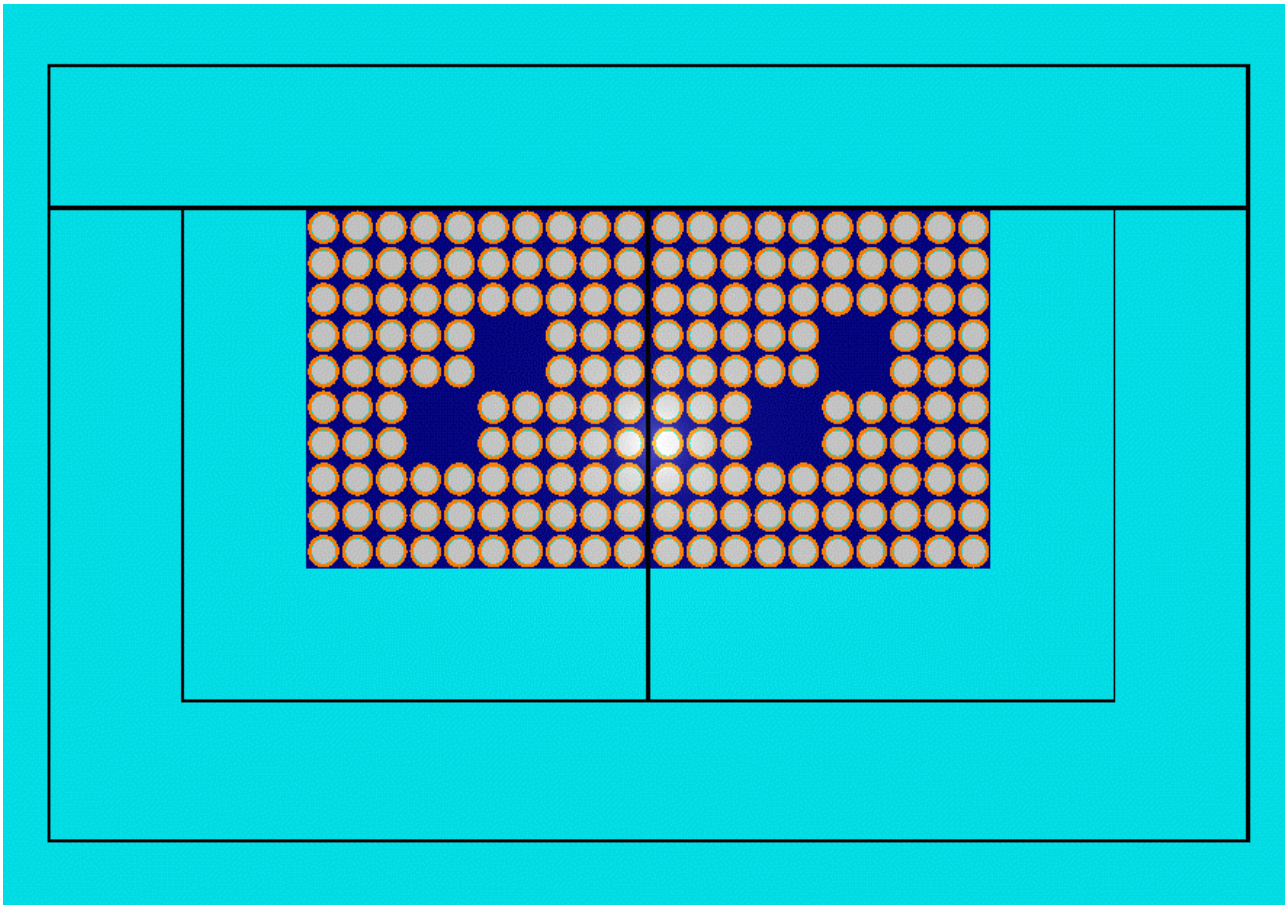

Figure 6-9 RAJ-II Hypothetical Accident Condition Model with Fuel Assembly Orientation 1

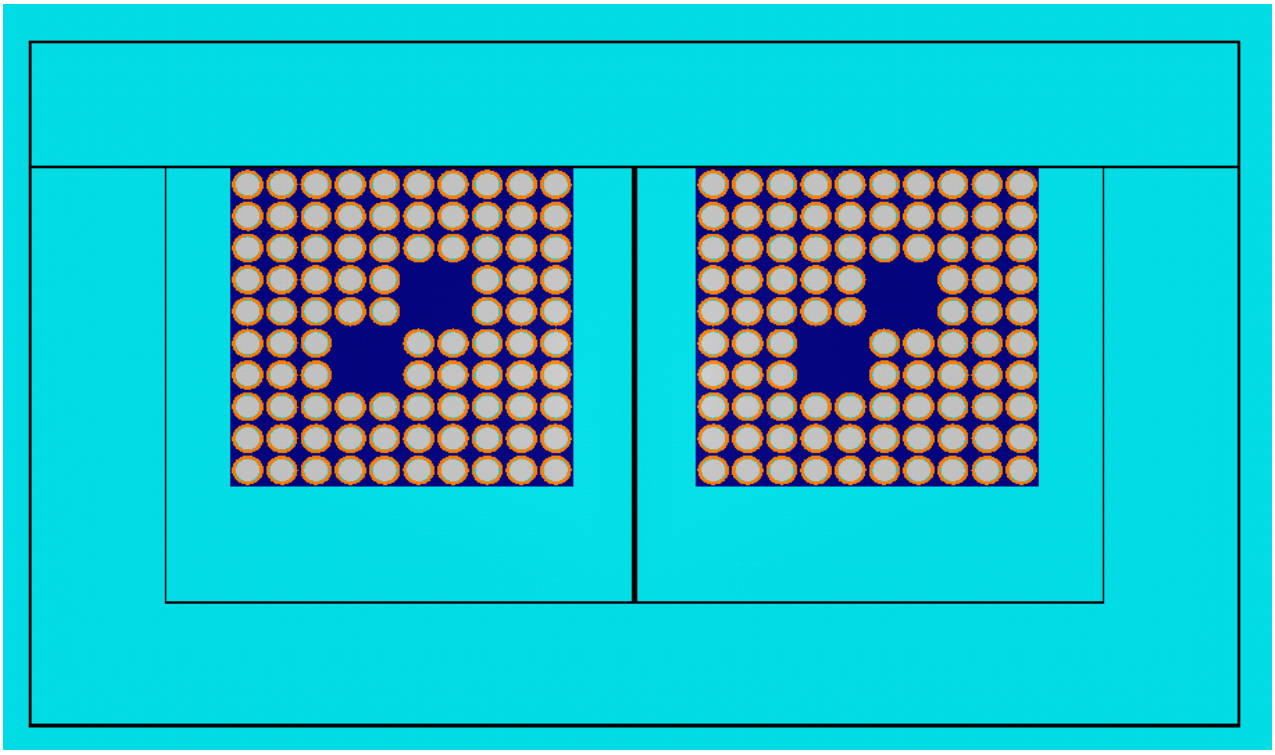

Figure 6-10 RAJ-II Hypothetical Accident Condition Model with Fuel Assembly Orientation 2

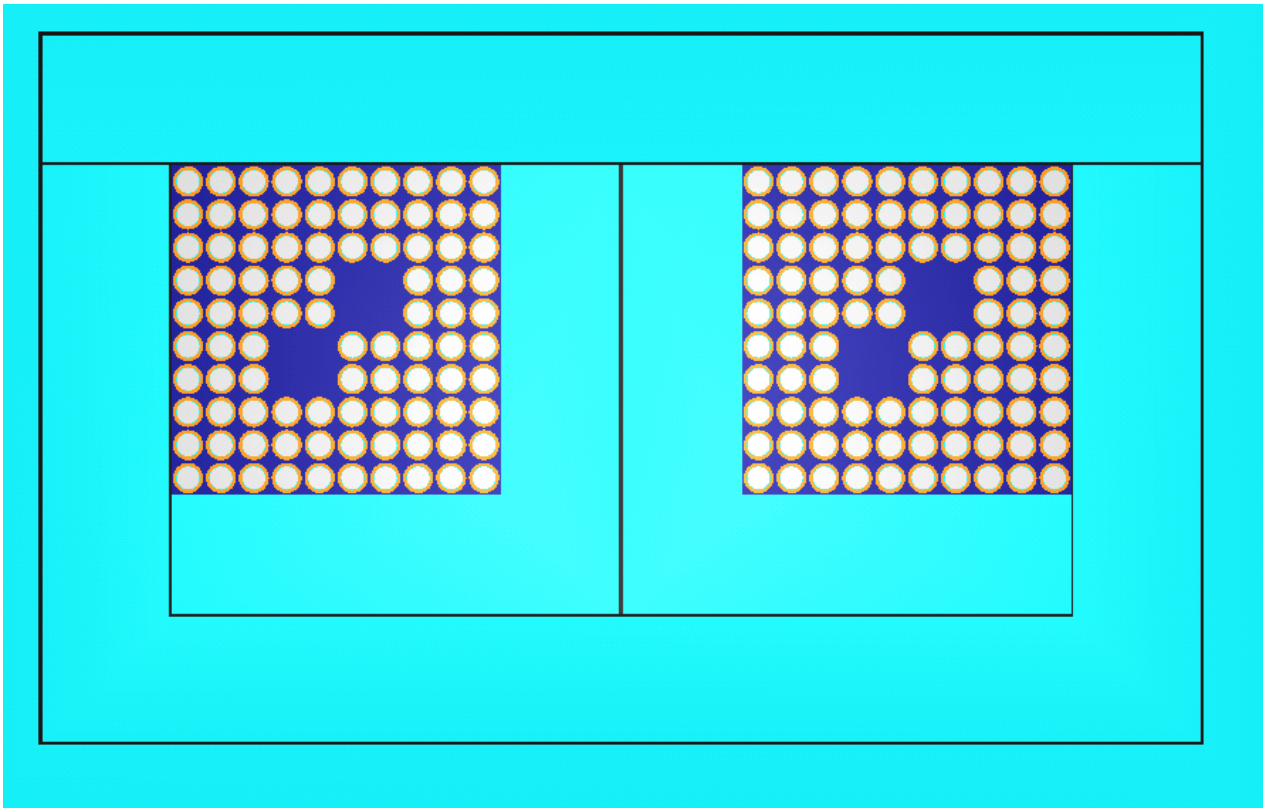

Figure 6-11 RAJ-II Hypothetical Accident Condition Model with Fuel Assembly Orientation 3

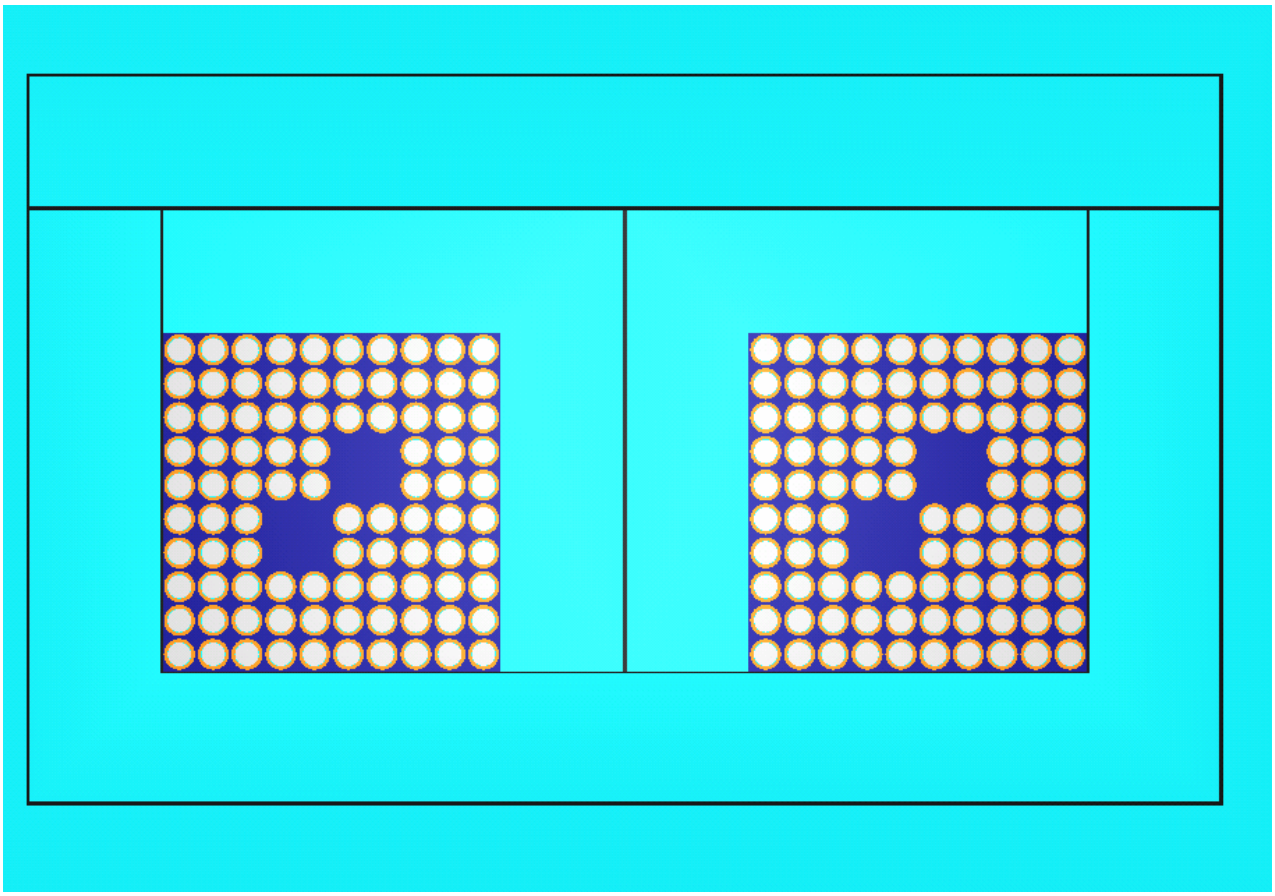

Figure 6-12 RAJ-II Hypothetical Accident Condition Model with Fuel Assembly Orientation 4

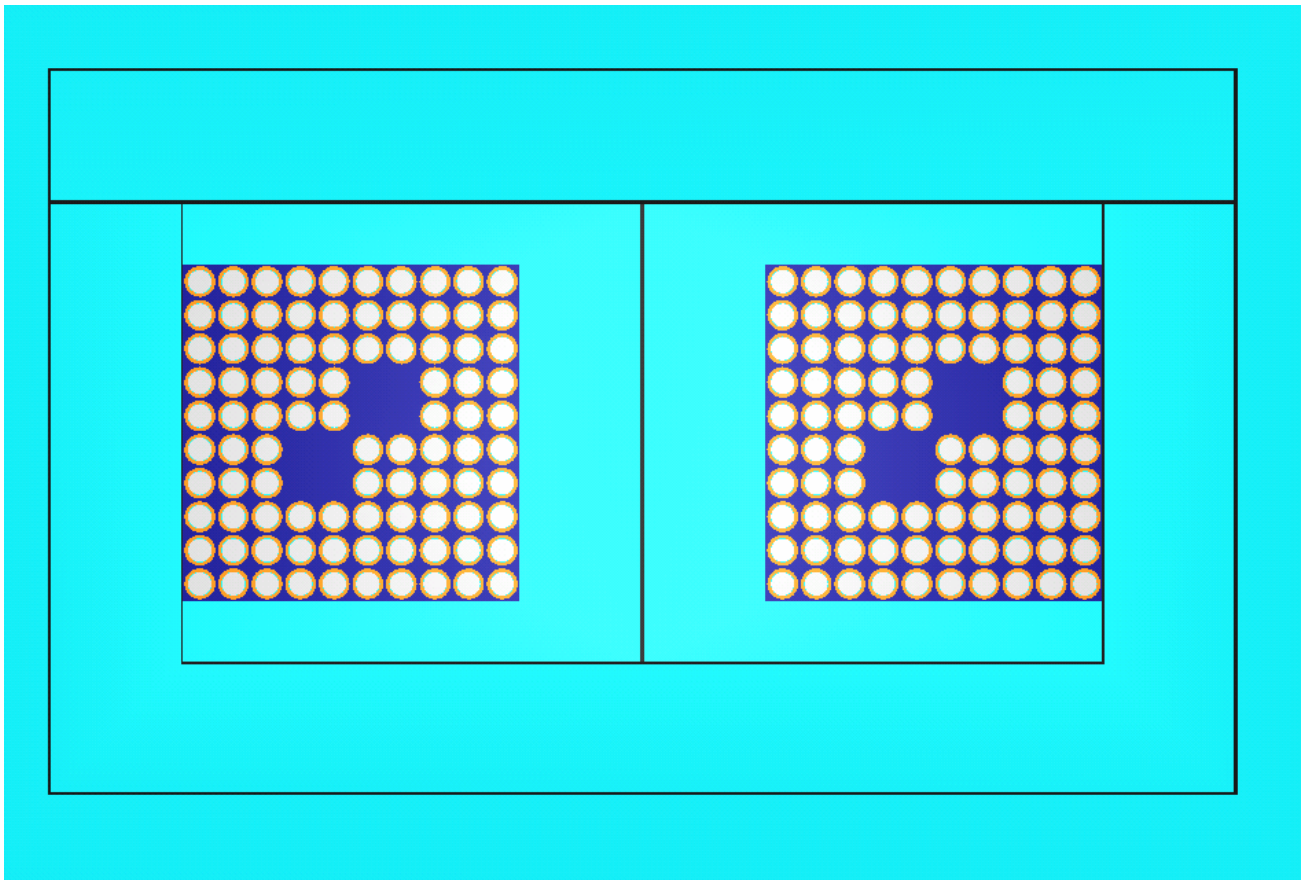

Figure 6-13 RAJ-II Hypothetical Accident Condition Model with Fuel Assembly Orientation 5

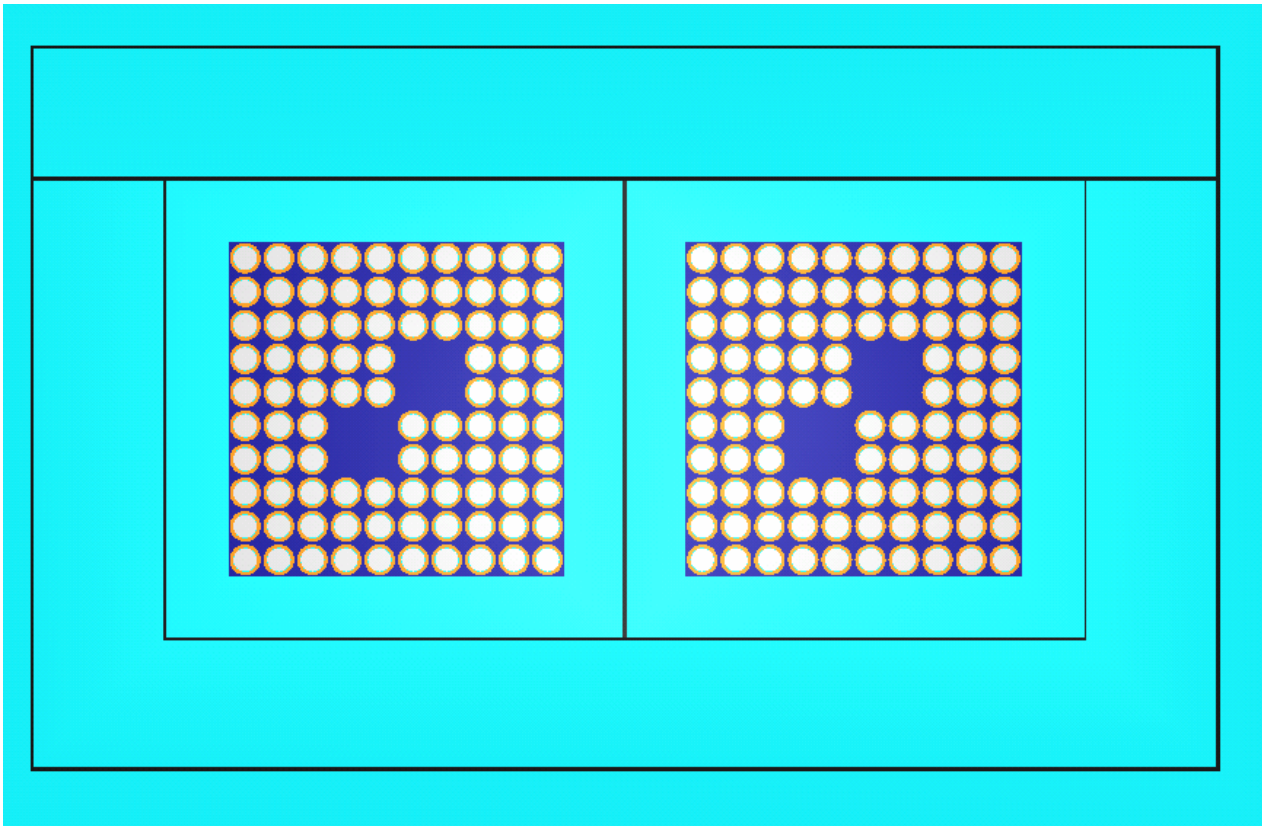

Figure 6-14 RAJ-II Hypothetical Accident Condition Model with Fuel Assembly Orientation 6

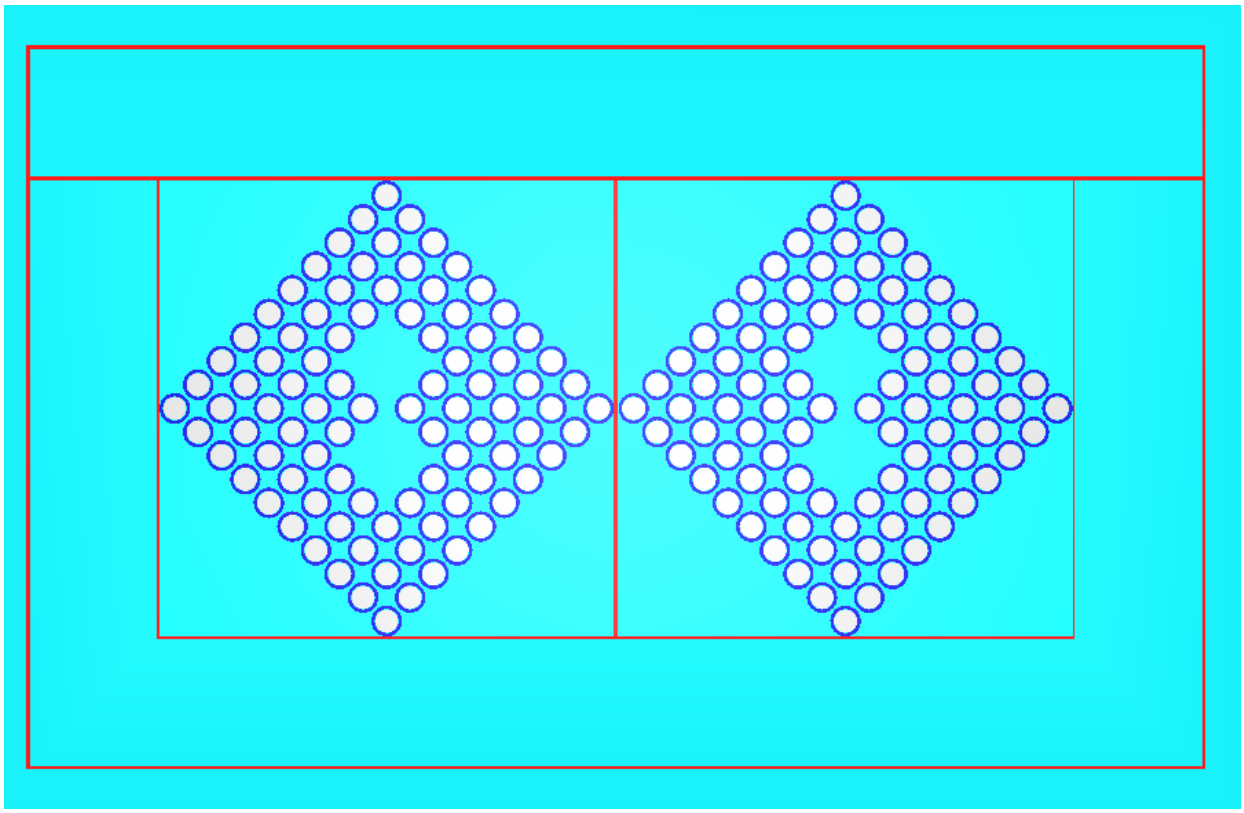

Figure 6-15 RAJ-II Hypothetical Accident Condition Model with Fuel Assembly Orientation 7

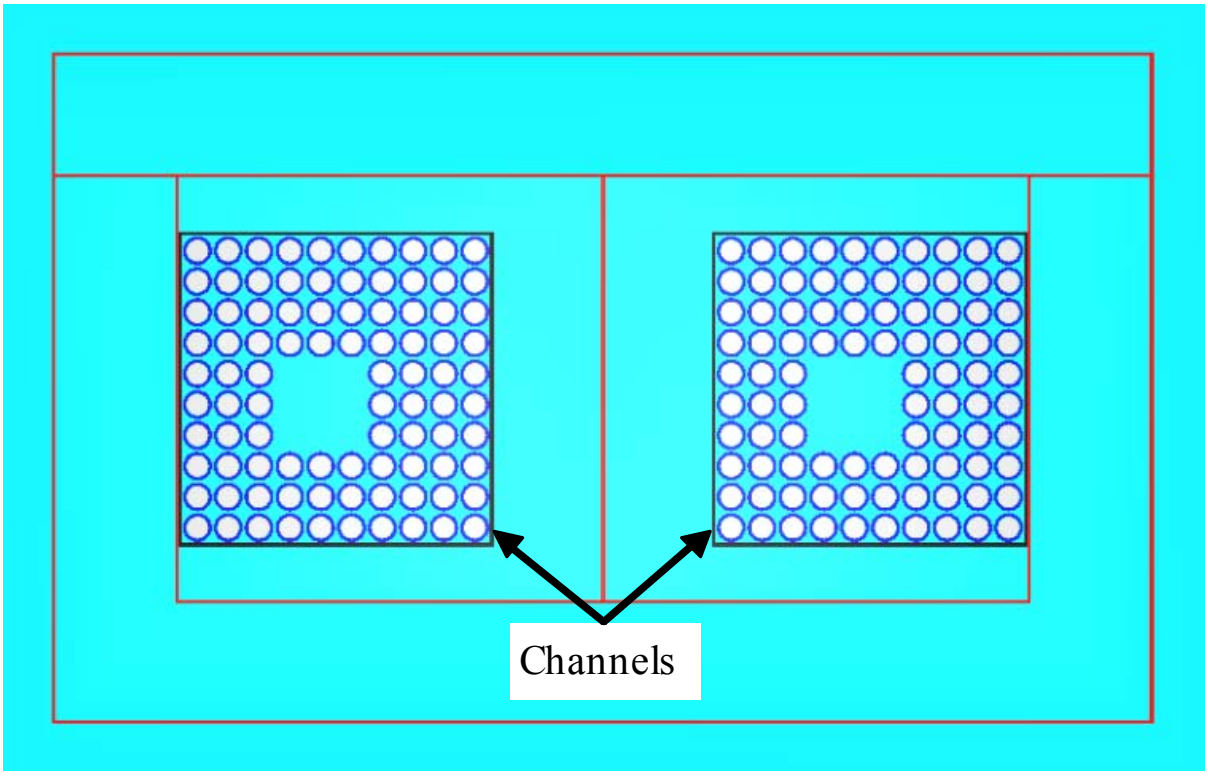

Figure 6-16 RAJ-II Hypothetical Accident Condition Model with Channels

6.3.1.3 RAJ-II Fuel Rod Transport Model

The RAJ-II fuel rod transport models are developed for single packages and package arrays under normal transport and hypothetical accident conditions. Cylindrical fuel rods containing UO_2, enriched to 5 wt. percent U-235, are modeled loose, bundled together, or in the RAJ-II inner container in 5-inch stainless steel pipe or protective case.

6.3.1.3.1 RAJ-II Single Package Fuel Rod Transport NCT Model

The RAJ-II single package normal conditions of transport described in Section 6.3.1.1.1 are used for the single package fuel rod transport models.

The fuel rods are modeled inside the inner container, flush with the polyethylene foam. A 0.0152 cm thick polyethylene layer is modeled around each fuel rod to simulate any protective material present. The worst case fuel rod parameters are shown in Table 6-6 RAJ-II Fuel Rod Transport Model Fuel Parameters.

Table 6-6 RAJ-II Fuel Rod Transport Model Fuel Parameters

Fuel Rod Type	Pellet OD (cm)	Fuel Rod ID (cm)	Fuel Rod OD (cm)	Fuel Rod Length (cm)
10x10	0.9	1.000	1.000	385
9 x 9	0.9600	1.0200	1.0200	381
8 x 8	1.05	1.1000	1.1000	381

Calculations performed with the fuel rod transport, package array, HAC model determine the fuel assembly modeling for the fuel rod transport, single package, Normal Conditions of Transport (NCT) model. The calculations investigate transporting loose fuel rods, bundled fuel rods, and fuel rods in 5-inch stainless steel pipe within each RAJ-II shipping compartment. A fuel rod pitch sensitivity study is conducted for each fuel rod type to determine the number of fuel rods that can be transported in a loose configuration within the RAJ-II fuel assembly compartment. A square pitch fuel rod array is used for the sensitivity study since scoping calculations showed no statistically significant difference in system reactivity between fuel rods in a square pitch array and those in a triangular pitch array within the container geometry. The pitch sensitivity study results in the minimum and maximum allowable fuel rod quantity for shipping in a loose configuration. The loose rod analysis is used to bound a fuel rod shipment in which fuel rods are strapped or bundled together. A fuel rod pitch sensitivity analysis is also performed to determine the fuel rod quantity that may be transported inside a 5-inch stainless steel pipe. A triangular pitch fuel rod array is used for the sensitivity study since scoping calculations showed it to result in a higher system reactivity than a square pitch rod array inside a 5-inch stainless steel pipe. The stainless steel material is conservatively neglected when performing the calculations, therefore, any container with a volume equivalent to or less than the 5-inch stainless steel pipe is acceptable for fuel rod transport, as long as the fuel rod quantity is limited to that for the pipe.

The 8x8 worst case fuel rod is used for the RAJ-II fuel rod transport, single package, NCT model since it is determined to be the most reactive rod in the fuel rod transport, package array, HAC pitch sensitivity studies. The RAJ-II fuel rod transport, single package NCT model is shown in Figure 6-17 RAJ-II Fuel Rod Transport Single Package NCT Model. The worst case fuel parameters for the 8x8 rod are presented in Table 6-6. As shown in Table 6-6, the fuel rod cladding is not modeled for the 8x8 fuel rod. Although the cladding material is removed, the fuel rod external boundary is maintained (i.e. pellet clad gap to fuel rod OD is maintained, polyethylene coating applied to fuel rod OD region).

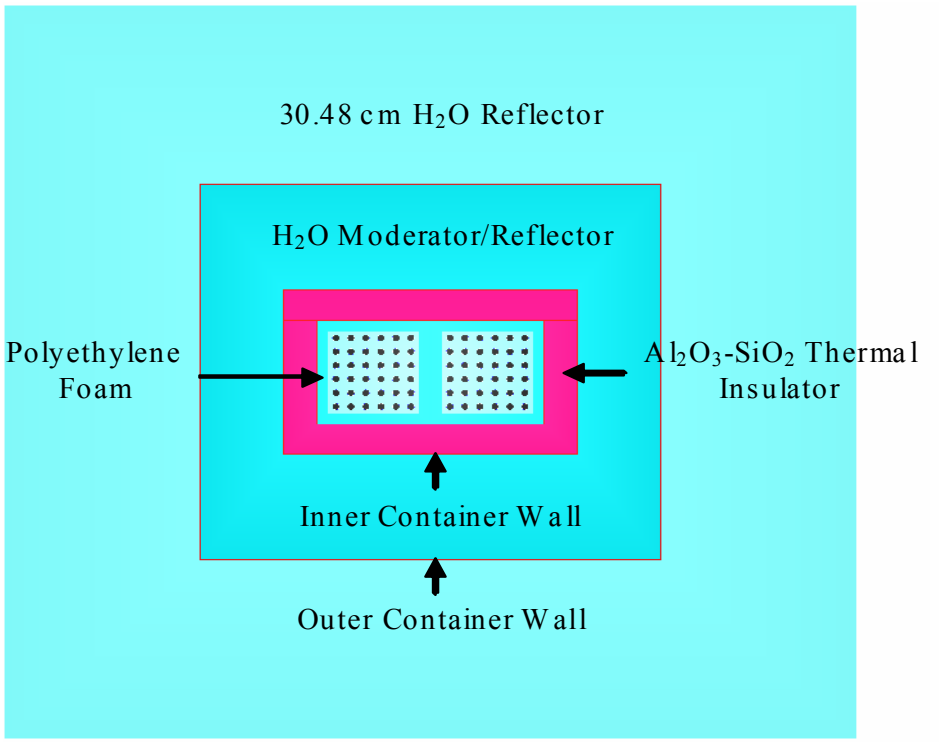

Figure 6-17 RAJ-II Fuel Rod Transport Single Package NCT Model

6.3.1.3.2 RAJ-II Single Package Fuel Rod Transport HAC Model

The RAJ-II single package hypothetical accident conditions described in Section 6.3.1.1.2 are used for the single package fuel rod transport models.

The fuel rods are modeled as filling the inner container fuel assembly compartment, since the polyethylene foam is removed due to the HAC. A 0.0152 cm thick polyethylene layer is modeled around each fuel rod to simulate any protective material present. Worst case fuel rod parameters determined from the package array HAC parameter sensitivity analyses (Section 6.3.1.1.2), are used for the fuel rod transport models. The worst case fuel rod parameters are shown in Table 6-6 RAJ-II Fuel Rod Transport Model Fuel Parameters.

Calculations performed with the fuel rod transport, package array, HAC model determine the fuel assembly modeling for the fuel rod transport, single package, HAC model. The calculations

investigate transporting loose fuel rods, bundled fuel rods, fuel rods in a 5-inch stainless steel pipe and protective case within each RAJ-II shipping compartment. A fuel rod pitch sensitivity study is conducted for each fuel rod type to determine the number of fuel rods that can be transported in a loose configuration within the RAJ-II fuel assembly compartment. A square pitch fuel rod array is used for the sensitivity study since scoping calculations showed no statistically significant difference in system reactivity between fuel rods in a square pitch array and those in a triangular pitch array within the container geometry. The pitch sensitivity study results in the minimum and maximum allowable fuel rod quantity for shipping in a loose configuration. The loose rod analysis is used to bound a fuel rod shipment in which fuel rods are strapped together. A fuel rod pitch sensitivity analysis is also performed to determine the fuel rod quantity that may be transported inside a 5-inch stainless steel, Type 304 pipe. A triangular pitch fuel rod array is used for the sensitivity study since scoping calculations showed it to result in a higher system reactivity than a square pitch rod array inside a 5-inch stainless steel pipe. The stainless steel material is conservatively neglected when performing the calculations, therefore, any container with a volume equivalent to or less than the 5-inch stainless steel pipe is acceptable for fuel rod transport, as long as the fuel rod quantity is limited to that for the pipe.

The 8x8 worst case fuel rod is used for the RAJ-II fuel rod transport, single package, HAC model since it is determined to be the most reactive rod in the fuel rod transport, package array, HAC pitch sensitivity studies. The RAJ-II fuel rod transport, single package HAC model is shown in Figure 6-18 RAJ-II Fuel Rod Transport Single Package HAC Model. The worst case fuel parameters for the 8x8 rod are presented in Table 6-6. As shown in Table 6-6, the fuel rod cladding is not modeled for the 8x8 fuel rod. Although the cladding material is removed, the fuel rod external boundary is maintained (i.e., pellet clad gap to fuel rod OD is maintained, polyethylene coating applied to fuel rod OD region).

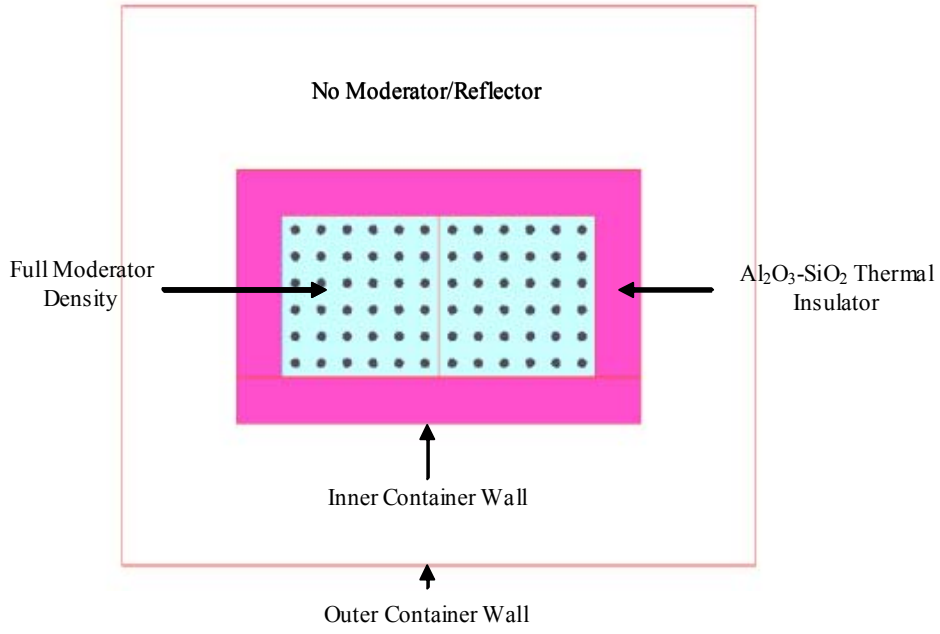

Figure 6-18 RAJ-II Fuel Rod Transport Single Package HAC Model

6.3.1.3.3 RAJ-II Package Array Fuel Rod Transport NCT Model

The RAJ-II package array normal conditions of transport described in Section 6.3.1.2.1 are used for the package array, normal conditions of transport, fuel rod transport models.

The fuel rods are modeled inside the inner container, flush with the polyethylene foam. A 0.0152 cm thick polyethylene layer is modeled around each fuel rod to simulate any protective material present. Worst case fuel rod parameters determined from the package array HAC parameter sensitivity analyses (Section 6.3.1.2.2), are used for the fuel rod transport models. The worst case fuel rod parameters are shown in Table 6-6.

Calculations performed with the fuel rod transport, package array, HAC model determine the fuel assembly modeling for the fuel rod transport, package array, Normal Conditions of Transport (NCT) model. The calculations investigate transporting loose fuel rods, bundled fuel rods, and fuel rods in 5-inch stainless steel pipe within each RAJ-II shipping compartment. A fuel rod pitch sensitivity study is conducted for each fuel rod type to determine the number of fuel rods that can be transported in a loose configuration within the RAJ-II fuel assembly compartment. A square pitch fuel rod array is used for the sensitivity study since scoping calculations showed no statistically significant difference in system reactivity between fuel rods in a square pitch array and those in a triangular pitch array within the container geometry. The pitch sensitivity study results in the minimum and maximum allowable fuel rod quantity for shipping in a loose configuration. The loose rod analysis is used to bound a fuel rod shipment in which fuel rods are strapped or bundled together.

A fuel rod pitch sensitivity analysis is also performed to determine the fuel rod quantity that may be transported inside a 5-inch stainless steel pipe. A triangular pitch fuel rod array is used for the sensitivity study since scoping calculations showed it to result in a higher system reactivity than a square pitch rod array inside a 5-inch stainless steel pipe. The stainless steel material is conservatively neglected when performing the calculations, therefore, any container with a volume equivalent to or less than the 5-inch stainless steel pipe is acceptable for fuel rod transport, as long as the fuel rod quantity is limited to that for the pipe.

The 8x8 worst case fuel rod is used for the RAJ-II fuel rod transport, package array, NCT model since it is determined to be the most reactive rod in the fuel rod transport, package array, HAC pitch sensitivity studies. A portion of the RAJ-II fuel rod transport, 21x3x24 package array, NCT model is shown in Figure 6-19. The worst case fuel parameters for the 8x8 rod are presented in Table 6-6. As shown in Table 6-6, the fuel rod cladding is not modeled for the 8x8 fuel rod. Although the cladding material is removed, the fuel rod external boundary is maintained (i.e., pellet clad gap to fuel rod OD is maintained, polyethylene coating applied to fuel rod OD region).

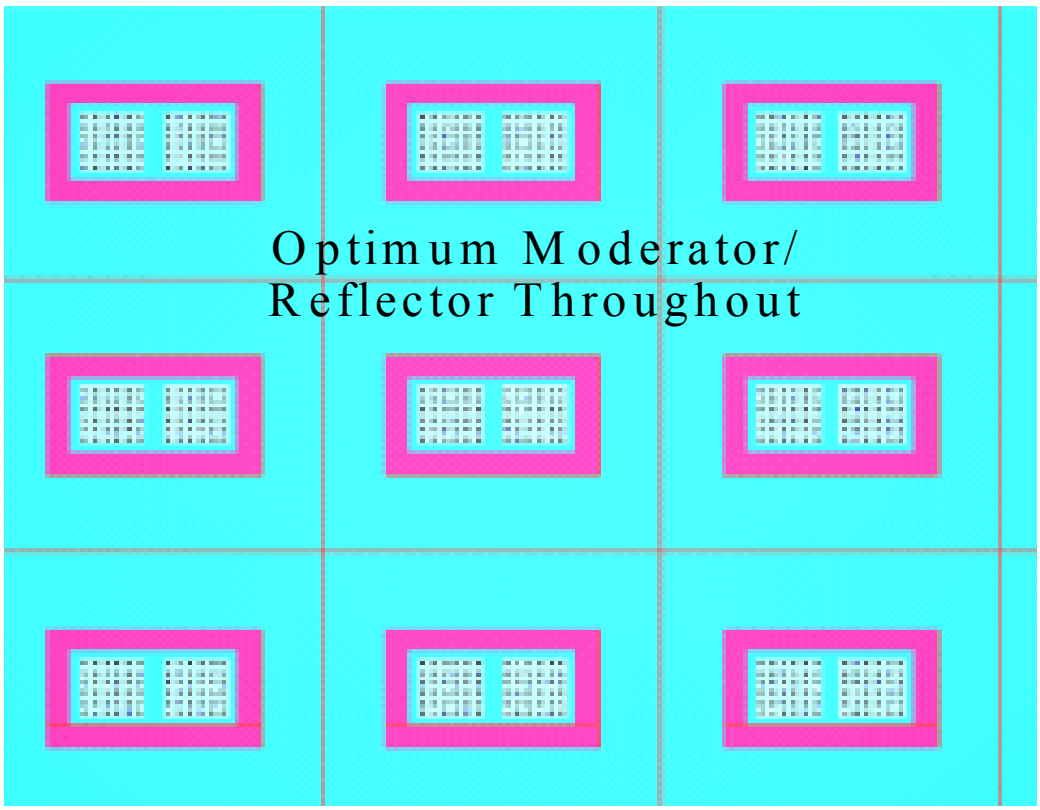

Figure 6-19 RAJ-II Fuel Rod Transport Package Array NCT Model

6.3.1.3.4 RAJ-II Package Array Fuel Rod Transport HAC Model

The RAJ-II package array hypothetical accident conditions described in Section 6.3.1.2.2 are used for the package array, HAC, fuel rod transport models.

The fuel rods are modeled filling the inner container for the hypothetical accident conditions. A 0.0152 cm thick polyethylene layer is modeled around each fuel rod to simulate any protective material present. Worst case fuel rod parameters determined from the package array HAC parameter sensitivity analyses (Section 6.3.1.2.2), are used for the fuel rod transport models. The worst case fuel rod parameters are shown in Table 6-6.

Calculations are conducted to investigate transporting loose fuel rods, bundled fuel rods, and fuel rods in 5-inch stainless steel pipe within each RAJ-II shipping compartment. A fuel rod pitch sensitivity study is conducted for each fuel rod type, to determine the number of fuel rods that can be transported in a loose configuration within the RAJ-II fuel assembly compartment. For convenience, a square pitch array is used to conduct the sensitivity study, since scoping calculations revealed little difference in the reactivity between square and triangular pitch arrays. The pitch sensitivity study results in the minimum and maximum allowable fuel rod quantity for shipping rods in a loose configuration. The loose rod analysis is used to bound a fuel rod shipment in which fuel rods are strapped or bundled together.

A fuel rod pitch sensitivity analysis is also performed to determine the fuel rod quantity that may be transported inside a 5-inch stainless steel pipe. Triangular pitch fuel rod arrays are used to

find the maximum allowable quantity. The stainless steel material is conservatively neglected when performing the calculations, therefore, any container with a volume equivalent to or less than the 5-inch stainless steel pipe is acceptable for fuel rod transport, as long as the fuel rod quantity is limited to that for the pipe.

The fuel rod type with the most reactive configuration is chosen for the RAJ-II fuel rod transport, package array, HAC model. A portion of the RAJ-II fuel rod transport package array HAC model is shown in Figure 6-20.

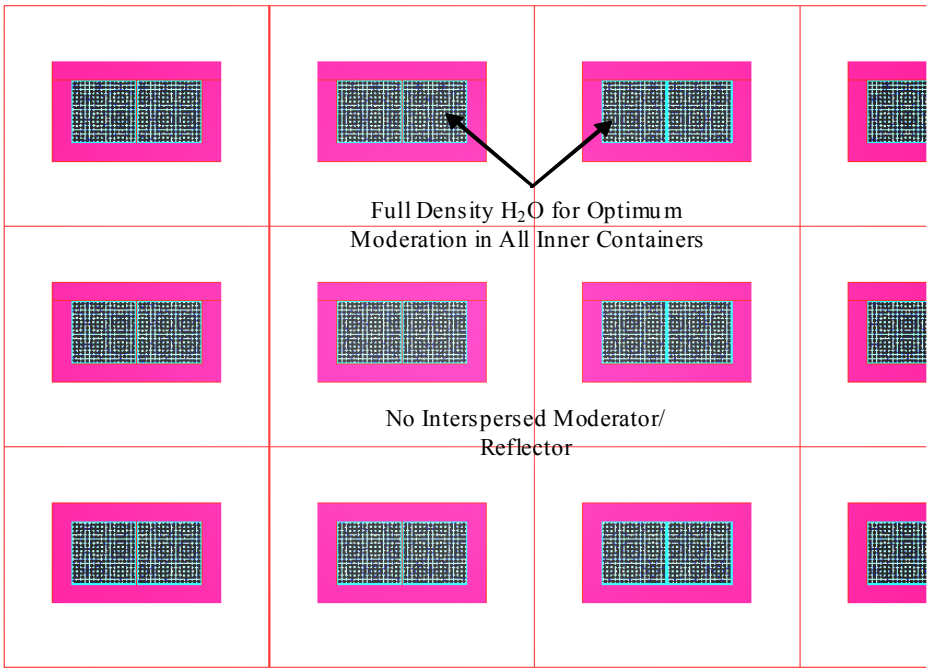

Figure 6-20 RAJ-II Fuel Rod Transport Package Array HAC Model

6.3.2 Material Properties

6.3.2.1 Material Tolerances

Table 6-7 Dimensional Tolerances provides sheet metal thickness dimensional tolerance from ASTM A240 and ASTM A480 (the former refers to the latter for specific tolerances). The table also provides the thicknesses used in the damaged and undamaged container models.

Table 6-7 Dimensional Tolerances

Stainless Steel Sheet Gauge	Nominal Thickness (mm)	Permissible Variations* (mm)	Model Thickness Used (in.) [cm] (description)
2 mm.	2.00 mm	± 0.18	0.0689 [0.175] (outer container wall)
1.5 mm	1.50 mm	± 0.15	0.0535 [0.136] (inner container wall)
1.0 mm.	1.00 mm	± 0.13	0.0344 [0.0875] (inner container fuel assembly compartments)

* ASTM-A240/A240M- 97b, Table A1.2, *Standard Specification for Heat Resisting Chromium and Chromium-Nickel Stainless Steel Plate, Sheet, and Strip for Pressure Vessels*, August 1997.

6.3.2.2 MATERIAL SPECIFICATIONS

Table 6-8 Material Specifications for the RAJ-II contains the material compositions for the RAJ-II shipping container. The UO_2 stack density is taken as 98% of theoretical. The presence of Gd_2O_3 in the UO_2-Gd_2O_3 pellet reduces the density from 10.74 to 10.67 g/cm^3.

Table 6-8 Material Specifications for the RAJ-II

Material	Density (g/cm^3)	Constituent	Atomic Density (atoms/b-cm)
$U(5.0)O_2$ 98% Theoretical Density	10.74	U-235 U-238 O	1.2128×10^{-3} 2.2753×10^{-2} 4.7931×10^{-2}
$U(5.0)O_2$-Gd_2O_3 98% Theoretical Density 2 wt% Gd_2O_3 (75% credit for Gd)	10.67	U-235 U-238 O Gd-152 Gd-154 Gd-155 Gd-156 Gd-157 Gd-158 Gd-160	1.18663×10^{-03} 2.22611×10^{-02} 4.76929×10^{-02} 1.06320×10^{-6} 1.15892×10^{-5} 7.86790×10^{-5} 1.08822×10^{-4} 8.31978×10^{-5} 1.32053×10^{-4} 1.16211×10^{-4}
Zirconium	6.49	Zr	4.2846×10^{-2}
Stainless Steel 304	7.94	Fe Cr Ni Mn Si C P	5.8545×10^{-2} 1.7473×10^{-2} 7.7402×10^{-3} 1.7407×10^{-3} 1.7025×10^{-3} 3.1877×10^{-4} 6.9468×10^{-5}

Material	Density (g/cm^3)	Constituent	Atomic Density (atoms/b-cm)
Polyethylene Foam	≤ 0.05 – 0.075	C H	$3.4374x10^{-3}$ $6.8748x10^{-3}$
Low Density Polyethylene (LDPE) Insert	0.925	C H	$3.9745x10^{-2}$ $7.9490x10^{-2}$
Polyethylene Cluster Assembly	0.949	C H	$4.0776x10^{-2}$ $8.1552x10^{-2}$
Alumina Silicate [Al_2O_3(49%)-SiO_2(51%)]	0.25	Al Si O	$1.4474x10^{-3}$ $1.2783x10^{-3}$ $4.7277x10^{-3}$
Paper Honeycomb $C_6H_{10}O_5$	0.04 – 0.08	C H O	$1.7840x10^{-3}$ $2.9733x10^{-3}$ $1.4867x10^{-3}$
Full Density Water	1.0	H O	$6.6769x10^{-2}$ $3.3385x10^{-2}$

Polyethylene inserts or polyethylene cluster separators are positioned between fuel rods at various locations along the axis of the fuel assembly to avoid stressing the axial grids during transportation. The inserts are shown in Figure 6-1 while the separators are shown in Figure 6-2. The Low Density Polyethylene (LDPE) insert has a 0.925 g/cm^3 density and an approximate volume of 25 cm^3. Therefore, a 10x10 assembly with 9 polyethylene inserts has a 225 cm^3 total LDPE volume required for one location along the fuel assembly.

The cluster separator is composed of LDPE (0.925 g/cm^3) fingers and a High Density Polyethylene (HDPE, 0.959 g/cm^3) holder (The LDPE and HDPE densities are based on accepted industry definitions). The LDPE fingers (10x10) occupy an approximate volume of 38 cm^3 while the HDPE holder has an approximate volume of 85 cm^3. A volume average density of 0.949 g/cm^3 is calculated for the polyethylene cluster assembly, i.e.

$$\left[\frac{\left(38cm^3 \times 0.925g/cm^3\right)+\left(85cm^3 \times 0.959g/cm^3\right)}{123cm^3}\right]$$

For a 10x10 assembly, two cluster separators, shown in Figure 6-2, are placed at numerous locations along the fuel assembly. A total polyethylene volume of 246 cm^3 is calculated for each location in which the cluster separators are placed. The RAJ-II criticality calculations use the 10x10 cluster separator characteristics for the fuel types investigated. However, the polyethylene characteristics are only used to establish a polyethylene mass limit so that an accurate measurement of polyethylene characteristics by the user is unnecessary. Other plastics with equivalent hydrogen mass limits are acceptable. The following equation can be used to determine plastic equivalence (e.g., ABS plastic).

$$M_{eq,i} = M_{poly} \times \frac{0.137}{(\rho_{mix,i} \times wf_{H,i})}$$

The formula for polyethylene mass equivalence is:

$$M_{eq,i} = M_{poly} \times [(rho_{mix,poly})(wf_{H,\ poly})]/[(rho_{mix,i})(wf_{H,i})]$$

$$= M_{poly} \times [(0.949\ g/cm^3)(0.144)]/[(rho_{mix,i})(wf_{H,i})]$$

$$= M_{poly} \times (0.137\ g/cm^3)/[(rho_{mix,i})(wf_{H,i})]$$

The fuel parameters used to calculate volume fractions for the water and polyethylene mixture in the RAJ-II normal condition model are shown in Table 6-9 RAJ-II Normal Condition Model Fuel Parameters. The volume fractions of polyethylene and water for the worst case fuel assembly type analyzed are shown in Table 6-10 RAJ-II Normal Condition Model Polyethylene and Water Volume Fractions and Table 6-11 Single Package Normal and HAC Model Fuel Parameters. The volume fractions in Table 6-10 are entered into the model input standard composition specification area. Mixtures representing the polyethylene inserts between fuel rods are created using the compositions specified, and used in the KENO V.a calculation. The mixtures are also used in the lattice cell description to provide the lump shape and dimensions for resonance cross-section processing, the lattice corrections for cross-section processing, and the information necessary to create cell-weighted cross-sections.

Table 6-9 RAJ-II Normal Condition Model Fuel Parameters

Fuel Assembly	Fuel Rod OR (cm)	Number of Fuel Rods	Fuel Rod Pitch (cm)	Fuel Rod Length (cm)	Cluster Separator Volume Surrounding Fuel (cm^3)	Number of Part Length Fuel Rods
GNF 10x10	0.505	92	1.350	385	10,200	12

Table 6-10 RAJ-II Normal Condition Model Polyethylene and Water Volume Fractions

Fuel Assembly	Assembly Volume (cm^3)	Fuel Rod Volume (cm^3)	Interstitial Volume (cm^3)	Polyethylene Volume (cm^3)	Vf_{poly}	Vf_{H2O}
GNF 10x10	66,676.46	26,527.22	40,149.24	10,200	0.25405	0.74595

Table 6-11 Single Package Normal and HAC Model Fuel Parameters

Fuel Assembly	Partial Fuel Rods (#)	Pitch (cm)	Pellet Diameter (cm)	Clad Inner Diameter (cm)	Clad Outer Diameter (cm)
GNF 10X10	12	1.350	0.895	0.9338	1.010

In the hypothetical accident condition model, the polyethylene inserts are assumed to melt when subjected to the tests specified in 10 CFR Part 71. The polyethylene is assumed to uniformly coat the fuel rods in each fuel assembly forming a cylindrical layer of polyethylene around each fuel rod. Different coating thicknesses are investigated, and a maximum thickness is determined to set a polyethylene mass limit for each fuel assembly type considered for transport. The fuel assembly parameters used to calculate the polyethylene mass limits are shown in Table 6-12 Fuel Assembly Parameters for Polyethylene Mass Calculations. For the fuel parameter sensitivity study and the worst case fuel assembly models, the polyethylene is smeared into the fuel rod cladding to accommodate the limitations in the lattice cell modeling for cross-section processing in SCALE. A visual representation of the smeared clad/polyethylene mixture compared to a discrete treatment is shown in Figure 6-21 Visual Representation of the Clad/Polyethylene Smeared Mixture versus Discrete Modeling. The polyethylene mass and the volume fractions of polyethylene and zirconium clad for each fuel assembly analyzed are shown in Table 6-13 Polyethylene Mass and Volume Fraction Calculations. The volume fractions in Table 6-13 are entered into the model input standard composition specification area. Mixtures representing the polyethylene inserts between fuel rods are created using the compositions specified, and used in the KENO V.a calculation. The mixtures are also used in the lattice cell description to provide the lump shape and dimensions for resonance cross-section processing, the lattice corrections for cross-section processing, and the information necessary to create cell-weighted cross-sections.

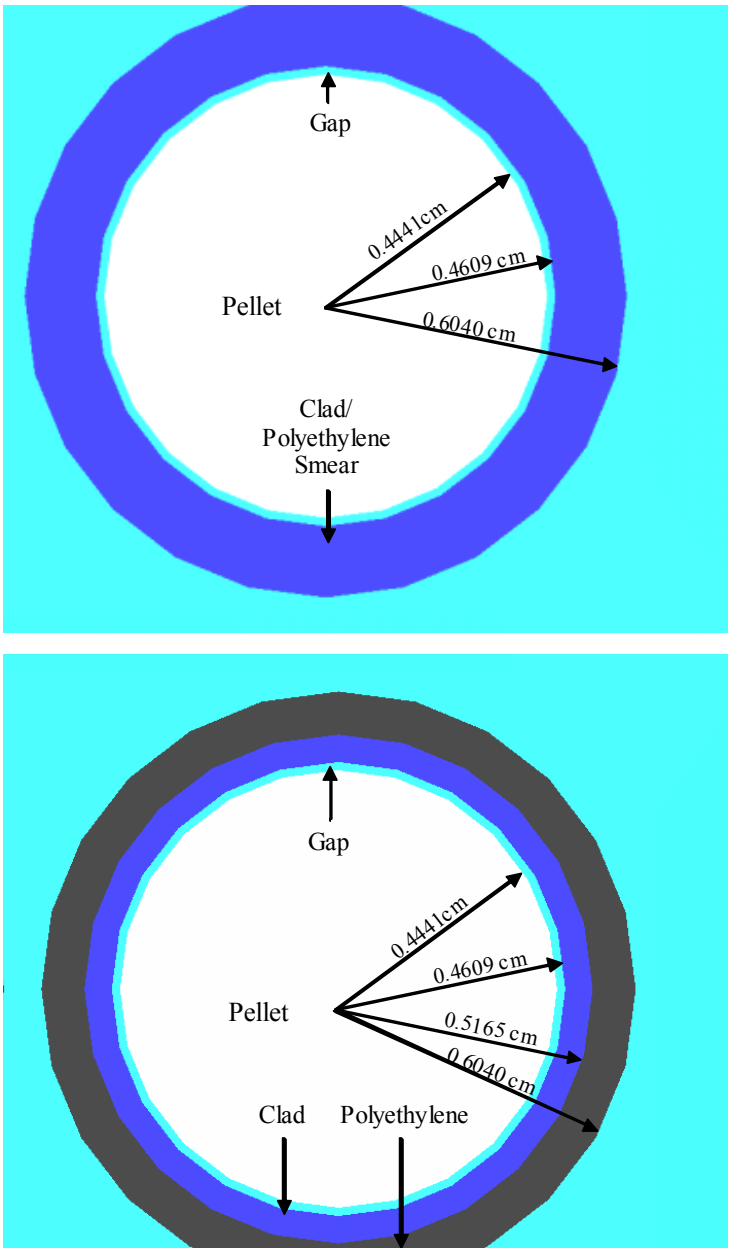

Figure 6-21 Visual Representation of the Clad/Polyethylene Smeared Mixture versus Discrete Modeling

Table 6-12 Fuel Assembly Parameters for Polyethylene Mass Calculations

Fuel Assembly Design	Fuel Rod OR (cm)	Number of Fuel Rods	Fuel Rod Pitch (cm)	Fuel Rod Length (cm)	Fuel Rod IR (cm)
ATRIUM 10x10	0.5165	91	1.284	383.54	0.4609
GNF 10x10	0.50927	92	1.2954	381	0.46609
Framatome 9x9	0.54991	72	1.4478	381	0.48006
GNF 9x9	0.55499	74	1.43764	381	0.49149
GNF 8x8	0.6096	60	1.6256	381	0.53594

Table 6-13 Polyethylene Mass and Volume Fraction Calculations

Radius (cm)	Thickness (cm)	Total Poly Volume[a] (cm^3)	Total Poly Mass[b] (g)	$Volume_{poly}$ Per Fuel Rod[c] (cm^3)	$Volume_{clad}$ Per Fuel Rod[d] (cm^3)	Vf_{clad}[e]	Vf_{poly}[f]
Two ATRIUM 10x10 Fuel Assemblies							
0.51650	0.00000	0	0	0.00	65.47985	1.00000	0.00000
0.56504	0.04854	11512.03	10924.92	63.25	65.47985	0.50865	0.49135
0.59071	0.07421	18019.18	17100.20	99.01	65.47985	0.39809	0.60191
0.60395	0.08745	21487	20391.16	118.06	65.47985	0.35676	0.64324
0.61369	0.08000	24087.04	22858.60	132.35	65.47985	0.33100	0.66900
0.62343	0.10693	26729.6	25366.39	146.87	65.47985	0.30836	0.69164
0.63317	0.11667	29414.68	27914.53	161.62	65.47985	0.28833	0.71167
Two GNF 10x10 Fuel Assemblies							
0.50927	0.00000	0	0	0.00	50.41067	1.00000	0.00000
0.55824	0.04897	11512.03	10924.92	62.57	50.41067	0.44621	0.55379
0.59086	0.08159	19768.04	18759.87	107.43	50.41067	0.31937	0.68063
0.59743	0.08816	21487	20391.16	116.78	50.41067	0.30152	0.69848
0.60723	0.09796	24087.04	22858.6	130.91	50.41067	0.27802	0.72198
0.61703	0.10776	26729.6	25366.39	145.27	50.41067	0.25762	0.74238
0.62683	0.11756	29414.68	27914.53	159.86	50.41067	0.23974	0.76026
Two Framatome 9x9 Fuel Assemblies							
0.5499	0.0000	0	0	0.00	86.11243	1.00000	0.00000
0.6470	0.0971	20021.07	19000	139.04	86.11243	0.38247	0.61753
0.6610	0.1111	23182.3	22000	160.99	86.11243	0.34849	0.65151
0.6702	0.1203	25289.78	24000	175.62	86.11243	0.32901	0.67099
0.6792	0.1293	27397.26	26000	190.26	86.11243	0.31158	0.68842
0.6882	0.1383	29504.74	28000	204.89	86.11243	0.29591	0.70409
0.6970	0.1471	31612.22	30000	219.53	86.11243	0.28174	0.71826
Two GNF 9x9 Fuel Assemblies							
0.55499	0.00000	0	0	0.00	79.53889	1.00000	0.00000
0.65344	0.09845	21074.82	20000	142.40	79.53889	0.35839	0.64161
0.66248	0.10749	23182.3	22000	156.64	79.53889	0.33678	0.66322
0.67140	0.11641	25289.78	24000	170.88	79.53889	0.31763	0.68237

Radius (cm)	Thickness (cm)	Total Poly Volume[a] (cm^3)	Total Poly Mass[b] (g)	$Volume_{poly}$ Per Fuel Rod[c] (cm^3)	$Volume_{clad}$ Per Fuel Rod[d] (cm^3)	Vf_{clad}[e]	Vf_{poly}[f]
0.68020	0.12521	27397.26	26000	185.12	79.53889	0.30054	0.69946
0.68889	0.13390	29504.74	28000	199.36	79.53889	0.28519	0.71481
0.69747	0.14248	31612.22	30000	213.60	79.53889	0.27134	0.72866
Two GNF 8x8 Fuel Assemblies							
0.60960	0.00000	0	0	0.00	100.9989	1.00000	0.00000
0.71484	0.10524	20021.07	19000	166.84	100.9989	0.37709	0.62291
0.73008	0.12048	23182.3	22000	193.19	100.9989	0.34332	0.65668
0.74006	0.13046	25289.78	24000	210.75	100.9989	0.32398	0.67602
0.74990	0.14030	27397.26	26000	228.31	100.9989	0.30670	0.69330
0.75962	0.15002	29504.74	28000	245.87	100.9989	0.29117	0.70883
0.76922	0.15962	31612.22	30000	263.44	100.9989	0.27714	0.72286

The following example calculations are for two Atrium 10x10 assemblies with a total 21,487 cm^3 polyethylene volume:

a. Total Polyethylene Volume = (Total Fuel Rod Number)x(2 Fuel Assemblies)x(Polyethylene Area)x(Fuel Rod Length)

$$Volume = (91\,fuelrods)(2\,fuelassemblies)\left\{(\pi)\left[(0.60395cm)^2 - (0.5165cm)^2\right]\right\}(383.54cm) = 21487cm^3$$

b. Total Polyethylene Mass = (Total Polyethylene Volume)x(Polyethylene Density)

$$Mass = \left(21487cm^3\right)\left(0.949\frac{g}{cm^3}\right) = 20391.16g$$

c. Polyethylene Volume per Fuel Rod = Total Polyethylene Volume/Total Fuel Rod Number

$$\frac{Volume_{Poly}}{FuelRod} = \frac{21487cm^3}{(91\,fuelrods)(2\,fuelassemblies)} = 118.06cm^3$$

d. Clad Volume per Fuel Rod = [(Fuel Rod Area to Outer Clad)-(Fuel Rod Area to Inner Clad)]x Fuel Rod Length

$$\frac{Volume_{clad}}{FuelRod} = (\pi)\left[(0.5165cm)^2 - (0.4609cm)^2\right](383.54cm) = 65.48cm^3$$

e. Clad Volume Fraction = Clad Volume/Total Clad and Polyethylene Volumes

$$VF_{clad} = 65.48cm^3 \Big/ \left[(118.06cm^3)(65.48cm^3)\right] = 0.35676$$

f. Polyethylene Volume Fraction = Polyethylene Volume/ Total Clad and Polyethylene Volumes

$$VF_{Poly} = 118.06cm^3 \Big/ \left[(118.06cm^3)(65.48cm^3)\right] = 0.64323$$

6.3.3 Computer Codes and Cross-Section Libraries

The calculational methodology employed in the analyses is based on that embodied in SCALE - PC (version 4.4a), as documented in Reference 8. The neutron cross-section library employed in the analyses and the supporting validation analyses was the 44 group ENDF/B-V library distributed with version 4.4a of the SCALE package. Each case was run using the CSAS25 sequence of codes, i.e., BONAMI, NITAWL, and KENO V.a. For each case, 400 generations with 2,500 neutrons per generation were run to ensure proper behavior about the mean value. The methodology and results of the validation of SCALE 4.4a on the PC is outlined in Section 6.10, and results in an Upper Safety Limit (USL) that is the basis for comparison to ensure subcriticality.

For the performace of the Uranium-Carbide and PWR loose rod provision analysis, the GEMER Monte Carlo code was used. GEMER is a Monte Carlo neutron transport code developed by combining geometry and Monte Carlo features from the KENO IV and MERIT Monte Carlo codes and be adding enhance geometry, picture geometry checking and editing features (Ref. 4). Hence, GEMER is the evolution of Geometry Enhanced MERIT. The MERIT code is premised on the Battelle Northwest Laboratory's BMC code and is characterized by its explicit treatment of resolved resonance in material cross section set. Functionally, the GEMER Monte Carlo code is similar in analytic capability to other industry recognized codes such as KENO Va. or MCNP.

Cross sections in GEMER are currently processed from the ENDF/B-IV library in multigroup and resonance parameter formats. Cross-sections are prepared in the 190 energy group format and those in the resonance energy range have the form of resonance parameters. The resonance parameters describe the cross sections in the resonance range and Monte Carlo sampling in this range is done from resonance kernels rather than from broad group cross sections (i.e., explicit treatment of resolved resonance's using a single level Breit-Wigner equation at each collision in the resonance energy range). Thus there is a single unique cross section set associated with each available isotope and dependence is not placed on Dancoff (flux shadowing) correction factors or effective scattering cross sections. This treatment of cross-sections with explicit resonance parameters is especially suited to the analysis of uranium compounds in the form of heterogeneous accumulations, lattices, or systems containing nuclear poisons.

Thermal scattering of hydrogen is represented by the Hayward Kernel S(α,β) data in the ENDF/B-IV library. The types of reactions considered in the GEMER Monte Carlo calculation are fission, capture, elastic, inelastic, and (n, 2n) reactions; absorption is implicitly treated by applying the non-absorption probability to neutron weights on each collision. As part of the solutions, GEMER produces eigenvalue, micro- and macro-group fluxes, reaction rates, cross sections, and neutron balance by isotopes.

6.3.4 Demonstration of Maximum Reactivity

The objectives for the RAJ-II shipping container analysis are to demonstrate package criticality safety and determine fuel loading criteria. To accomplish these objectives, calculations are performed to determine the most reactive fuel configuration inside the RAJ-II assembly compartments. Once the fuel configuration is determined, moderator and reflector conditions are investigated. Finally, package orientation (for arrays) is examined. When the worst case fuel configuration, moderator/reflector conditions, and package orientation are found, the single package and package array calculations under both normal and hypothetical accident conditions are performed.

6.3.4.1 Fuel Assembly Orientation Study (2N=448)

The package array dimensions for the fuel assembly orientation are 14x2x16 (width x depth x height). Initial calculations are performed to find the worst case fuel assembly orientation inside each RAJ-II fuel compartment. Nominal fuel assembly dimensions are used for these initial calculations (Table 6-4). Note that in all cases with cladding, zirconium is used to conservatively represent any zirconium alloy. The package array HAC model described in Section 6.3.1.2.2 is used and the fuel assembly orientations depicted in Figure 6-9 through Figure

6-15 are applied. In addition, a polyethylene coating covers each fuel rod in the assembly, the fuel assembly is un-channeled, and the moderator density is 1.0 g/cm^3 in the RAJ-II inner container fuel region. The polyethylene foam is assumed to burn away, Alumina Silicate thermal insulator envelopes the inner container, and no water is in either the outer container or between packages in the array. The results of the calculations are shown in Table 6-14 RAJ-II Array HAC Fuel Assembly Orientation. Based on the results in Table 6-14, assembly orientation 6, is bounding for all designs. Therefore, orientation 6 with the assembly centered in each fuel compartment is used in the remaining design calculations. It is also noted that most results in Table 6-14 exceed the 0.94254 USL. For this reason, gadolinia-urania fuel rods are added to the fuel assemblies to provide reactivity hold-down.

Table 6-14 RAJ-II Array HAC Fuel Assembly Orientation

Fuel Assembly	Interspersed Moderator Density (g/cm^3)	Polyethylene Mass Per Assembly (kg)	Assembly Orientation	k_{eff}	σ	$k_{eff} + 2\sigma$
FANP 10x10	0.0	10.2	1	0.9375	0.0010	0.9395
FANP 10x10	0.0	10.2	2	0.9529	0.0008	0.9545
FANP 10x10	0.0	10.2	3	0.8973	0.0008	0.8989
FANP 10x10	0.0	10.2	4	0.8965	0.0010	0.8985
FANP 10x10	0.0	10.2	5	0.9248	0.0010	0.9268
FANP 10x10	0.0	10.2	6	0.9741	0.0009	**0.9759**
FANP 10x10	0.0	10.2	7	0.9486	0.0009	0.9504
GNF 10x10	0.0	10.2	1	0.9586	0.0010	0.9606
GNF 10x10	0.0	10.2	2	0.9721	0.0009	0.9739
GNF 10x10	0.0	10.2	3	0.9184	0.0008	0.9200
GNF 10x10	0.0	10.2	4	0.9183	0.0009	0.9201
GNF 10x10	0.0	10.2	5	0.9431	0.0008	0.9447
GNF 10x10	0.0	10.2	6	0.9909	0.0010	**0.9929**
GNF 10x10	0.0	10.2	7	0.9652	0.0008	0.9668
FANP 9x9[a]	0.0	11	1	0.9486	0.0009	0.9504
FANP 9x9	0.0	11	2	0.9559	0.0009	0.9577
FANP 9x9	0.0	11	3	0.9052	0.0008	0.9068
FANP 9x9	0.0	11	4	0.9056	0.0008	0.9072
FANP 9x9	0.0	11	5	0.9293	0.0010	0.9313
FANP 9x9	0.0	11	6	0.9791	0.0008	**0.9807**
FANP 9x9	0.0	11	7	0.9362	0.0009	0.9380
GNF 9x9	0.0	11	1	0.9491	0.0008	0.9507
GNF 9x9	0.0	11	2	0.9577	0.0008	0.9593
GNF 9x9	0.0	11	3	0.9051	0.0008	0.9067
GNF 9x9	0.0	11	4	0.9042	0.0009	0.9060
GNF 9x9	0.0	11	5	0.9287	0.0009	0.9305
GNF 9x9	0.0	11	6	0.9787	0.0008	**0.9803**
GNF 9x9	0.0	11	7	0.9556	0.0008	0.9572
GNF 8x8	0.0	11	1	0.9506	0.0009	0.9524
GNF 8x8	0.0	11	2	0.9563	0.0008	0.9579
GNF 8x8	0.0	11	3	0.9048	0.0008	0.9064
GNF 8x8	0.0	11	4	0.9052	0.0009	0.9070
GNF 8x8	0.0	11	5	0.9299	0.0009	0.9317
GNF 8x8	0.0	11	6	0.9764	0.0008	**0.9780**
GNF 8x8	0.0	11	7	0.9554	0.0009	0.9572

a. The Framatome D-lattice 9x9 assembly was modeled. However, the results presented here are applicable to the C-lattice as well
b. Limiting case shown in bold

6.3.4.2 Fuel Assembly Gadolinia Rod Study (2N=448)

Fuel assemblies with lattice average U-235 enrichments of 5.0 wt% are qualified for transport in the RAJ-II shipping container by crediting the gadolinia-urania fuel rods present in the assembly. The gadolinia-urania fuel rods decrease system reactivity such that the $k_{eff} + 2\sigma$ remains below the 0.94254 USL. The gadolinia content of each gadolinia-urania fuel rod is limited to 75% of the value specified in Table 6-1. Scoping studies are performed using numerous gadolinia-urania fuel rod placement patterns in the orientation 6 models, from the fuel assembly orientation study, to find the pattern that yields the highest reactivity for each fuel assembly type. Of the patterns investigated, three patterns that produce the highest reactivity for each fuel assembly type are shown in Figure 6-22 - Figure 6-24. The calculations are performed using optimum moderator conditions. The results for the 14x2x16 RAJ-II container array transporting 10x10, 9x9, or 8x8 fuel assembies with gadolinia-urania fuel rods arranged in the patterns displayed in Figure 6-22 - Figure 6-24 are listed in Table 6-15. As shown in Table 6-15, the gadolinia-urania fuel rods hold the system reactivity below the 0.94254 USL. Based on the gadolinia-urania fuel rod pattern optimization calculations:

- Gadolinia-urania fuel rod Pattern G is selected for future FANP 10x10 fuel assembly sensitivity calculations,
- Gadolinia-urania fuel rod Pattern B is selected for future GNF 10x10 fuel assembly sensitivity calculations,
- Gadolinia-urania fuel rod Pattern A is selected for future FANP and GNF 9x9 fuel assembly sensitivity calculations,
- Gadolinia-urania fuel rod Pattern I is selected for future GNF 8x8 fuel assembly sensitivity calculations.

Table 6-15 RAJ-II Shipping Container 14x2x16 Array with Gadolinia-Urania Fuel Rods

Assembly Type	Pattern Designation	U-235 Enrich (wt%)	Gad Rod #	Pitch (cm)	Pellet Diameter (cm)	Clad ID (cm)	Clad OD (cm)	k_{eff}	σ	$k_{eff} + 2\sigma$
FANP 10x10	B	5.0	12	1.284	0.8882	0.9218	1.033	0.8716	0.0008	0.8732
FANP 10x10	F	5.0	12	1.284	0.8882	0.9218	1.033	0.8699	0.0008	0.8715
FANP 10x10	G	5.0	12	1.284	0.8882	0.9218	1.033	0.8732	0.0008	**0.8748**
GNF 10x10	B	5.0	12	1.2954	0.8941	0.9322	1.019	0.8886	0.0008	**0.8902**
GNF 10x10	G	5.0	12	1.2954	0.8941	0.9322	1.019	0.8871	0.0008	0.8887
GNF 10x10	H	5.0	12	1.2954	0.8941	0.9322	1.019	0.8880	0.0009	0.8898
FANP 9x9	A	5.0	10	1.4478	0.9398	0.9601	1.099	0.8644	0.0007	**0.8658**
FANP 9x9	B	5.0	10	1.4478	0.9398	0.9601	1.099	0.8605	0.0008	0.8621
FANP 9x9	E	5.0	10	1.4478	0.9398	0.9601	1.099	0.8354	0.0009	0.8372
GNF 9x9	A	5.0	10	1.4376	0.9550	0.9830	1.110	0.8579	0.0008	**0.8596**
GNF 9x9	B	5.0	10	1.4376	0.9550	0.9830	1.110	0.8572	0.0008	0.8588
GNF 9x9	F	5.0	10	1.4376	0.9550	0.9830	1.110	0.8524	0.0009	0.8540
GNF 8x8	E	5.0	7	1.6256	1.0439	1.0719	1.219	0.8779	0.0009	0.8797
GNF 8x8	G	5.0	7	1.6256	1.0439	1.0719	1.219	0.8726	0.0008	0.8742
GNF 8x8	I	5.0	7	1.6256	1.0439	1.0719	1.219	0.8800	0.0009	**0.8818**

a. Limiting case(s) shown in bold

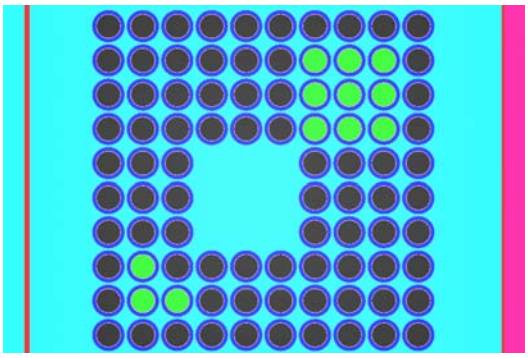

FANP 10x10 5.0 wt% ^{235}U, Pattern B

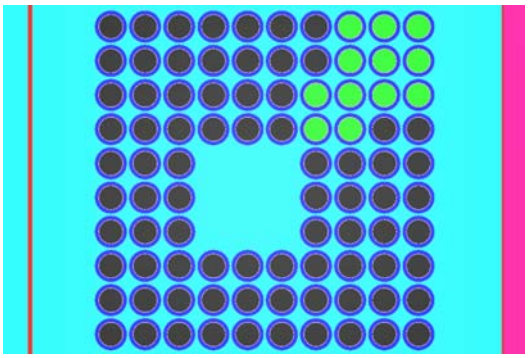

FANP 10x10 5.0 wt% ^{235}U, Pattern F

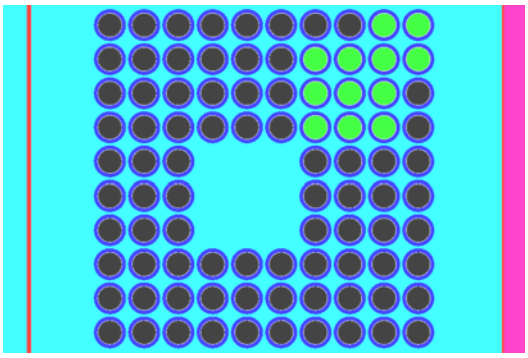

FANP 10x10 5.0 wt% ^{235}U, Pattern G

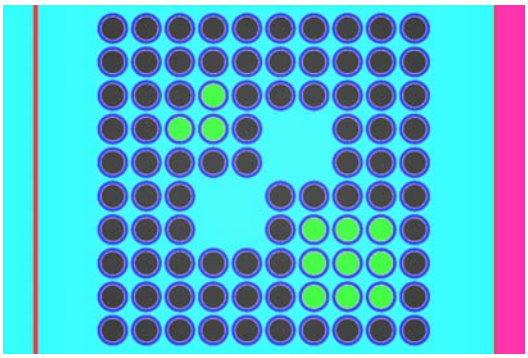

GNF 10x10 5.0 wt% ^{235}U, Pattern B

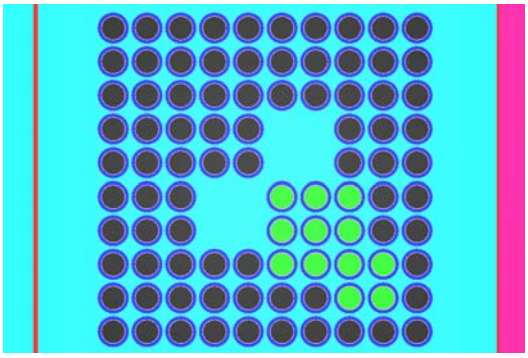

GNF 10x10 5.0 wt% ^{235}U, Pattern G

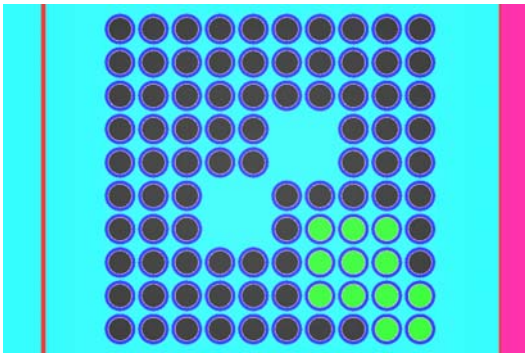

GNF 10x10 5.0 wt% ^{235}U, Pattern H

Figure 6-22 Gadolinia-Urania Fuel Rod Placement Pattern for 10x10 Fuel Assemblies at 5.0 wt% ^{235}U

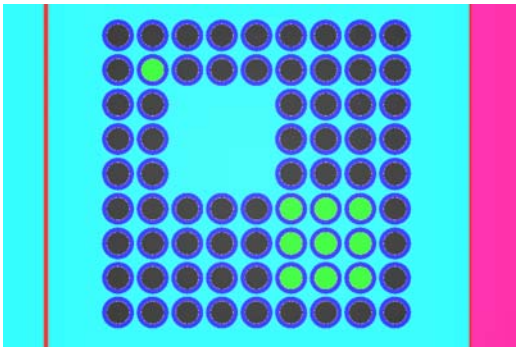

FANP 9x9 5.0 wt% ^{235}U, Pattern A

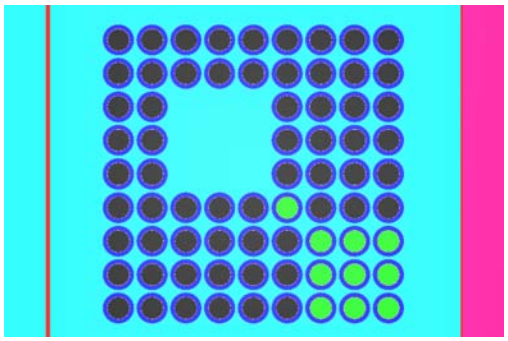

FANP 9x9 5.0 wt% ^{235}U, Pattern B

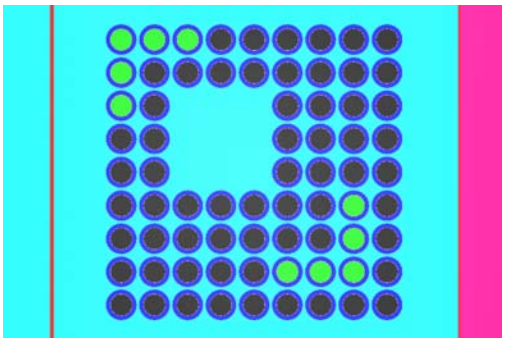

FANP 9x9 5.0 wt% ^{235}U, Pattern E

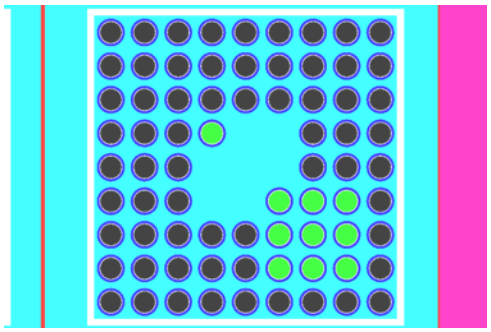

GNF 9x9 5.0 wt% ^{235}U, Pattern A

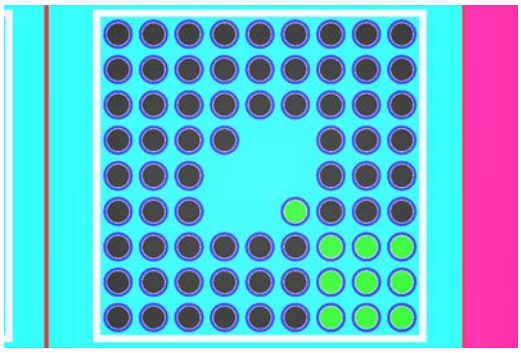

GNF 9x9 5.0 wt% ^{235}U, Pattern B

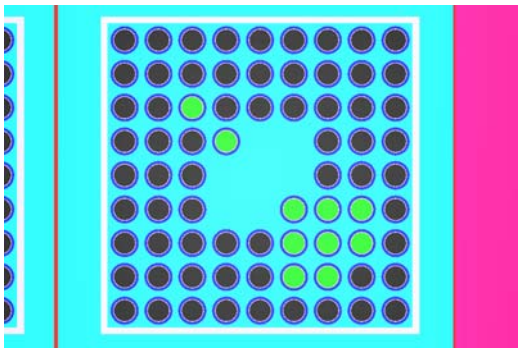

GNF 9x9 5.0 wt% ^{235}U, Pattern F

Figure 6-23 Gadolinia-Urania Fuel Rod Placement Pattern for 9x9 Fuel Assemblies at 5.0 wt% ^{235}U

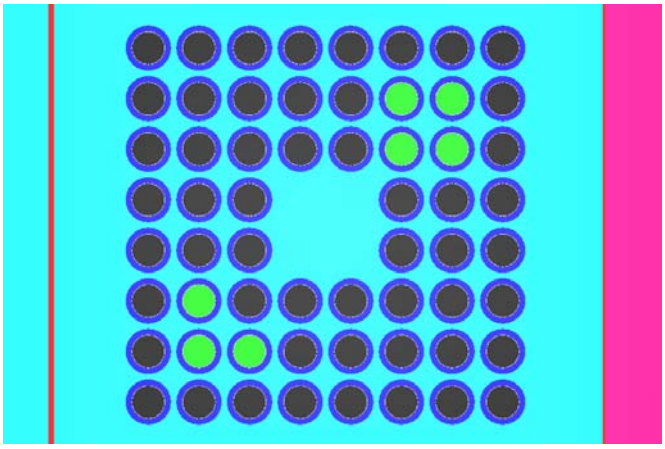

GNF 8x8 5.0 wt% ^{235}U, Pattern E

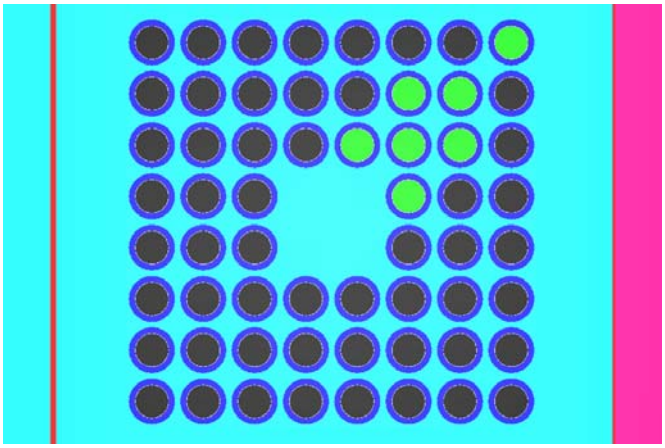

GNF 8x8 5.0 wt% ^{235}U, Pattern G

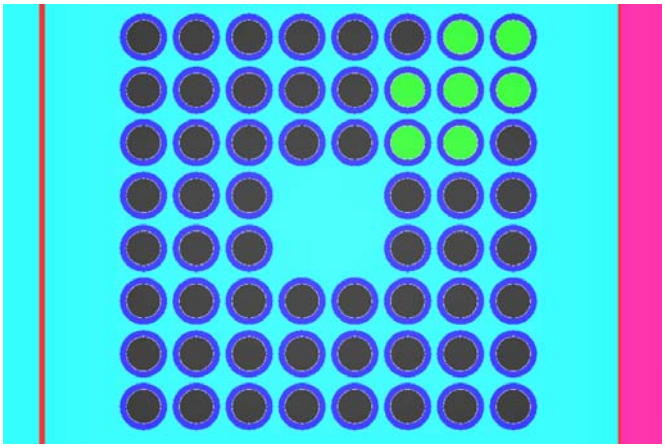

GNF 8x8 5.0 wt% ^{235}U, Pattern I

Figure 6-24 Gadolinia-Urania Fuel Rod Placement Pattern for 8x8 Fuel Assemblies at 5.0 wt% ^{235}U

6.3.4.3 Fuel Assembly Channel Study (2N=448)

A calculation is performed to determine if the presence of channels around the fuel assembly increases system reactivity. The orientation 6 models with the gadolina-urania fuel rod patterns that produced the highest system reactivity from the previous studies are used and a zirconium channel is placed around each assembly as shown in Figure 6-16 RAJ-II Hypothetical Accident Condition Model with Channels. The channel thickness is varied from 0.17 cm to 0.3048 cm and the impact on reactivity is assessed. The fuel assembly channel is located in the reflector region for each fuel assembly. It has no effect on the assembly H/X ratio since it is not located within the fuel envelope. Therefore, removing it would not have the same impact on system reactivity as removing the internal grid structure. The results are shown in Table 6-16. Comparing the results in Table 6-16 and Table 6-15 indicates reactivity increases with the presence of channels due to increased neutron leakage from the inner fuel compartment, resulting in increased neutron interaction among containers in the array. Therefore, channels will be included in subsequent calculations.

Table 6-16 RAJ-II Sensitivity Analysis for Channeled Fuel Assemblies

Assembly Type	Channel Thickness (cm)	Poly Mass per Assembly (kg)	Pitch (cm)	Pellet Diameter (cm)	Clad ID (cm)	Clad OD (cm)	k_{eff}	σ	$k_{eff} + 2\sigma$
FANP 10x10	0.1700	10.2	1.284	0.8882	0.9218	1.033	0.8801	0.0008	0.8817
FANP 10x10	0.2032	10.2	1.284	0.8882	0.9218	1.033	0.8786	0.0008	0.8802
FANP 10x10	0.2540	10.2	1.284	0.8882	0.9218	1.033	0.8815	0.0009	**0.8833**
FANP 10x10	0.3048	10.2	1.284	0.8882	0.9218	1.033	0.8810	0.0008	0.8826
GNF 10x10	0.1700	10.2	1.2954	0.8941	0.9322	1.019	0.8922	0.0009	0.8940
GNF 10x10	0.2032	10.2	1.2954	0.8941	0.9322	1.019	0.8948	0.0008	0.8964
GNF 10x10	0.2540	10.2	1.2954	0.8941	0.9322	1.019	0.8947	0.0008	0.8963
GNF 10x10	0.3048	10.2	1.2954	0.8941	0.9322	1.019	0.8953	0.0008	**0.8969**
FANP 9x9	0.1700	11	1.4478	0.9398	0.9601	1.0998	0.8719	0.0009	0.8737
FANP 9x9	0.2032	11	1.4478	0.9398	0.9601	1.0998	0.8724	0.0009	0.8742
FANP 9x9	0.2540	11	1.4478	0.9398	0.9601	1.0998	0.8739	0.0008	0.8756
FANP 9x9	0.3048	11	1.4478	0.9398	0.9601	1.0998	0.8755	0.0009	**0.8773**
GNF 9x9	0.1700	11	1.4376	0.9550	0.9830	1.11	0.8626	0.0009	0.8644
GNF 9x9	0.2032	11	1.4376	0.9550	0.9830	1.11	0.8651	0.0009	0.8669
GNF 9x9	0.2540	11	1.4376	0.9550	0.9830	1.11	0.8654	0.0010	**0.8674**
GNF 9x9	0.3048	11	1.4376	0.9550	0.9830	1.11	0.8659	0.0008	0.8676
GNF 8x8	0.1700	11	1.6256	1.0439	1.0719	1.2192	0.8834	0.0010	0.8854
GNF 8x8	0.2032	11	1.6256	1.0439	1.0719	1.2192	0.8857	0.0008	0.8873
GNF 8x8	0.2540	11	1.6256	1.0439	1.0719	1.2192	0.8884	0.0009	0.8902
GNF 8x8	0.3048	11	1.6256	1.0439	1.0719	1.2192	0.8900	0.0009	**0.8918**

a. Limiting case(s) shown in bold

6.3.4.4 Polyethylene Mass Study (2N=448)

The effect that polyethylene mass has on reactivity for each fuel assembly design is considered for transport in the RAJ-II shipping container. The results of the previous sensitivity studies are taken into consideration for the polyethylene mass study. The worst case channeled (0.3048 cm thick channels) models, used in the previous study, are used for the polyethylene mass study. The polyethylene and clad volume fractions, shown in Table 6-13, are used in the model material description to represent the polyethylene and clad mixture. They are also used in the lattice cell description for resonance cross-section processing. The polyethylene coating thickness around the fuel rods is varied, and the effect on reactivity is determined. The results of the calculations, Table 6-26, are displayed in Figure 6-25 RAJ-II Array HAC Polyethylene Sensitivity. Although the polyethylene addition increases reactivity, the increase is gradual and the resulting system k_{eff} remains subcritical. Based on the results in Figure 6-25:

- a polyethylene mass of 10.2 kg/assembly (20.4 kg/container) is chosen for further FANP and GNF 10x10 calculations,

- an 11 kg/assembly (22 kg/container) polyethylene mass is selected for subsequent FANP 9x9, GNF 9x9, and GNF 8x8 fuel assembly calculations.

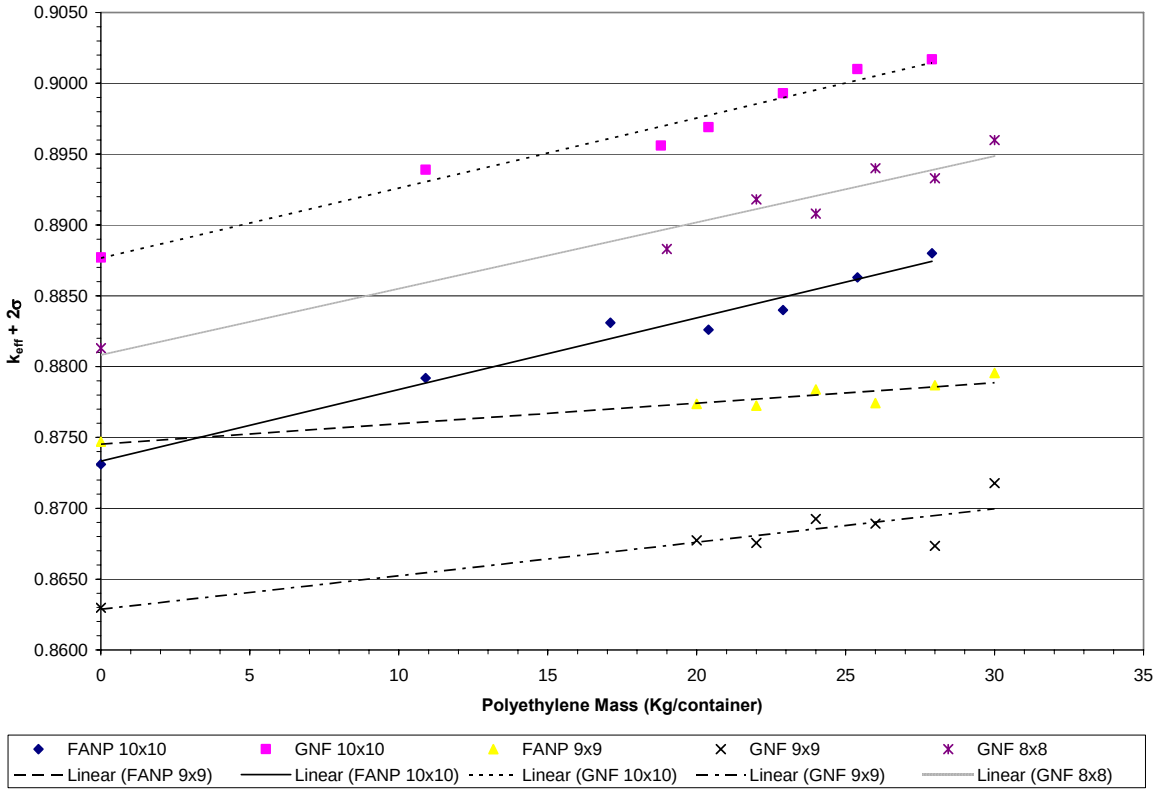

Figure 6-25 RAJ-II Array HAC Polyethylene Sensitivity

6.3.4.5 Fuel Rod Pitch Sensitivity Study (2N=448)

A fuel rod pitch sensitivity study is conducted using the worst case models from the polyethylene sensitivity study. The minimum fuel rod pitch is chosen to be at the point that the polyethylene coating on adjacent fuel rods contact. The maximum fuel rod pitch is chosen to be 4.1% greater than the reference fuel designs to bound the damage sustained during the 9 meter drop. The results are shown in Figure 6-26 RAJ-II Fuel Rod Pitch Sensitivity Study. Based on the results in Figure 6-26, the fuel assemblies are under-moderated such that increasing the pitch increases system reactivity. Based on the pitch sensitivity calculations (Table 6-27):

- a 1.350 cm fuel rod pitch is selected as the upper limit for FANP and GNF 10x10 pitch range,
- a 1.510 cm fuel rod pitch is selected as the upper limit for FANP and GNF 9x9 pitch range,
- a 1.6923 cm fuel rod pitch is selected as the upper limit for GNF 8x8 pitch range.

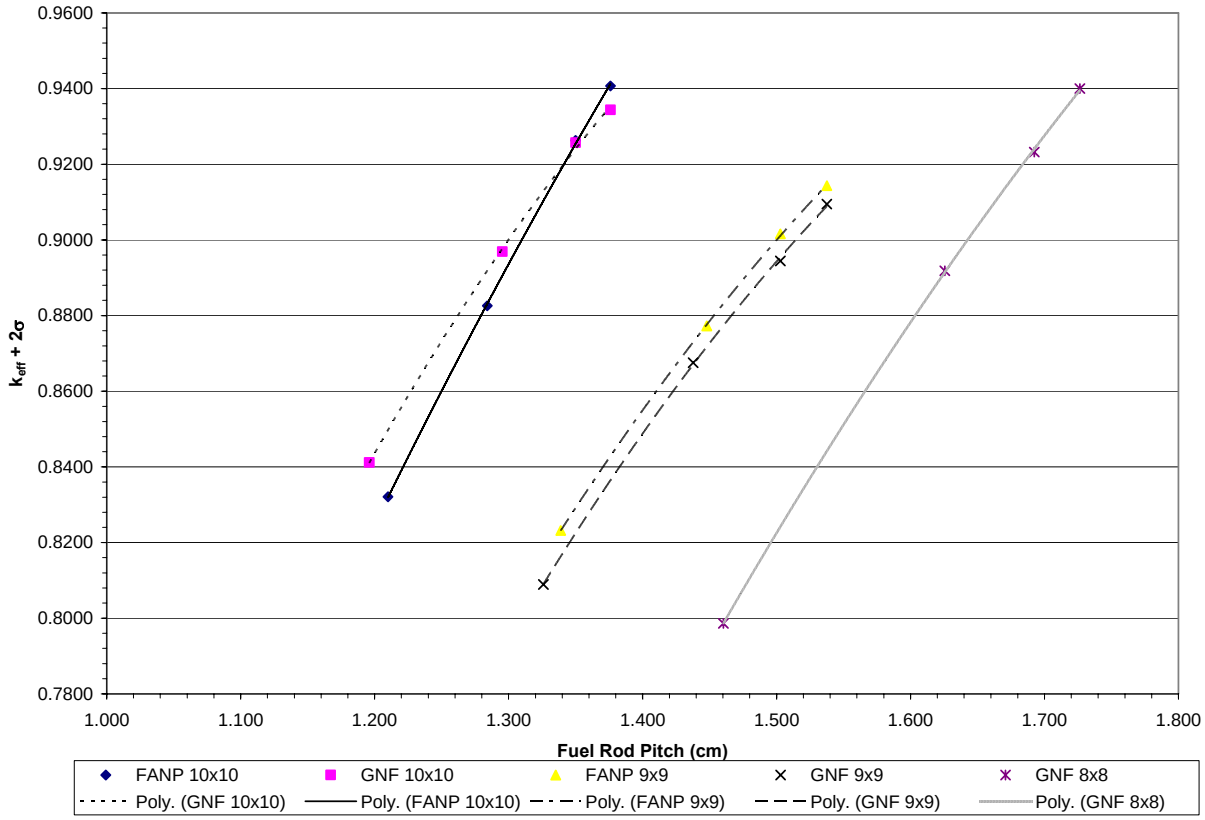

Figure 6-26 RAJ-II Fuel Rod Pitch Sensitivity Study

6.3.4.6 Fuel Pellet Diameter Sensitivity Study (2N=448)

With a polyethylene quantity chosen, the worst case orientation known, the channeled fuel effect assessed, and the worst case gadolinia-urania fuel rod patterns identified, a fuel pellet diameter sensitivity study is conducted. For the pellet diameter sensitivity study, the package array HAC model described in Section 6.3.1.2.2 is used for the study, fuel assembly orientation 6 is selected based on the results in Table 6-14, the maximum polyethylene amount for each fuel assembly design is chosen, the worst case gadolinia-urania rod pattern is selected, the inner container fuel compartment is maintained at optimum density water, an Alumina Silicate themal insulator envelopes the inner container fuel compartment, and water is removed from the outer container and between packages in the array. The results are shown in Figure 6-27 RAJ-II Array HAC Pellet Diameter Sensitivity Study. The results in Figure 6-27, demonstrate that reactivity increases as pellet diameter is increased. Pellet diameters of 0.895 cm for the FANP and GNF 10x10 designs, 0.96 cm for the Framatome and GNF 9x9 designs, and 1.05 cm for the GNF 8x8 design are found acceptable as the upper bounds for the fuel assembly design pellet ranges (Table 6-28).

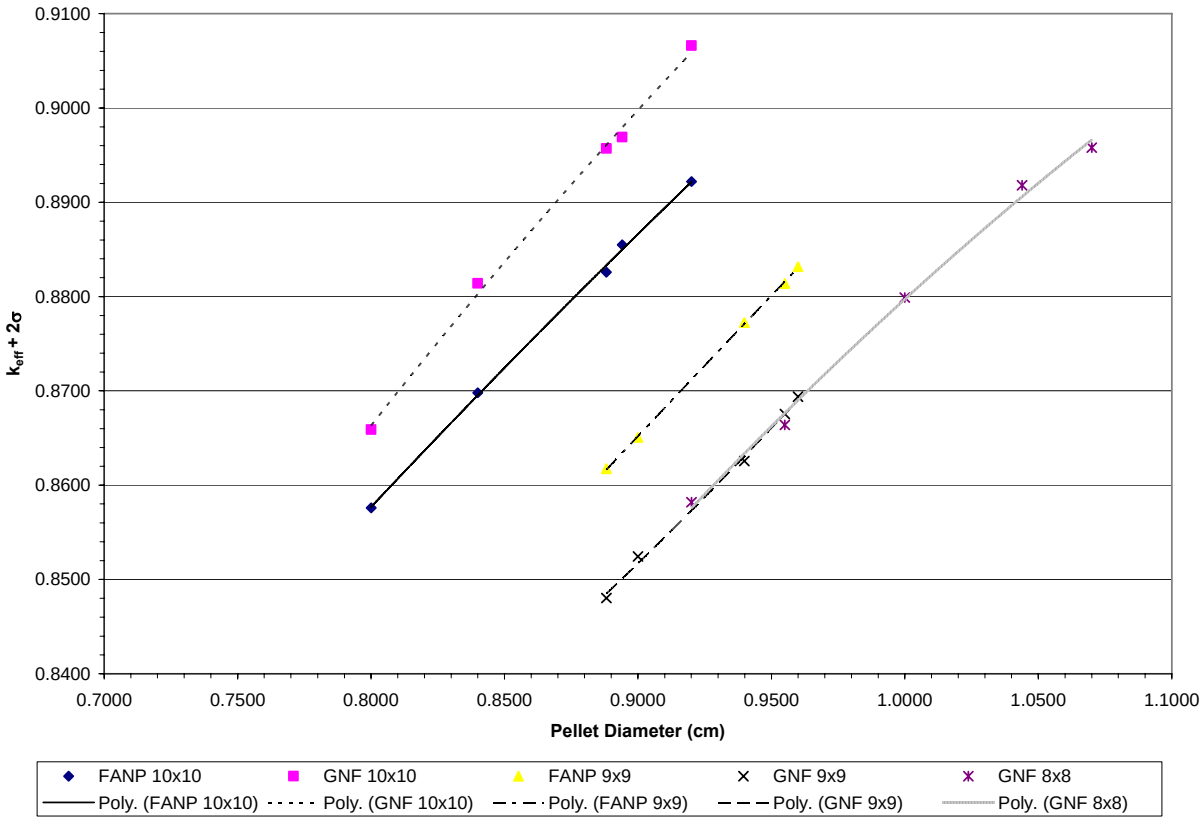

Figure 6-27 RAJ-II Array HAC Pellet Diameter Sensitivity Study

6.3.4.7 Fuel Rod Clad Thickness Sensitivity Study (2N=448)

Two sets of calculations are performed to assess the reactivity sensitivity to changes in cladding thickness. For the clad thickness sensitivity studies, the package array HAC model described in

Section 6.3.1.2.2 is used for the study, fuel assembly orientation 6 is selected based on the results in Table 6-14, the maximum polyethylene amount for each fuel assembly design is chosen, the worst case gadolinia-urania rod pattern is selected, the inner container fuel compartment is maintained at optimum density moderation, an Alumina Silicate themal insulator envelopes the inner container fuel compartment, and water is removed from the outer container and between packages in the array. For the first set of calculations, the inner clad diameter is adjusted to determine the effect on reactivity while the outer clad diameter is fixed at its nominal value shown in Table 6-4. The minimum value for the parameter search range is the pellet OD, while the maximum value for the range is the clad OD. The second set of calculations involves adjustments to the outer clad diameter while the inner clad diameter is held at its nominal value Table 6-4. Figure 6-28 RAJ-II Array HAC Fuel Rod Clad ID Sensitivity Study displays the results for the inner clad diameter sensitivity calculations, and Figure 6-29 RAJ-II Array HAC Fuel Rod Clad OD Sensitivity Study shows the results for the outer clad diameter sensitivity study. Both sets of results demonstrate that a decrease in the clad thickness results in an increase in system reactivity. The results also indicate that reactivity increases as the clad OD is decreased and increases as the clad ID is increased. Based on these results and fabrication constraints (Table 6-30 and Table 6-31):

- a 0.933 cm upper bound clad ID, and a 1.00 cm lower bound clad OD are selected for the FANP and GNF 10x10 parameter ranges,

- a 1.02 cm upper bound clad ID, and a 1.09 cm lower bound clad OD are selected for the FANP and GNF 9x9 parameter ranges,

- a 1.10 cm upper bound clad ID, and a 1.17 cm lower bound clad OD are selected for the GNF 8x8 parameter range.

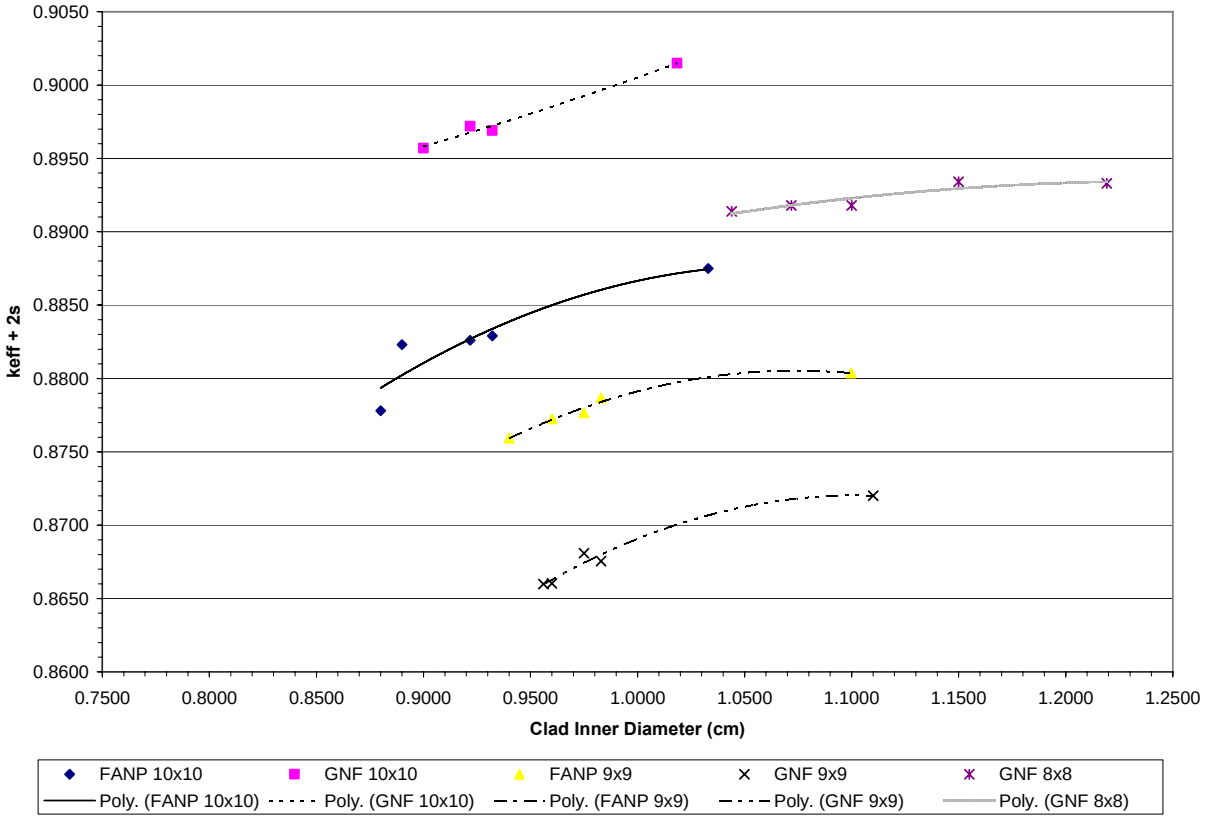

Figure 6-28 RAJ-II Array HAC Fuel Rod Clad ID Sensitivity Study

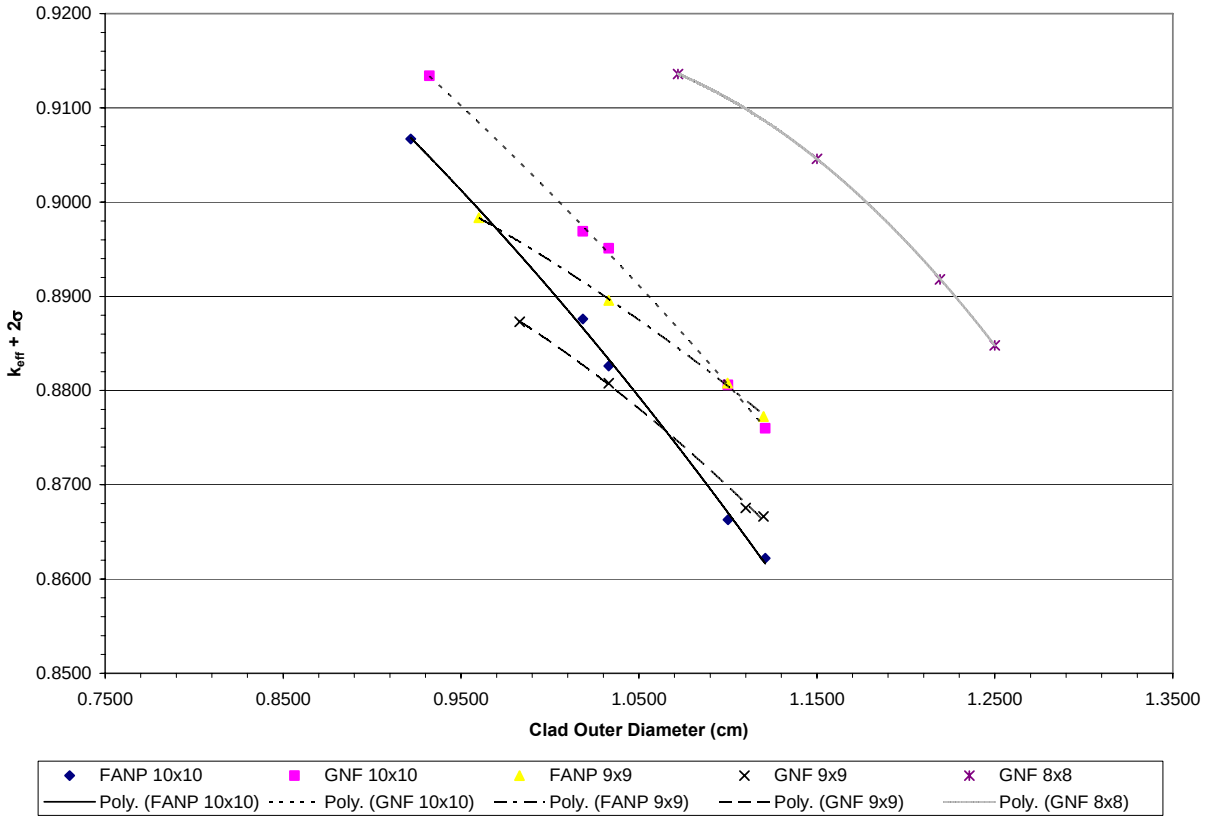

Figure 6-29 RAJ-II Array HAC Fuel Rod Clad OD Sensitivity Study

6.3.4.8 Worst Case Parameter Fuel Designs (2N=448)

The previous calculations have varied single parameters and assessed the impact on reactivity. Since the ranges investigated are to be a part of the fuel loading criteria, an assessment must be made for more than one parameter change at a time. To validate the parameter ranges selected to appear in the fuel loading criteria, a fuel design is developed by assembling the worst case parameters for each design considered for transport in the RAJ-II container. Table 6-17 RAJ-II Array HAC Worst Case Parameter Fuel Designs contains the worst case parameters for each design. The worst case models from the clad ID and OD sensitivity study are used to conduct the worst case fuel parameter study. The polyethylene is smeared into the fuel rod cladding to accommodate the limitations in the lattice cell modeling for cross-section processing in SCALE. A search for the worst case gadolinia-urania fuel rod pattern is also conducted to validate the worst case fuel design. Numerous patterns were investigated for each fuel assembly with the worst case fuel parameters determined from the sensitivity studies. Of the patterns investigated, three patterns that produce the highest reactivity for each fuel assembly type are shown in Figure 6-22 - Figure 6-24. Additional calculations are performed to investigate the number of gadolinia-urania fuel rods needed based on fuel assembly U-235 enrichment. For each fuel assembly U-235 enrichment, a gadolinia-urania fuel rod pattern optimization study is conducted. The three patterns that produce the highest reactivity for each fuel assembly based on U-235 enrichment are shown in Figure 6-30 - Figure 6-32 . All results are listed in Table 6-17 and are

below the USL of 0.94254. Based on the results listed in Table 6-17, all worst case fuel assembly designs result in maximum system reactivities that are within the statistical uncertainty of one another.

Table 6-17 RAJ-II Array HAC Worst Case Parameter Fuel Designs

Assembly Type	Gadolinia -Urania Fuel Rod Number	^{235}U Enrich ment (wt%)	Poly Mass per Assembly (kg)	Pitch (cm)	Pellet Diameter (cm)	Clad ID (cm)	Clad OD (cm)	k_{eff}	σ	$k_{eff} + 2\sigma$
FANP 10x10	12	5.0	10.2	1.350	0.895	0.933	1.00	0.9368	0.0008	0.9384
FANP 10x10	10	4.6	10.2	1.350	0.895	0.933	1.00	0.9360	0.0009	0.9378
FANP 10x10	9	4.3	10.2	1.350	0.895	0.933	1.00	0.9325	0.0010	0.9345
FANP 10x10	8	4.2	10.2	1.350	0.895	0.933	1.00	0.9366	0.0009	**0.9384**
FANP 10x10	6	3.9	10.2	1.350	0.895	0.933	1.00	0.9353	0.0007	0.9367
FANP 10x10	4	3.6	10.2	1.350	0.895	0.933	1.00	0.9341	0.0009	0.9359
FANP 10x10	2	3.3	10.2	1.350	0.895	0.933	1.00	0.9305	0.0009	0.9323
FANP 10x10	0	2.9	10.2	1.350	0.895	0.933	1.00	0.9274	0.0008	0.9290
GNF 10x10	12	5.0	10.2	1.350	0.895	0.933	1.00	0.9393	0.0008	0.9409
GNF 10x10	10	4.6	10.2	1.350	0.895	0.933	1.00	0.9349	0.0010	0.9369
GNF 10x10	9	4.3	10.2	1.350	0.895	0.933	1.00	0.9346	0.0008	0.9362
GNF 10x10	8	4.2	10.2	1.350	0.895	0.933	1.00	0.9395	0.0009	**0.9413**
GNF 10x10	6	3.9	10.2	1.350	0.895	0.933	1.00	0.9377	0.0009	0.9395
GNF 10x10	4	3.6	10.2	1.350	0.895	0.933	1.00	0.9370	0.0008	0.9386
GNF 10x10	2	3.3	10.2	1.350	0.895	0.933	1.00	0.9344	0.0009	0.9362
GNF 10x10	0	2.9	10.2	1.350	0.895	0.933	1.00	0.9317	0.0007	0.9331
FANP 9x9	10	5.0	11	1.510	0.96	1.02	1.09	0.9191	0.0008	0.9207
FANP 9x9	8	4.7	11	1.510	0.96	1.02	1.09	0.9294	0.0008	**0.9310**
FANP 9x9	6	4.2	11	1.510	0.96	1.02	1.09	0.9242	0.0010	0.9262
FANP 9x9	4	3.8	11	1.510	0.96	1.02	1.09	0.9264	0.0007	0.9278
FANP 9x9	2	3.5	11	1.510	0.96	1.02	1.09	0.9257	0.0007	0.9271
FANP 9x9	0	3.0	11	1.510	0.96	1.02	1.09	0.9214	0.0008	0.9230
GNF 9x9	10	5.0	11	1.510	0.96	1.02	1.09	0.9151	0.0008	0.9167
GNF 9x9	8	4.8	11	1.510	0.96	1.02	1.09	0.9368	0.0009	**0.9386**
GNF 9x9	6	4.2	11	1.510	0.96	1.02	1.09	0.9294	0.0009	0.9312
GNF 9x9	4	3.8	11	1.510	0.96	1.02	1.09	0.9333	0.0007	0.9347
GNF 9x9	2	3.5	11	1.510	0.96	1.02	1.09	0.9311	0.0008	0.9327
GNF 9x9	0	3.0	11	1.510	0.96	1.02	1.09	0.9290	0.0008	0.9306
GNF 8x8	7	5.0	11	1.6923	1.05	1.10	1.17	0.9356	0.0008	**0.9372**
GNF 8x8	6	4.7	11	1.6923	1.05	1.10	1.17	0.9323	0.0009	0.9341
GNF 8x8	4	4.1	11	1.6923	1.05	1.10	1.17	0.9305	0.0008	0.9321
GNF 8x8	2	3.7	11	1.6923	1.05	1.10	1.17	0.9321	0.0008	0.9337
GNF 8x8	0	3.1	11	1.6923	1.05	1.10	1.17	0.9311	0.0008	0.9327

a. Limiting case(s) shown in bold

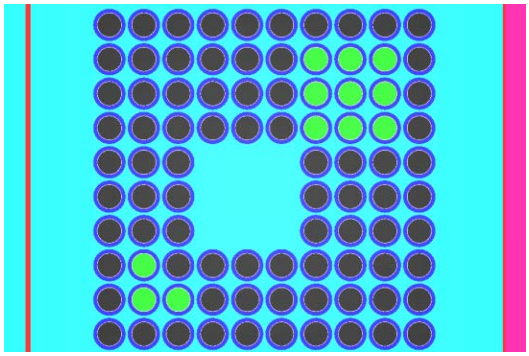

FANP 10x10 5.0 wt% ^{235}U, Pattern B

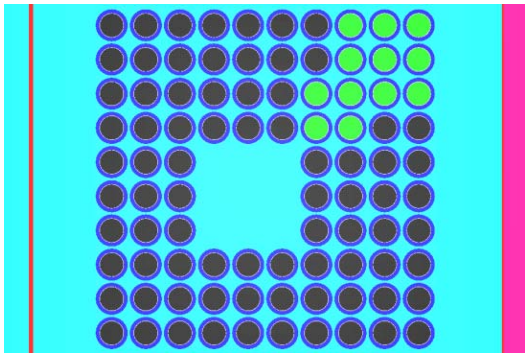

FANP 10x10 5.0 wt% ^{235}U, Pattern F

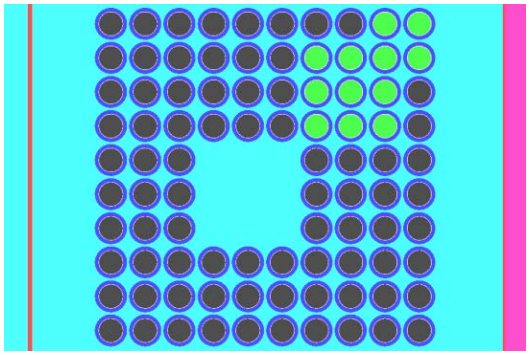

FANP 10x10 5.0 wt% ^{235}U, Pattern G

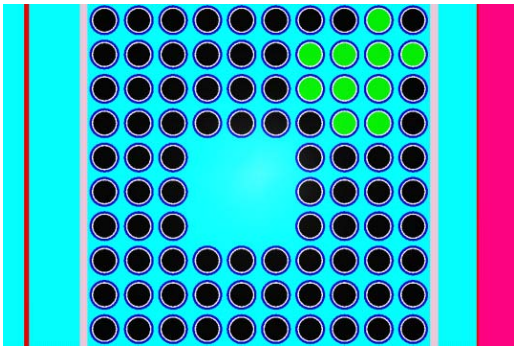

FANP 10x10 4.6 wt% ^{235}U, Pattern E

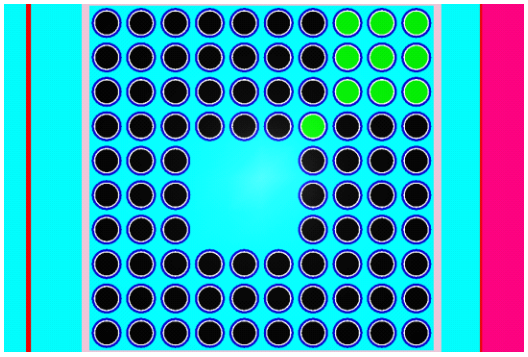

FANP 10x10 4.6 wt% ^{235}U, Pattern F

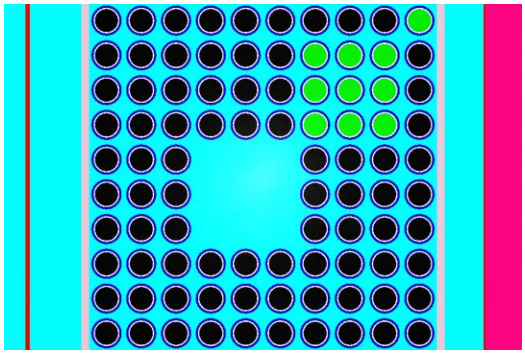

FANP 10x10 4.6 wt% ^{235}U, Pattern G

Figure 6-30 Gadolinia-Urania Fuel Rod Placement Pattern for 10x10 Fuel Assemblies

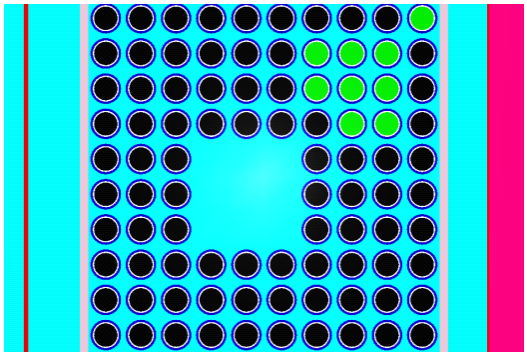

FANP 10x10 4.3 wt% ^{235}U, Pattern E

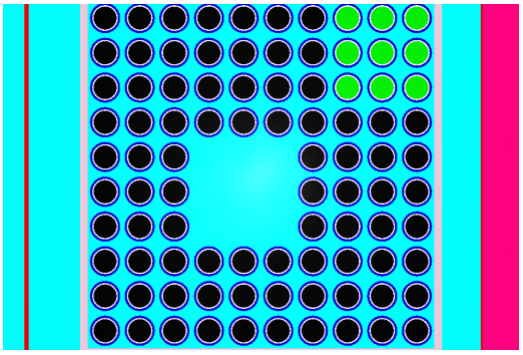

FANP 10x10 4.3 wt% ^{235}U, Pattern F

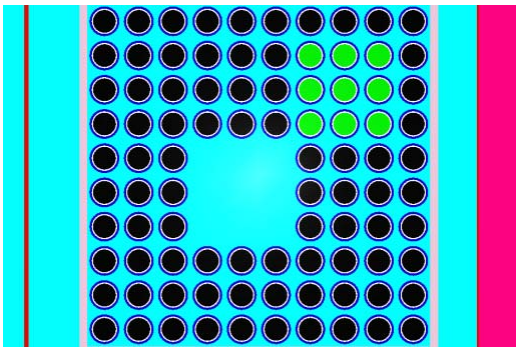

FANP 10x10 4.3 wt% ^{235}U, Pattern G

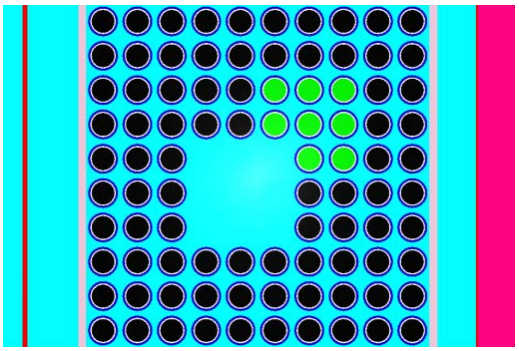

FANP 10x10 4.2 wt% ^{235}U, Pattern D

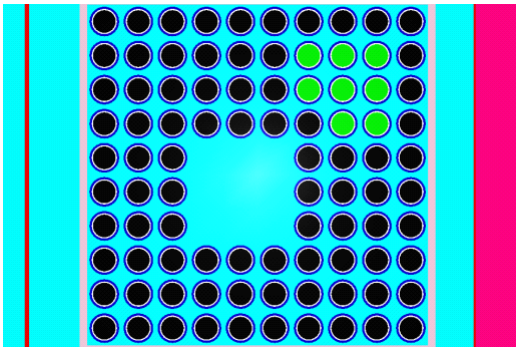

FANP 10x10 4.2 wt% ^{235}U, Pattern E

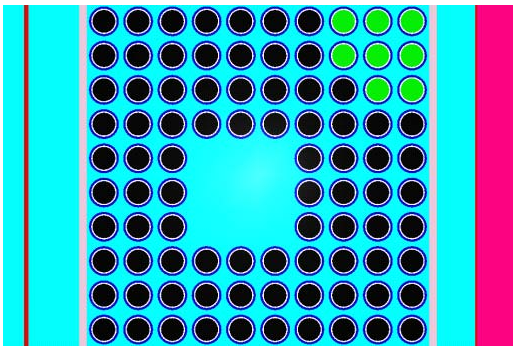

FANP 10x10 4.2 wt% ^{235}U, Pattern F

Figure 6-30 Gadolinia-Urania Fuel Rod Placement Pattern for 10x10 Fuel Assemblies (Continued)

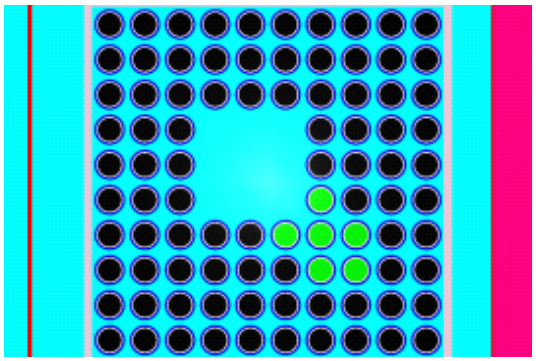

FANP 10x10 3.9 wt% ^{235}U, Pattern E

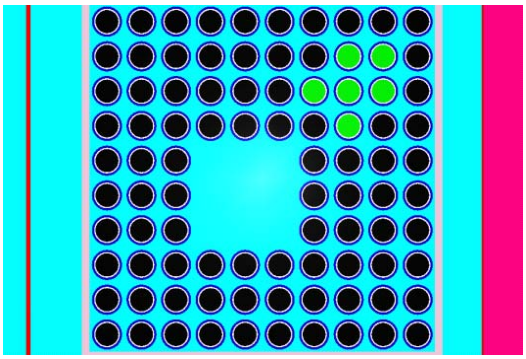

FANP 10x10 3.9 wt% ^{235}U, Pattern F

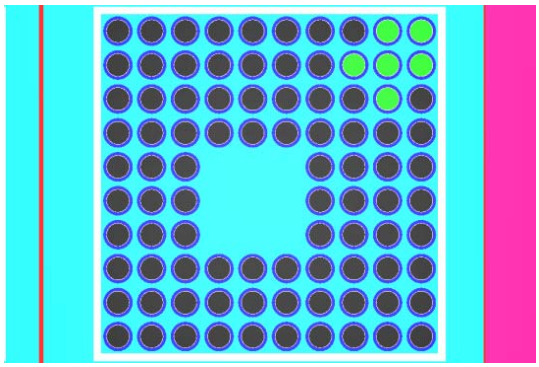

FANP 10x10 3.9 wt% ^{235}U, Pattern G

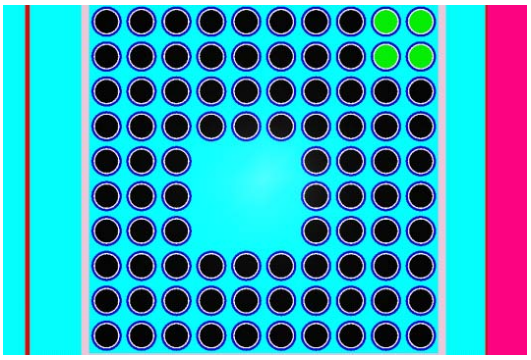

FANP 10x10 3.6 wt% ^{235}U, Pattern H

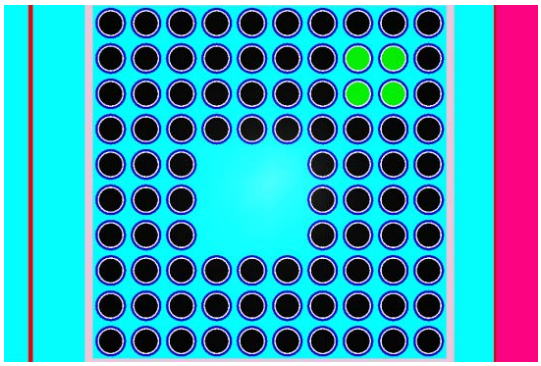

FANP 10x10 3.6 wt% ^{235}U, Pattern I

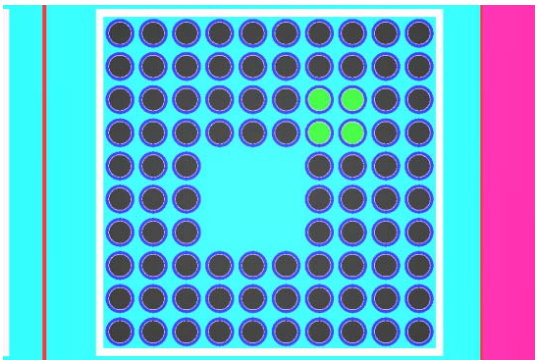

FANP 10x10 3.6 wt% ^{235}U, Pattern J

Figure 6-30 Gadolinia-Urania Fuel Rod Placement Pattern for 10x10 Fuel Assemblies (Continued)

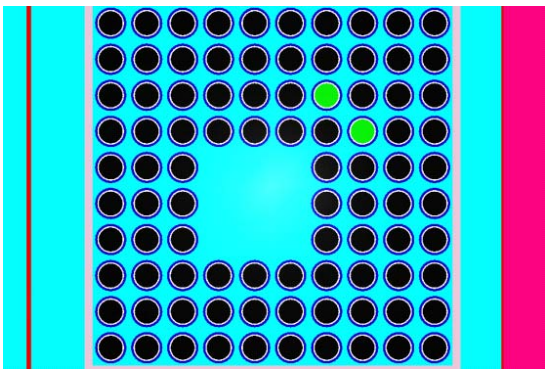

FANP 10x10 3.3 wt% ^{235}U, Pattern F

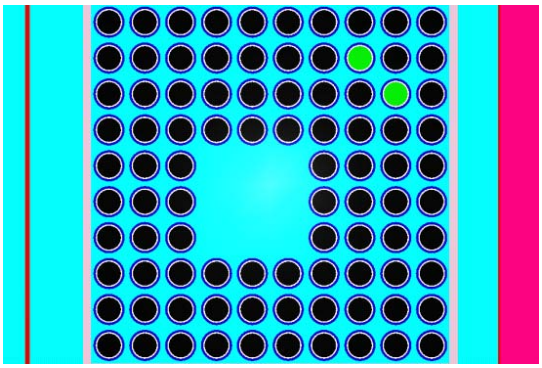

FANP 10x10 3.3 wt% ^{235}U, Pattern G

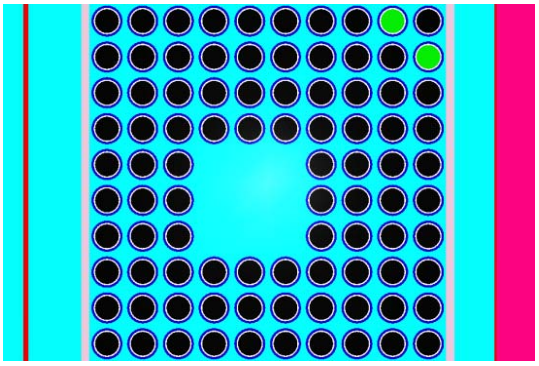

FANP 10x10 3.3 wt% ^{235}U, Pattern H

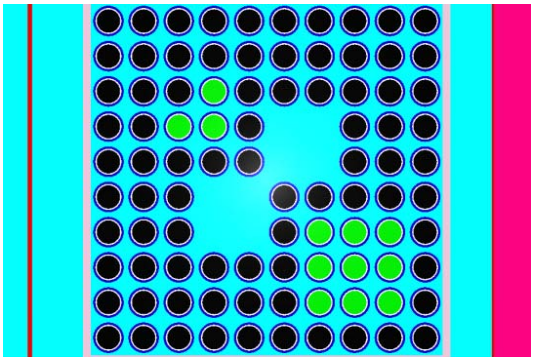

GNF 10x10 5.0 wt% ^{235}U, Pattern B

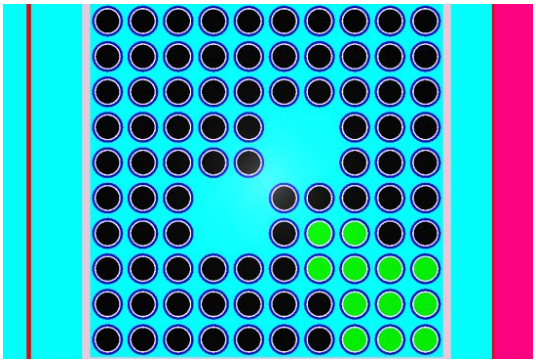

GNF 10x10 5.0 wt% ^{235}U, Pattern F

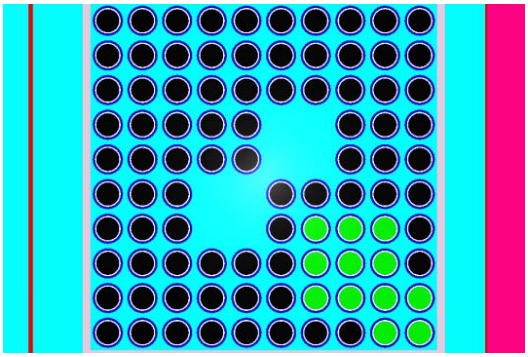

GNF 10x10 5.0 wt% ^{235}U, Pattern H

Figure 6-30 Gadolinia-Urania Fuel Rod Placement Pattern for 10x10 Fuel Assemblies (Continued)

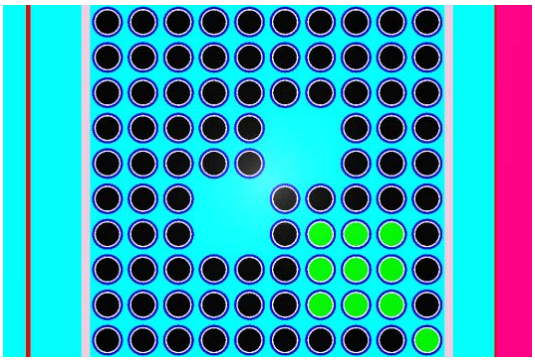

GNF 10x10 4.6 wt% ^{235}U, Pattern F

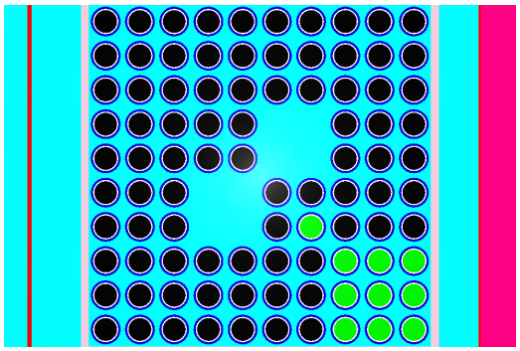

GNF 10x10 4.6 wt% ^{235}U, Pattern G

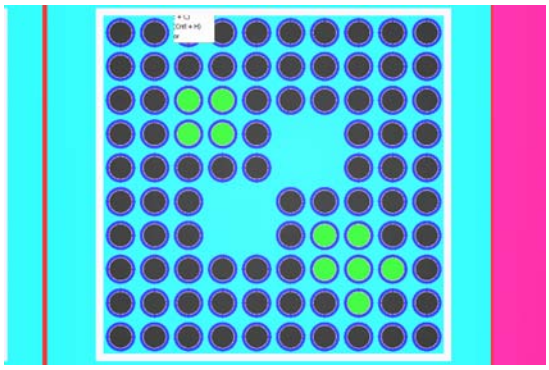

GNF 10x10 4.6 wt% ^{235}U, Pattern I

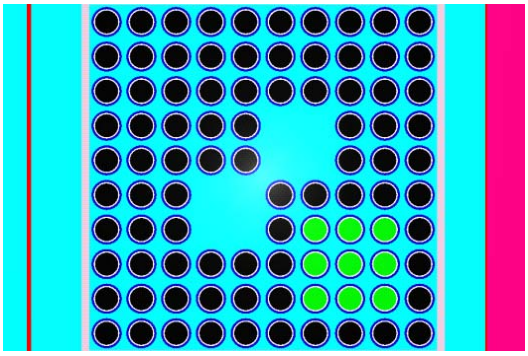

GNF 10x10 4.3 wt% ^{235}U, Pattern F

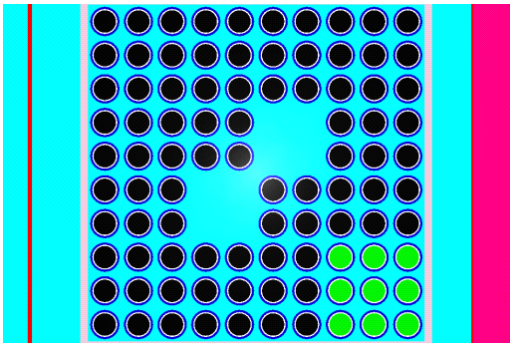

GNF 10x10 4.3 wt% ^{235}U, Pattern G

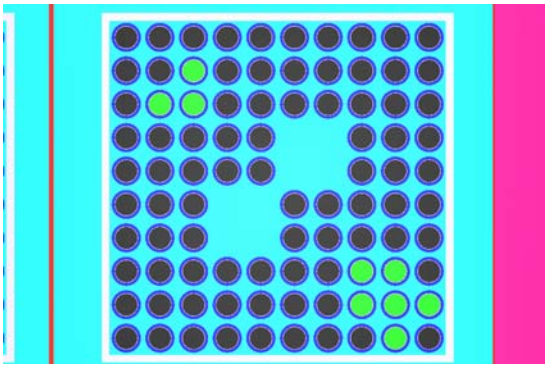

GNF 10x10 4.3 wt% ^{235}U, Pattern J

Figure 6-30 Gadolinia-Urania Fuel Rod Placement Pattern for 10x10 Fuel Assemblies (Continued)

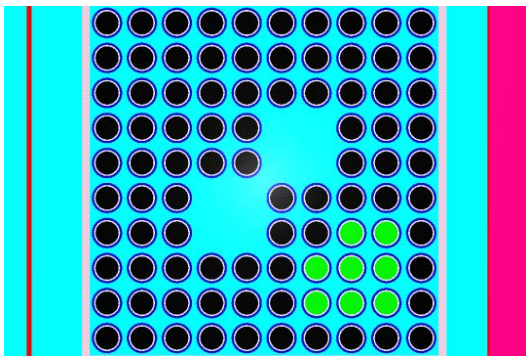

GNF 10x10 4.2 wt%^{235}U, Pattern F

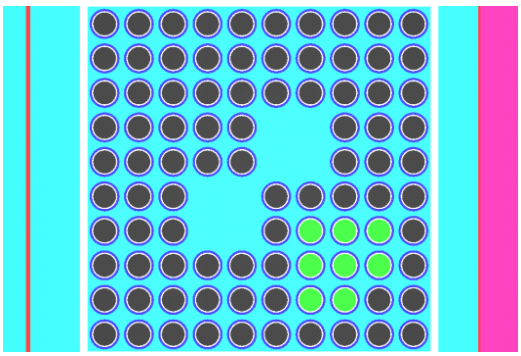

GNF 10x10 4.2 wt%^{235}U, Pattern I

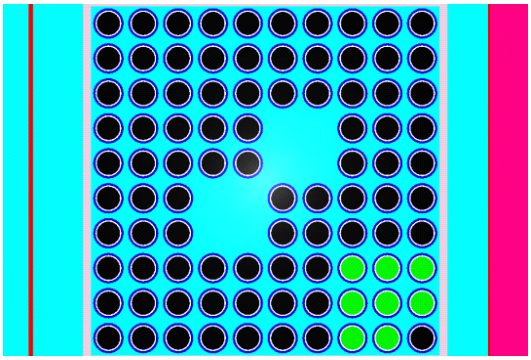

GNF 10x10 4.2 wt%^{235}U, Pattern J

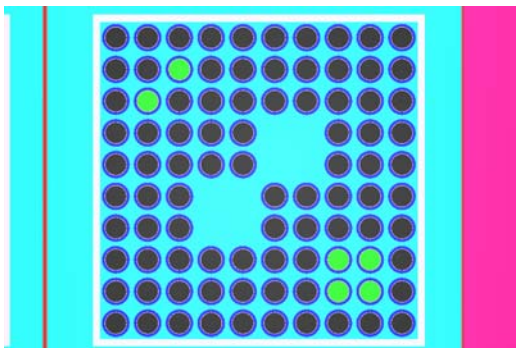

GNF 10x10 3.9 wt%^{235}U, Pattern G

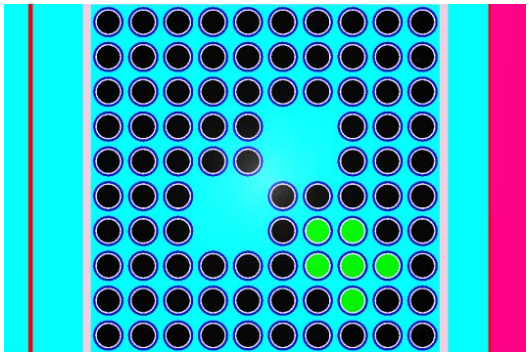

GNF 10x10 3.9 wt%^{235}U, Pattern J

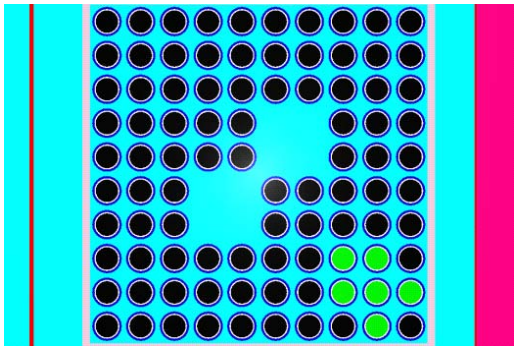

GNF 10x10 3.9 wt%^{235}U, Pattern K

Figure 6-30 Gadolinia-Urania Fuel Rod Placement Pattern for 10x10 Fuel Assemblies (Continued)

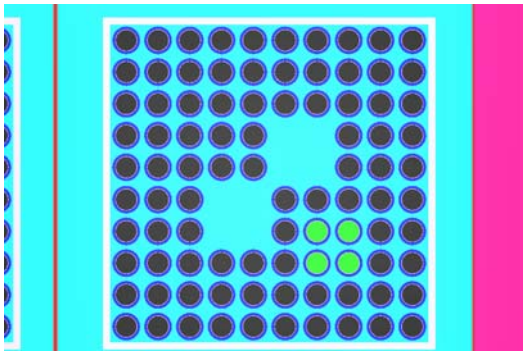

GNF 10x10 3.6 wt% ^{235}U, Pattern F

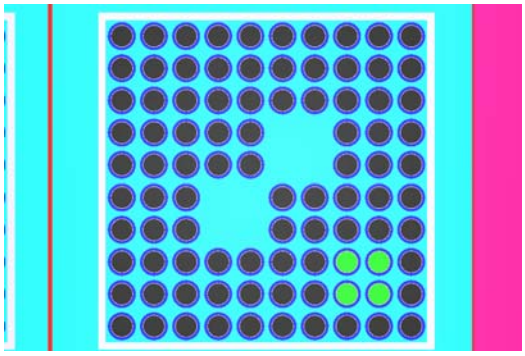

GNF 10x10 3.6 wt% ^{235}U, Pattern G

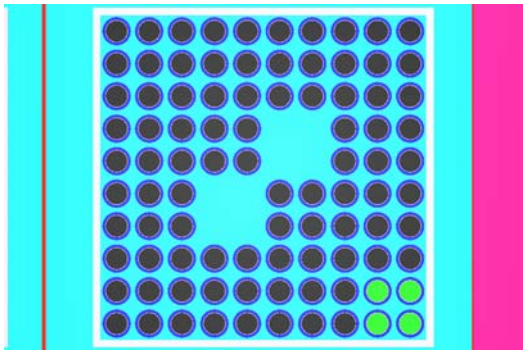

GNF 10x10 3.6 wt% ^{235}U, Pattern H

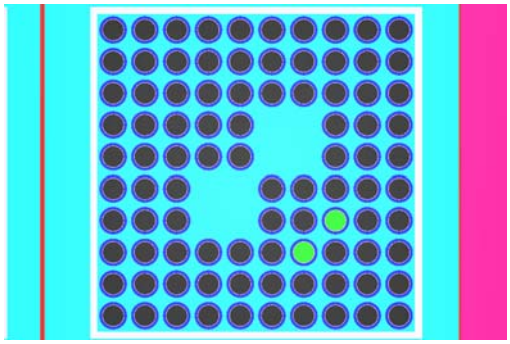

GNF 10x10 3.3 wt% ^{235}U, Pattern A

Figure 6-30 Gadolinia-Urania Fuel Rod Placement Pattern for 10x10 Fuel Assemblies (Continued)

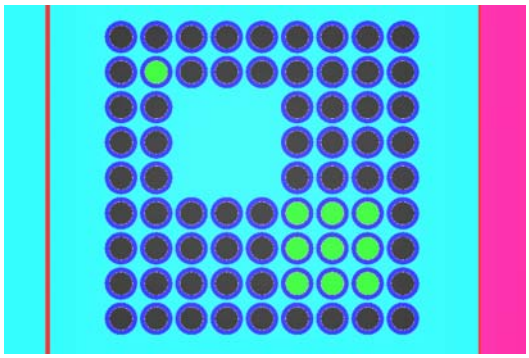

FANP 9x9 5.0 wt% ^{235}U, Pattern A

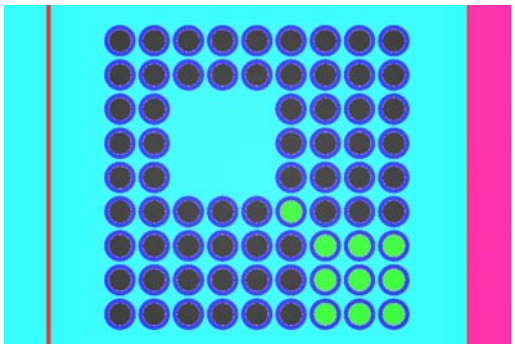

FANP 9x9 5.0 wt% ^{235}U, Pattern B

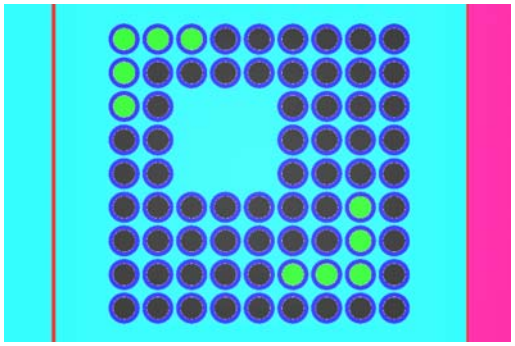

FANP 9x9 5.0 wt% ^{235}U, Pattern E

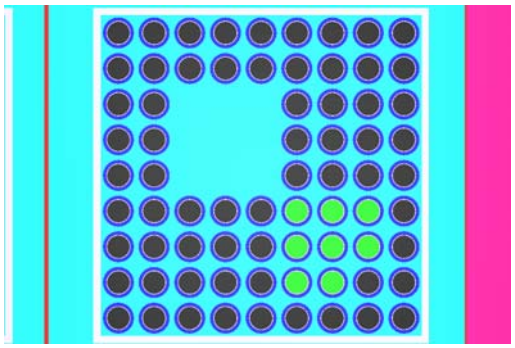

FANP 9x9 4.7 wt% ^{235}U, Pattern A

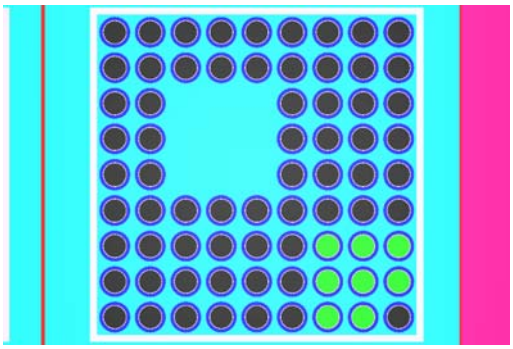

FANP 9x9 4.7 wt% ^{235}U, Pattern B

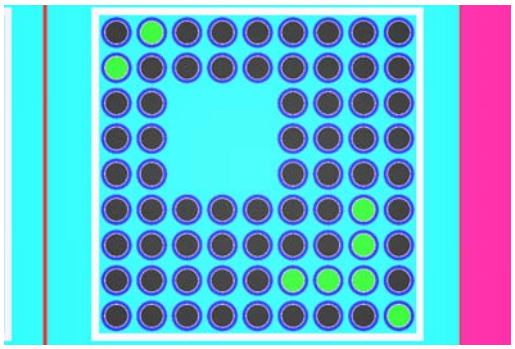

FANP 9x9 4.7 wt% ^{235}U, Pattern E

Figure 6-31 Gadolinia-Urania Fuel Rod Placement Pattern for 9x9 Fuel Assemblies

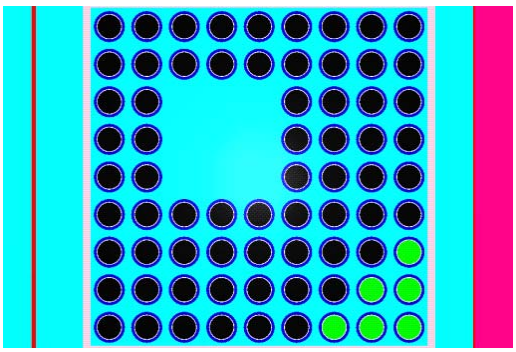

FANP 9x9 4.2 wt% U-235, Pattern A

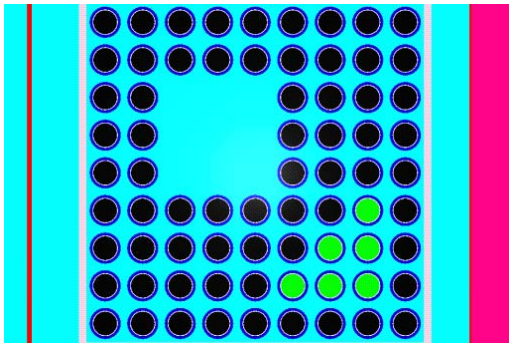

FANP 9x9 4.2 wt% U-235, Pattern B

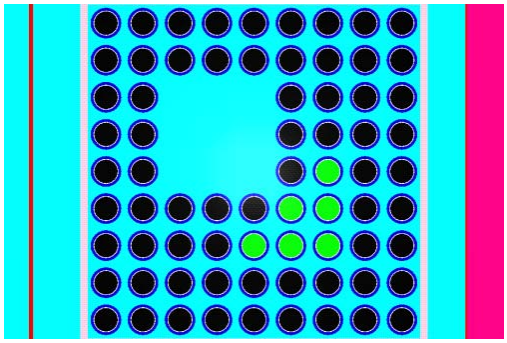

FANP 9x9 4.2 wt% U-235, Pattern C

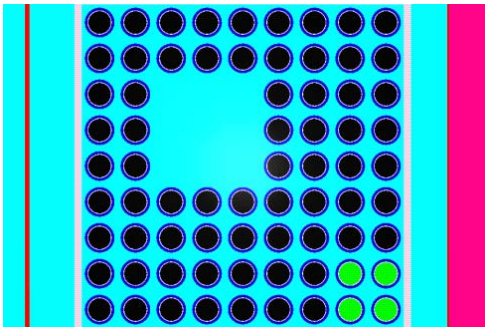

FANP 9x9 3.8 wt% U-235, Pattern A

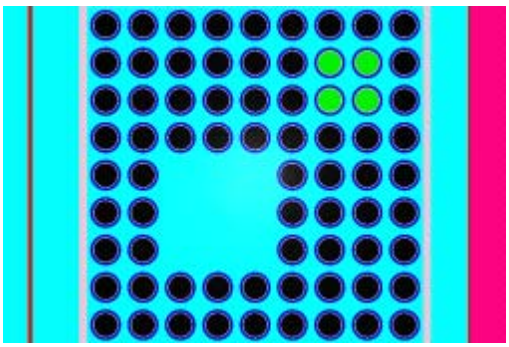

FANP 9x9 3.8 wt% U-235, Pattern B

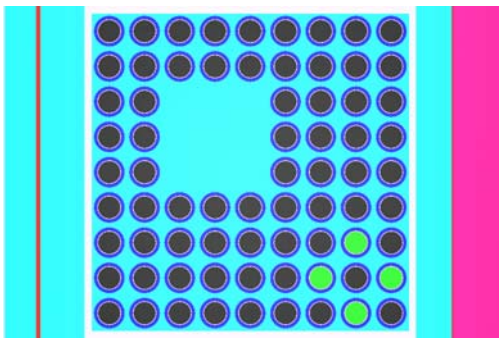

FANP 9x9 3.8 wt% U-235, Pattern F

Figure 6-31 Gadolinia-Urania Fuel Rod Placement Pattern for 9x9 Fuel Assemblies (Continued)

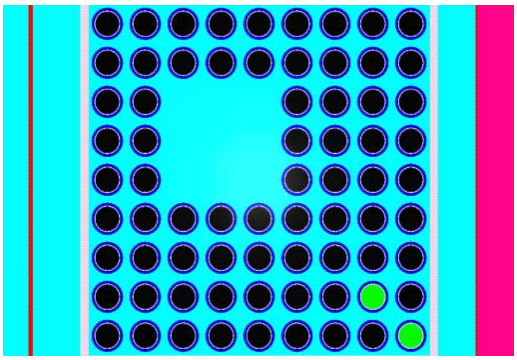

FANP 9x9 3.5 wt% U-235, Pattern B

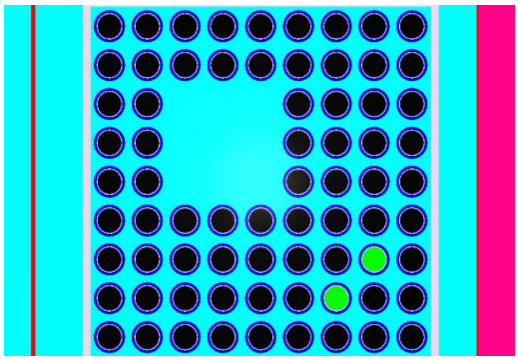

FANP 9x9 3.5 wt% U-235, Pattern C

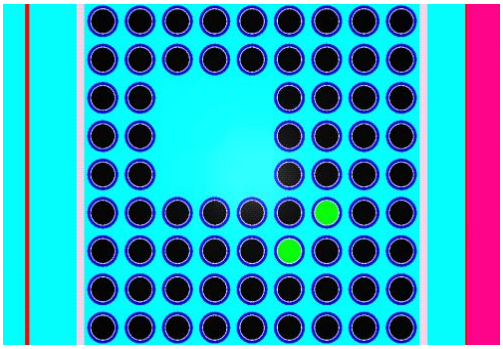

FANP 9x9 3.5 wt% U-235, Pattern D

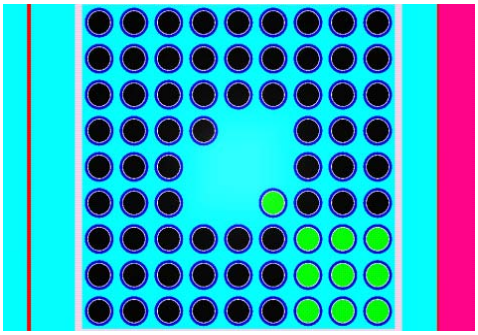

GNF 9x9 5.0 wt% U-235, Pattern B

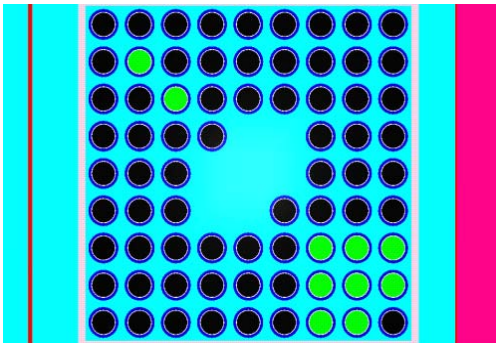

GNF 9x9 5.0 wt% U-235, Pattern G

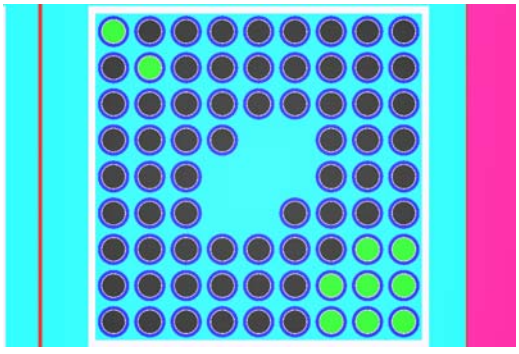

GNF 9x9 5.0 wt% U-235, Pattern H

Figure 6-31 Gadolinia–Urania Fuel Rod Placement Pattern for 9X9 Fuel Assemblies (Continued)

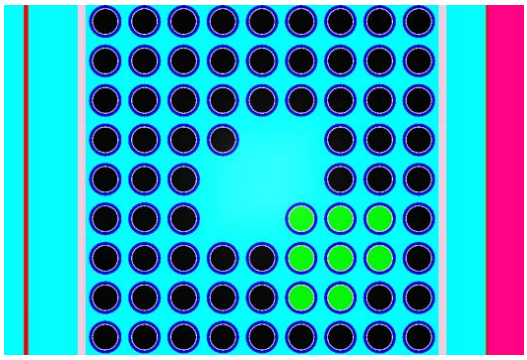

GNF 9x9 4.8 wt% U-235, Pattern A

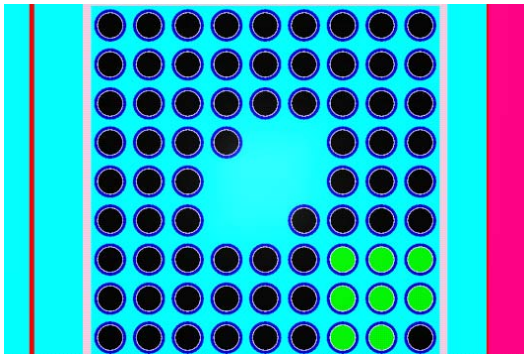

GNF 9x9 4.8 wt% U-235, Pattern B

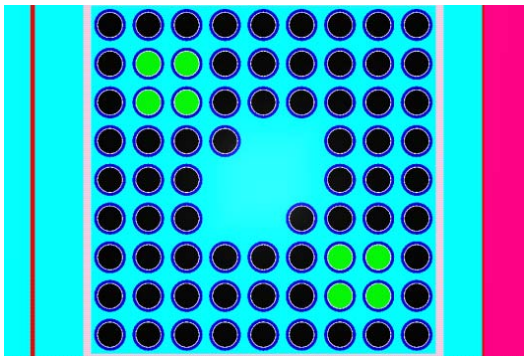

GNF 9x9 4.8 wt% U-235, Pattern H

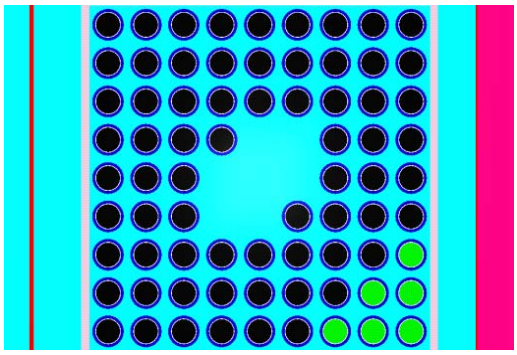

GNF 9x9 4.2 wt% U-235, Pattern A

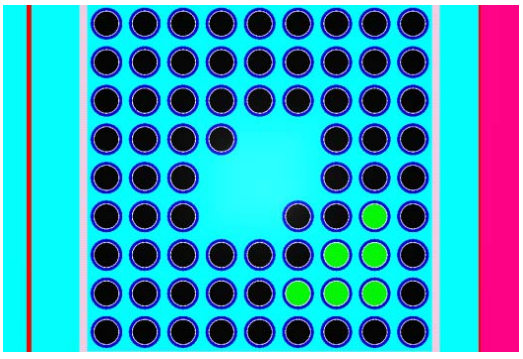

GNF 9x9 4.2 wt% U-235, Pattern B

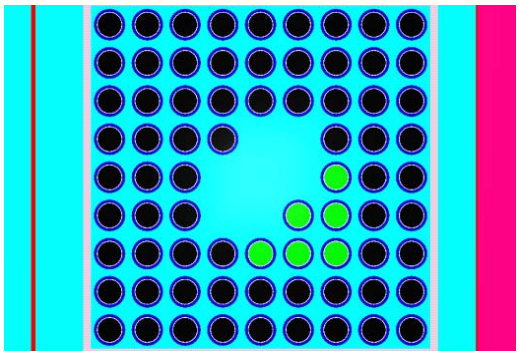

GNF 9x9 4.2 wt% U-235, Pattern C

Figure 6-31 Gadolinia–Urania Fuel Rod Placement Pattern for 9X9 Fuel Assemblies (Continued)

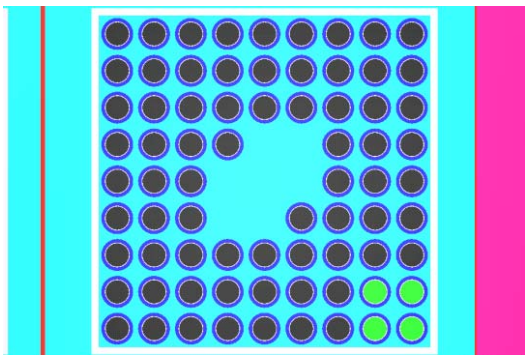

GNF 9x9 3.8 wt% ^{235}U, Pattern A

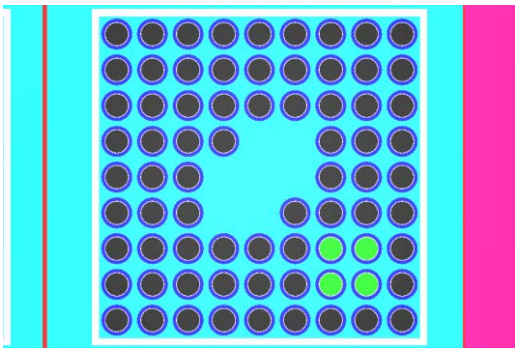

GNF 9x9 3.8 wt% ^{235}U, Pattern B

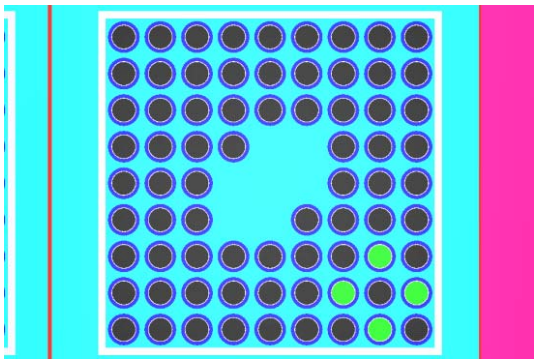

GNF 9x9 3.8 wt% ^{235}U, Pattern F

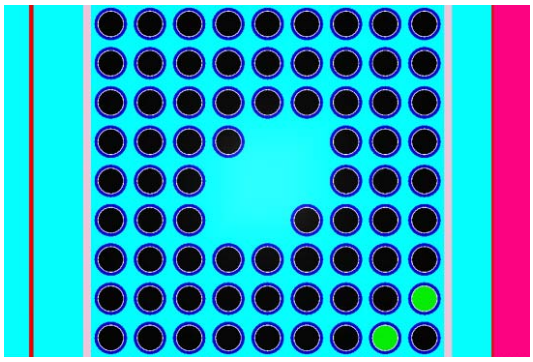

GNF 9x9 3.5 wt% ^{235}U, Pattern A

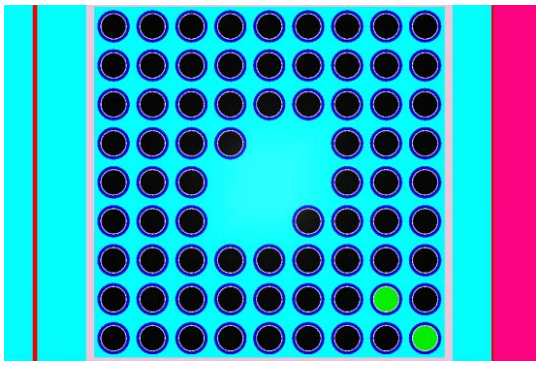

GNF 9x9 3.5 wt% ^{235}U, Pattern B

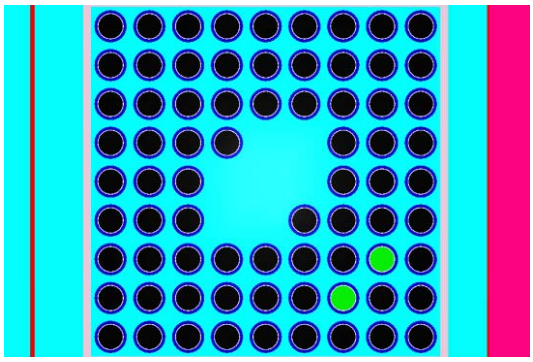

GNF 3.5 wt% ^{235}U, Pattern C

Figure 6-31 Gadolinia–Urania Fuel Rod Placement Pattern for 9X9 Fuel Assemblies (Continued)

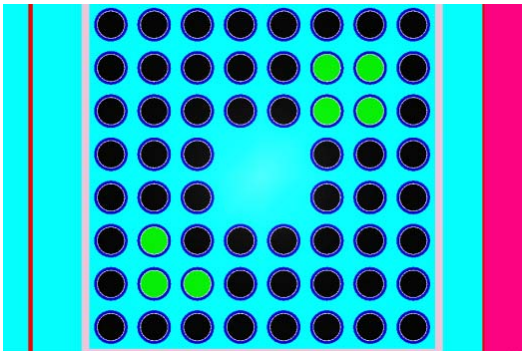

GNF 8x8 5.0 wt% ^{235}U, Pattern E

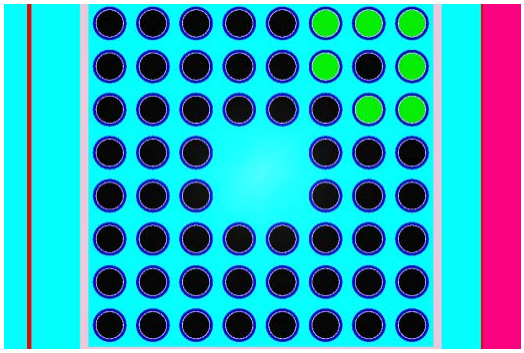

GNF 8x8 5.0 wt% ^{235}U, Pattern H

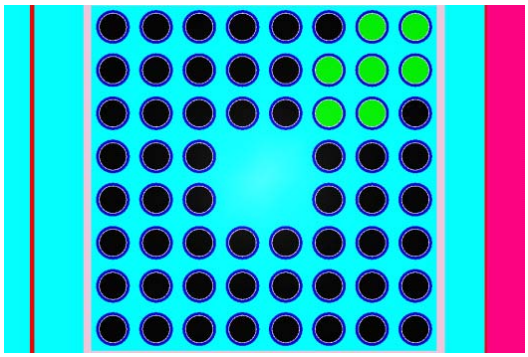

GNF 8x8 5.0 wt% ^{235}U, Pattern I

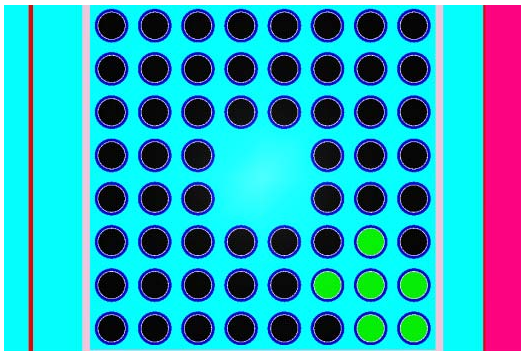

GNF 8x8 4.7 wt% ^{235}U, Pattern B

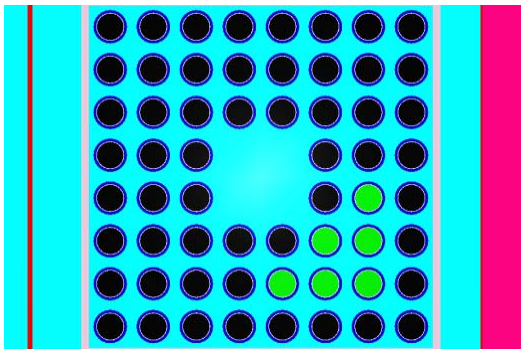

GNF 8x8 4.7 wt% ^{235}U, Pattern C

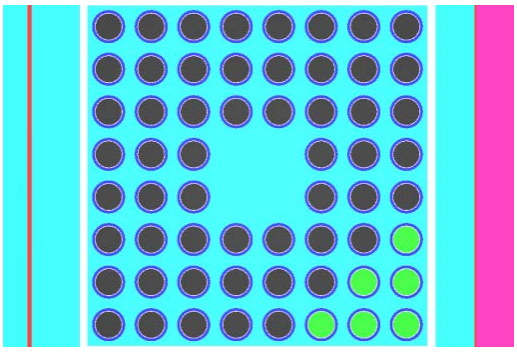

GNF 8x8 4.7 wt% ^{235}U, Pattern D

Figure 6-32 Gadolinia-Urania Fuel Rod Placement Pattern for 8x8 Fuel Assemblies

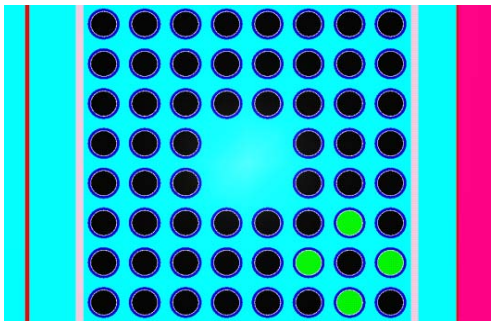

GNF 8x8 4.1 wt%^{235}U, Pattern B

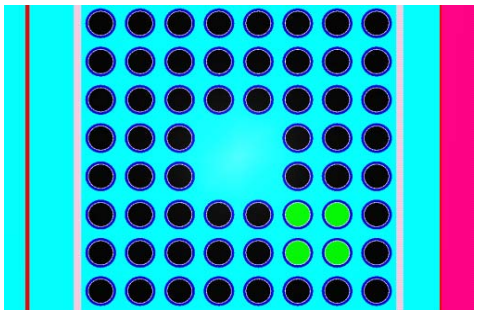

GNF 8x8 4.1 wt%^{235}U, Pattern C

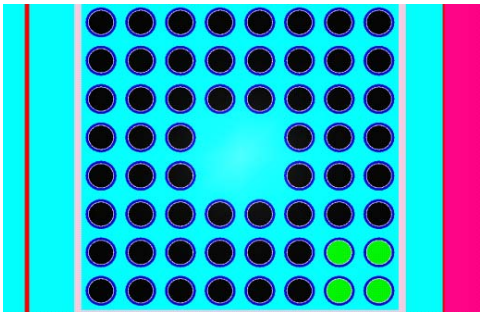

GNF 8x8 4.1 wt%^{235}U, Pattern D

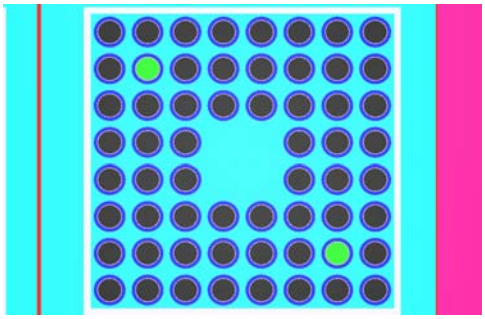

GNF 8x8 3.7 wt%^{235}U, Pattern A

Figure 6-32 Gadolinia-Urania Fuel Rod Placement Pattern for 8x8 Fuel Assemblies (Continued)

6.3.4.9 Part Length Fuel Rod Study (2N=448)

The FANP 10x10, FANP 9x9, GNF 10x10, and GNF 9x9 worst case designs are used to investigate the impact that part length fuel rods have on system reactivity. The worst case part length fuel rod patterns identified by performing scoping studies for the 10x10 designs are shown in Figure 6-33 and Figure 6-34. The worst case part length fuel rod patterns identified by performing scoping studies for the 9x9 designs are shown in Figure 6-35 and Figure 6-36. The fuel rod lengths for the part length rods are half that of the normal rod, and calculations showed that reducing the length further decreases system reactivity. To maintain the same amount of polyethylene when the part length rods are inserted, the polyethylene is redistributed to all rods in the assembly. The worst case models from the moderator density sensitivity study are used to conduct the part length fuel rod study, and the worst case fuel parameters listed in Table 6-17 are utilized. The part length fuel rod study results are contained in Table 6-18. All results for the FANP 9x9, the FANP 10x10, and the GNF 9x9 are below the USL of 0.94254. Several cases for the GNF 10x10 fuel design are above the USL of 0.94254. Therefore, an increased clad thickness is investigated for the 10x10 designs to reduce the system reactivity; these cases are included at the end of Table 6-18. The increased clad thickness for the 10x10 designs reduce system reactivity and all 10x10 results are below the USL of 0.94254. Comparing the results in Table 6-18 with those in Table 6-17 reveals the system reactivity remains about the same for the 9x9 fuel assembly designs with part length fuel rods. The FANP 10x10 and GNF 10x10 fuel designs are more reactive with the part length fuel rod configuration. Based on the results in Table 6-17 and Table 6-18:

- The maximum system reactivity with FANP 10x10 fuel assemblies having part length fuel rods and gadolinia-urania fuel is statistically greater than the maximum system reactivity with FANP 10x10 fuel assemblies having gadolinia-urania fuel and no part length fuel rods. The configuration that yields the highest $k_{eff} + 2\sigma$ consists of fuel assemblies with a lattice average enrichment of 5.0 wt% U-235, 12 gadolinia-urania fuel rods enriched to 2.0 wt% gadolinia arranged in Pattern G, and 10 part length fuel rods. With the clad thickness for the fuel assemblies increased from 0.0335 cm to 0.0381 cm, the $k_{eff} + 2\sigma$ for this configuration is 0.9394.

- The maximum system reactivity with GNF 10x10 fuel assemblies having part length fuel rods and gadolinia-urania fuel is statistically greater than the maximum system reactivity with GNF 10x10 fuel assemblies having gadolinia-urania fuel and no part length fuel rods. The configuration that yields the highest $k_{eff} + 2\sigma$ consists of fuel assemblies with a lattice average enrichment of 5.0 wt% U-235, 12 gadolinia-urania fuel rods enriched to 2.0 wt% gadolinia arranged in Pattern H, and 12 part length fuel rods. With the clad thickness for the fuel assemblies increased from 0.0335 cm to 0.0381 cm, the $k_{eff} + 2\sigma$ for this configuration is 0.9418.

- Based on fuel parameter changes made to the 10x10 designs to lower reactivity, a 0.9338 cm upper bound clad ID, and a 1.01 cm lower bound clad OD are established for the GNF 10x10 parameter ranges. The 0.9330 cm upper bound clad ID and 1.00 cm lower bound clad OD may still be used for the FANP 10x10 design since the fuel assembly with this configuration remained below the USL of 0.94254.

- The most reactive FANP 9x9 configuration consists of fuel assemblies with a lattice average enrichment of 4.7 wt% U-235 and 8 gadolinia-urania fuel rods enriched to 2.0 wt% gadolinia arranged in Pattern A and 8 part length rods. The $k_{eff} + 2\sigma$ for this configuration is 0.9303.

- The most reactive GNF 9x9 configuration consists of fuel assemblies with a lattice average enrichment of 4.7 wt% U-235 and 8 gadolinia-urania fuel rods enriched to 2.0 wt% gadolinia arranged in Pattern B and 8 part length fuel rods. The $k_{eff} + 2\sigma$ for this configuration is 0.9407.

- The most reactive GNF 8x8 configuration consists of fuel assemblies with a lattice average enrichment of 5.0 wt% U-235, 7 gadolinia-urania fuel rods enriched to 2.0 wt% gadolinia arranged in Pattern I, and no part length fuel rods. The $k_{eff} + 2\sigma$ for this configuration is 0.9372 (Table 6-17). The GNF 8x8 fuel assembly is not evaluated for part length fuel rods.

The GNF 10x10 assembly is chosen as the overall bounding fuel type since the $k_{eff} + 2\sigma$ is among the largest numerical values, however, the system reactivity of the 10x10, and 9x9 worst case fuel assembly designs in the 14x2x16 RAJ-II container array are statistically indistinquishable.

Table 6-18 RAJ-II Array HAC Part Length Fuel Rod Calculations

Assembly Type	Number of Part Length Rods	Gadolinia -Urania Fuel Rod Number	^{235}U Enrichment (wt%)	Pitch (cm)	Pellet Diameter (cm)	Clad ID (cm)	Clad OD (cm)	k_{eff}	σ	$k_{eff} + 2\sigma$
FANP 10x10	8	0	2.9	1.350	0.895	0.933	1.00	0.9228	0.0008	0.9244
FANP 10x10	8	2	3.3	1.350	0.895	0.933	1.00	0.9282	0.0008	0.9298
FANP 10x10	8	4	3.6	1.350	0.895	0.933	1.00	0.9332	0.0008	0.9348
FANP 10x10	8	6	3.9	1.350	0.895	0.933	1.00	0.9327	0.0008	0.9343
FANP 10x10	8	8	4.2	1.350	0.895	0.933	1.00	0.9367	0.0008	0.9383
FANP 10x10	8	9	4.3	1.350	0.895	0.933	1.00	0.9282	0.0008	0.9298
FANP 10x10	8	10	4.6	1.350	0.895	0.933	1.00	0.9363	0.0009	0.9381
FANP 10x10	8	12	5.0	1.350	0.895	0.933	1.00	0.9403	0.0008	**0.9419**
FANP 10x10	10	0	2.9	1.350	0.895	0.933	1.00	0.9224	0.0008	0.9240
FANP 10x10	10	2	3.3	1.350	0.895	0.933	1.00	0.9283	0.0008	0.9299
FANP 10x10	10	4	3.6	1.350	0.895	0.933	1.00	0.9330	0.0007	0.9344
FANP 10x10	10	6	3.9	1.350	0.895	0.933	1.00	0.9333	0.0008	0.9349
FANP 10x10	10	8	4.2	1.350	0.895	0.933	1.00	0.9367	0.0008	0.9383
FANP 10x10	10	9	4.3	1.350	0.895	0.933	1.00	0.9301	0.0008	0.9317
FANP 10x10	10	10	4.6	1.350	0.895	0.933	1.00	0.9379	0.0009	0.9397
FANP 10x10	10	12	5.0	1.350	0.895	0.933	1.00	0.9399	0.0008	**0.9415**
FANP 10x10	12	0	2.9	1.350	0.895	0.933	1.00	0.9234	0.0008	0.9250
FANP 10x10	12	2	3.3	1.350	0.895	0.933	1.00	0.9281	0.0008	0.9297
FANP 10x10	12	4	3.6	1.350	0.895	0.933	1.00	0.9329	0.0008	0.9345
FANP 10x10	12	6	3.9	1.350	0.895	0.933	1.00	0.9319	0.0008	0.9335

Assembly Type	Number of Part Length Rods	Gadolinia -Urania Fuel Rod Number	^{235}U Enrichment (wt%)	Pitch (cm)	Pellet Diameter (cm)	Clad ID (cm)	Clad OD (cm)	k_{eff}	σ	$k_{eff} + 2\sigma$
FANP 10x10	12	8	4.2	1.350	0.895	0.933	1.00	0.9356	0.0008	0.9372
FANP 10x10	12	9	4.3	1.350	0.895	0.933	1.00	0.9294	0.0007	0.9308
FANP 10x10	12	10	4.6	1.350	0.895	0.933	1.00	0.9371	0.0008	0.9387
FANP 10x10	12	12	5.0	1.350	0.895	0.933	1.00	0.9404	0.0009	**0.9422**
FANP 10x10	14	0	2.9	1.350	0.895	0.933	1.00	0.9225	0.0008	0.9241
FANP 10x10	14	2	3.3	1.350	0.895	0.933	1.00	0.9274	0.0008	0.9290
FANP 10x10	14	4	3.6	1.350	0.895	0.933	1.00	0.9326	0.0009	0.9344
FANP 10x10	14	6	3.9	1.350	0.895	0.933	1.00	0.9313	0.0008	0.9329
FANP 10x10	14	8	4.2	1.350	0.895	0.933	1.00	0.9348	0.0010	0.9368
FANP 10x10	14	9	4.3	1.350	0.895	0.933	1.00	0.9310	0.0008	0.9326
FANP 10x10	14	10	4.6	1.350	0.895	0.933	1.00	0.9371	0.0008	0.9387
FANP 10x10	14	12	5.0	1.350	0.895	0.933	1.00	0.9393	0.0009	**0.9411**
GNF 10x10	8	0	2.9	1.350	0.895	0.933	1.00	0.9321	0.0007	0.9335
GNF 10x10	8	2	3.3	1.350	0.895	0.933	1.00	0.9327	0.0007	0.9341
GNF 10x10	8	4	3.6	1.350	0.895	0.933	1.00	0.9395	0.0010	0.9415
GNF 10x10	8	6	3.9	1.350	0.895	0.933	1.00	0.9367	0.0008	0.9383
GNF 10x10	8	8	4.2	1.350	0.895	0.933	1.00	0.9402	0.0008	**0.9418**
GNF 10x10	8	9	4.3	1.350	0.895	0.933	1.00	0.9369	0.0009	0.9387
GNF 10x10	8	10	4.6	1.350	0.895	0.933	1.00	0.9376	0.0009	0.9394
GNF 10x10	8	12	5.0	1.350	0.895	0.933	1.00	0.9386	0.0010	0.9406
GNF 10x10	10	0	2.9	1.350	0.895	0.933	1.00	0.9300	0.0008	0.9316
GNF 10x10	10	2	3.3	1.350	0.895	0.933	1.00	0.9319	0.0008	0.9335
GNF 10x10	10	4	3.6	1.350	0.895	0.933	1.00	0.9380	0.0009	0.9398
GNF 10x10	10	6	3.9	1.350	0.895	0.933	1.00	0.9347	0.0008	0.9363
GNF 10x10	10	8	4.2	1.350	0.895	0.933	1.00	0.9419	0.0010	**0.9439**
GNF 10x10	10	9	4.3	1.350	0.895	0.933	1.00	0.9374	0.0008	0.9390
GNF 10x10	10	10	4.6	1.350	0.895	0.933	1.00	0.9385	0.0009	0.9403
GNF 10x10	10	12	5.0	1.350	0.895	0.933	1.00	0.9412	0.0008	0.9428
GNF 10x10	12	0	2.9	1.350	0.895	0.933	1.00	0.9300	0.0007	0.9314
GNF 10x10	12	2	3.3	1.350	0.895	0.933	1.00	0.9316	0.0007	0.9330
GNF 10x10	12	4	3.6	1.350	0.895	0.933	1.00	0.9377	0.0009	0.9395
GNF 10x10	12	6	3.9	1.350	0.895	0.933	1.00	0.9352	0.0008	0.9368
GNF 10x10	12	8	4.2	1.350	0.895	0.933	1.00	0.9408	0.0009	0.9426
GNF 10x10	12	9	4.3	1.350	0.895	0.933	1.00	0.9374	0.0008	0.9390
GNF 10x10	12	10	4.6	1.350	0.895	0.933	1.00	0.9406	0.0009	0.9424
GNF 10x10	12	12	5.0	1.350	0.895	0.933	1.00	0.9415	0.0008	**0.9431**
GNF 10x10	14	0	2.9	1.350	0.895	0.933	1.00	0.9277	0.0008	0.9293
GNF 10x10	14	2	3.3	1.350	0.895	0.933	1.00	0.9305	0.0008	0.9321
GNF 10x10	14	4	3.6	1.350	0.895	0.933	1.00	0.9374	0.0009	0.9392
GNF 10x10	14	6	3.9	1.350	0.895	0.933	1.00	0.9347	0.0008	0.9363
GNF 10x10	14	8	4.2	1.350	0.895	0.933	1.00	0.9401	0.0009	**0.9419**
GNF 10x10	14	9	4.3	1.350	0.895	0.933	1.00	0.9370	0.0009	0.9388
GNF 10x10	14	10	4.6	1.350	0.895	0.933	1.00	0.9381	0.0009	0.9399
GNF 10x10	14	12	5.0	1.350	0.895	0.933	1.00	0.9401	0.0008	0.9417
FANP 9x9	8	0	3.0	1.510	0.96	1.02	1.09	0.9168	0.0008	0.9184
FANP 9x9	8	2	3.5	1.510	0.96	1.02	1.09	0.9219	0.0008	0.9235
FANP 9x9	8	4	3.8	1.510	0.96	1.02	1.09	0.9234	0.0009	0.9252
FANP 9x9	8	6	4.2	1.510	0.96	1.02	1.09	0.9227	0.0007	0.9241
FANP 9x9	8	8	4.7	1.510	0.96	1.02	1.09	0.9287	0.0008	**0.9303**

Assembly Type	Number of Part Length Rods	Gadolinia -Urania Fuel Rod Number	^{235}U Enrichment (wt%)	Pitch (cm)	Pellet Diameter (cm)	Clad ID (cm)	Clad OD (cm)	k_{eff}	σ	$k_{eff} + 2\sigma$
FANP 9x9	8	10	5.0	1.510	0.96	1.02	1.09	0.9165	0.0008	0.9181
FANP 9x9	10	0	3.0	1.510	0.96	1.02	1.09	0.9139	0.0008	0.9155
FANP 9x9	10	2	3.5	1.510	0.96	1.02	1.09	0.9195	0.0008	0.9211
FANP 9x9	10	4	3.8	1.510	0.96	1.02	1.09	0.9189	0.0008	0.9205
FANP 9x9	10	6	4.2	1.510	0.96	1.02	1.09	0.9208	0.0008	0.9224
FANP 9x9	10	8	4.7	1.510	0.96	1.02	1.09	0.9256	0.0009	**0.9274**
FANP 9x9	10	10	5.0	1.510	0.96	1.02	1.09	0.9135	0.0009	0.9153
FANP 9x9	12	0	3.0	1.510	0.96	1.02	1.09	0.9100	0.0007	0.9114
FANP 9x9	12	2	3.5	1.510	0.96	1.02	1.09	0.9155	0.0007	0.9169
FANP 9x9	12	4	3.8	1.510	0.96	1.02	1.09	0.9168	0.0008	0.9184
FANP 9x9	12	6	4.2	1.510	0.96	1.02	1.09	0.9147	0.0007	0.9161
FANP 9x9	12	8	4.7	1.510	0.96	1.02	1.09	0.9208	0.0008	**0.9224**
FANP 9x9	12	10	5.0	1.510	0.96	1.02	1.09	0.9087	0.0009	0.9105
GNF 9x9	8	0	3.0	1.510	0.96	1.02	1.09	0.9261	0.0008	0.9277
GNF 9x9	8	2	3.5	1.510	0.96	1.02	1.09	0.9311	0.0008	0.9327
GNF 9x9	8	4	3.8	1.510	0.96	1.02	1.09	0.9303	0.0008	0.9319
GNF 9x9	8	6	4.2	1.510	0.96	1.02	1.09	0.9293	0.0008	0.9309
GNF 9x9	8	8	4.7	1.510	0.96	1.02	1.09	0.9391	0.0008	**0.9407**
GNF 9x9	8	10	5.0	1.510	0.96	1.02	1.09	0.9140	0.0008	0.9156
GNF 9x9	10	0	3.0	1.510	0.96	1.02	1.09	0.9249	0.0009	0.9267
GNF 9x9	10	2	3.5	1.510	0.96	1.02	1.09	0.9315	0.0008	0.9331
GNF 9x9	10	4	3.8	1.510	0.96	1.02	1.09	0.9287	0.0008	0.9303
GNF 9x9	10	6	4.2	1.510	0.96	1.02	1.09	0.9297	0.0009	0.9315
GNF 9x9	10	8	4.7	1.510	0.96	1.02	1.09	0.9377	0.0008	**0.9393**
GNF 9x9	10	10	5.0	1.510	0.96	1.02	1.09	0.9048	0.0008	0.9064
GNF 9x9	12	0	3.0	1.510	0.96	1.02	1.09	0.9235	0.0008	0.9251
GNF 9x9	12	2	3.5	1.510	0.96	1.02	1.09	0.9294	0.0009	0.9312
GNF 9x9	12	4	3.8	1.510	0.96	1.02	1.09	0.9288	0.0009	0.9306
GNF 9x9	12	6	4.2	1.510	0.96	1.02	1.09	0.9263	0.0008	0.9279
GNF 9x9	12	8	4.7	1.510	0.96	1.02	1.09	0.9370	0.0009	**0.9388**
GNF 9x9	12	10	5.0	1.510	0.96	1.02	1.09	0.9056	0.0008	0.9072
FANP 10x10	8	0	2.9	1.350	0.895	0.9338	1.01	0.9203	0.0008	0.9219
FANP 10x10	8	2	3.3	1.350	0.895	0.9338	1.01	0.9150	0.0008	0.9166
FANP 10x10	8	4	3.6	1.350	0.895	0.9338	1.01	0.9290	0.0008	0.9306
FANP 10x10	8	6	3.9	1.350	0.895	0.9338	1.01	0.9303	0.0008	0.9319
FANP 10x10	8	8	4.2	1.350	0.895	0.9338	1.01	0.9292	0.0008	0.9308
FANP 10x10	8	9	4.3	1.350	0.895	0.9338	1.01	0.9293	0.0008	0.9309
FANP 10x10	8	10	4.6	1.350	0.895	0.9338	1.01	0.9335	0.0008	0.9351
FANP 10x10	8	12	5.0	1.350	0.895	0.9338	1.01	0.9353	0.0009	**0.9371**
FANP 10x10	10	0	2.9	1.350	0.895	0.9338	1.01	0.9218	0.0008	0.9234
FANP 10x10	10	2	3.3	1.350	0.895	0.9338	1.01	0.9265	0.0008	0.9281
FANP 10x10	10	4	3.6	1.350	0.895	0.9338	1.01	0.9320	0.0008	0.9336
FANP 10x10	10	6	3.9	1.350	0.895	0.9338	1.01	0.9311	0.0008	0.9327
FANP 10x10	10	8	4.2	1.350	0.895	0.9338	1.01	0.9345	0.0008	0.9361
FANP 10x10	10	9	4.3	1.350	0.895	0.9338	1.01	0.9296	0.0009	0.9314
FANP 10x10	10	10	4.6	1.350	0.895	0.9338	1.01	0.9369	0.0009	0.9387
FANP 10x10	10	12	5.0	1.350	0.895	0.9338	1.01	0.9376	0.0009	**0.9394**
FANP 10x10	12	0	2.9	1.350	0.895	0.9338	1.01	0.9216	0.0008	0.9232
FANP 10x10	12	2	3.3	1.350	0.895	0.9338	1.01	0.9256	0.0008	0.9272

Assembly Type	Number of Part Length Rods	Gadolinia -Urania Fuel Rod Number	^{235}U Enrichment (wt%)	Pitch (cm)	Pellet Diameter (cm)	Clad ID (cm)	Clad OD (cm)	k_{eff}	σ	$k_{eff} + 2\sigma$
FANP 10x10	12	4	3.6	1.350	0.895	0.9338	1.01	0.9314	0.0009	0.9332
FANP 10x10	12	6	3.9	1.350	0.895	0.9338	1.01	0.9319	0.0007	0.9333
FANP 10x10	12	8	4.2	1.350	0.895	0.9338	1.01	0.9345	0.0008	0.9361
FANP 10x10	12	9	4.3	1.350	0.895	0.9338	1.01	0.9277	0.0008	0.9293
FANP 10x10	12	10	4.6	1.350	0.895	0.9338	1.01	0.9347	0.0009	0.9365
FANP 10x10	12	12	5.0	1.350	0.895	0.9338	1.01	0.9370	0.0009	**0.9388**
FANP 10x10	14	0	2.9	1.350	0.895	0.9338	1.01	0.9207	0.0008	0.9223
FANP 10x10	14	2	3.3	1.350	0.895	0.9338	1.01	0.9247	0.0009	0.9265
FANP 10x10	14	4	3.6	1.350	0.895	0.9338	1.01	0.9291	0.0008	0.9307
FANP 10x10	14	6	3.9	1.350	0.895	0.9338	1.01	0.9301	0.0009	0.9319
FANP 10x10	14	8	4.2	1.350	0.895	0.9338	1.01	0.9324	0.0008	0.9340
FANP 10x10	14	9	4.3	1.350	0.895	0.9338	1.01	0.9293	0.0008	0.9309
FANP 10x10	14	10	4.6	1.350	0.895	0.9338	1.01	0.9352	0.0008	0.9368
FANP 10x10	14	12	5.0	1.350	0.895	0.9338	1.01	0.9370	0.0009	**0.9388**
GNF 10x10	8	0	2.9	1.350	0.895	0.9338	1.01	0.9292	0.0008	0.9308
GNF 10x10	8	2	3.3	1.350	0.895	0.9338	1.01	0.9296	0.0009	0.9314
GNF 10x10	8	4	3.6	1.350	0.895	0.9338	1.01	0.9357	0.0010	0.9377
GNF 10x10	8	6	3.9	1.350	0.895	0.9338	1.01	0.9354	0.0009	0.9372
GNF 10x10	8	8	4.2	1.350	0.895	0.9338	1.01	0.9399	0.0008	**0.9415**
GNF 10x10	8	9	4.3	1.350	0.895	0.9338	1.01	0.9346	0.0010	0.9366
GNF 10x10	8	10	4.6	1.350	0.895	0.9338	1.01	0.9376	0.0009	0.9394
GNF 10x10	8	12	5.0	1.350	0.895	0.9338	1.01	0.9375	0.0008	0.9391
GNF 10x10	10	0	2.9	1.350	0.895	0.9338	1.01	0.9292	0.0008	0.9308
GNF 10x10	10	2	3.3	1.350	0.895	0.9338	1.01	0.9296	0.0008	0.9312
GNF 10x10	10	4	3.6	1.350	0.895	0.9338	1.01	0.9371	0.0008	0.9387
GNF 10x10	10	6	3.9	1.350	0.895	0.9338	1.01	0.9370	0.0008	0.9386
GNF 10x10	10	8	4.2	1.350	0.895	0.9338	1.01	0.9372	0.0008	0.9388
GNF 10x10	10	9	4.3	1.350	0.895	0.9338	1.01	0.9363	0.0009	0.9381
GNF 10x10	10	10	4.6	1.350	0.895	0.9338	1.01	0.9345	0.0009	0.9363
GNF 10x10	10	12	5.0	1.350	0.895	0.9338	1.01	0.9375	0.0008	**0.9391**
GNF 10x10	12	0	2.9	1.350	0.895	0.9338	1.01	0.9276	0.0008	0.9292
GNF 10x10	12	2	3.3	1.350	0.895	0.9338	1.01	0.9309	0.0008	0.9325
GNF 10x10	12	4	3.6	1.350	0.895	0.9338	1.01	0.9373	0.0009	0.9391
GNF 10x10	12	6	3.9	1.350	0.895	0.9338	1.01	0.9347	0.0009	0.9365
GNF 10x10	12	8	4.2	1.350	0.895	0.9338	1.01	0.9374	0.0009	0.9392
GNF 10x10	12	9	4.3	1.350	0.895	0.9338	1.01	0.9333	0.0009	0.9351
GNF 10x10	12	10	4.6	1.350	0.895	0.9338	1.01	0.9378	0.0008	0.9394
GNF 10x10	12	12	5.0	1.350	0.895	0.9338	1.01	0.9404	0.0007	**0.9418**
GNF 10x10	14	0	2.9	1.350	0.895	0.9338	1.01	0.9261	0.0008	0.9277
GNF 10x10	14	2	3.3	1.350	0.895	0.9338	1.01	0.9299	0.0008	0.9315
GNF 10x10	14	4	3.6	1.350	0.895	0.9338	1.01	0.9345	0.0008	0.9361
GNF 10x10	14	6	3.9	1.350	0.895	0.9338	1.01	0.9351	0.0009	0.9369
GNF 10x10	14	8	4.2	1.350	0.895	0.9338	1.01	0.9376	0.0009	0.9394
GNF 10x10	14	9	4.3	1.350	0.895	0.9338	1.01	0.9353	0.0008	0.9369
GNF 10x10	14	10	4.6	1.350	0.895	0.9338	1.01	0.9368	0.0009	0.9386
GNF 10x10	14	12	5.0	1.350	0.895	0.9338	1.01	0.9398	0.0008	**0.9414**

a. Limiting case(s) shown in bold

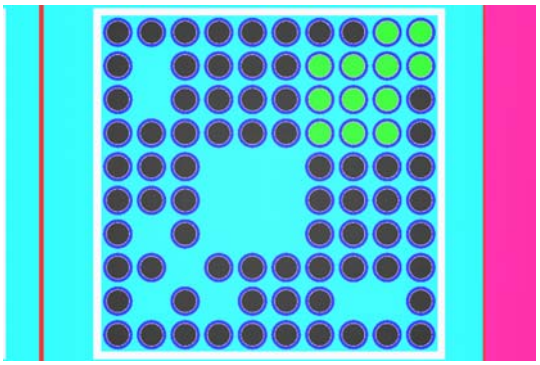

FANP 10x10 5.0 wt% ^{235}U, 8 Part Length Rods

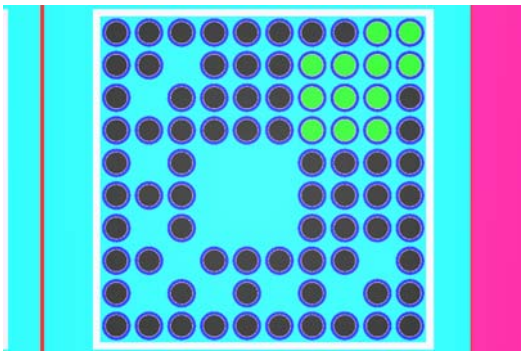

FANP 10x10 5.0 wt% ^{235}U, 10 Part Length Rods

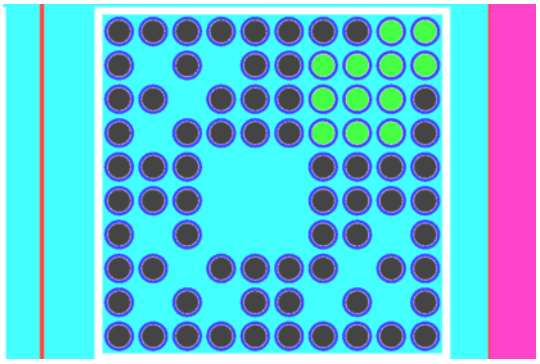

FANP 10x10 5.0 wt% ^{235}U, 12 Part Length Rods

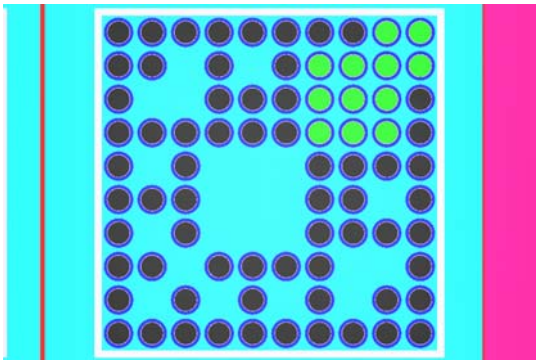

FANP 10x10 5.0 wt% ^{235}U, 14 Part Length Rods

Figure 6-33 FANP 10x10 Worst Case Fuel Parameters Model with Part Length Fuel Rods

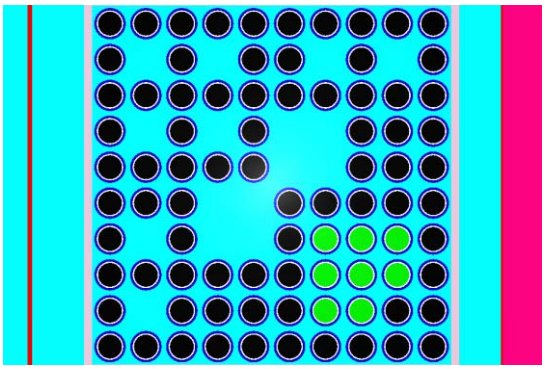

GNF 10x10 4.2 wt% ^{235}U, 8 Part Length Rods

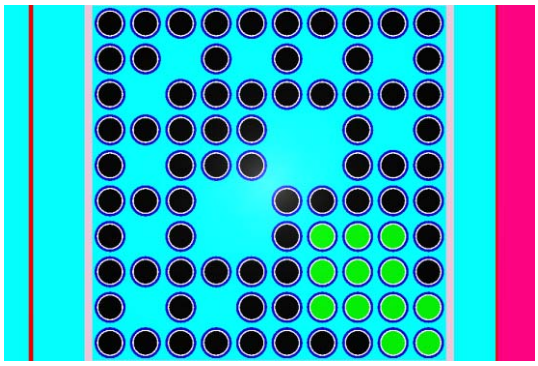

GNF 10x10 5.0 wt% ^{235}U, 10 Part Length Rods

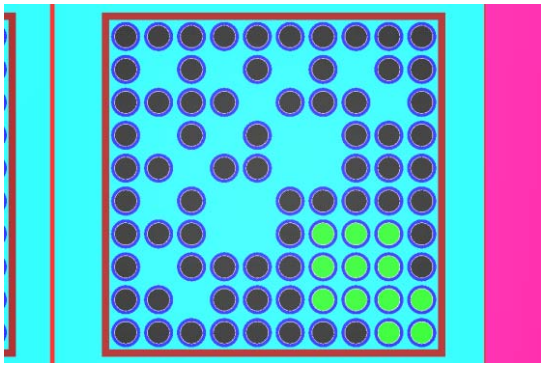

GNF 10x10 5.0 wt% ^{235}U, 12 Part Length Rods

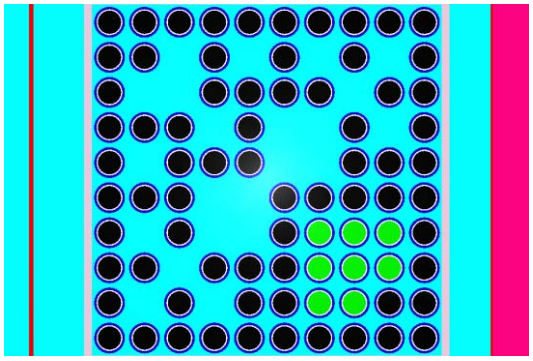

GNF 10x10 4.2 wt% ^{235}U, 14Part Length Rods

Figure 6-34 GNF 10x10 Worst Case Fuel Parameters Model with Part Length Fuel Rods

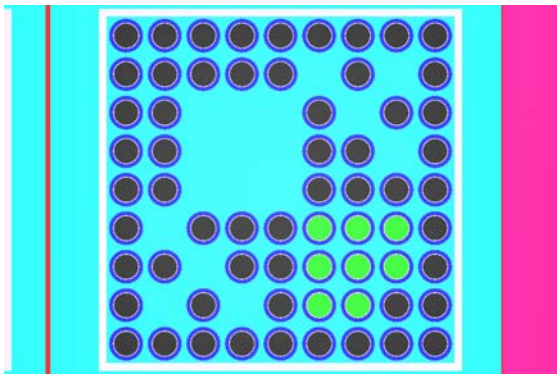

FANP 9x9 4.7 wt% ^{235}U, 8 Part Length Rods

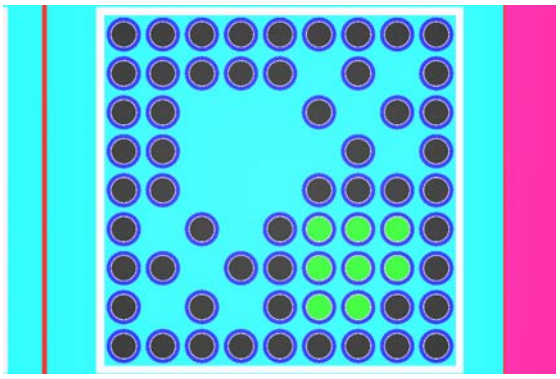

FANP 9x9 4.7 wt% ^{235}U, 10 Part Length Rods

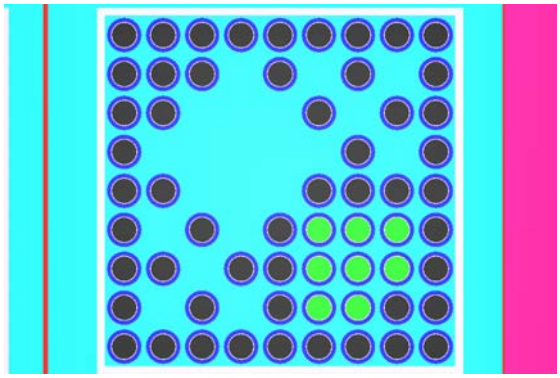

FANP 9x9 4.7 wt% ^{235}U, 12 Part Length Rods

Figure 6-35 FANP 9x9 Worst Case Fuel Parameters Model with Part Length Fuel Rods

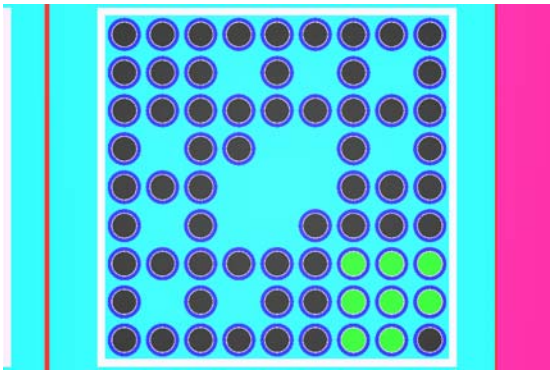

GNF 9x9 4.8 wt% ^{235}U, 8 Part Length Rods

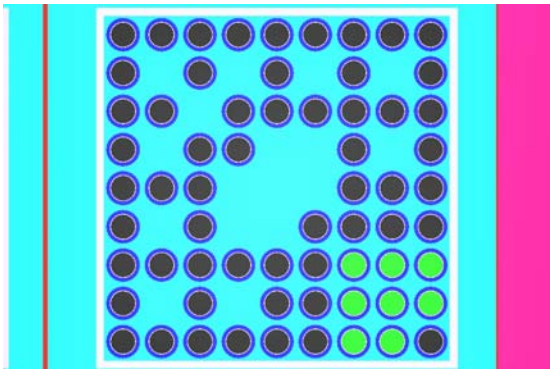

GNF 9x9 4.8 wt% ^{235}U, 10 Part Length Rods

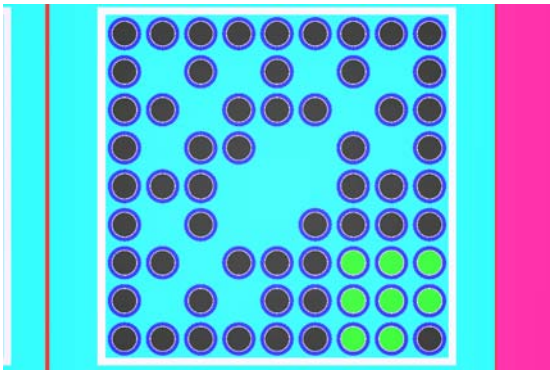

GNF 9x9 4.8 wt% ^{235}U, 12 Part Length Rods

Figure 6-36 GNF 9x9 Worst Case Fuel Parameters Model with Part Length Fuel Rods

6.3.4.10 Moderator Density Study (2N=448)

The worst case design from Table 6-18 RAJ-II Array HAC Part Length Fuel Rod Calculations is used to conduct a moderator density sensitivity analysis. The GNF 10x10 fuel bundle is chosen for the study since it resulted in the highest reactivity in Table 6-18. Previous calculations demonstrated the worst case condition for maximum reactivity is a configuration in which there is no moderator between the RAJ-II shipping packages. The moderator density study is conducted by varying the moderator density inside the inner container fuel compartment. The outer region of the inner container is filled with the Alumina Silicate thermal insulating material. The results of the moderator density study, Table 6-31, are shown in Figure 6-37. As shown in Figure 6-37, all cases peak at full moderator density. Therefore, a moderator density of 1.0 g/cm^3 is chosen as the worst case moderator condition for the RAJ-II inner container fuel compartment.

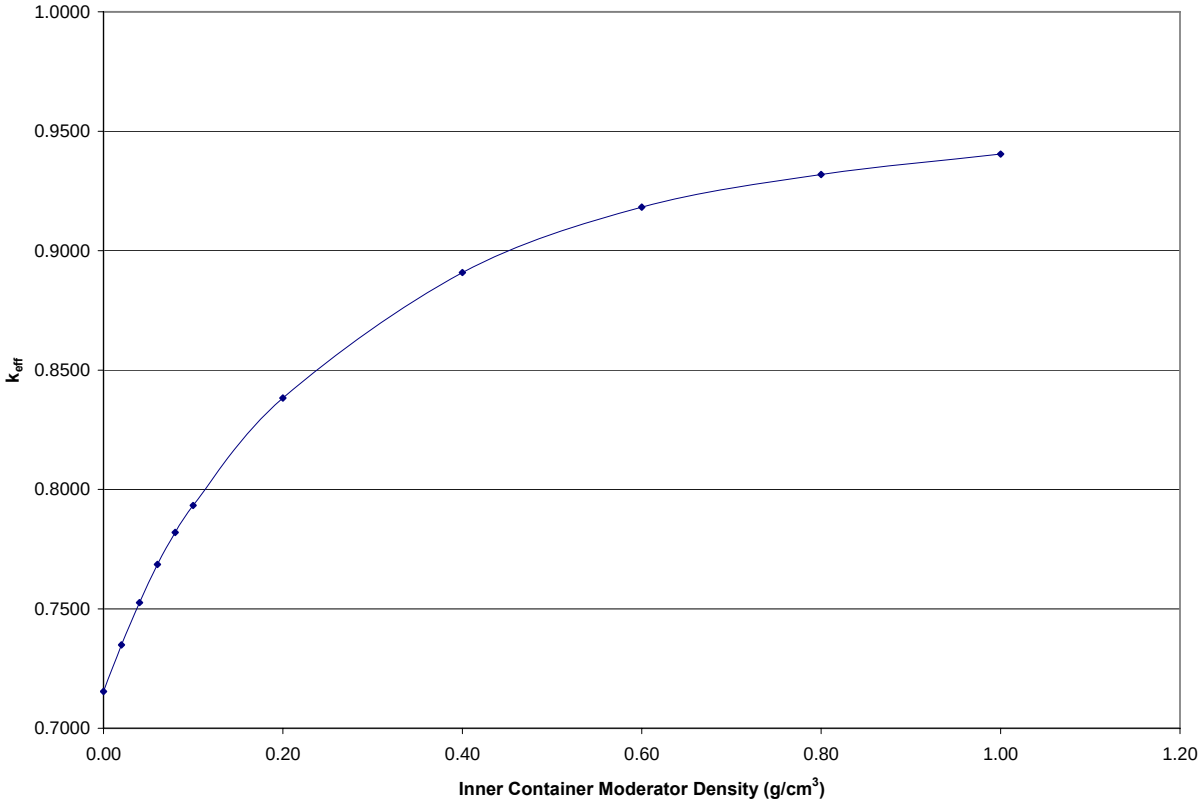

Figure 6-37 Moderator Density Sensitivity Study for the RAJ-II HAC Worst Case Parameter Fuel Design

6.3.4.11 Material Distribution Reactivity Study (2N=448, 2N=100)

A study is performed to determine the worst packing material distribution within the RAJ-II inner container. The material normally present around the inner container fuel compartment is a thermal insulator consisting of Alumina Silicate. The material normally lining the inner container

fuel compartment is a polyethylene foam material which has a density in the range 0.05 – 0.075 g/cm^3.

The first part of the material distribution study investigates replacing the Alumina Silicate alternately with full density water and void while the inner container fuel compartment is filled with full density water. The GNF 10x10 fuel bundle is chosen for the study since it resulted in the highest reactivity in Table 6-18. In addition, the worst case RAJ-II model is used in a 14x2x16 array (2N=448). The results are shown in Table 6-19. The first three cases in Table 6-19 show the most reactive condition is achieved with the Alumina Silicate thermal insulator in place. Therefore, the Alumina Silicate thermal insulator will remain a part of the worst case RAJ-II model.

The second part of the material distribution study investigates placing the polyethylene foam material in its proper location within the RAJ-II fuel assembly compartment. Until this point, the polyethylene foam was assumed to burn away in the fire that also melted the polyethylene spacers. It should be noted that it is extremely unlikely that this configuration would exist post thermal excursion. The polyethylene foam would be as susceptible to the fire as the polyethylene spacers. However, the incomplete foam burn is considered in this study for conservatism. The GNF 10x10 fuel bundle is chosen for the study since it resulted in the highest reactivity in Table 6-18. In addition, the worst case RAJ-II model is used in a 14x2x16 array (2N=448). The results are shown in Table 6-19. As shown in Table 6-19, the most reactive condition is achieved with the full thickness of ethafoam in place. Since the k_{eff} values exceed the 0.94254 USL with the polyethylene foam in place, the package array size is reduced to 10x1x10 (2N=100) to meet the acceptance criterion (last row in Table 6-19). The full thickness of ethafoam will be maintained for the remaining RAJ-II calculations since that configuration resulted in the highest k_{eff} value.

Table 6-19 RAJ-II Inner Container Thermal Insulator Region and Polyethylene Foam Material Study

Fuel Type	Array Size	Inner Container Foam Space	Insulator Space Fill	k_{eff}	σ	$k_{eff} + 2\sigma$
GNF 10x10	14x2x16 (2N=448)	Water	Thermal Ins.	0.9404	0.0007	0.9418
GNF 10x10	14x2x16 (2N=448)	Water	Water	0.7938	0.0009	0.7956
GNF 10x10	14x2x16 (2N=448)	Water	None	0.9362	0.0008	0.9378
GNF 10x10	14x2x16 (2N=448)	¼ Foam Thickness-Water	Thermal Ins.	0.9618	0.0009	0.9636
GNF 10x10	14x2x16 (2N=448)	½ Foam Thickness-Water	Thermal Ins.	0.9808	0.0009	0.9826
GNF 10x10	14x2x16 (2N=448)	5/8 Foam Thickness-Water	Thermal Ins.	0.9902	0.0008	0.9918

Fuel Type	Array Size	Inner Container Foam Space	Insulator Space Fill	k_{eff}	σ	k_{eff} + 2σ
GNF 10x10	14x2x16 (2N=448)	¾ Foam Thickness-Water	Thermal Ins.	0.9943	0.0008	0.9959
GNF 10x10	14x2x16 (2N=448)	7/8 Foam Thickness-Water	Thermal Ins.	0.9965	0.0008	0.9981
GNF 10x10	14x2x16 (2N=448)	Full Foam Thickness	Thermal Ins.	0.9971	0.0010	**0.9991**
GNF 10x10	10x1x10 (2N=100)	Full Foam Thickness	Thermal Ins.	0.9378	0.0009	0.9396

6.3.4.12 Inner Container Partial Flooding Study (2N=100)

Calculations are run in which the fuel bundle rows are partially filled within the RAJ-II inner fuel compartment as shown in Figure 6-39. The GNF 10x10 fuel bundle is chosen for the analysis since it produced the highest reactivity in Figure 6-37. The RAJ-II HAC model from the polyethylene foam study is used with an array size of 10x1x10 (2N=100). The results are shown in Table 6-20. As shown in Table 6-20, the most reactive condition exists when water fully covers each fuel bundle. Therefore, the inner container fuel compartment will be fully flooded with water in the worst case RAJ-II model.

Table 6-20 RAJ-II Inner Container Partially Filled with Moderator

Fuel Type	Fuel Rows Filled	Moderator Density (g/cm^3)	k_{eff}	σ	k_{eff} + 2σ
GNF 10x10	1	1.00	0.6643	0.0007	0.6657
GNF 10x10	3	1.00	0.7678	0.0009	0.7696
GNF 10x10	5	1.00	0.8653	0.0008	0.8669
GNF 10x10	7	1.00	0.9212	0.0008	0.9228
GNF 10x10	9	1.00	0.9355	0.0009	0.9373
GNF 10x10	10	1.00	0.9378	0.0009	**0.9396**

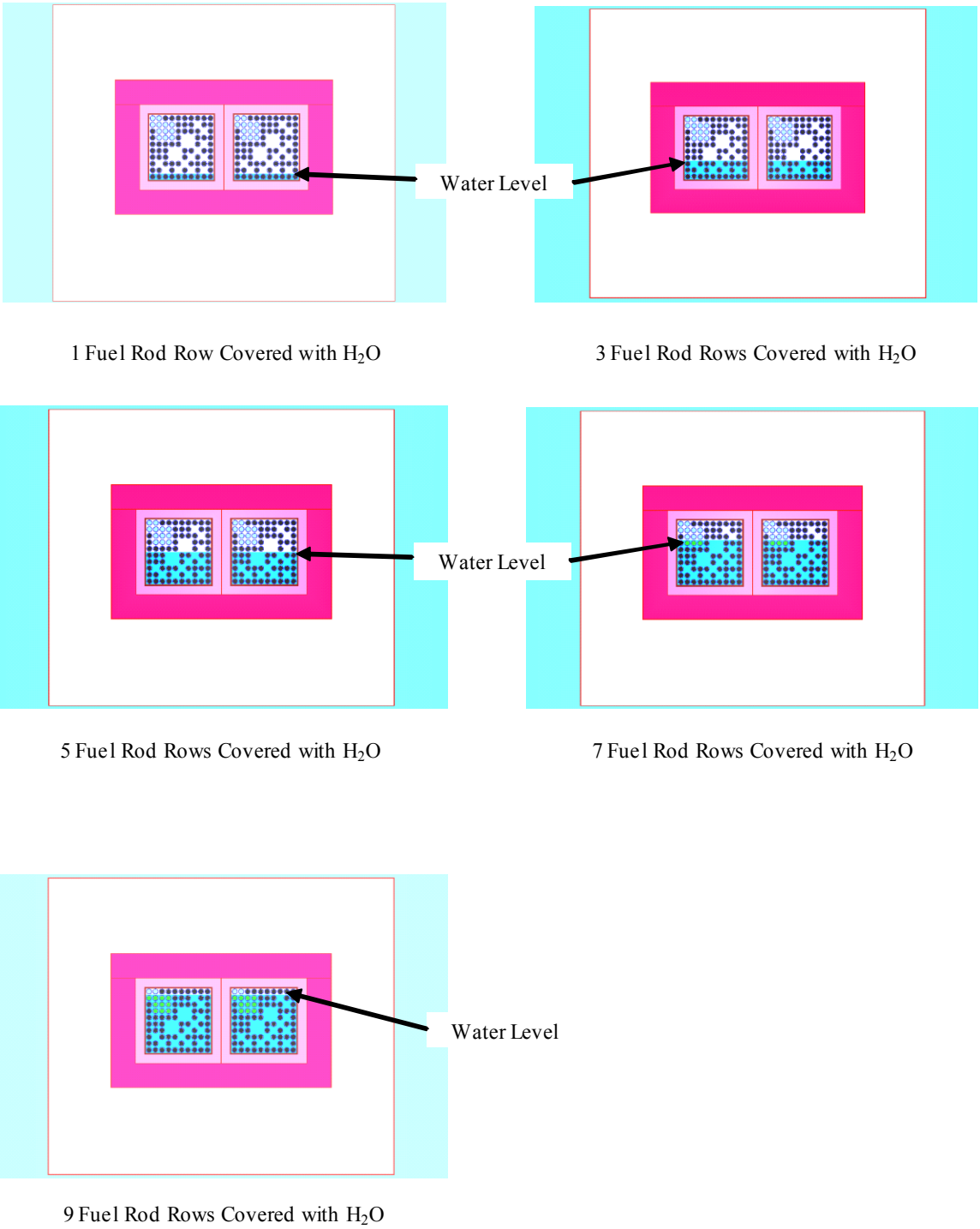

Figure 6-38 RAJ-II Inner Container Fuel Compartment Flooding Cases

6.3.4.13 RAJ-II Container Spacing Study (2N=100)

Calculations performed previously assume the RAJ-II shipping containers are resting next to one another with no spacing between them. A container pitch sensitivity study is conducted to determine if reactivity increases as containers are moved away from one another. The HAC model used in the inner container partial flooding study is used for the pitch sensitivity study with an array size of 10x1x10 (2N=100). The GNF 10x10 fuel assemblies with an average lattice enrichment of 5.0 wt% U-235, 12 gadolinia-urania fuel rods enriched to 2.0 wt % gadolinia, and 12 part length fuel rods is used. The worst case fuel parameters listed in Table 6-18 for the GNF 10x10 fuel design are utilized. The edge-to-edge separation is increased from 0 to 10 cm and the reactivity impact is observed. The results shown in Table 6-21 show a decrease in reactivity with increased spacing between containers. Therefore, the most reactive container configuration occurs when there is minimum spacing between containers.

Table 6-21 RAJ-II Array Spacing Sensitivity Study

Assembly Type	Interspersed Moderator Density (g/cm^3)	Container Pitch (cm)	Pitch (cm)	Pellet Diameter (cm)	Clad ID (cm)	Clad OD (cm)	k_{eff}	σ	$k_{eff} + 2\sigma$
GNF 10x10	0.0	71.926	1.350	0.895	0.9338	1.01	0.9378	0.0009	**0.9396**
GNF 10x10	0.0	74.426	1.350	0.895	0.9338	1.01	0.9259	0.0009	0.9277
GNF 10x10	0.0	76.926	1.350	0.895	0.9338	1.01	0.9122	0.0008	0.9138
GNF 10x10	0.0	81.926	1.350	0.895	0.9338	1.01	0.8865	0.0008	0.8881

6.4 SINGLE PACKAGE EVALUATION

Based on the sensitivity studies performed in this section, the single package and package array normal transport condition and HAC calculations are performed using the GNF 10x10 at an average lattice enrichment of 5.0 wt % U-235, twelve 2.0 wt% gadolinia fuel rods, and 12 part length fuel rods.

6.4.1 Configuration

The single package model described in Section 6.3.1.1 is used to demonstrate criticality safety of the RAJ-II shipping container using the worst case fuel design. The GNF 10x10 at an average lattice enrichment of 5.0 wt % U-235, twelve 2.0 wt% gadolinia fuel rods, and 12 part length fuel rods is used for the NTC and HAC evaluations. A moderator density study is conducted under both hypothetical accident and normal conditions. In the HAC study, the water density in the inner package is varied while the void in the outer container is maintained. For the normal conditions of transport, the moderator density is uniformly varied.

6.4.2 Single Package Results

The results for the single package normal conditions of transport evaluation are displayed in Figure 6-39. The results for the single package HAC evaluation are shown in Figure 6-40. The results in the figures indicate reactivity for the single package increases with increasing moderator density. The highest k_{eff} is achieved for both cases at full density moderation in the inner container. The polyethylene foam remains in place for the NTC single package configuration, but the polyethylene foam is removed from the HAC single package configuration. Removing the polyethylene foam in the HAC single package model, decreases neutron leakage which increases reactivity for a single container. In addition, full density moderation is included in the outer container for the single package NTC configuration. In both cases, the k_{eff} remains far below the USL of 0.94254. The maximum $k_{eff} + 2\sigma$ for the single package normal conditions of transport case is 0.6689 (Table 6-32), and the maximum $k_{eff} + 2\sigma$ for the single package HAC case is 0.6951 (Table 6-33). Therefore, criticality safety is established for the single package RAJ-II container.

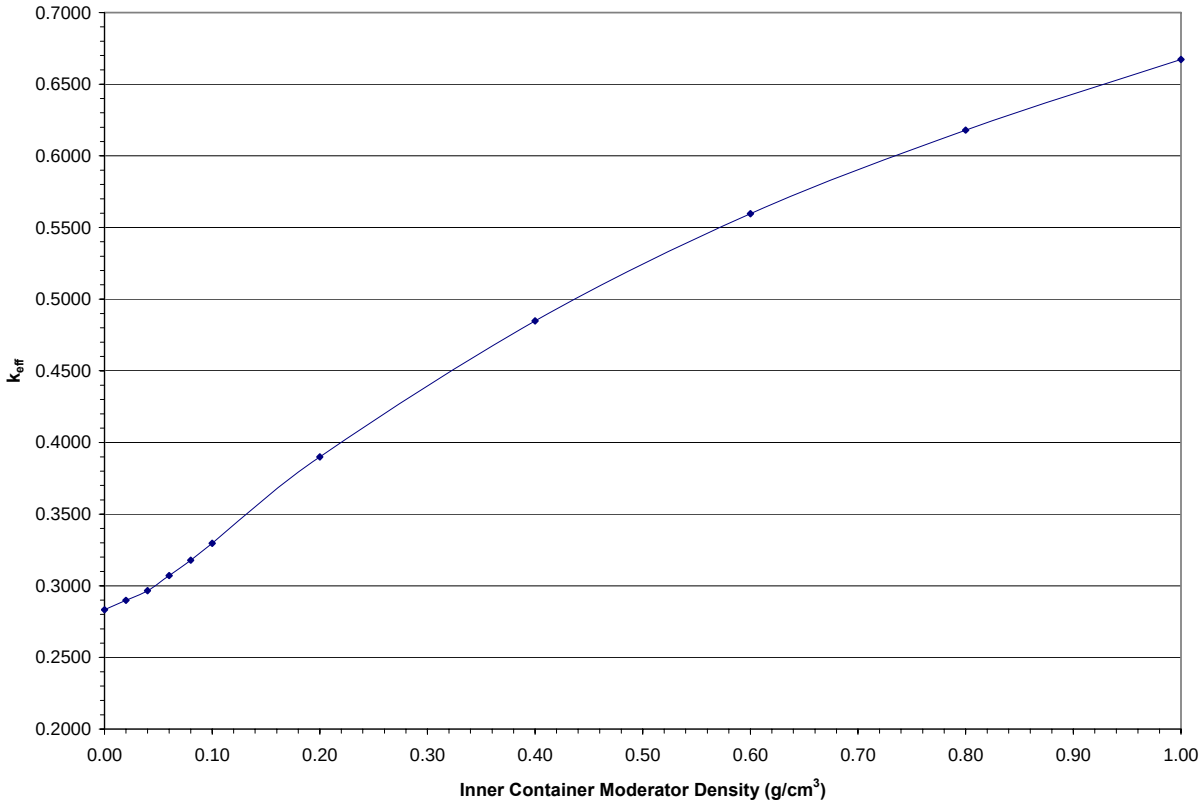

Figure 6-39 RAJ-II Single Package Normal Conditions of Transport Results

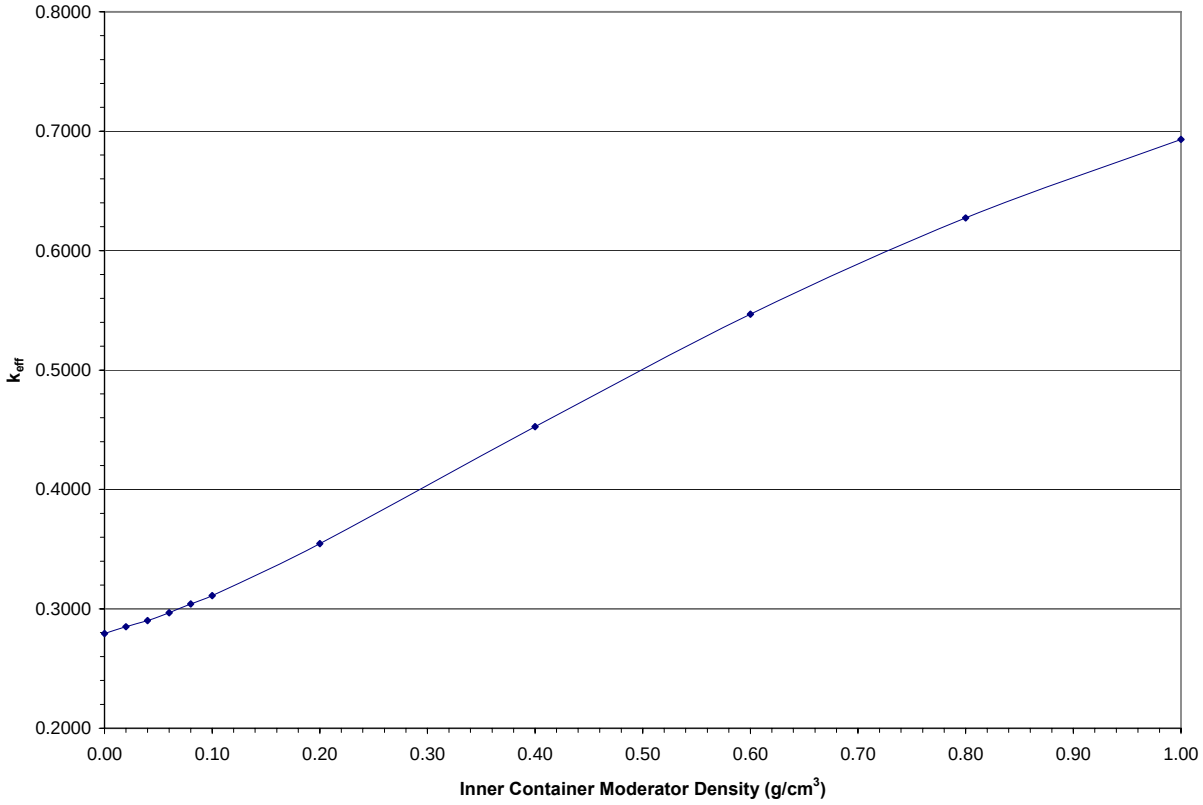

Figure 6-40 RAJ-II Single Package HAC Results

6.5 EVALUATION OF PACKAGE ARRAYS UNDER NORMAL CONDITIONS OF TRANSPORT

6.5.1 Configuration

The package array normal condition model described in Section 6.3.1.2.1 is used to demonstrate criticality safety of the RAJ-II shipping container using the GNF 10x10 worst case fuel design at an average lattice enrichment of 5.0 wt % U-235, twelve 2.0 wt% gadolinia fuel rods, and 12 part length fuel rods. The calculation using the normal conditions of transport model involves a moderator density sensitivity study. In the model, the moderator density is uniformly varied and the system reactivity is observed.

6.5.2 Package Array NCT Results

The results of the package array normal condition model calculations are shown in Figure 6-41. The reactivity peaks with no moderator present . A decreasing trend continues until the moderator density reaches 0.4 g/cm^3 at which point reactivity increases almost linearly to full water density. The maximum $k_{eff} + 2\sigma$ obtained is 0.8535 (Table 6-34) which is below the USL

of 0.94254. Therefore, criticality safety of the RAJ-II shipping container is demonstrated under normal conditions of transport.

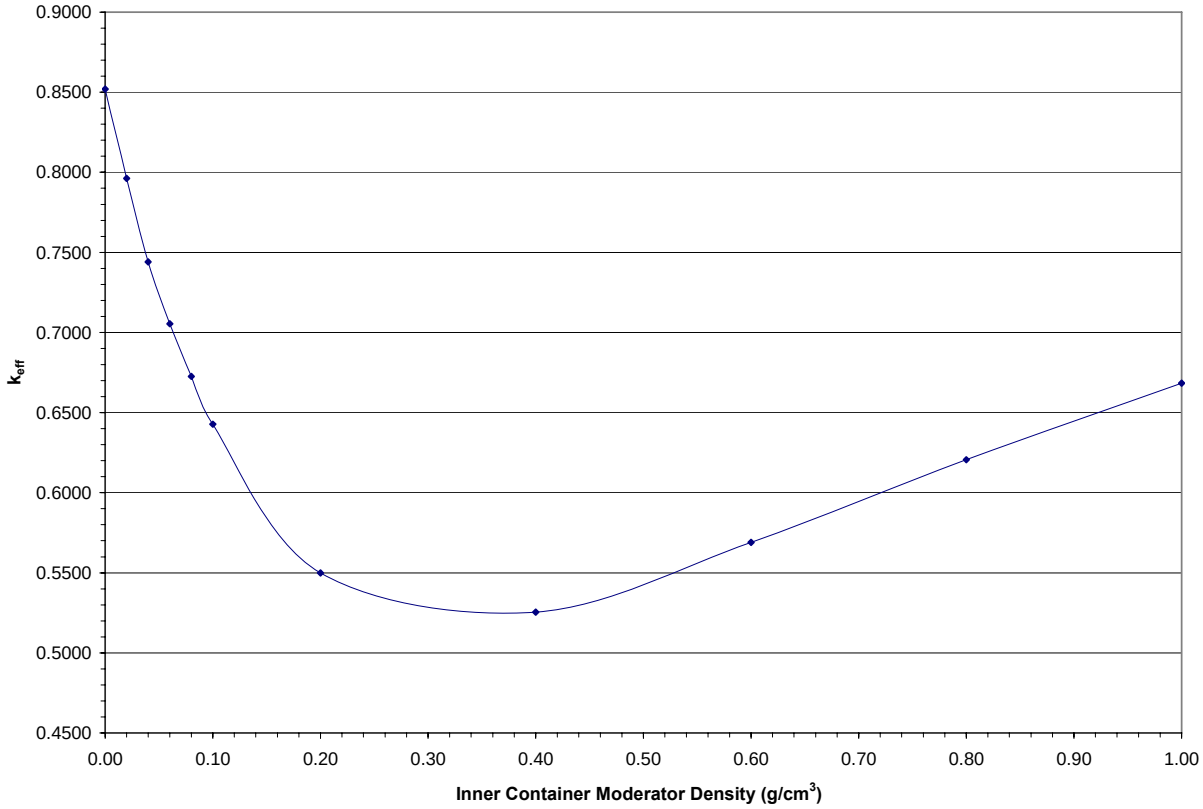

Figure 6-41 RAJ-II Package Array Under Normal Conditions of Transport Results

6.6 PACKAGE ARRAYS UNDER HYPOTHETICAL ACCIDENT CONDITIONS

6.6.1 Configuration

The package array hypothetical accident condition model described in Section 6.3.1.2.2 is used to demonstrate criticality safety of a 10x1x10 array (2N=100) of RAJ-II shipping containers using the GNF 10x10 worst case fuel design at an average lattice enrichment of 5.0 wt % U-235, twelve 2.0 wt% gadolinia fuel rods, and 12 part length fuel rods. The calculation using the HAC model involves a moderator density sensitivity study. In the study, no moderator is present in the outer container while the moderator density inside the inner container is varied. The polyethylene foam inside the inner container fuel compartment is modeled because previous calculations demonstrated this configuration to be the most reactive.

6.6.2 Package Array HAC Results

The results of the package array (2N=10x1x10=100 array) HAC model calculations are shown in Figure 6-42. The system reactivity begins at its lowest value and increases with increasing interspersed moderator density. This trend highlights the neutronics of the problem. Initially, no moderator, other than the polyethylene surrounding the fuel rods, is present to thermalize neutrons that enter the inner container. As the inner container moderator density increases, higher energy neutrons pass into adjacent containers and thermalize in the vicinity of the fuel creating a more reactive situation. The maximum $k_{eff} + 2\sigma$ for the package array HAC case is 0.9396 (Table 6-35) which is below the USL of 0.94254. Therefore, criticality safety of the RAJ-II shipping container is demonstrated for the package array under hypothetical accident conditions.

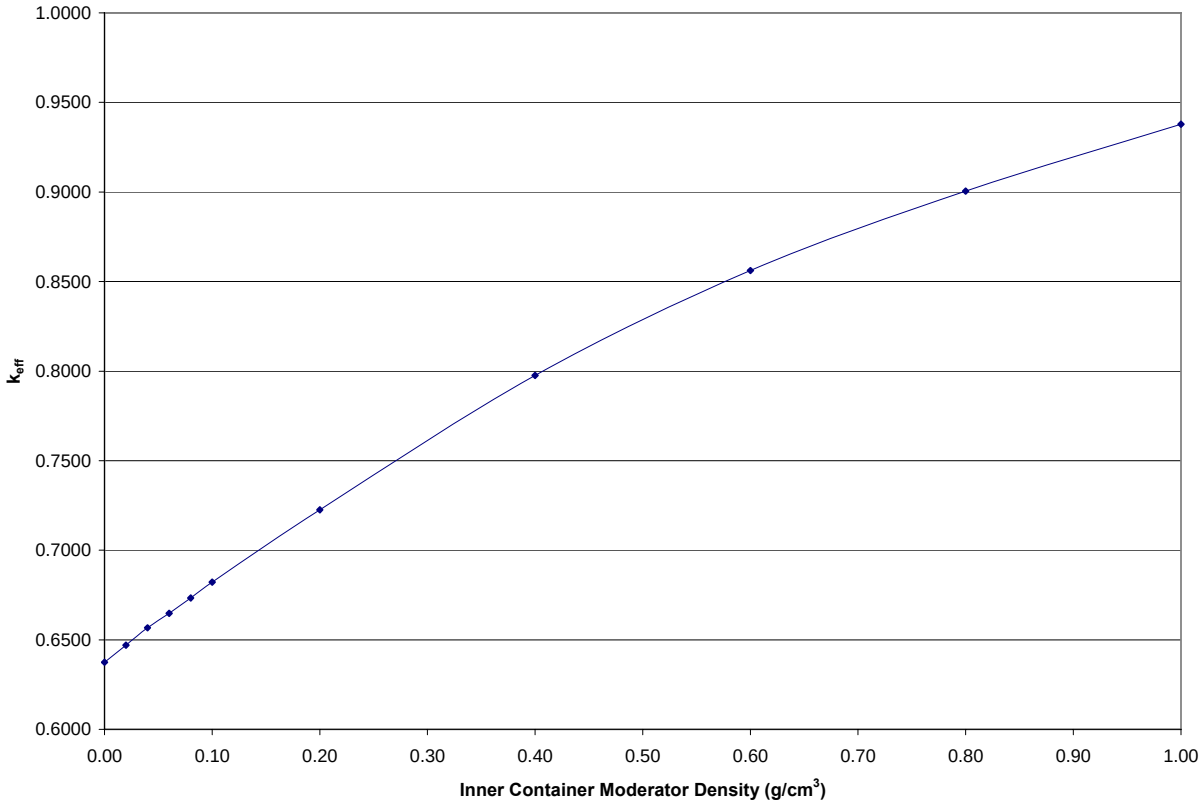

Figure 6-42 RAJ-II Package Array Hypothetical Accident Condition Results

6.6.2.1 Pu-239 Effect on Reactivity for the RAJ-II Package Array Hypothetical Accident Condition

Because the fuel scheduled for transport in the RAJ-II could have a small Pu-239 content, the effect on the RAJ-II Package HAC reactivity is investigated. The maximum plutonium concentration (3.04×10^{-9} gPu-239/gU) listed in Table 1-3 of the SAR is added to the worst case package array HAC model (10x1x10 array), determined in the previous sections, and the k_{eff} is calculated. The results showed no statistically significant difference between the cases with and without plutonium. The $k_{eff} \pm 2\sigma$ for the worst case with plutonium is 0.9406. The $k_{eff} + 2\sigma$ for the worst case without plutonium, calculated in Section 6.6.2, is 0.9396. Both results remain below the USL of 0.94254. Therefore, the plutonium is justifiably neglected in the RAJ-II evaluation.

6.7 Fuel Rod Transport in the RAJ-II

Studies are conducted to allow transport of UO_2 fuel rods in the RAJ-II container. Several configurations are investigated including: loose fuel rods, fuel rods bundled together, and fuel rods contained in 5-inch stainless steel pipe/protective case. The model uses the 10x10, 9x9, or 8x8 worst case fuel rod designs developed in Section 6.3.4. A 6-mil layer of polyethylene encircles each fuel rod in the model to bound protective packing material that may be used for fuel rod transport.

6.7.1 Loose Fuel Rod Study

The package array model under hypothetical accident conditions is used for fuel rod calculations in the RAJ-II, since it was demonstrated to be more reactive than the normal conditions of transport, package array model. The worst case fuel rods are arranged in a square pitch array inside each RAJ-II transport compartment. Scoping studies indicated little difference between the square and triangular pitch array, therefore the square pitch array is chosen for convenience. The inner container is filled with full density water and the outer container has no water, which facilitates leakage of neutrons into neighboring containers. The fuel rod pitch is varied, and the results are illustrated with curves. The curves are shown Figure 6-43 Fuel Rod Pitch Sensitivity Study and corresponding calculational data listed in Table 6-22 Fuel Rod Pitch Sensitivity Study Results. The results demonstrate that a fully loaded inner compartment in which the rods are all in contact with each other is a supercritical configuration. As a result, a minimum number of fuel rods to ensure subcriticality cannot be established for the RAJ-II shipping container. A maximum fuel rod quantity to ensure subcriticality can be established for the loose configuration. For all three fuel designs, a maximum of 25 fuel rods may be safely transported in each RAJ- II fuel assembly compartment. The 8x8 rod design is limiting as shown in Figure 6-43 and Table 6-22 Fuel Rod Pitch Sensitivity Study Results.

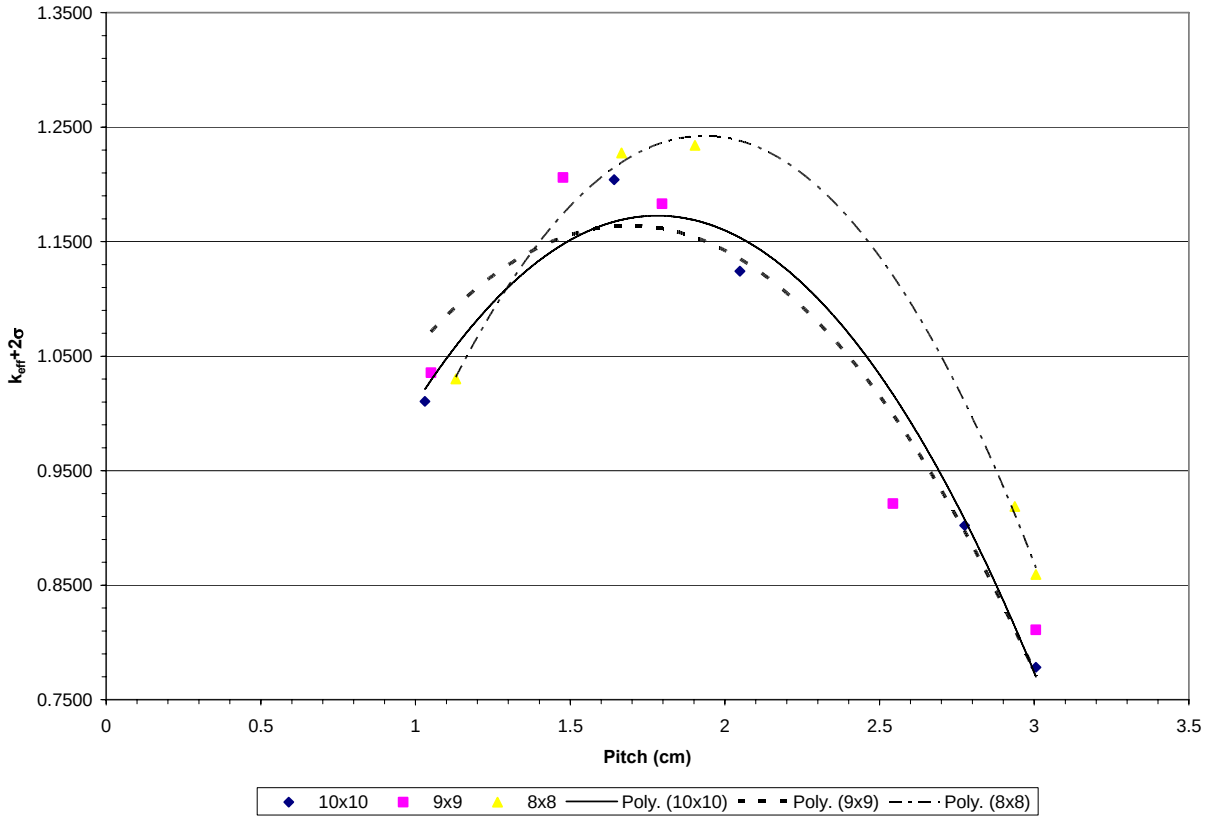

Figure 6-43 Fuel Rod Pitch Sensitivity Study

Table 6-22 Fuel Rod Pitch Sensitivity Study Results

Fuel Rod Type	Fuel Rod Pitch (cm)	Fuel Rod Number	Fuel Pellet OD (cm)	Clad Inner Diameter (cm)	Clad Outer Diameter (cm)	k_{eff}	σ	k_{eff} + 2σ
10x10	1.0305	289	0.9	1.000	1.000	1.0092	0.0007	1.0106
10x10	1.6416	100	0.9	1.000	1.000	1.2024	0.0009	1.2042
10x10	2.0484	64	0.9	1.000	1.000	1.1224	0.0009	1.1242
10x10	2.7754	34	0.9	1.000	1.000	0.9005	0.0008	0.9021
10x10	3.0056	25	0.9	1.000	1.000	0.7769	0.0007	0.7783
9x9	1.0505	256	0.9600	1.0200	1.0200	1.0341	0.0007	1.0355
9x9	1.4770	121	0.9600	1.0200	1.0200	1.2045	0.0008	1.2061
9x9	1.7972	81	0.9600	1.0200	1.0200	1.1816	0.0008	1.1832
9x9	2.5432	34	0.9600	1.0200	1.0200	0.9196	0.0008	0.9212
9x9	3.0056	25	0.9600	1.0200	1.0200	0.8096	0.0007	0.8110
8x8	1.1305	225	1.05	1.1000	1.1000	1.0288	0.0007	1.0302
8x8	1.6662	100	1.05	1.1000	1.1000	1.2259	0.0008	1.2275
8x8	1.9035	81	1.05	1.1000	1.1000	1.2328	0.0007	1.2342
8x8	2.9370	30	1.05	1.1000	1.1000	0.9172	0.0008	0.9188
8x8	3.0056	25	1.05	1.1000	1.1000	0.8577	0.0008	0.8593

The results in Table 6-22 Fuel Rod Pitch Sensitivity Study Results are based on calculations performed with full water density inside the inner container. It appears the maximum fuel rod quantity allowable for the 10x10 and 9x9 fuel rods should be 34, while that for the 8x8 fuel rods should be 30. However, the rod configurations at full moderator densities represent an overmoderated condition in which reactivity peaks at a reduced moderator density. Therefore, calculations are performed with 25 fuel rods in each transport compartment for each fuel rod type, and the moderator density inside the inner container is varied from 0.4 g/cm^3 to 1.00 g/cm^3 to investigate the possibility that reactivity peaks at a lower moderator density. The results of these calculations are shown in Table 6-23. The peak reactivity for all the fuel rod types occurs at a moderator density of 0.6 g/cm^3 and are all below the USL of 0.94254. Therefore, criticality safety for loose fuel rod transport with a maximum of 25 rods in each transport compartment is demonstrated.

Table 6-23 Fuel Rod Maximum Quantity at Reduced Moderator Densities

Fuel Rod Type	Fuel Rod Pitch (cm)	Fuel Rod Number	Inner Container Moderator Density (g/cm^3)	Fuel Pellet OD (cm)	Clad Inner Diameter (cm)	Clad Outer Diameter (cm)	k_{eff}	σ	$k_{eff} + 2\sigma$
10x10	3.0056	25	0.40	0.9	1.000	1.000	0.7875	0.0009	0.7893
10x10	3.0056	25	0.60	0.9	1.000	1.000	0.8113	0.0008	**0.8129**
10x10	3.0056	25	0.80	0.9	1.000	1.000	0.8012	0.0007	0.8026
10x10	3.0056	25	1.00	0.9	1.000	1.000	0.7769	0.0007	0.7783
9x9	3.0056	25	0.40	0.9600	1.0200	1.0200	0.8128	0.0008	0.8144
9x9	3.0056	25	0.60	0.9600	1.0200	1.0200	0.8404	0.0008	**0.8420**
9x9	3.0056	25	0.80	0.9600	1.0200	1.0200	0.8321	0.0008	0.8337
9x9	3.0056	25	1.00	0.9600	1.0200	1.0200	0.8096	0.0007	0.8110
8x8	3.0056	25	0.40	1.05	1.1000	1.1000	0.8529	0.0008	0.8545
8x8	3.0056	25	0.60	1.05	1.1000	1.1000	0.8832	0.0008	**0.8848**
8x8	3.0056	25	0.80	1.05	1.1000	1.1000	0.8799	0.0009	0.8817
8x8	3.0056	25	1.00	1.05	1.1000	1.1000	0.8577	0.0008	0.8593

a. Limiting case(s) shown in bold

6.7.2 Fuel Rods Bundled Together

Based on the results in the previous calculation, there is no advantage to bundling fuel rods together since close packed rods do not guarantee subcriticality. Besides, the straps holding the fuel rods together in the bundle may fail during an accident, and the rods could move about the transport compartment without restraint. Therefore, the maximum number of fuel rods allowable in each RAJ-II fuel compartment when fuel rods are transported in bundles is 25 for all types.

6.7.3 Fuel Rods Transported in 5-Inch Stainless Steel Pipe

A fuel rod pitch sensitivity study is conducted for the transport of fuel rods inside 5-inch stainless steel pipe, residing in the RAJ-II fuel compartment. The package array model under hypothetical accident conditions is used for fuel rod calculations in the RAJ-II container, since it was demonstrated to be more reactive than the normal conditions of transport, package array model. The GNF 10x10, the GNF 9x9, and the GNF 8x8, the UC and PWR worst case fuel rod designs are used for the study. Since the 5-inch stainless steel pipe presents a more difficult volume to accommodate rods in a square pitch, a triangular pitch array is used for the rod configuration. The pipe's stainless steel wall is also neglected for conservatism. The fuel rod configuration inside the pipe is shown in Figure 6-44 for the GNF 8x8 fuel rods. The volume inside the pipe is filled with water at a density sufficient for optimum moderation. The inner fuel compartment volume outside the pipe is modeled with no material present to maximize neutron interaction among packages in the array.

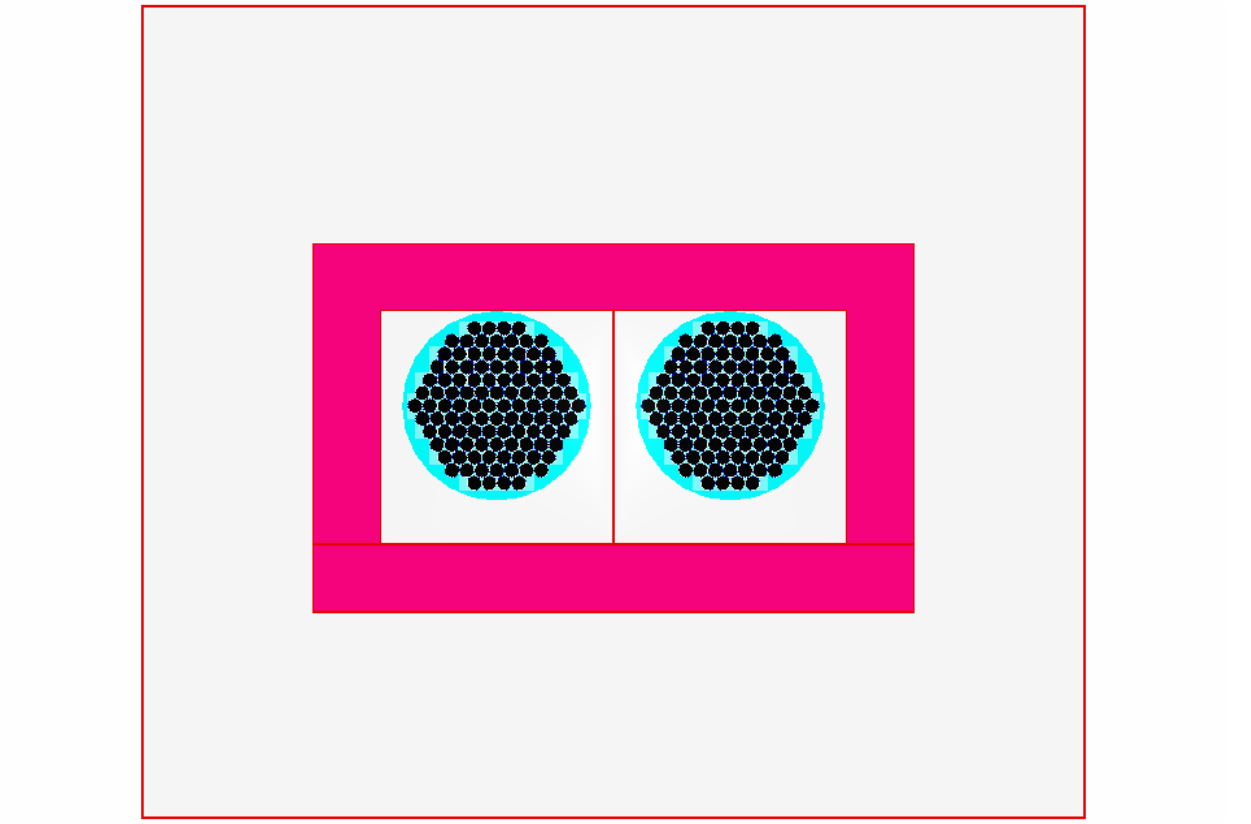

Figure 6-44 RAJ-II with Fuel Rods in 5-Inch Stainless Steel Pipes for Transport

The results for fuel rod transport in a SS pipe within the RAJ-II container for the all rod designs are displayed in Figure 6-45. As shown in Figure 6-45, optimum peaks are formed above the USL of 0.94254. Therefore, the stainless steel pipe may be used to ship a limited number of fuel rods. The maximum number of 10x10 fuel rods that may be transported in the stainless steel pipe is 30. The maximum number of 9x9 fuel rods that may be transported in the stainless steel pipe is 26. The maximum number of 8x8 fuel rods that may be transported in the stainless steel pipe is 22. The $k_{eff} + 2\sigma$ values (Table 6-36) for all fuel rod types with the appropriate fuel rod quantity are below the USL of 0.94254. Therefore, criticality safety is demonstrated for fuel rod transport inside a SS pipe within the RAJ-II container.

The optimum peak for the 10x10 fuel rods is greater than that for the 9x9 or 8x8 fuel rods in the SS pipe. Since the reactivity peak for the 8x8 fuel rod in the loose rod study is greater than that for the 10x10 fuel rods in the SS pipe, it is chosen as the bounding fuel assembly type.

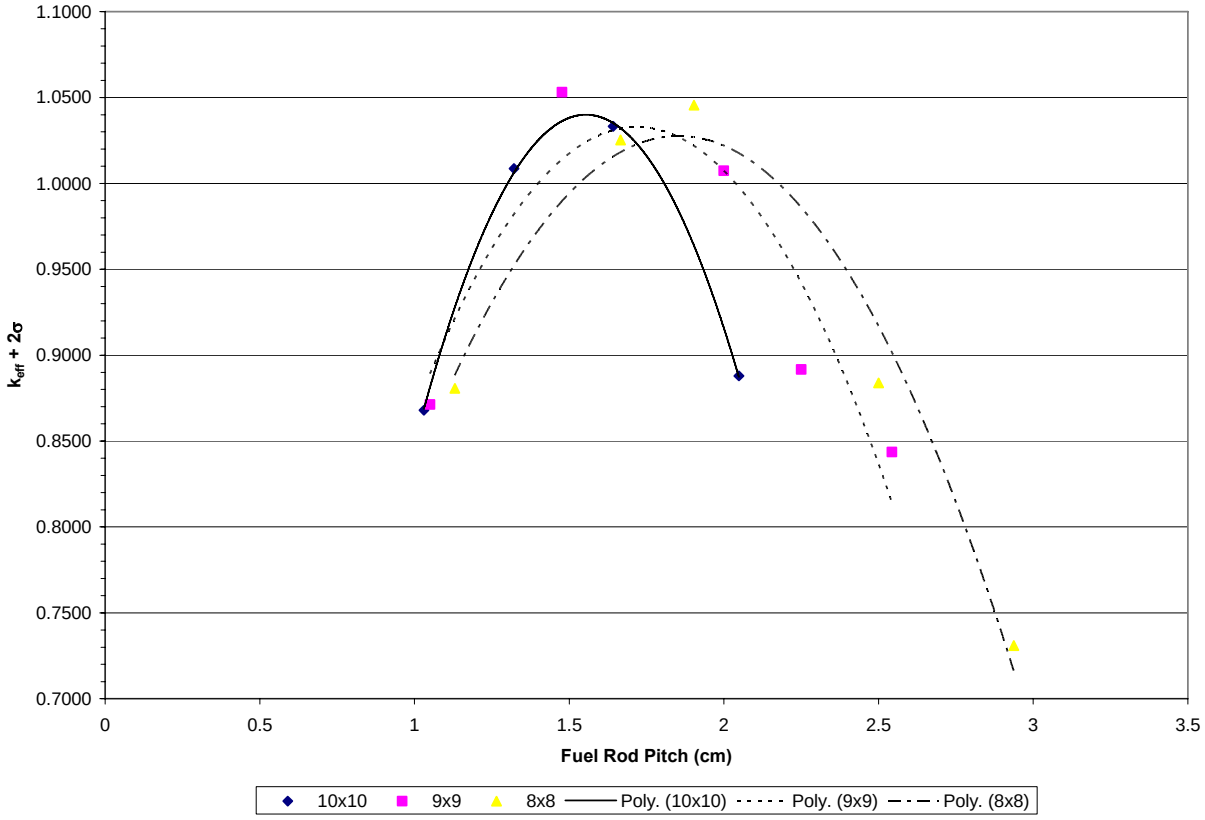

Figure 6-45 RAJ-II Fuel Rod Transport in Stainless Steel Pipe

This addendum to the RAJ-II SAR includes analysis of Uranium-Carbide and UO2 PWR rods inside the 5" stainless steel pipe. Loose rods in the product container are evaluated in this analysis ACEL's CANDU Uranium-Carbide (UC) or generic Uranium-Dioxide (UO_2) fuel rods with a maximum U-235 (pellet) enrichment of 5.0%. The analysis is also applicable to UC or UO_2 fuel rods with GdO_2 or boron, provided that the maximum enrichment and dimensional limits are met since the presence of GdO_2 or boron in the fuel rods will result in a reduction in the applicable neutron multiplication factors. The same applies to fuel rods clad with stainless steel since stainless steel (with the same or greater clad thickness) is a better neutron absorber than zircaloy.

Three different fuel rods have been considered in this analysis, as designated by the labels "CANDU-14", "CANDU-25" and "PWR". The CANDU-14 and CANDU-25 types are those corresponding to the fuel rods in typical CANDU 14 element and 25 element fuel bundle assemblies (Table 6-2). The PWR type is that corresponding to generic PWR fuel rods.

The optimum condition for interspersed water in 8x1x8 and 4x2x6 arrays of damaged containers has been determined as in the case for the infinite arrays of undamaged containers by scoping calculations independently varying the W/F ratios inside the product containers and the interspersed water outside. The results of the scoping calculations are that the optimum interspersed water is again the 0.0 case, presumably because the fuel region inside the Product Containers is already fully moderated by the water and plastic sleeving surrounding the fuel rods.

Based on the results of the horizontally infinite arrays of damaged packages, calculations have been made for the 8x1x8 arrays of damaged RAJ-II containers for most reactive water-to-fuel ratios inside the product containers without interspersed water outside the product containers. **Tables 6-24** and **6-25** show the results for three types of rods. The maximum $k_{eff} + 2\sigma$ for 8x1x8 arrays of RAJ-II containers is 0.9131 which occurs for loose CANDU-14 UC fuel rods at a W/F ratio of 2.68. As in the case for the horizontally infinite arrays of undamaged RAJ-II, this result also bounds the k_{eff} values of the CANDU-25 UC fuel rod and generic PWR UO_2 designs.

Table 6-24 Results for 8x1x8 Array of Containers with Loose Fuel Rods

Type of Rods	W/F Ratio	k_{eff}	σ	$k_{eff} + 2\sigma$
CANDU-14 (UC)	2.12	0.90794	0.00076	0.90946
CANDU-25 (UC)	2.68	0.91162	0.00074	**0.91310**
PWR (UO_2)	2.24	0.85480	0.00074	0.85628

Table 6-25 Results for 4x2x6 Array of Containers with Loose Fuel Rods

Type of Rods	W/F Ratio	k_{eff}	σ	$k_{eff} + 2\sigma$
CANDU-14 (UC)	2.12	0.82820	0.00073	0.82966
CANDU-25 (UC)	2.68	0.83361	0.00072	**0.83505**
PWR (UO_2)	2.24	0.77301	0.00075	0.77451

6.7.4 Fuel Rods Transported in Stainless Steel Protective Case

The fuel rod pitch sensitivity study conducted for the transport of fuel rods inside the 5-inch stainless steel pipe described in Section 6.7.3 bounds the transport of fuel rods in the protective case. The protective case cross-section is 89 mm (3.50 inches) by 80 mm (3.15 inches). Based on this small cross-sectional area, the total number of fuel rods that will fit in the protective case is less than the total for the 5-inch pipe. Based on the calculations for the stainless steel pipe, the maximum number of 10x10 fuel rods that may be transported in the protective case is 30, the maximum number of 9x9 fuel rods that may be transported in in the protective case is 26, the maximum number of 8x8 fuel rods that may be transported in in the protective case is 22.

6.7.5 Single Package Fuel Rod Transport Evaluation

6.7.5.1 Configuration

The single package model described in Section 6.3.1.1 is used to demonstrate criticality safety of the RAJ-II shipping container using the worst case fuel design. The single package is evaluated under both normal conditions of transport and hypothetical accident conditions. The evaluation consists of a moderator density sensitivity study. For the normal conditions of transport model, the moderator density is uniformly varied. In contrast, the moderator density is fixed in the inner container for the hypothetical accident condition model, and the moderator in the outer container is varied. Based on the results in Table 6-22, the GNF 8x8 worst case fuel rod design is used for the study since it produced the highest reactivity peak among all fuel rods considered.

6.7.5.2 Single Package Fuel Rod Transport Result

The results for the single package, loose fuel rod, normal conditions of transport evaluation are displayed in Figure 6-46. The results for the single package, loose fuel rod, HAC evaluation are shown in Figure 6-47. The results in the figures indicate reactivity for the single package increases with increasing moderator density. The highest k_{eff} is achieved for both cases at full density moderation. In both cases, the k_{eff} remains far below the USL of 0.94254. The maximum $k_{eff} + 2\sigma$ for the single package normal conditions of transport case is 0.6381 (Table 6-37), and the maximum $k_{eff} + 2\sigma$ for the single package HAC case is 0.6548 (Table 6-38). Therefore, criticality safety is established for the single package RAJ-II container transporting up to 25 loose fuel rods.

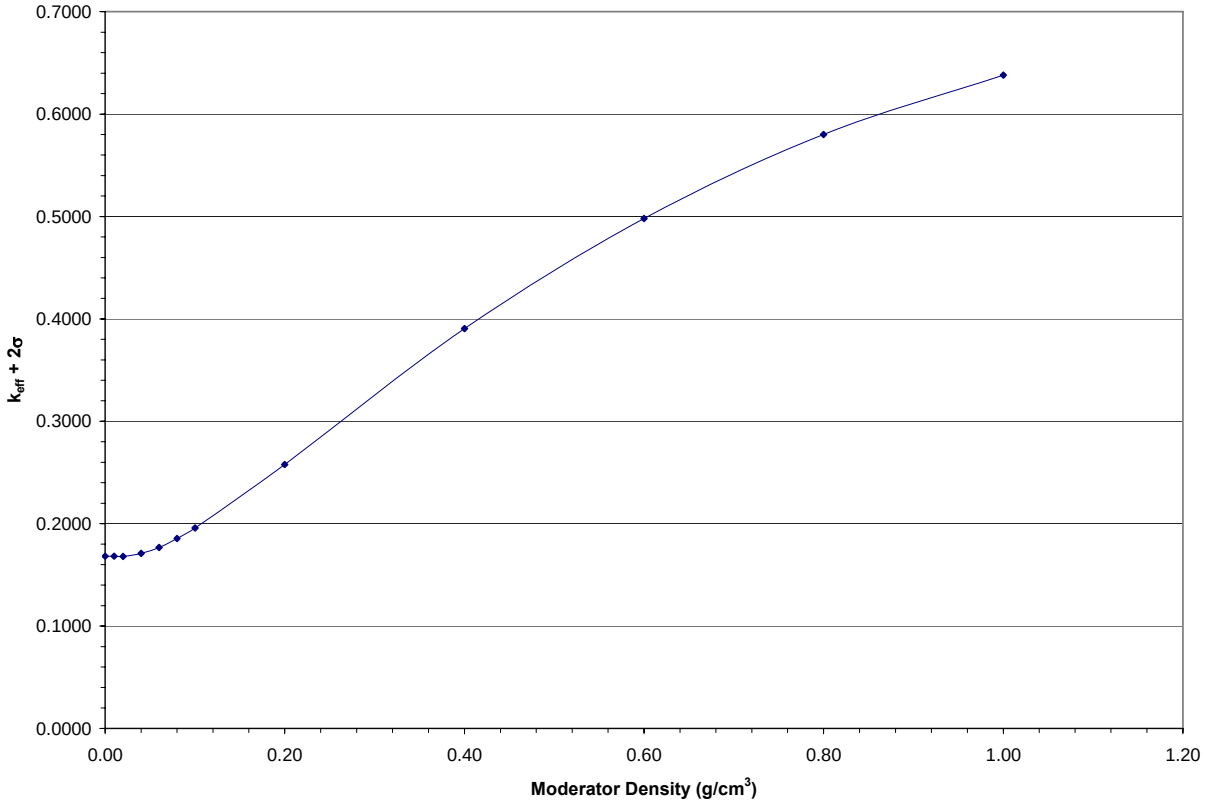

Figure 6-46 RAJ-II Fuel Rod Single Package Under Normal Conditions of Transport

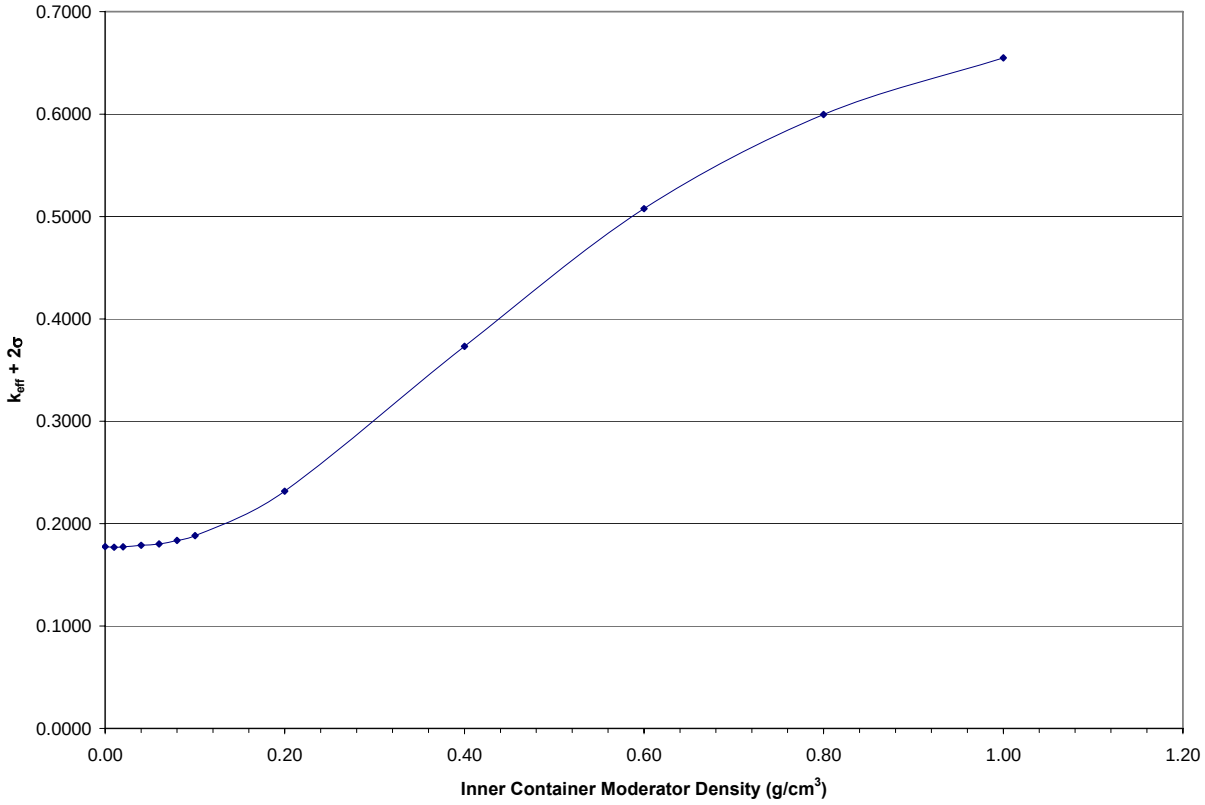

Figure 6-47 RAJ-II Fuel Rod Transport Single Package HAC

6.7.6 Evaluation of Package Arrays with Fuel Rods Under Normal Conditions of Transport

The package array normal condition model described in Section 6.3.1.2.1 is used to demonstrate criticality safety of the RAJ-II shipping container when transporting fuel rods. Based on the results in Table 6-22, the GNF 8x8 worst case fuel rod design is used for the study since it produced the highest reactivity peak among all fuel rod designs considered. The calculation using the package array normal conditions of transport model for fuel rod transport involves a moderator density sensitivity study. In the model, the moderator density is uniformly varied and the system reactivity is observed.

6.7.6.1 Package Array NCT Fuel Rod Transport Results

The results of the package array fuel rod transport normal condition model calculations are shown in Figure 6-48. As shown, the reactivity initially increases then decreases as the moderator density increases until a density of 0.4 g/cm^3 is reached, then it increases essentially linearly until full density is reached. The maximum $k_{eff} + 2\sigma$ obtained is 0.6381 (Table 6-39) which is below the USL of 0.94254. Therefore, criticality safety of the RAJ-II shipping container with fuel rods is demonstrated under normal conditions of transport.

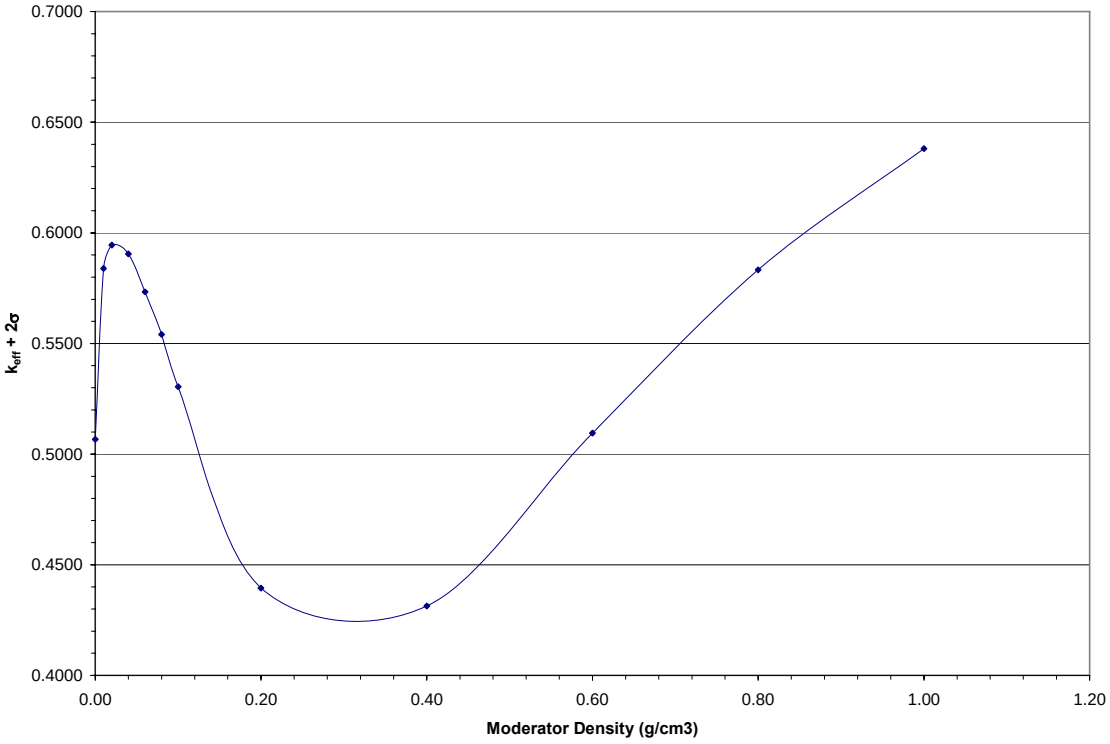

Figure 6-48 RAJ-II Package Array Under Normal Conditions of Transport with Loose Fuel Rods

6.7.7 Fuel Rod Transport Package Arrays Under Hypothetical Accident Conditions

The package array hypothetical accident condition model described in Section 6.3.1.2.2 is used to demonstrate criticality safety of a 10x1x10 array (2N=100) of RAJ-II shipping containers when transporting loose fuel rods. Based on the results in Table 6-22, the GNF 8x8 worst case fuel rod design is used for the study since it produced the highest reactivity peak among the fuel rod designs considered. The calculation using the HAC model involves a moderator density sensitivity study. In the study, there is no interspersed moderator, and the moderator density inside the inner container is varied. The polyethylene foam lines the inner container fuel compartment since the configuration resulted in the most reactive conditions.

6.7.7.1 Package Array HAC Fuel Rod Transport Results

The results of the package array HAC model calculations are shown in

Figure 6-49. The reactivity begins at its lowest value and increases with increasing internal moderator density until a peak is reached at a density of 0.6 g/cm^3. The maximum $k_{eff} + 2\sigma$ for the package array fuel rod transport HAC case is 0.8745 (Table 6-40), which is below the USL of 0.94254. Therefore, criticality safety of the RAJ-II shipping container is demonstrated for the package array under hypothetical accident conditions when fuel rods are being transported.

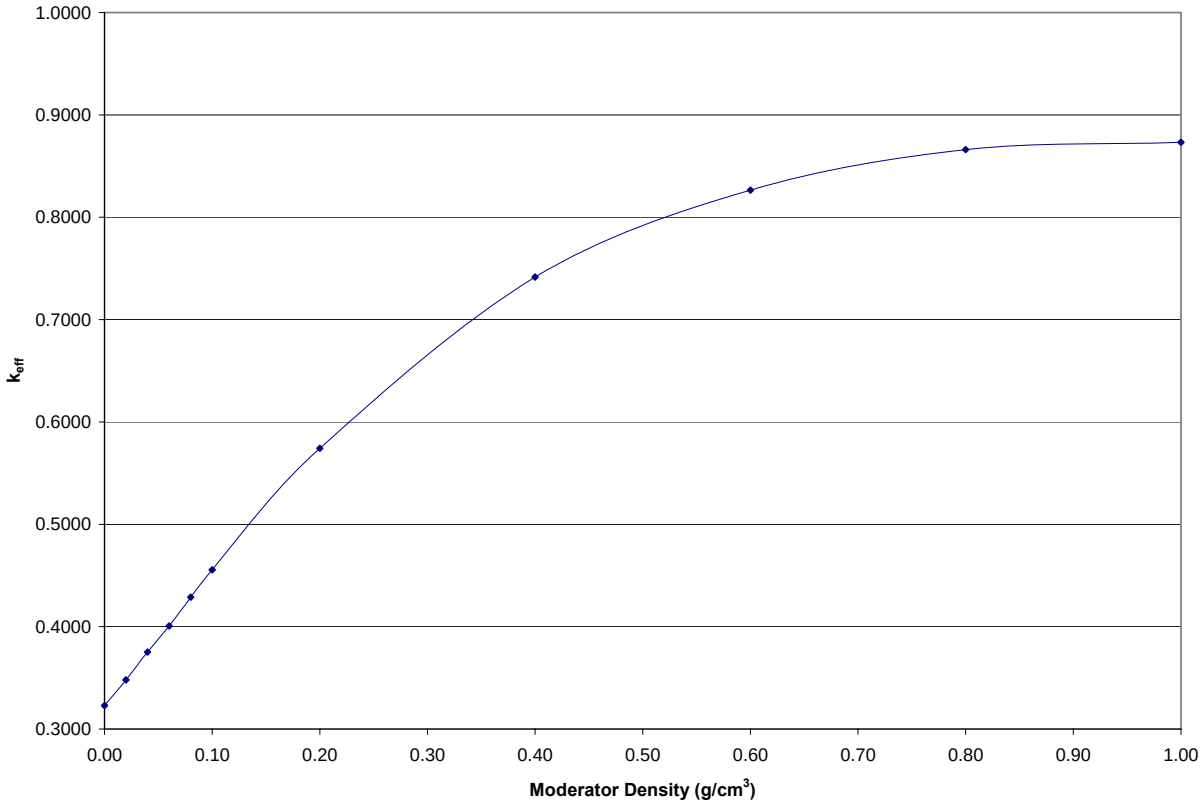

Figure 6-49 RAJ-II Fuel Rod Transport Under HAC

6.8 FISSILE MATERIAL PACKAGES FOR AIR TRANSPORT

This package is not intended for the air transport of fissile material.

6.9 CONCLUSION

Based on the calculations that have been documented, the RAJ-II shipping container is qualified to transport UO_2 fuel assemblies, including 10x10, 9x9, and 8x8 BWR designs, in accordance with the criticality safety requirements of the IAEA and 10 CFR 71. The fuel assemblies may be channeled or un-channeled.

The calculations documented in Chapter 6.0 also demonstrate a finite 10x1x10 array of damaged, or a 21x3x24 array of un-damaged packages remains below a k_{eff} of 0.95 with optimum interspersed moderation. Therefore, the calculations support a CSI of 1.0.

In addition, the calculations demonstrate UO_2 fuel rods may be packaged within the RAJ-II inner container in 5-inch stainless steel pipe/protective case, loose, or bundled together. The UO_2 fuel rods may consist of 10x10, 9x9, or 8x8 fuel rod designs.

The calculations documented in Chapter 6.0 also demonstrate the 10x10 fuel assemblies may be transported with 8, 10, 12, or 14 part length fuel rods, and 9x9 fuel assemblies may be transported with 8, 10 and 12 part length fuel rods.

6.10 BENCHMARK EVALUATIONS

6.10.1 Applicability of Benchmark Experiments

The criticality calculation method is verified by comparison with critical experiment data which is sufficiently diverse to establish that the method bias and uncertainty will apply to conditions considered in the RAJ-II shipping container criticality analysis. A set of 27 critical experiments are analyzed using SCALE-PC to demonstrate its applicability to criticality analysis and to establish a set of Upper Subcritical Limits (USLs) that define acceptance criteria. Benchmark experiments are selected with compositions, configurations, and nuclear characteristics that are comparable to those encountered in the RAJ-II shipping container loaded with fuel as described in Table 6-1. The critical experiments are described in detail in References 2-5 and 9-12 and summarized in Section 6.11.10.

The critical experiments consisted of water moderated, oxide fuel arrays in square lattices. Fourteen experiments were 15x8 fuel rod lattices, with 4.31 weight percent (w/o) U-235 enrichment, and different absorber plates in the water gaps between rods. The absorber plates include aluminum, Type 304L stainless steel, Type 304L stainless steel with various boron enrichments, zircaloy-4, and Boral™. Thirteen experiments were 15x15 fuel rod lattices using multiple enrichments, no absorbers between rod clusters, and gadonium absorber integral to the fuel in most cases (9 cases). The lattice arrays in these experiments had enrichments of 2.46, 2.73, 2.74, 2.75, 2.76, 2.77, or 2.78 w/o U-235. Comparison with these experiments demonstrates the applicability of the criticality calculation method.

6.10.2 Bias Determination

A set of Upper Subcritical Limits is determined using the results from the 27 critical experiments and USL Method 1, Confidence Band with Administrative Margin, described in Section 4.0 of NUREG/CR-6361 (Reference 7). The USL Method 1 applies a statistical calculation of the method bias and its uncertainty plus an administrative margin (0.05 Δk) to a linear fit of the critical experiment benchmark data. The USLs are determined as a function of the critical experiment system parameters; enrichment, water-to-fuel ratio, hydrogen-to- U-235 ratio, pin pitch, average energy of the lethargy causing fission, and the average energy group causing fission.

- The following equation is determined for the USL as a function of enrichment:
  $USL = 0.9388 + (8.6824 \times 10^{-4})x$ for all x
  The variance of the equation fit is 3.6827×10^{-6}. The applicable range for enrichment is $2.46 \leq x \leq 4.31$.

- The following equation is determined for the USL as a function of water-to-fuel ratio:
  $USL = 0.9398 + (6.6864 \times 10^{-4})x$ for all x
  The variance of the equation fit is 3.8188×10^{-6}. The applicable range for water-to-fuel ratio is $1.8714 \leq x \leq 3.8832$.

- The following equation is determined for the USL as a function of hydrogen-to-U-235:
  $USL = 0.9380 + (1.4976 \times 10^{-5})x$ for all x
  The variance of the equation fit is 4.1692×10^{-6}. The applicable range for hydrogen-to-U-235 ratio is $200.56 \leq 255.92$.

- The following equation is determined for the USL as a function of pin pitch:
  $USL = 0.9387 + (1.4894 \times 10^{-3})x$ for all x
  The variance of the equation fit is 3.7993×10^{-6}. The applicable range for pin pitch is $1.6358 \leq x \leq 2.54$.

- The following equation is determined for the USL as a function of average energy of the lethargy causing fission:
  $USL = 0.9423 - (3.8725 \times 10^{-3})x$ for all x
  The variance of the equation fit is 4.1339×10^{-6}. The applicable range for average energy of the lethargy causing fission is $0.1127 \leq x \leq 0.3645$.

- The following equation is determined for the USL as a function of the average energy group causing fission:
  $USL = 0.9281 + (3.9834 \times 10^{-4})x$ for all x
  The variance of the equation fit is 4.0641×10^{-6}. The applicable range for the average energy group causing fission is $32.89 \leq x \leq 35.77$.

Of the preceding equations, the USL as a function of enrichment is the best correlated to the data since the variance of the equation fit is the smallest. Therefore, the USL as a function of enrichment is used to determine a minimum USL for each fuel assembly type considered for use

with the RAJ-II shipping container (Table 6-1). Figure 6-50 shows the USL as a function of enrichment. USL values are calculated as a function of enrichment for each candidate fuel design. All candidate fuel designs have the same maximum enrichment of 5.0 wt. percent U-235. Although the 5.0 wt. percent U-235 enrichment falls outside the range of applicability, ANSI/ANS-8.1 (Reference 6) allows the range of applicability to be extended beyond the range of conditions represented by the benchmarks, as long as that extrapolation is not large. As outlined in Reference 7, k(x)-w(x) is used to extend the USL curve beyond the range of applicability. Figure 6-50 displays the USL curve extrapolation using k(x)-w(x); the extrapolated USL value corresponding to the 5.0 wt. percent U-235 enrichment is 0.94323. Since the extrapolated value results in a higher USL than the maximum enrichment within the range of applicability would produce, the USL corresponding to the 4.31 wt. percent U-235 enrichment is conservatively selected. Therefore, the USL for the RAJ-II shipping container is 0.94254.

The following equation is used to develop the k_{eff} for the transportation of fuel in the RAJ-II shipping container:

$$k_{eff} = k_{case} + 2\sigma$$

where:

k_{case} = KENO V.a k_{eff} for a particular case of interest
σ = uncertainty in calculated KENO V.a k_{eff} for a particular case of interest

The k_{eff} for each container configuration analyzed in the RAJ-II shipping container criticality analysis is compared to the minimum USL (0.94254) to ensure subcriticality.

The GEMER program has been validated against experiments that have uranium form, chemical composition and moderation/reflection conditions similar to those of this application. For low-enriched UO_2 lattice systems without poison, the calculational bias and bias uncertainty of GEMER is given by (Ref. 13):

$$b^* = -0.017$$

A minimum margin of subcriticality is applied as:

$$\Delta k_m = 0.05$$

Since the GEMER validation benchmarks for heterogeneous UO_2 systems do not include uranium-carbide (UC) fuel types in the Area of Applicability (AOA), an additional margin Δk_{AOA} = 0.01 will be applied for loose UC rods since no UC critical benchmarks are currently available. Therefore,

For UO_2 Rods: $USL = 1 + b^* - \Delta k_m = 1 + (-0.017) - 0.05 = 0.933$

For UC Rods: $USL = 1 + b^* - \Delta k_m - \Delta k_{AOA} = 1 + (-0.017) - 0.05 - 0.01 = 0.923$

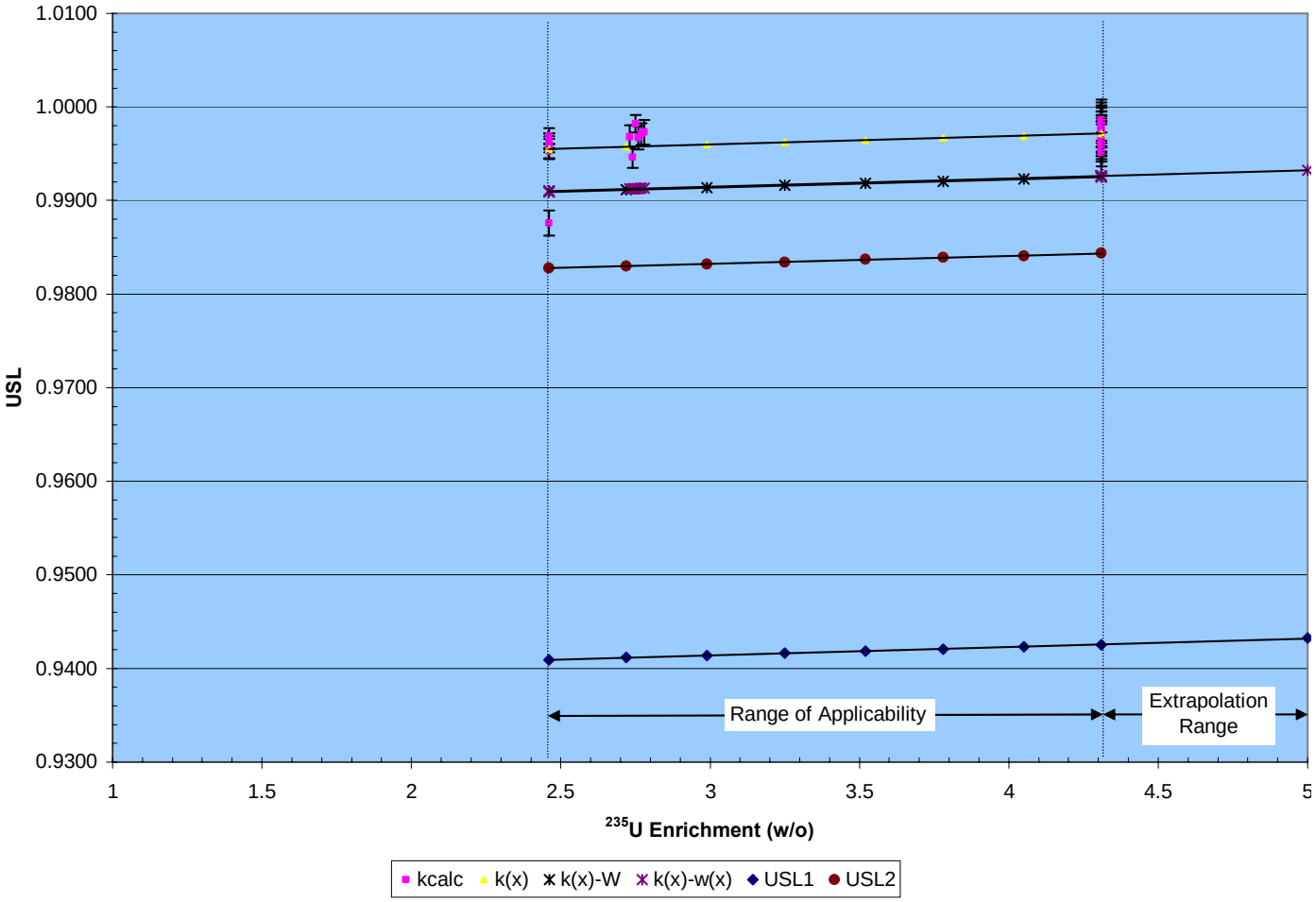

Figure 6-50 USL as a Function of Enrichment

6.11 APPENDIX

6.11.1 Single Package Normal Conditions of Transport Input

```
=CSAS25             PARM=SIZE=500000
RAJ-II CONTAINER, HAC, NO INTERSPERSED H2O, 100% INNER H2O DENSITY, 5.0 W/O
235U, 12 GAD RODS, SINGLE PACKAGE
44GROUPNDF5                 LATTICECELL
UO2             1  DEN=10.74    1.0  293 92235 5.0 92238 95.0   END
ZR              2  1.00              293                         END
H2O             3  1.00              293                         END
ARBMUO2         10.74 2 1 1 1 92000 1
                           8016 2 4 0.97840 293 92235  5.0
                                                92238 95.0  END
ARBMGD2O3       7.407 2 0 1 1 64000 2
                           8016 3 4 0.02160 293             END
H2O             5  1.00              293                         END
SS304           6  1.00              293                         END
POLYETHYLENE    7  DEN=0.080000 1.0  293                         END
POLYETHYLENE    8  DEN=0.949 0.25405 293                         END
H2O             8  DEN=1.00  0.74595 293                         END
H2O             9  1.00              293                         END
ARBMAL2O3       0.25 2 0 1 0 13027 2 8016 3 10  0.49            END
ARBMSIO2        0.25 2 0 1 0 14000 1 8016 2 10  0.51            END
ZR              11 1.00              293                         END
END COMP
SQUAREPITCH 1.3500 0.8950 1 8 1.01000 2 0.9338 0                END
MORE DATA
RES=4 CYLINDER 0.4475  DAN(4)=2.3197146E-01
END MORE DATA
RAJ-II CONTAINER, HAC, NO INTERSPERSED H2O, 100% INNER H2O DENSITY, 5.0 W/O
235U, 12 GAD RODS, SINGLE PACKAGE
READ PARM TME=400 GEN=400 NPG=2500 NSK=50 NUB=YES RUN=YES END PARM
READ GEOM

UNIT  1
COM=!CONTAINER INNER BOX!
'DEFINE GEOMETRY FOR SEPARATOR PLATE BETWEEN ASSEMBLY COMPARTMENTS
CUBOID     6  1  2P0.0875   2P228.34  2P8.829
'DEFINE REGION FOR ASSEMBLY COMPARTMENTS WITHIN INNER BOX
CUBOID     9  1  2P17.713   2P228.34  2P8.829
'INSERT FOAM POLYETHYLENE
HOLE       4      -8.9003       0.00    0.00
HOLE       5       8.9003       0.00    0.00
'DEFINE WALLS FOR ASSEMBLY COMPARTMENTS WITHIN INNER BOX
CUBOID     6  1  2P17.800   2P228.34    8.829  -8.9165
'DEFINE REGION OUTSIDE THE WALLS OF THE ASSEMBLY COMPARTMENTS
CUBOID    10  1  2P22.798   2P228.34    8.829  -13.839
'DEFINE THE INNER WALLS OF THE BOX ENDS
CUBOID     6  1  2P22.798   2P228.48    8.829  -13.979
'DEFINE INNER CORE OF BOX ENDS
CUBOID    10  1  2P22.798   2P233.44    8.829  -13.979
'DEFINE OUTER WALLS OF THE INNER BOX
```

```
CUBOID     6  1  2P22.938   2P233.58    8.829  -13.979

UNIT 2
COM=!INNER BOX LID!
'DEFINE INNER CORE OF INNER BOX LID
CUBOID    10 1  2P22.798    2P233.44   2P2.48
'DEFINE WALLS FOR INNER BOX LID
CUBOID    6  1  2P22.938    2P233.58   2P2.62

UNIT 3
COM=!INNER BOX WITH ENDS AND LID!
ARRAY 1 3*0

UNIT 4
COM=!FOAM POLYETHYLENE FOR LEFT ASSEMBLY COMPARTMENT!
CUBOID     9  1  2P7.055   2P228.34  2P7.055
HOLE      70      -6.7500  -192.50  -6.750
'FOAM POLYETHYLENE FOR ASSEMBLY COMPARTMENTS
CUBOID     7  1  2P8.8126   2P228.34  2P8.829

UNIT 5
COM=!FOAM POLYETHYLENE FOR RIGHT ASSEMBLY COMPARTMENT!
CUBOID     9  1  2P7.055   2P228.34  2P7.055
HOLE      70      -6.7500  -192.50  -6.750
'FOAM POLYETHYLENE FOR ASSEMBLY COMPARTMENT
CUBOID     7  1  2P8.8126   2P228.34  2P8.829

UNIT 10
COM=!5 W/O FUEL PINS W/O GAD!
'DEFINE THE FUEL PELLET
YCYLINDER 1  1    0.4475   192.5  0
'DEFINE THE PELLET-CLAD GAP
YCYLINDER 0  1    0.4669   192.5  0
'DEFINE THE FUEL ROD CLADDING/POLY
YCYLINDER 2  1    0.5050   192.5  0
'DEFINE THE FUEL ROD PITCH FILLED WITH POLYETHYLENE
CUBOID    8  1  2P0.6750    192.5  0  2P0.6750

UNIT 20
COM=!SPACE WITHIN FUEL ASSEMBLY LATTICE!
CUBOID    8  1  2P0.6750   192.5  0  2P0.6750

UNIT 40
COM=!5 W/O FUEL PINS W (2.0 WT % X 0.75) GAD!
'DEFINE THE FUEL PELLET
YCYLINDER 4  1    0.4475   192.5  0
'DEFINE THE PELLET-CLAD GAP
YCYLINDER 0  1    0.4669   192.5  0
'DEFINE THE FUEL ROD CLADDING/POLY
YCYLINDER 2  1    0.5050   192.5  0
'DEFINE THE FUEL ROD PITCH FILLED WITH POLYETHYLENE
CUBOID    8  1  2P0.6750    192.5  0  2P0.6750

UNIT 50
COM=!LOWER HALF FUEL ASSEMBLY WITH CLUSTER SEPARATOR!
ARRAY 2 3*0
```

```
UNIT 60
COM=!UPPER HALF FUEL ASSEMBLY WITH CLUSTER SEPARATOR!
ARRAY 3 3*0

UNIT 70
COM=!COMPLETE FUEL ASSEMBLY!
ARRAY 4 3*0
REFLECTOR 11 1  2R0.3048 2R0.0  2R0.3048  1

GLOBAL
UNIT 400
COM=!OUTER CONTAINER BODY AND LID!
'DEFINE INNER REGION OF THE OUTER CONTAINER
CUBOID   3  1   2P35.788    2P253.188  2P31.900
'INNER CONTAINER PLACEMENT WITHIN OUTER CONTAINER
HOLE 3         -22.938      -233.58    -14.024
'DEFINE WALLS OF THE OUTER CONTAINER AND LID
CUBOID   6  1   2P35.963    2P253.363  2P32.075

'GLOBAL
'UNIT 500
'ARRAY 10 3*0
REFLECTOR  5  1  6R30.48  1
END GEOM

READ ARRAY
ARA=1 NUX=1 NUY=1 NUZ=2
FILL 1 2
END FILL
ARA=2 NUX=10 NUY=1 NUZ=10
FILL 10 10 10 10 10 10 10 10 40 40
     10 10 20 10 10 10 40 40 40 40
     10 20 10 10 10 10 40 40 40 10
     10 10 10 20 20 10 40 40 40 10
     10 20 10 20 20 10 10 10 10 10
     10 10 20 10 10 20 20 10 10 10
     10 20 10 20 10 20 20 10 10 10
     10 10 10 10 20 10 10 10 20 10
     10 20 10 20 10 20 10 20 10 10
     10 10 10 10 10 10 10 10 10 10
END FILL
ARA=3 NUX=10 NUY=1 NUZ=10
FILL 10 10 10 10 10 10 10 10 40 40
     10 10 10 10 10 10 40 40 40 40
     10 10 10 10 10 10 40 40 40 10
     10 10 10 20 20 10 40 40 40 10
     10 10 10 20 20 10 10 10 10 10
     10 10 10 10 10 20 20 10 10 10
     10 10 10 10 10 20 20 10 10 10
     10 10 10 10 10 10 10 10 10 10
     10 10 10 10 10 10 10 10 10 10
     10 10 10 10 10 10 10 10 10 10
END FILL
ARA=4  NUX=1  NUY=2  NUZ=1
FILL 50 60
END FILL
ARA=10 NUX=21 NUY=3 NUZ=24
```

```
FILL F400
END FILL
END ARRAY

READ BNDS ALL=VACUUM
END BNDS
END DATA
END
```

6.11.2 Single Package Hypothetical Accident Conditions Input

```
=CSAS25             PARM=SIZE=500000
RAJ-II CONTAINER, HAC, 12 PART LENGTH RODS, 12 GAD RODS, 1.350 CM PITCH,
PATTERN H, SINGLE PACKAGE
44GROUPNDF5                 LATTICECELL
UO2            1  DEN=10.74 1.0 293 92235 5.0 92238 95.0      END
ZR             2             0.26380  293                     END
POLYETHYLENE   2  DEN=0.949  0.73620  293                     END
H2O            3  0.01 293                                    END
ARBMUO2        10.74 2 1 1 1 92000 1
                              8016 2 4 0.97840 293 92235  5.0
                                                   92238 95.0 END
ARBMGD2O3      7.407 2 0 1 1 64000 2
                              8016 3 4 0.02160 293           END
H2O            5  1.00 293                                    END
SS304          6  1.00 293                                    END
H2O            7  1.00 293                                    END
H2O            8  1.00 293                                    END
ZR             9  1.00 293                                    END
ARBMAL2O3      0.25 2 0 1 0 13027 2 8016 3 10  0.49           END
ARBMSIO2       0.25 2 0 1 0 14000 1 8016 2 10  0.51           END
END COMP
SQUAREPITCH 1.3500 0.8950 1 7 1.19720 2 0.9338 0              END
MORE DATA
RES=4 CYLINDER 0.4475  DAN(4)=2.2023524E-01
END MORE DATA
RAJ-II CONTAINER, HAC, 12 PART LENGTH RODS, 12 GAD RODS, 1.350 CM PITCH,
PATTERN H, SINGLE PACKAGE
READ PARM TME=400 GEN=400 NPG=2500 NSK=50 NUB=YES RUN=YES END PARM
READ GEOM

UNIT  1
COM=!CONTAINER INNER BOX!
'DEFINE GEOMETRY FOR SEPARATOR PLATE BETWEEN ASSEMBLY COMPARTMENTS
CUBOID     6  1  2P0.0875   225.20  -228.34  2P8.829
'DEFINE REGION FOR ASSEMBLY COMPARTMENTS WITHIN INNER BOX
CUBOID     7  1  2P17.713   225.20  -228.34  2P8.829
'PLACE THE FUEL ASSEMBLIES INSIDE INNER BOX
HOLE       70     -15.290  -192.50  -6.477
HOLE       70       2.336  -192.50  -6.477
'DEFINE WALLS FOR ASSEMBLY COMPARTMENTS WITHIN INNER BOX
CUBOID     6  1  2P17.800   225.20  -228.34  8.829  -8.9165
'DEFINE REGION OUTSIDE THE WALLS OF THE ASSEMBLY COMPARTMENTS
CUBOID     10 1  2P22.798   225.20  -228.34  8.829  -13.839
'DEFINE THE INNER WALLS OF THE BOX ENDS
CUBOID     6  1  2P22.798   225.34  -228.48  8.829  -13.979
'DEFINE INNER CORE OF BOX ENDS -8.1CM IN Y FOR TOTAL DEFORMATION
CUBOID     10 1  2P22.798   225.34  -233.44  8.829  -13.979
'DEFINE OUTER WALLS OF THE INNER BOX -8.1CM IN Y FOR TOTAL DEFORMATION
CUBOID     6  1  2P22.938   225.48  -233.58  8.829  -13.979

UNIT 2
COM=!INNER BOX LID!
'DEFINE INNER CORE OF INNER BOX LID -8.1CM IN Y FOR TOTAL DEFORMATION
```

```
CUBOID    10 1  2P22.798    2P229.39   2P2.48
'DEFINE WALLS FOR INNER BOX LID -8.1CM IN Y FOR TOTAL DEFORMATION
CUBOID    6  1  2P22.938    2P229.53   2P2.62

UNIT 3
COM=!INNER BOX WITH ENDS AND LID!
ARRAY 1 3*0

UNIT 10
COM=!5 W/O FUEL PINS W/O GAD!
'DEFINE THE FUEL PELLET
YCYLINDER 1  1    0.4475   192.5  0
'DEFINE THE PELLET-CLAD GAP
YCYLINDER 0  1    0.4669   192.5  0
'DEFINE THE FUEL ROD CLADDING/POLY
YCYLINDER 2  1    0.5986   192.5  0
'DEFINE THE FUEL ROD PITCH FILLED WITH POLYETHYLENE
CUBOID    7  1  2P0.6750    192.5  0  2P0.6750

UNIT 20
COM=!SPACE WITHIN FUEL ASSEMBLY LATTICE!
CUBOID    7  1  2P0.6750   192.5  0  2P0.6750

UNIT 30
COM=!ARRAY FOR COMPLETE FUEL ASSEMBLY!
ARRAY 2 3*0
REFLECTOR 9  1  2R0.3048 2R0.0  2R0.3048  1

UNIT 40
COM=!5 W/O FUEL PINS W (2.0 WT % X 0.75) GAD!
'DEFINE THE FUEL PELLET
YCYLINDER 4  1    0.4475   192.5  0
'DEFINE THE PELLET-CLAD GAP
YCYLINDER 0  1    0.4669   192.5  0
'DEFINE THE FUEL ROD CLADDING/POLY
YCYLINDER 2  1    0.5986   192.5  0
'DEFINE THE FUEL ROD PITCH FILLED WITH POLYETHYLENE
CUBOID    7  1  2P0.6750    192.5  0  2P0.6750

UNIT 50
COM=!LOWER HALF FUEL ASSEMBLY WITH CLUSTER SEPARATOR!
ARRAY 2 3*0

UNIT 60
COM=!UPPER HALF FUEL ASSEMBLY WITH CLUSTER SEPARATOR!
ARRAY 3 3*0

UNIT 70
COM=!COMPLETE FUEL ASSEMBLY!
ARRAY 4 3*0
REFLECTOR 9  1  2R0.3048 2R0.0  2R0.3048  1

GLOBAL
UNIT 400
COM=!OUTER CONTAINER BODY AND LID!
'DEFINE INNER REGION OF THE OUTER CONTAINER
'MINUS 4.7CM IN Y AND -2.4CM IN Z FOR TOTAL DEFORMATION
```

```
CUBOID    0  1   2P35.788  247.960  -253.190  29.500  -31.900
'INNER CONTAINER PLACEMENT WITHIN OUTER CONTAINER
HOLE 3          -22.938      -229.53    -14.024
'DEFINE WALLS OF THE OUTER CONTAINER AND LID
CUBOID    6  1   2P35.963  248.135  -253.365  29.675  -32.075

'GLOBAL
'UNIT 500
'ARRAY 10 3*0
REFLECTOR  5  1  6R30.48  1
END GEOM

READ ARRAY
ARA=1 NUX=1 NUY=1 NUZ=2
FILL 1 2
END FILL
ARA=2 NUX=10 NUY=1 NUZ=10
FILL 10 10 10 10 10 10 10 10 40 40
     10 10 20 10 10 10 40 40 40 40
     10 20 10 10 10 10 40 40 40 10
     10 10 10 20 20 10 40 40 40 10
     10 20 10 20 20 10 10 10 10 10
     10 10 20 10 10 20 20 10 10 10
     10 20 10 20 10 20 20 10 10 10
     10 10 10 10 20 10 10 10 20 10
     10 20 10 20 10 20 10 20 10 10
     10 10 10 10 10 10 10 10 10 10
END FILL
ARA=3 NUX=10 NUY=1 NUZ=10
FILL 10 10 10 10 10 10 10 10 40 40
     10 10 10 10 10 10 40 40 40 40
     10 10 10 10 10 10 40 40 40 10
     10 10 10 20 20 10 40 40 40 10
     10 10 10 20 20 10 10 10 10 10
     10 10 10 10 10 20 20 10 10 10
     10 10 10 10 10 20 20 10 10 10
     10 10 10 10 10 10 10 10 10 10
     10 10 10 10 10 10 10 10 10 10
     10 10 10 10 10 10 10 10 10 10
END FILL
ARA=4  NUX=1  NUY=2  NUZ=1
FILL 50 60
END FILL
END ARRAY

READ BNDS ALL=VACUUM
END BNDS
END DATA
END
```

6.11.3 Package Array Normal Conditions of Transport Input

```
=CSAS25             PARM=SIZE=500000
RAJ-II CONTAINER, HAC, NO INTERSPERSED H2O, 100% INNER H2O DENSITY, 5.0 W/O
235U, 12 GAD RODS, 21 X 3 X 24 ARRAY
44GROUPNDF5                 LATTICECELL
UO2             1  DEN=10.74    1.0  293 92235 5.0 92238 95.0   END
ZR              2  1.00              293                        END
H2O             3  1.00              293                        END
ARBMUO2         10.74 2 1 1 1 92000 1
                              8016 2 4 0.97840 293 92235  5.0
                                                   92238 95.0  END
ARBMGD2O3       7.407 2 0 1 1 64000 2
                              8016 3 4 0.02160 293             END
H2O             5  1.00              293                        END
SS304           6  1.00              293                        END
POLYETHYLENE    7  DEN=0.080000 1.0  293                        END
POLYETHYLENE    8  DEN=0.949 0.25405 293                        END
H2O             8  DEN=1.00  0.74595 293                        END
H2O             9  1.00              293                        END
ARBMAL2O3       0.25 2 0 1 0 13027 2 8016 3 10  0.49            END
ARBMSIO2        0.25 2 0 1 0 14000 1 8016 2 10  0.51            END
ZR              11 1.00              293                        END
END COMP
SQUAREPITCH 1.3500 0.8950 1 8 1.01000 2 0.9338 0                END
MORE DATA
RES=4 CYLINDER 0.4475  DAN(4)=2.3197146E-01
END MORE DATA
RAJ-II CONTAINER, HAC, NO INTERSPERSED H2O, 100% INNER H2O DENSITY, 5.0 W/O
235U, 12 GAD RODS, 21 X 3 X 24 ARRAY
READ PARM TME=400 GEN=400 NPG=2500 NSK=50 NUB=YES RUN=YES END PARM
READ GEOM

UNIT  1
COM=!CONTAINER INNER BOX!
'DEFINE GEOMETRY FOR SEPARATOR PLATE BETWEEN ASSEMBLY COMPARTMENTS
CUBOID     6  1  2P0.0875   2P228.34  2P8.829
'DEFINE REGION FOR ASSEMBLY COMPARTMENTS WITHIN INNER BOX
CUBOID     9  1  2P17.713   2P228.34  2P8.829
'INSERT FOAM POLYETHYLENE
HOLE       4      -8.9003       0.00    0.00
HOLE       5       8.9003       0.00    0.00
'DEFINE WALLS FOR ASSEMBLY COMPARTMENTS WITHIN INNER BOX
CUBOID     6  1  2P17.800   2P228.34    8.829  -8.9165
'DEFINE REGION OUTSIDE THE WALLS OF THE ASSEMBLY COMPARTMENTS
CUBOID    10  1  2P22.798   2P228.34    8.829  -13.839
'DEFINE THE INNER WALLS OF THE BOX ENDS
CUBOID     6  1  2P22.798   2P228.48    8.829  -13.979
'DEFINE INNER CORE OF BOX ENDS
CUBOID    10  1  2P22.798   2P233.44    8.829  -13.979
'DEFINE OUTER WALLS OF THE INNER BOX
CUBOID     6  1  2P22.938   2P233.58    8.829  -13.979

UNIT 2
```

```
COM=!INNER BOX LID!
'DEFINE INNER CORE OF INNER BOX LID
CUBOID    10 1  2P22.798    2P233.44   2P2.48
'DEFINE WALLS FOR INNER BOX LID
CUBOID    6  1  2P22.938    2P233.58   2P2.62

UNIT 3
COM=!INNER BOX WITH ENDS AND LID!
ARRAY 1 3*0

UNIT 4
COM=!FOAM POLYETHYLENE FOR LEFT ASSEMBLY COMPARTMENT!
CUBOID     9  1  2P7.055   2P228.34  2P7.055
HOLE      70      -6.7500  -192.50  -6.750
'FOAM POLYETHYLENE FOR ASSEMBLY COMPARTMENTS
CUBOID     7  1  2P8.8126   2P228.34  2P8.829

UNIT 5
COM=!FOAM POLYETHYLENE FOR RIGHT ASSEMBLY COMPARTMENT!
CUBOID     9  1  2P7.055   2P228.34  2P7.055
HOLE      70      -6.7500  -192.50  -6.750
'FOAM POLYETHYLENE FOR ASSEMBLY COMPARTMENT
CUBOID     7  1  2P8.8126   2P228.34  2P8.829

UNIT 10
COM=!5 W/O FUEL PINS W/O GAD!
'DEFINE THE FUEL PELLET
YCYLINDER 1  1    0.4475   192.5  0
'DEFINE THE PELLET-CLAD GAP
YCYLINDER 0  1    0.4669   192.5  0
'DEFINE THE FUEL ROD CLADDING/POLY
YCYLINDER 2  1    0.5050   192.5  0
'DEFINE THE FUEL ROD PITCH FILLED WITH POLYETHYLENE
CUBOID    8  1  2P0.6750    192.5  0  2P0.6750

UNIT 20
COM=!SPACE WITHIN FUEL ASSEMBLY LATTICE!
CUBOID    8  1  2P0.6750   192.5  0  2P0.6750

UNIT 40
COM=!5 W/O FUEL PINS W (2.0 WT % X 0.75) GAD!
'DEFINE THE FUEL PELLET
YCYLINDER 4  1    0.4475   192.5  0
'DEFINE THE PELLET-CLAD GAP
YCYLINDER 0  1    0.4669   192.5  0
'DEFINE THE FUEL ROD CLADDING/POLY
YCYLINDER 2  1    0.5050   192.5  0
'DEFINE THE FUEL ROD PITCH FILLED WITH POLYETHYLENE
CUBOID    8  1  2P0.6750    192.5  0  2P0.6750

UNIT 50
COM=!LOWER HALF FUEL ASSEMBLY WITH CLUSTER SEPARATOR!
ARRAY 2 3*0

UNIT 60
COM=!UPPER HALF FUEL ASSEMBLY WITH CLUSTER SEPARATOR!
ARRAY 3 3*0
```

```
UNIT 70
COM=!COMPLETE FUEL ASSEMBLY!
ARRAY 4 3*0
REFLECTOR 11 1  2R0.3048 2R0.0  2R0.3048  1

UNIT 400
COM=!OUTER CONTAINER BODY AND LID!
'DEFINE INNER REGION OF THE OUTER CONTAINER
CUBOID   3  1   2P35.788    2P253.188  2P31.900
'INNER CONTAINER PLACEMENT WITHIN OUTER CONTAINER
HOLE 3         -22.938      -233.58    -14.024
'DEFINE WALLS OF THE OUTER CONTAINER AND LID
CUBOID   6  1   2P35.963    2P253.363  2P32.075

GLOBAL
UNIT 500
ARRAY 10 3*0
REFLECTOR  5  1  6R30.48  1
END GEOM

READ ARRAY
ARA=1 NUX=1 NUY=1 NUZ=2
FILL 1 2
END FILL
ARA=2 NUX=10 NUY=1 NUZ=10
FILL 10 10 10 10 10 10 10 10 40 40
     10 10 20 10 10 10 40 40 40 40
     10 20 10 10 10 10 40 40 40 10
     10 10 10 20 20 10 40 40 40 10
     10 20 10 20 20 10 10 10 10 10
     10 10 20 10 10 20 20 10 10 10
     10 20 10 20 10 20 20 10 10 10
     10 10 10 10 20 10 10 10 20 10
     10 20 10 20 10 20 10 20 10 10
     10 10 10 10 10 10 10 10 10 10
END FILL
ARA=3 NUX=10 NUY=1 NUZ=10
FILL 10 10 10 10 10 10 10 10 40 40
     10 10 10 10 10 10 40 40 40 40
     10 10 10 10 10 10 40 40 40 10
     10 10 10 20 20 10 40 40 40 10
     10 10 10 20 20 10 10 10 10 10
     10 10 10 10 10 20 20 10 10 10
     10 10 10 10 10 20 20 10 10 10
     10 10 10 10 10 10 10 10 10 10
     10 10 10 10 10 10 10 10 10 10
     10 10 10 10 10 10 10 10 10 10
END FILL
ARA=4  NUX=1  NUY=2  NUZ=1
FILL 50 60
END FILL
ARA=10 NUX=21 NUY=3 NUZ=24
FILL F400
END FILL
END ARRAY
```

```
READ BNDS ALL=VACUUM
END BNDS
END DATA
END
```

6.11.4 Package Array Hypothetical Accident Conditions Input

6.11.4.1 GNF 10x10

```
=CSAS25             PARM=SIZE=500000
RAJ-II CONTAINER, HAC, 100% H2O DENSITY, WORSTCASE, GNF 10x10, 10 X 1 X 10
ARRAY
44GROUPNDF5                 LATTICECELL
UO2             1  DEN=10.74 1.0 293 92235 5.0 92238 95.0      END
ZR              2             0.26380  293                     END
POLYETHYLENE    2  DEN=0.949  0.73620  293                     END
H2O             3  0.01 293                                    END
ARBMUO2         10.74 2 1 1 1 92000 1
                           8016 2 4 0.97840 293 92235  5.0
                                                92238 95.0 END
ARBMGD2O3       7.407 2 0 1 1 64000 2
                           8016 3 4 0.02160 293            END
H2O             5  1.00 293                                 END
SS304           6  1.00 293                                 END
H2O             7  1.00 293                                 END
POLYETHYLENE    8  DEN=0.080000 1.0  293                     END
ZR              9  1.00 293                                 END
ARBMAL2O3       0.25 2 0 1 0 13027 2 8016 3 10  0.49         END
ARBMSIO2        0.25 2 0 1 0 14000 1 8016 2 10  0.51         END
END COMP
SQUAREPITCH 1.3500 0.8950 1 7 1.19720 2 0.9338 0             END
MORE DATA
RES=4 CYLINDER 0.4475  DAN(4)=2.2023524E-01
END MORE DATA
RAJ-II CONTAINER, HAC, 100% H2O DENSITY, WORSTCASE, GNF 10x10, 10 X 1 X 10
ARRAY
READ PARM TME=400 GEN=400 NPG=2500 NSK=50 NUB=YES RUN=YES END PARM
READ GEOM

UNIT  1
COM=!CONTAINER INNER BOX!
'DEFINE GEOMETRY FOR SEPARATOR PLATE BETWEEN ASSEMBLY COMPARTMENTS
CUBOID     6  1  2P0.0875   225.20  -228.34  2P8.829
'DEFINE REGION FOR ASSEMBLY COMPARTMENTS WITHIN INNER BOX
CUBOID     7  1  2P17.713   225.20  -228.34  2P8.829
'INSERT FOAM POLYETHYLENE AND FUEL
HOLE       4      -8.9001     0.00      0.00
HOLE       5       8.9001     0.00      0.00
'DEFINE WALLS FOR ASSEMBLY COMPARTMENTS WITHIN INNER BOX
CUBOID     6  1  2P17.800   225.20  -228.34  8.829  -8.9165
'DEFINE REGION OUTSIDE THE WALLS OF THE ASSEMBLY COMPARTMENTS
CUBOID     10 1  2P22.798   225.20  -228.34  8.829  -13.839
'DEFINE THE INNER WALLS OF THE BOX ENDS
CUBOID     6  1  2P22.798   225.34  -228.48  8.829  -13.979
'DEFINE INNER CORE OF BOX ENDS -8.1CM IN Y FOR TOTAL DEFORMATION
CUBOID     10 1  2P22.798   225.34  -233.44  8.829  -13.979
'DEFINE OUTER WALLS OF THE INNER BOX -8.1CM IN Y FOR TOTAL DEFORMATION
CUBOID     6  1  2P22.938   225.48  -233.58  8.829  -13.979
```

```
UNIT 2
COM=!INNER BOX LID!
'DEFINE INNER CORE OF INNER BOX LID -8.1CM IN Y FOR TOTAL DEFORMATION
CUBOID    10 1  2P22.798    2P229.39   2P2.48
'DEFINE WALLS FOR INNER BOX LID -8.1CM IN Y FOR TOTAL DEFORMATION
CUBOID    6  1  2P22.938    2P229.53   2P2.62

UNIT 3
COM=!INNER BOX WITH ENDS AND LID!
ARRAY 1 3*0

UNIT 4
COM=!FOAM POLYETHYLENE FOR LEFT ASSEMBLY COMPARTMENT!
CUBOID     7  1  2P7.055   225.20  -228.34  2P7.055
HOLE      70      -6.7500 -192.50   -6.750
'FOAM POLYETHYLENE FOR ASSEMBLY COMPARTMENTS
CUBOID     8  1  2P8.8126  225.20  -228.34  2P8.829

UNIT 5
COM=!FOAM POLYETHYLENE FOR RIGHT ASSEMBLY COMPARTMENT!
CUBOID     7  1  2P7.055   225.20  -228.34  2P7.055
HOLE      70      -6.7500 -192.50   -6.750
'FOAM POLYETHYLENE FOR ASSEMBLY COMPARTMENT
CUBOID     8  1  2P8.8126  225.20  -228.34  2P8.829

UNIT 10
COM=!5 W/O FUEL PINS W/O GAD!
'DEFINE THE FUEL PELLET
YCYLINDER 1  1    0.4475   192.5  0
'DEFINE THE PELLET-CLAD GAP
YCYLINDER 0  1    0.4669   192.5  0
'DEFINE THE FUEL ROD CLADDING/POLY
YCYLINDER 2  1    0.5986   192.5  0
'DEFINE THE FUEL ROD PITCH FILLED WITH POLYETHYLENE
CUBOID    7  1  2P0.6750    192.5  0  2P0.6750

UNIT 20
COM=!SPACE WITHIN FUEL ASSEMBLY LATTICE!
CUBOID    7  1  2P0.6750   192.5  0  2P0.6750

UNIT 30
COM=!ARRAY FOR COMPLETE FUEL ASSEMBLY!
ARRAY 2 3*0
REFLECTOR 9  1  2R0.3048 2R0.0  2R0.3048  1

UNIT 40
COM=!5 W/O FUEL PINS W (2.0 WT % X 0.75) GAD!
'DEFINE THE FUEL PELLET
YCYLINDER 4  1    0.4475   192.5  0
'DEFINE THE PELLET-CLAD GAP
YCYLINDER 0  1    0.4669   192.5  0
'DEFINE THE FUEL ROD CLADDING/POLY
YCYLINDER 2  1    0.5986   192.5  0
'DEFINE THE FUEL ROD PITCH FILLED WITH POLYETHYLENE
CUBOID    7  1  2P0.6750    192.5  0  2P0.6750

UNIT 50
```

```
COM=!LOWER HALF FUEL ASSEMBLY WITH CLUSTER SEPARATOR!
ARRAY 2 3*0

UNIT 60
COM=!UPPER HALF FUEL ASSEMBLY WITH CLUSTER SEPARATOR!
ARRAY 3 3*0

UNIT 70
COM=!COMPLETE FUEL ASSEMBLY!
ARRAY 4 3*0
REFLECTOR 9  1  2R0.3048 2R0.0  2R0.3048  1

UNIT 400
COM=!OUTER CONTAINER BODY AND LID!
'DEFINE INNER REGION OF THE OUTER CONTAINER
'MINUS 4.7CM IN Y AND -2.4CM IN Z FOR TOTAL DEFORMATION
CUBOID    0  1   2P35.788  247.960  -253.190  29.500  -31.900
'INNER CONTAINER PLACEMENT WITHIN OUTER CONTAINER
HOLE 3          -22.938      -229.53    -14.024
'DEFINE WALLS OF THE OUTER CONTAINER AND LID
CUBOID    6  1   2P35.963  248.135  -253.365  29.675  -32.075

GLOBAL
UNIT 500
ARRAY 10 3*0
REFLECTOR  5  1  6R30.48  1
END GEOM

READ ARRAY
ARA=1 NUX=1 NUY=1 NUZ=2
FILL 1 2
END FILL
ARA=2 NUX=10 NUY=1 NUZ=10
FILL 10 10 10 10 10 10 10 10 40 40
     10 10 20 10 10 10 40 40 40 40
     10 20 10 10 10 10 40 40 40 10
     10 10 10 20 20 10 40 40 40 10
     10 20 10 20 20 10 10 10 10 10
     10 10 20 10 10 20 20 10 10 10
     10 20 10 20 10 20 20 10 10 10
     10 10 10 10 20 10 10 10 20 10
     10 20 10 20 10 20 10 20 10 10
     10 10 10 10 10 10 10 10 10 10
END FILL
ARA=3 NUX=10 NUY=1 NUZ=10
FILL 10 10 10 10 10 10 10 10 40 40
     10 10 10 10 10 10 40 40 40 40
     10 10 10 10 10 10 40 40 40 10
     10 10 10 20 20 10 40 40 40 10
     10 10 10 20 20 10 10 10 10 10
     10 10 10 10 10 20 20 10 10 10
     10 10 10 10 10 20 20 10 10 10
     10 10 10 10 10 10 10 10 10 10
     10 10 10 10 10 10 10 10 10 10
     10 10 10 10 10 10 10 10 10 10
END FILL
ARA=4  NUX=1  NUY=2  NUZ=1
```

```
FILL 50 60
END FILL
ARA=10 NUX=10 NUY=1 NUZ=10
FILL F400
END FILL
END ARRAY

READ BNDS ALL=VACUUM
END BNDS
END DATA
END
```

6.11.5 Single Package Loose Rods Normal Conditions of Transport Input

```
=CSAS25             PARM=SIZE=500000
RAJ-II CONTAINER, 8, NTC, 100% H20, 2.8150 CM PITCH, LOOSE FUEL RODS, SINGLE
PACKAGE
44GROUPNDF5                 LATTICECELL
UO2            1  DEN=10.74    1.0  293 92235 5.0 92238 95.0   END
POLYETHYLENE   2  DEN=0.925    1.0  293                         END
H2O            3  1.00              293                         END
UO2            4  DEN=10.4799  1.0  293 92235 3.25 92238 96.75 END
GD             4  DEN=0.17374  1.0  293                         END
O              4  DEN=0.026514 1.0  293                         END
H2O            5  1.00              293                         END
SS304          6  1.00              293                         END
H2O            8  1.00              293                         END
H2O            9  1.00              293                         END
ARBMAL2O3      0.25 2 0 1 0 13027 2 8016 3 10  0.49             END
ARBMSIO2       0.25 2 0 1 0 14000 1 8016 2 10  0.51             END
ZR             11 1.00              293                         END
END COMP
SQUAREPITCH 2.8150 1.0500 1 8 1.13048 2 1.100 0               END
RAJ-II CONTAINER, 8, NTC, 100% H20, 2.8150 CM PITCH, LOOSE FUEL RODS, SINGLE
PACKAGE
READ PARM TME=400 GEN=400 NPG=2500 NSK=50 NUB=YES END PARM
READ GEOM

UNIT  1
COM=!CONTAINER INNER BOX!
'DEFINE GEOMETRY FOR SEPARATOR PLATE BETWEEN ASSEMBLY COMPARTMENTS
CUBOID     6  1  2P0.0875   2P228.34  2P8.829
'DEFINE REGION FOR ASSEMBLY COMPARTMENTS WITHIN INNER BOX
CUBOID     3  1  2P17.713   2P228.34  2P8.829
'INSERT FOAM POLYETHYLENE
HOLE       4      -8.9003       0.00    0.00
HOLE       5       8.9003       0.00    0.00
'DEFINE WALLS FOR ASSEMBLY COMPARTMENTS WITHIN INNER BOX
CUBOID     6  1  2P17.800   2P228.34    8.829  -8.9165
'DEFINE REGION OUTSIDE THE WALLS OF THE ASSEMBLY COMPARTMENTS
CUBOID    10  1  2P22.798   2P228.34    8.829  -13.839
'DEFINE THE INNER WALLS OF THE BOX ENDS
CUBOID     6  1  2P22.798   2P228.48    8.829  -13.979
'DEFINE INNER CORE OF BOX ENDS
CUBOID    10  1  2P22.798   2P233.44    8.829  -13.979
'DEFINE OUTER WALLS OF THE INNER BOX
CUBOID     6  1  2P22.938   2P233.58    8.829  -13.979

UNIT 2
COM=!INNER BOX LID!
'DEFINE INNER CORE OF INNER BOX LID
CUBOID    10 1  2P22.798    2P233.44   2P2.48
'DEFINE WALLS FOR INNER BOX LID
CUBOID    6  1  2P22.938    2P233.58   2P2.62
```

```
UNIT 3
COM=!INNER BOX WITH ENDS AND LID!
ARRAY 1 3*0

UNIT 4
COM=!FOAM POLYETHYLENE FOR LEFT ASSEMBLY COMPARTMENT!
CUBOID     3  1  2P7.0378   2P228.34  2P7.054
HOLE      30      -7.0376  -191.77   -7.0376
'FOAM POLYETHYLENE FOR ASSEMBLY COMPARTMENTS
CUBOID     7  1  2P8.8126   2P228.34  2P8.829

UNIT 5
COM=!FOAM POLYETHYLENE FOR RIGHT ASSEMBLY COMPARTMENT!
CUBOID     3  1  2P7.0378   2P228.34  2P7.054
HOLE      30      -7.0376  -191.77   -7.0376
'FOAM POLYETHYLENE FOR ASSEMBLY COMPARTMENT
CUBOID     7  1  2P8.8126   2P228.34  2P8.829

UNIT 10
COM=!5 W/O FUEL PINS W/O GAD!
'DEFINE THE FUEL PELLET
YCYLINDER 1  1    0.52500  381  0
'DEFINE THE PELLET-CLAD GAP
YCYLINDER 0  1    0.55000  381  0
'DEFINE THE FUEL ROD CLADDING
YCYLINDER 2  1    0.56524  381  0
'DEFINE THE FUEL ROD PITCH FILLED WITH WATER
CUBOID    8  1  2P1.40750  381  0  2P1.40750

UNIT 20
COM=!SPACE WITHIN FUEL ASSEMBLY LATTICE!
CUBOID    8  1  2P1.40750  381  0  2P1.40750

UNIT 30
COM=!ARRAY FOR COMPLETE FUEL ASSEMBLY!
ARRAY 2 3*0

UNIT 400
COM=!OUTER CONTAINER BODY AND LID!
'DEFINE INNER REGION OF THE OUTER CONTAINER
CUBOID   3  1   2P35.788    2P253.188  2P31.900
'INNER CONTAINER PLACEMENT WITHIN OUTER CONTAINER
HOLE 3         -22.938      -233.58    -14.024
'DEFINE WALLS OF THE OUTER CONTAINER AND LID
CUBOID   6  1   2P35.963    2P253.363  2P32.075

GLOBAL
UNIT 500
ARRAY 10 3*0
REFLECTOR  5  1  6R30.48  1
END GEOM

READ ARRAY
ARA=1 NUX=1 NUY=1 NUZ=2
FILL 1 2
END FILL
ARA=2 NUX=5  NUY=1 NUZ=5
```

```
FILL 10 10 10 10 10
     10 10 10 10 10
     10 10 10 10 10
     10 10 10 10 10
     10 10 10 10 10
END FILL
ARA=10 NUX=21 NUY=3  NUZ=24
FILL F400
END FILL
END ARRAY

READ BNDS ALL=VACUUM
END BNDS
END DATA
END
```

6.11.6 Single Package Loose Fuel Rods Hypothetical Accident Conditions Input

```
=CSAS25             PARM=SIZE=500000
RAJ-II CONTAINER, 8, HAC, 100% H2O, WORST CASE MODEL, 3.0056 CM PITCH, LOOSE
FUEL RODS, SINGLE PACKAGE
44GROUPNDF5                 LATTICECELL
UO2            1  DEN=10.74 1.0 293 92235 5.0 92238 95.0      END
POLYETHYLENE   2  DEN=0.925    1.0    293                     END
H2O            3  1.00               293                     END
UO2            4  DEN=10.4799  1.0 293 92235 3.25 92238 96.75 END
GD             4  DEN=0.17374  1.0 293                       END
O              4  DEN=0.026514 1.0 293                       END
H2O            5  1.00 293                                  END
SS304          6  1.00 293                                  END
H2O            7  DEN=1.00  1.0 293                         END
H2O            8  DEN=1.00     1.0    293                   END
ZR             9  1.00 293                                  END
ARBMAL2O3      0.25 2 0 1 0 13027 2 8016 3 10  0.49          END
ARBMSIO2       0.25 2 0 1 0 14000 1 8016 2 10  0.51          END
END COMP
SQUAREPITCH 3.0056 1.0500 1 8 1.13048 2 1.100 0              END
RAJ-II CONTAINER, 8, HAC, 100% H2O, WORST CASE MODEL, 3.0056 CM PITCH, LOOSE
FUEL RODS, SINGLE PACKAGE
READ PARM TME=400 GEN=400 NPG=2500 NSK=50 NUB=YES END PARM
READ GEOM

UNIT  1
COM=!CONTAINER INNER BOX!
'DEFINE GEOMETRY FOR SEPARATOR PLATE BETWEEN ASSEMBLY COMPARTMENTS
CUBOID     6  1  2P0.0875   225.20  -228.34  2P8.829
'DEFINE REGION FOR ASSEMBLY COMPARTMENTS WITHIN INNER BOX
CUBOID     7  1  2P17.713   225.20  -228.34  2P8.829
'PLACE THE FUEL ASSEMBLIES INSIDE INNER BOX
HOLE       30     -16.413  -190.50  -7.514
HOLE       30       1.386  -190.50  -7.514
'DEFINE WALLS FOR ASSEMBLY COMPARTMENTS WITHIN INNER BOX
CUBOID     6  1  2P17.800   225.20  -228.34  8.829  -8.9165
'DEFINE REGION OUTSIDE THE WALLS OF THE ASSEMBLY COMPARTMENTS
CUBOID     10 1  2P22.798   225.20  -228.34  8.829  -13.839
'DEFINE THE INNER WALLS OF THE BOX ENDS
CUBOID     6  1  2P22.798   225.34  -228.48  8.829  -13.979
'DEFINE INNER CORE OF BOX ENDS -8.1CM IN Y FOR TOTAL DEFORMATION
CUBOID     10 1  2P22.798   225.34  -233.44  8.829  -13.979
'DEFINE OUTER WALLS OF THE INNER BOX -8.1CM IN Y FOR TOTAL DEFORMATION
CUBOID     6  1  2P22.938   225.48  -233.58  8.829  -13.979

UNIT 2
COM=!INNER BOX LID!
'DEFINE INNER CORE OF INNER BOX LID -8.1CM IN Y FOR TOTAL DEFORMATION
CUBOID    10 1  2P22.798    2P229.39   2P2.48
'DEFINE WALLS FOR INNER BOX LID -8.1CM IN Y FOR TOTAL DEFORMATION
CUBOID    6  1  2P22.938    2P229.53   2P2.62

UNIT 3
```

```
COM=!INNER BOX WITH ENDS AND LID!
ARRAY 1 3*0

UNIT 10
COM=!5 W/O FUEL PINS W/O GAD!
'DEFINE THE FUEL PELLET
YCYLINDER 1  1    0.52500  381  0
'DEFINE THE PELLET-CLAD GAP
YCYLINDER 0  1    0.55000  381  0
'DEFINE THE FUEL ROD CLADDING
YCYLINDER 2  1    0.56524  381  0
'DEFINE THE FUEL ROD PITCH FILLED WITH WATER
CUBOID    8  1  2P1.50280  381  0  2P1.50280

UNIT 20
COM=!SPACE WITHIN FUEL ASSEMBLY LATTICE!
CUBOID    8  1  2P1.50280  381  0  2P1.50280

UNIT 30
COM=!ARRAY FOR COMPLETE FUEL ASSEMBLY!
ARRAY 2 3*0

GLOBAL
UNIT 400
COM=!OUTER CONTAINER BODY AND LID!
'DEFINE INNER REGION OF THE OUTER CONTAINER
'MINUS 4.7CM IN Y AND -2.4CM IN Z FOR TOTAL DEFORMATION
CUBOID    0  1   2P35.788  247.960  -253.190  29.500  -31.900
'INNER CONTAINER PLACEMENT WITHIN OUTER CONTAINER
HOLE 3          -22.938      -229.53    -14.024
'DEFINE WALLS OF THE OUTER CONTAINER AND LID
CUBOID    6  1   2P35.963  248.135  -253.365  29.675  -32.075

'GLOBAL
'UNIT 500
'ARRAY 10 3*0
REFLECTOR  5  1  6R30.48  1
END GEOM

READ ARRAY
ARA=1 NUX=1 NUY=1 NUZ=2
FILL 1 2
END FILL
ARA=2 NUX=5  NUY=1 NUZ=5
FILL 10 10 10 10 10
     10 10 10 10 10
     10 10 10 10 10
     10 10 10 10 10
     10 10 10 10 10
END FILL
ARA=10 NUX=14 NUY=2 NUZ=16
FILL F400
END FILL
END ARRAY

READ BNDS ALL=VACUUM
END BNDS
END DATA
```

6.11.7 Package Array Loose Fuel Rods Normal Conditions of Transport Input

```
=CSAS25             PARM=SIZE=500000
RAJ-II CONTAINER, 8, NTC, 100% H20, 2.8150 CM PITCH, LOOSE FUEL RODS, 21 x 3
x 24
44GROUPNDF5                 LATTICECELL
UO2            1  DEN=10.74    1.0  293 92235 5.0 92238 95.0   END
POLYETHYLENE   2  DEN=0.925    1.0  293                         END
H2O            3  1.00              293                         END
UO2            4  DEN=10.4799  1.0  293 92235 3.25 92238 96.75 END
GD             4  DEN=0.17374  1.0  293                         END
O              4  DEN=0.026514 1.0  293                         END
H2O            5  1.00              293                         END
SS304          6  1.00              293                         END
POLYETHYLENE   7  DEN=0.067967 1.0  293                         END
H2O            8  1.00              293                         END
H2O            9  1.00              293                         END
ARBMAL2O3      0.25 2 0 1 0 13027 2 8016 3 10  0.49              END
ARBMSIO2       0.25 2 0 1 0 14000 1 8016 2 10  0.51              END
ZR             11 1.00              293                         END
END COMP
SQUAREPITCH 2.8150 1.0500 1 8 1.13048 2 1.100 0                END
RAJ-II CONTAINER, 8, NTC, 100% H20, 2.8150 CM PITCH, LOOSE FUEL RODS, 21 x 3
x 24
READ PARM TME=400 GEN=400 NPG=2500 NSK=50 NUB=YES END PARM
READ GEOM

UNIT  1
COM=!CONTAINER INNER BOX!
'DEFINE GEOMETRY FOR SEPARATOR PLATE BETWEEN ASSEMBLY COMPARTMENTS
CUBOID     6  1  2P0.0875   2P228.34  2P8.829
'DEFINE REGION FOR ASSEMBLY COMPARTMENTS WITHIN INNER BOX
CUBOID     3  1  2P17.713   2P228.34  2P8.829
'INSERT FOAM POLYETHYLENE
HOLE       4      -8.9003       0.00    0.00
HOLE       5       8.9003       0.00    0.00
'DEFINE WALLS FOR ASSEMBLY COMPARTMENTS WITHIN INNER BOX
CUBOID     6  1  2P17.800   2P228.34    8.829  -8.9165
'DEFINE REGION OUTSIDE THE WALLS OF THE ASSEMBLY COMPARTMENTS
CUBOID    10  1  2P22.798   2P228.34    8.829  -13.839
'DEFINE THE INNER WALLS OF THE BOX ENDS
CUBOID     6  1  2P22.798   2P228.48    8.829  -13.979
'DEFINE INNER CORE OF BOX ENDS
CUBOID    10  1  2P22.798   2P233.44    8.829  -13.979
'DEFINE OUTER WALLS OF THE INNER BOX
CUBOID     6  1  2P22.938   2P233.58    8.829  -13.979

UNIT 2
COM=!INNER BOX LID!
'DEFINE INNER CORE OF INNER BOX LID
CUBOID    10 1  2P22.798    2P233.44   2P2.48
'DEFINE WALLS FOR INNER BOX LID
CUBOID    6  1  2P22.938    2P233.58   2P2.62
```

```
UNIT 3
COM=!INNER BOX WITH ENDS AND LID!
ARRAY 1 3*0

UNIT 4
COM=!FOAM POLYETHYLENE FOR LEFT ASSEMBLY COMPARTMENT!
CUBOID     3  1  2P7.0378   2P228.34  2P7.054
HOLE      30      -7.0376  -191.77   -7.0376
'FOAM POLYETHYLENE FOR ASSEMBLY COMPARTMENTS
CUBOID     7  1  2P8.8126   2P228.34  2P8.829

UNIT 5
COM=!FOAM POLYETHYLENE FOR RIGHT ASSEMBLY COMPARTMENT!
CUBOID     3  1  2P7.0378   2P228.34  2P7.054
HOLE      30      -7.0376  -191.77   -7.0376
'FOAM POLYETHYLENE FOR ASSEMBLY COMPARTMENT
CUBOID     7  1  2P8.8126   2P228.34  2P8.829

UNIT 10
COM=!5 W/O FUEL PINS W/O GAD!
'DEFINE THE FUEL PELLET
YCYLINDER 1  1    0.52500  381  0
'DEFINE THE PELLET-CLAD GAP
YCYLINDER 0  1    0.55000  381  0
'DEFINE THE FUEL ROD CLADDING
YCYLINDER 2  1    0.56524  381  0
'DEFINE THE FUEL ROD PITCH FILLED WITH WATER
CUBOID    8  1  2P1.40750  381  0  2P1.40750

UNIT 20
COM=!SPACE WITHIN FUEL ASSEMBLY LATTICE!
CUBOID    8  1  2P1.40750  381  0  2P1.40750

UNIT 30
COM=!ARRAY FOR COMPLETE FUEL ASSEMBLY!
ARRAY 2 3*0

UNIT 400
COM=!OUTER CONTAINER BODY AND LID!
'DEFINE INNER REGION OF THE OUTER CONTAINER
CUBOID   3  1   2P35.788    2P253.188  2P31.900
'INNER CONTAINER PLACEMENT WITHIN OUTER CONTAINER
HOLE 3         -22.938      -233.58    -14.024
'DEFINE WALLS OF THE OUTER CONTAINER AND LID
CUBOID   6  1   2P35.963    2P253.363  2P32.075

GLOBAL
UNIT 500
ARRAY 10 3*0
REFLECTOR  5  1  6R30.48  1
END GEOM

READ ARRAY
ARA=1 NUX=1 NUY=1 NUZ=2
FILL 1 2
END FILL
ARA=2 NUX=5  NUY=1 NUZ=5
```

```
FILL 10 10 10 10 10
     10 10 10 10 10
     10 10 10 10 10
     10 10 10 10 10
     10 10 10 10 10
END FILL
ARA=10 NUX=21 NUY=3  NUZ=24
FILL F400
END FILL
END ARRAY

READ BNDS ALL=VACUUM
END BNDS
END DATA
END
```

6.11.8 Package Array Loose Fuel Rods Hypothetical Accident Conditions Input

```
=CSAS25             PARM=SIZE=500000
RAJ-II CONTAINER, 8, HAC, 100% H2O, WORST CASE MODEL, 3.0056 CM PITCH, LOOSE
FUEL RODS, 10 X 1 X 10 ARRAY
44GROUPNDF5                 LATTICECELL
UO2            1  DEN=10.74 1.0 293 92235 5.0 92238 95.0      END
POLYETHYLENE   2  DEN=0.925    1.0    293                     END
H2O            3  1.00                293                     END
H2O            5  1.00 293                                    END
SS304          6  1.00 293                                    END
POLYETHYLENE   7  DEN=0.08000  1.0  293                       END
H2O            8  DEN=1.00     1.0    293                     END
ZR             9  1.00 293                                    END
ARBMAL2O3      0.25 2 0 1 0 13027 2 8016 3 10  0.49           END
ARBMSIO2       0.25 2 0 1 0 14000 1 8016 2 10  0.51           END
END COMP
SQUAREPITCH 3.0056 1.0500 1 8 1.13048 2 1.100 0               END
RAJ-II CONTAINER, 8, HAC, 100% H2O, WORST CASE MODEL, 3.0056 CM PITCH, LOOSE
FUEL RODS, 10 X 1 X 10 ARRAY
READ PARM TME=400 GEN=400 NPG=2500 NSK=50 NUB=YES END PARM
READ GEOM

UNIT  1
COM=!CONTAINER INNER BOX!
'DEFINE GEOMETRY FOR SEPARATOR PLATE BETWEEN ASSEMBLY COMPARTMENTS
CUBOID     6  1  2P0.0875   225.20  -228.34  2P8.829
'DEFINE REGION FOR ASSEMBLY COMPARTMENTS WITHIN INNER BOX
CUBOID     7  1  2P17.713   225.20  -228.34  2P8.829
'PLACE THE FUEL ASSEMBLIES INSIDE INNER BOX
HOLE       30     -15.913  -190.50  -7.014
HOLE       30       1.886  -190.50  -7.014
'DEFINE WALLS FOR ASSEMBLY COMPARTMENTS WITHIN INNER BOX
CUBOID     6  1  2P17.800   225.20  -228.34  8.829  -8.9165
'DEFINE REGION OUTSIDE THE WALLS OF THE ASSEMBLY COMPARTMENTS
CUBOID     10 1  2P22.798   225.20  -228.34  8.829  -13.839
'DEFINE THE INNER WALLS OF THE BOX ENDS
CUBOID     6  1  2P22.798   225.34  -228.48  8.829  -13.979
'DEFINE INNER CORE OF BOX ENDS -8.1CM IN Y FOR TOTAL DEFORMATION
CUBOID     10 1  2P22.798   225.34  -233.44  8.829  -13.979
'DEFINE OUTER WALLS OF THE INNER BOX -8.1CM IN Y FOR TOTAL DEFORMATION
CUBOID     6  1  2P22.938   225.48  -233.58  8.829  -13.979

UNIT 2
COM=!INNER BOX LID!
'DEFINE INNER CORE OF INNER BOX LID -8.1CM IN Y FOR TOTAL DEFORMATION
CUBOID    10 1  2P22.798    2P229.39   2P2.48
'DEFINE WALLS FOR INNER BOX LID -8.1CM IN Y FOR TOTAL DEFORMATION
CUBOID    6  1  2P22.938    2P229.53   2P2.62

UNIT 3
COM=!INNER BOX WITH ENDS AND LID!
ARRAY 1 3*0
```

```
UNIT 10
COM=!5 W/O FUEL PINS W/O GAD!
'DEFINE THE FUEL PELLET
YCYLINDER 1  1    0.52500  381  0
'DEFINE THE PELLET-CLAD GAP
YCYLINDER 0  1    0.55000  381  0
'DEFINE THE FUEL ROD CLADDING
YCYLINDER 2  1    0.56524  381  0
'DEFINE THE FUEL ROD PITCH FILLED WITH WATER
CUBOID    8  1  2P1.50280  381  0  2P1.50280

UNIT 20
COM=!SPACE WITHIN FUEL ASSEMBLY LATTICE!
CUBOID    8  1  2P1.50280  381  0  2P1.50280

UNIT 30
COM=!ARRAY FOR COMPLETE FUEL ASSEMBLY!
ARRAY 2 3*0

UNIT 40
COM=!5 W/O FUEL PINS W/O GAD LEFT SIDE FOAM!
'DEFINE THE FUEL PELLET
YCYLINDER 1  1    0.52500  381  0
'DEFINE THE PELLET-CLAD GAP
YCYLINDER 0  1    0.55000  381  0
'DEFINE THE FUEL ROD CLADDING
YCYLINDER 2  1    0.56524  381  0
'DEFINE THE FUEL ROD PITCH FILLED WITH WATER
CUBOID    8  1    1.50280  -1.00280 381  0  2P1.50280

UNIT 46
COM=!5 W/O FUEL PINS W/O GAD LEFT SIDE TOP FOAM!
'DEFINE THE FUEL PELLET
YCYLINDER 1  1    0.52500  381  0
'DEFINE THE PELLET-CLAD GAP
YCYLINDER 0  1    0.55000  381  0
'DEFINE THE FUEL ROD CLADDING
YCYLINDER 2  1    0.56524  381  0
'DEFINE THE FUEL ROD PITCH FILLED WITH WATER
CUBOID    8  1    1.50280  -1.00280 381  0    1.00280  -1.50280

UNIT 47
COM=!5 W/O FUEL PINS W/O GAD LEFT SIDE BOTTOM FOAM!
'DEFINE THE FUEL PELLET
YCYLINDER 1  1    0.52500  381  0
'DEFINE THE PELLET-CLAD GAP
YCYLINDER 0  1    0.55000  381  0
'DEFINE THE FUEL ROD CLADDING
YCYLINDER 2  1    0.56524  381  0
'DEFINE THE FUEL ROD PITCH FILLED WITH WATER
CUBOID    8  1    1.50280  -1.00280 381  0    1.50280  -1.00280

UNIT 50
COM=!5 W/O FUEL PINS W/O GAD RIGHT SIDE FOAM!
'DEFINE THE FUEL PELLET
YCYLINDER 1  1    0.52500  381  0
'DEFINE THE PELLET-CLAD GAP
```

```
YCYLINDER 0  1    0.55000  381  0
'DEFINE THE FUEL ROD CLADDING
YCYLINDER 2  1    0.56524  381  0
'DEFINE THE FUEL ROD PITCH FILLED WITH WATER
CUBOID    8  1    1.00280  -1.50280 381  0  2P1.50280

UNIT 56
COM=!5 W/O FUEL PINS W/O GAD RIGHT SIDE TOP FOAM!
'DEFINE THE FUEL PELLET
YCYLINDER 1  1    0.52500  381  0
'DEFINE THE PELLET-CLAD GAP
YCYLINDER 0  1    0.55000  381  0
'DEFINE THE FUEL ROD CLADDING
YCYLINDER 2  1    0.56524  381  0
'DEFINE THE FUEL ROD PITCH FILLED WITH WATER
CUBOID    8  1    1.00280  -1.50280 381  0    1.00280  -1.50280

UNIT 57
COM=!5 W/O FUEL PINS W/O GAD RIGHT BOTTOM SIDE FOAM!
'DEFINE THE FUEL PELLET
YCYLINDER 1  1    0.52500  381  0
'DEFINE THE PELLET-CLAD GAP
YCYLINDER 0  1    0.55000  381  0
'DEFINE THE FUEL ROD CLADDING
YCYLINDER 2  1    0.56524  381  0
'DEFINE THE FUEL ROD PITCH FILLED WITH WATER
CUBOID    8  1    1.00280  -1.50280 381  0    1.50280  -1.00280

UNIT 60
COM=!5 W/O FUEL PINS W/O GAD TOP SIDE FOAM!
'DEFINE THE FUEL PELLET
YCYLINDER 1  1    0.52500  381  0
'DEFINE THE PELLET-CLAD GAP
YCYLINDER 0  1    0.55000  381  0
'DEFINE THE FUEL ROD CLADDING
YCYLINDER 2  1    0.56524  381  0
'DEFINE THE FUEL ROD PITCH FILLED WITH WATER
CUBOID    8  1  2P1.50280  381  0    1.00280  -1.50280

UNIT 70
COM=!5 W/O FUEL PINS W/O GAD BOTTOM SIDE FOAM!
'DEFINE THE FUEL PELLET
YCYLINDER 1  1    0.52500  381  0
'DEFINE THE PELLET-CLAD GAP
YCYLINDER 0  1    0.55000  381  0
'DEFINE THE FUEL ROD CLADDING
YCYLINDER 2  1    0.56524  381  0
'DEFINE THE FUEL ROD PITCH FILLED WITH WATER
CUBOID    8  1  2P1.50280  381  0    1.50280  -1.00280

UNIT 400
COM=!OUTER CONTAINER BODY AND LID!
'DEFINE INNER REGION OF THE OUTER CONTAINER
'MINUS 4.7CM IN Y AND -2.4CM IN Z FOR TOTAL DEFORMATION
CUBOID    0  1   2P35.788  247.960  -253.190  29.500  -31.900
'INNER CONTAINER PLACEMENT WITHIN OUTER CONTAINER
HOLE 3          -22.938      -229.53    -14.024
```

```
'DEFINE WALLS OF THE OUTER CONTAINER AND LID
CUBOID    6  1   2P35.963  248.135  -253.365  29.675  -32.075

GLOBAL
UNIT 500
ARRAY 10 3*0
REFLECTOR  5  1  6R30.48  1
END GEOM

READ ARRAY
ARA=1 NUX=1 NUY=1 NUZ=2
FILL 1 2
END FILL
ARA=2 NUX=5  NUY=1 NUZ=5
FILL 47 70 70 70 57
     40 10 10 10 50
     40 10 10 10 50
     40 10 10 10 50
     46 60 60 60 56
END FILL
ARA=10 NUX=10 NUY=1 NUZ=10
FILL F400
END FILL
END ARRAY

READ BNDS ALL=VACUUM
END BNDS
END DATA
END
```

6.11.9 Data Tables for Figures in RAJ-II CSE

Table 6-26 Data for Figure 6-25 RAJ-II Array HAC Polyethylene Sensitivity

Output File Name	Case Description	Interspersed Moderator Density (g/cm^3)	Polyethylene Mass (kg)	k_{eff}	σ	$k_{eff} + 2\sigma$
rajII_hac_a10_no interspersedh2o_ polyethylenesens itivity_1.284cmpit ch_14X2X16	Atrium 10XP+	0.00	0	0.8715	0.0008	0.8731
"	Atrium 10XP+	0.00	10.9	0.8774	0.0009	0.8792
"	Atrium 10XP+	0.00	17.1	0.8813	0.0009	0.8831
"	Atrium 10XP+	0.00	20.4	0.8810	0.0008	0.8826
"	Atrium 10XP+	0.00	22.9	0.8822	0.0009	0.8840
"	Atrium 10XP+	0.00	25.4	0.8847	0.0008	0.8863
"	Atrium 10XP+	0.00	27.9	0.8860	0.001	0.8880
rajII_hac_g10_no interspersedh2o_ polyethylenesens itivity_pitch1.295 4cm_14X2X16	GNF 10 x 10	0.00	0	0.8863	0.0007	0.8877
"	GNF 10 x 10	0.00	10.9	0.8923	0.0008	0.8939
"	GNF 10 x 10	0.00	17.1	0.8940	0.0008	0.8956
"	GNF 10 x 10	0.00	20.4	0.8955	0.0007	0.8969
"	GNF 10 x 10	0.00	22.9	0.8975	0.0009	0.8993
"	GNF 10 x 10	0.00	25.4	0.8994	0.0008	0.9010
"	GNF 10 x 10	0.00	27.9	0.9001	0.0008	0.9017
rajII_hac_f9_10g adrods_refassy_ 14x2x16_polysen s	FANP 9x9	0.00	0	0.8728	0.0009	0.8746
rajII_hac_f9_10g adrods_refassy_ 14x2x16_polysen s	FANP 9x9	0.00	20	0.8756	0.0009	0.8774

rajII_hac_f9_10gadrods_refassy_14x2x16_channels	FANP 9x9	0.00	22	0.8755	0.0009	0.8773
rajII_hac_f9_10gadrods_refassy_14x2x16_polysens	FANP 9x9	0.00	24	0.8769	0.0007	0.8783
rajII_hac_f9_10gadrods_refassy_14x2x16_polysens	FANP 9x9	0.00	26	0.8758	0.0008	0.8774
rajII_hac_f9_10gadrods_refassy_14x2x16_polysens	FANP 9x9	0.00	28	0.8766	0.0008	0.8782
rajII_hac_f9_10gadrods_refassy_14x2x16_polysens	FANP 9x9	0.00	30	0.8776	0.0009	0.8794
rajII_hac_g9_10gadrods_refassy_14X2X16_polyses	GNF 9x9	0.00	0	0.8612	0.0008	0.8628
rajII_hac_g9_10gadrods_refassy_14X2X16_polyses	GNF 9x9	0.00	20	0.8661	0.0009	0.8679
rajII_hac_g9_10gadrods_refassy_14X2X16_channels	GNF 9x9	0.00	22	0.8659	0.0008	0.8676
rajII_hac_g9_10gadrods_refassy_14X2X16_polyses	GNF 9x9	0.00	24	0.8676	0.0007	0.8690
rajII_hac_g9_10gadrods_refassy_14X2X16_polyses	GNF 9x9	0.00	26	0.8670	0.0009	0.8688
rajII_hac_g9_10gadrods_refassy_14X2X16_polyses	GNF 9x9	0.00	28	0.8656	0.0009	0.8674
rajII_hac_g9_10gadrods_refassy_14X2X16_polyses	GNF 9x9	0.00	30	0.8702	0.0008	0.8718

rajII_hac_g8_noi nterspersedh2o_ polyethylenesens itivity_1.6256cm_ 14X2X16	GNF 8x8	0.00	0	0.8795	0.0009	0.8813
“	GNF 8x8	0.00	19	0.8865	0.0009	0.8883
“	GNF 8x8	0.00	22	0.8900	0.0009	0.8918
“	GNF 8x8	0.00	24	0.8892	0.0008	0.8908
“	GNF 8x8	0.00	26	0.8924	0.0008	0.8940
“	GNF 8x8	0.00	28	0.8915	0.0009	0.8933
“	GNF 8x8	0.00	30	0.8942	0.0009	0.8960

Table 6-27 Data for Figure 6-26 RAJ-II Fuel Rod Pitch Sensitivity Study

Output File Name	Interspersed Moderator Density (g/cm^3)	Polyethylene Mass (kg)	Pitch (cm)	k_{eff}	σ	$k_{eff} + 2\sigma$
rajII_hac_a10_nointerspersedh2o_pitchsensitivity_14X2X16	0.00	20.4	1.210	0.8301	0.0010	0.8321
"	0.00	20.4	1.284	0.8810	0.0008	0.8826
"	0.00	20.4	1.350	0.9245	0.0009	0.9263
"	0.00	20.4	1.376	0.9391	0.0008	0.9407
rajII_hac_g10_nointerspersedh2o_pitchsensitivity_14X2X16	0.00	20.4	1.1960	0.8394	0.0009	0.8412
"	0.00	20.4	1.2954	0.8955	0.0007	0.8969
"	0.00	20.4	1.350	0.9241	0.0008	0.9257
"	0.00	20.4	1.3760	0.9328	0.0008	0.9344
rajII_hac_f9_10gadrods_refassy_14x2x16_pitch	0.00	22	1.3389	0.8219	0.0008	0.8235
"	0.00	22	1.4478	0.8755	0.0009	0.8773
"	0.00	22	1.5028	0.8998	0.0008	0.9014
rajII_hac_f9_10gadrods_refassy_14x2x16_channels	0.00	22	1.5376	0.9126	0.0009	0.9144
rajII_hac_g9_10gadrods_refassy_14X2X16_pitchsens	0.00	22	1.3260	0.8073	0.0008	0.8089
"	0.00	22	1.4376	0.8659	0.0008	0.8676
"	0.00	22	1.5028	0.8929	0.0008	0.8944
rajII_hac_g9_10gadrods_refassy_14X2X16_channels	0.00	22	1.5376	0.9076	0.0009	0.9095
rajII_hac_g8_nointerspersedh2o_pitchsensitivity_14X2X16	0.00	22	1.4603	0.7968	0.0009	0.7986
"	0.00	22	1.6256	0.8900	0.0009	0.8918
"	0.00	22	1.6923	0.9216	0.0008	0.9232
"	0.00	22	1.7264	0.9384	0.0008	0.9400

Table 6-28 Data for Figure 6-27 RAJ-II Array HAC Pellet Diameter Sensitivity Study

Output File Name	Interspersed Moderator Density (g/cm^3)	Pellet Diameter (cm)	k_{eff}	σ	$k_{eff} + 2\sigma$
rajII_hac_a10_nointerspersedh2o_pelletodsensitivity_14X2X16	0	0.8000	0.8560	0.0008	0.8576
"	0	0.8400	0.8680	0.0009	0.8698
"	0	0.8882	0.8810	0.0008	0.8826
"	0	0.8941	0.8839	0.0008	0.8855
"	0	0.9200	0.8906	0.0008	0.8922
rajII_hac_g10_nointerspersedh2o_pelletodsensitivity_14X2X16	0	0.8000	0.8641	0.0009	0.8659
"	0	0.8400	0.8796	0.0009	0.8814
"	0	0.8882	0.8941	0.0008	0.8957
"	0	0.8941	0.8955	0.0007	0.8969
"	0	0.9200	0.9050	0.0008	0.9066
rajII_hac_f9_10gadrods_refassy_14x2x16_pelletod	0	0.8882	0.8600	0.0008	0.8616
"	0	0.9000	0.8633	0.0009	0.8651
rajII_hac_f9_10gadrods_refassy_14x2x16_channels	0	0.9398	0.8755	0.0009	0.8773
rajII_hac_f9_10gadrods_refassy_14x2x16_pelletod	0	0.9550	0.8799	0.0008	0.8815
"	0	0.9600	0.8817	0.0007	0.8831
rajII_hac_g9_10gadrods_refassy_14X2X16_pelletodsens	0	0.8882	0.8462	0.0008	0.8478
"	0	0.9000	0.8509	0.0009	0.8527
"	0	0.9398	0.8609	0.0008	0.8625
rajII_hac_g9_10gadrods_refassy_14X2X16_channels	0	0.9550	0.8659	0.0008	0.8676
rajII_hac_g9_10gadrods_refassy_14X2X16_pelletodsens	0	0.9600	0.8678	0.0008	0.8694
rajII_hac_g8_nointerspersedh2o_pelletodsensitivity_14X2X16	0	0.9200	0.8566	0.0008	0.8582
"	0	0.9550	0.8648	0.0008	0.8664
"	0	1.0000	0.8783	0.0008	0.8799
"	0	1.0439	0.8900	0.0009	0.8918
"	0	1.0700	0.8940	0.0009	0.8958

Table 6-29 Data for Figure 6-28 RAJ-II Array HAC Fuel Rod Clad ID Sensitivity Study

Output File Name	Moderator Density (g/cm^3)	Clad Inner Diameter (cm)	k_{eff}	σ	$k_{eff} + 2\sigma$
rajII_hac_a10_nointersperse dh2o_cladidsensitivity _14X2X16	0	0.8800	0.8760	0.0009	0.8778
"	0	0.8900	0.8805	0.0009	0.8823
"	0	0.9218	0.8810	0.0008	0.8826
"	0	0.9322	0.8813	0.0008	0.8829
"	0	1.0330	0.8855	0.0010	0.8875
rajII_hac_g10_nointersperse dh2o_cladidsensitivity _14X2X16	0	0.9000	0.8937	0.0010	0.8957
"	0	0.9218	0.8956	0.0008	0.8972
"	0	0.9322	0.8955	0.0007	0.8969
"	0	1.0185	0.8999	0.0008	0.9015
rajII_hac_f9_10gadrods_r efassy_14x2x16_cladid	0	0.9400	0.8742	0.0009	0.8759
rajII_hac_f9_10gadrods_r efassy_14x2x16_channel s	0	0.9601	0.8755	0.0009	0.8773
rajII_hac_f9_10gadrods_r efassy_14x2x16_cladid	0	0.9750	0.8760	0.0009	0.8777
"	0	0.9830	0.8768	0.0009	0.8786
"	0	1.0998	0.8789	0.0008	0.8804
rajII_hac_g9_10gadrods_ refassy_14X2X16_cladid	0	0.9560	0.8641	0.0008	0.8657
"	0	0.9600	0.8643	0.0008	0.8659
"	0	0.9750	0.8660	0.0009	0.8678
rajII_hac_g9_10gadrods_ refassy_14X2X16_chann els	0	0.9830	0.8659	0.0008	0.8676
rajII_hac_g9_10gadrods_ refassy_14X2X16_cladid	0	1.1100	0.8702	0.0008	0.8718
rajII_hac_g8_nointersper sedh2o_cladidsensitivity_ 14X2X16	0	1.0440	0.8894	0.001	0.8914
"	0	1.0719	0.8900	0.0009	0.8918
"	0	1.1000	0.8900	0.0009	0.8918
"	0	1.1500	0.8918	0.0008	0.8934
"	0	1.2192	0.8917	0.0008	0.8933

Table 6-30 Data for Figure 6-29 RAJ-II Array HAC Fuel Rod Clad OD Sensitivity Study

Output File Name	Moderator Density (g/cm^3)	Clad Outer Diameter (cm)	k_{eff}	σ	$k_{eff} + 2\sigma$
rajII_hac_a10_nointerspersedh2o_cladodsensitivity_14X2X16	0	0.9218	0.9051	0.0008	0.9067
"	0	1.0185	0.8858	0.0009	0.8876
"	0	1.0330	0.8810	0.0008	0.8826
"	0	1.1000	0.8647	0.0008	0.8663
"	0	1.1210	0.8604	0.0009	0.8622
rajII_hac_g10_nointerspersedh2o_cladodsensitivity_14X2X16	0	0.9322	0.9118	0.0008	0.9134
"	0	1.0185	0.8955	0.0007	0.8969
"	0	1.0330	0.8935	0.0008	0.8951
"	0	1.1000	0.8790	0.0008	0.8806
"	0	1.1210	0.8742	0.0009	0.8760
rajII_hac_f9_10gadrods_refassy_14x2x16_cladod	0	0.9601	0.8967	0.0008	0.8984
"	0	1.0330	0.8876	0.0008	0.8892
"	0	1.0998	0.8792	0.0008	0.8808
rajII_hac_f9_10gadrods_refassy_14x2x16_channels	0	1.1200	0.8755	0.0009	0.8773
rajII_hac_g9_10gadrods_refassy_14X2X16_cladod	0	0.9830	0.8857	0.0008	0.8873
"	0	1.0330	0.8791	0.0009	0.8809
rajII_hac_g9_10gadrods_refassy_14X2X16_channels	0	1.1100	0.8659	0.0008	0.8676
rajII_hac_g9_10gadrods_refassy_14X2X16_cladod	0	1.1200	0.8644	0.0010	0.8664
rajII_hac_g8_nointerspersedh2o_cladodsensitivity_14X2X16	0	1.0719	0.9120	0.0008	0.9136
"	0	1.1500	0.9030	0.0008	0.9046
"	0	1.2192	0.8900	0.0009	0.8918
"	0	1.2500	0.8832	0.0008	0.8848

Table 6-31 Data For Figure 6-37 Moderator Density Sensitivity Study for the RAJ-II HAC Worst Case Parameter Fuel Design

Output File Name	Moderator Density (g/cm^3)	Clad Inner Diameter (cm)	Clad Outer Diameter (cm)	k_{eff}	σ	$k_{eff} + 2\sigma$
rajII_hac_g10_worstcase_moderatordensity_14X2X16	0.00	0.9338	1.010	0.7154	0.0006	0.7166
"	0.02	0.9338	1.010	0.7349	0.0007	0.7363
"	0.04	0.9338	1.010	0.7526	0.0007	0.7540
"	0.06	0.9338	1.010	0.7686	0.0006	0.7698
"	0.08	0.9338	1.010	0.7820	0.0007	0.7834
"	0.10	0.9338	1.010	0.7933	0.0008	0.7949
"	0.20	0.9338	1.010	0.8383	0.0007	0.8397
"	0.40	0.9338	1.010	0.8908	0.0007	0.8922
"	0.60	0.9338	1.010	0.9182	0.0009	0.9200
"	0.80	0.9338	1.010	0.9319	0.0008	0.9335
"	1.00	0.9338	1.010	0.9404	0.0007	0.9418

Table 6-32 Data for Figure 6-39 RAJ-II Single Package Normal Conditions of Transport Results

Output File Name	Fuel Assembly Type	Moderator Density (g/cm^3)	Gadolinia Rod (#)	Pitch (cm)	Pellet OD (cm)	Clad Inner Diameter (cm)	Clad Outer Diameter (cm)	k_{eff}	σ	$k_{eff} + 2\sigma$
rajII_normal_g10_5.0wtpct235u_h2odensitysensitivity_12gadrods_singlepackage	GNF 10 x 10	0.00	12	1.35	0.895	0.9338	1.010	0.2833	0.0005	0.2843
"	GNF 10 x 10	0.02	12	1.35	0.895	0.9338	1.010	0.2899	0.0005	0.2909
"	GNF 10 x 10	0.04	12	1.35	0.895	0.9338	1.010	0.2966	0.0006	0.2978
"	GNF 10 x 10	0.06	12	1.35	0.895	0.9338	1.010	0.3071	0.0006	0.3083
"	GNF 10 x 10	0.08	12	1.35	0.895	0.9338	1.010	0.3178	0.0006	0.3190
"	GNF 10 x 10	0.10	12	1.35	0.895	0.9338	1.010	0.3297	0.0005	0.3307
"	GNF 10 x 10	0.20	12	1.35	0.895	0.9338	1.010	0.3899	0.0006	0.3911
"	GNF 10 x 10	0.40	12	1.35	0.895	0.9338	1.010	0.4848	0.0008	0.4864
"	GNF 10 x 10	0.60	12	1.35	0.895	0.9338	1.010	0.5597	0.0008	0.5613
"	GNF 10 x 10	0.80	12	1.35	0.895	0.9338	1.010	0.6180	0.0007	0.6194
"	GNF 10 x 10	1.00	12	1.35	0.895	0.9338	1.010	0.6673	0.0008	0.6689

Table 6-33 Data for Figure 6-40 RAJ-II Single Package HAC Results

Output File Name	Fuel Assembly Type	Inner Container Moderator Density (g/cm^3)	Gadolinia Fuel Rods (#)	Pitch (cm)	Pellet OD (cm)	Clad Inner Diameter (cm)	Clad Outer Diameter (cm)	k_{eff}	σ	$k_{eff} + 2\sigma$
rajII_hac_g10__worstcase_moderatordensity_singlepackage	GNF 10 x 10	0.00	12	1.35	0.895	0.9338	1.010	0.2794	0.0005	0.2804
"	GNF 10 x 10	0.02	12	1.35	0.895	0.9338	1.010	0.2850	0.0005	0.2860
"	GNF 10 x 10	0.04	12	1.35	0.895	0.9338	1.010	0.2902	0.0005	0.2912
"	GNF 10 x 10	0.06	12	1.35	0.895	0.9338	1.010	0.2967	0.0006	0.2979
"	GNF 10 x 10	0.08	12	1.35	0.895	0.9338	1.010	0.3041	0.0006	0.3053
"	GNF 10 x 10	0.10	12	1.35	0.895	0.9338	1.010	0.3111	0.0005	0.3121
"	GNF 10 x 10	0.20	12	1.35	0.895	0.9338	1.010	0.3546	0.0006	0.3558
"	GNF 10 x 10	0.40	12	1.35	0.895	0.9338	1.010	0.4526	0.0007	0.4540
"	GNF 10 x 10	0.60	12	1.35	0.895	0.9338	1.010	0.5468	0.0008	0.5484
"	GNF 10 x 10	0.80	12	1.35	0.895	0.9338	1.010	0.6274	0.0008	0.6290
rajII_hac_g10_100pcth20density_worstcase_singlepackage	GNF 10 x 10	1.00	12	1.35	0.895	0.9338	1.010	0.6931	0.0010	0.6951

Table 6-34 Data for Figure 6-41 RAJ-II Package Array Under Normal Conditions of Transport Results

Output File Name	Fuel Assembly Type	Interspersed Moderator Density (g/cm^3)	Part Length Fuel Rods (#)	Pitch (cm)	Pellet OD (cm)	Clad Inner Diameter (cm)	Clad Outer Diameter (cm)	k_{eff}	σ	$k_{eff} + 2\sigma$
rajII_normal_g10_5.0wtpct235u_h2odensitysensitivity_12gadrods_21X3X24	GNF 10 x 10	0.00	12	1.35	0.895	0.9338	1.010	0.8519	0.0008	0.8535
"	GNF 10 x 10	0.02	12	1.35	0.895	0.9338	1.010	0.7962	0.0007	0.7976
"	GNF 10 x 10	0.04	12	1.35	0.895	0.9338	1.010	0.7441	0.0007	0.7455
"	GNF 10 x 10	0.06	12	1.35	0.895	0.9338	1.010	0.7054	0.0008	0.7070
"	GNF 10 x 10	0.08	12	1.35	0.895	0.9338	1.010	0.6726	0.0008	0.6742
"	GNF 10 x 10	0.10	12	1.35	0.895	0.9338	1.010	0.6427	0.0008	0.6443
"	GNF 10 x 10	0.20	12	1.35	0.895	0.9338	1.010	0.5500	0.0008	0.5516
"	GNF 10 x 10	0.40	12	1.35	0.895	0.9338	1.010	0.5254	0.0007	0.5268
"	GNF 10 x 10	0.60	12	1.35	0.895	0.9338	1.010	0.5690	0.0007	0.5704
"	GNF 10 x 10	0.80	12	1.35	0.895	0.9338	1.010	0.6206	0.0007	0.6220
"	GNF 10 x 10	1.00	12	1.35	0.895	0.9338	1.010	0.6683	0.0008	0.6699

Table 6-35 Data for Figure 6-42 RAJ-II Package Array Hypothetical Accident Condition Results

Output File Name	Fuel Assembly Type	Inner Container Moderator Density (g/cm^3)	Gadolinia-urania Fuel Rods (#)	Pitch (cm)	Pellet OD (cm)	Clad Inner Diameter (cm)	Clad Outer Diameter (cm)	k_{eff}	σ	$k_{eff} + 2\sigma$
rajII_hac_g10_12partlengthrods_worstcase_moderatordensity_10X1X10	GNF 10 x 10	0.00	12	1.35	0.895	0.9338	1.010	0.6375	0.0007	0.6389
"	GNF 10 x 10	0.02	12	1.35	0.895	0.9338	1.010	0.6470	0.0007	0.6484
"	GNF 10 x 10	0.04	12	1.35	0.895	0.9338	1.010	0.6567	0.0007	0.6581
"	GNF 10 x 10	0.06	12	1.35	0.895	0.9338	1.010	0.6648	0.0007	0.6662
"	GNF 10 x 10	0.08	12	1.35	0.895	0.9338	1.010	0.6734	0.0007	0.6748
"	GNF 10 x 10	0.10	12	1.35	0.895	0.9338	1.010	0.6822	0.0007	0.6836
"	GNF 10 x 10	0.20	12	1.35	0.895	0.9338	1.010	0.7226	0.0007	0.7240
"	GNF 10 x 10	0.40	12	1.35	0.895	0.9338	1.010	0.7976	0.0007	0.7990
"	GNF 10 x 10	0.60	12	1.35	0.895	0.9338	1.010	0.8561	0.0009	0.8579
"	GNF 10 x 10	0.80	12	1.35	0.895	0.9338	1.010	0.9005	0.0008	0.9021
"	GNF 10 x 10	1.00	12	1.35	0.895	0.9338	1.010	0.9378	0.0009	0.9396

Table 6-36 Data for Figure 6-45 RAJ-II Fuel Rod Transport in Stainless Steel Pipe

Output File Name	Fuel Assembly Type	Interspersed Moderator Density (g/cm^3)	Pitch (cm)	Fuel Rod (#)	Pellet OD (cm)	Clad Inner Diameter (cm)	Clad Outer Diameter (cm)	k_{eff}	σ	$k_{eff} + 2\sigma$
rajII_hac_8_worstcase_sspipe_14x2x16	8x8	1.000	1.1305	110	1.05	1.1000	1.1000	0.8793	0.0007	0.8807
"	8x8	1.000	1.6662	52	1.05	1.1000	1.1000	1.0235	0.0009	1.0253
"	8x8	1.000	1.9035	43	1.05	1.1000	1.1000	1.0440	0.0008	1.0456
rajII_hac_8_worstcase_sspipe_22fuelrods_14x2x16	8x8	1.000	2.5	22	1.05	1.1000	1.1000	0.8823	0.0008	0.8839
rajII_hac_8_worstcase_sspipe_14x2x16	8x8	1.000	2.937	14	1.05	1.1000	1.1000	0.7294	0.0008	0.7310
rajII_hac_9_worstcase_sspipe_14x2x16	9x9	1.000	1.0505	140	0.9600	1.0200	1.0200	0.8701	0.0006	0.8713
"	9x9	1.000	1.4770	72	0.9600	1.0200	1.0200	1.0515	0.0008	1.0531
"	9x9	1.000	2	38	0.9600	1.0200	1.0200	1.0056	0.0009	1.0074
rajII_hac_9_worstcase_sspipe_26fuelrods_14x2x16	9x9	1.000	2.25	26	0.9600	1.0200	1.0200	0.8900	0.0008	0.8916
rajII_hac_9_worstcase_sspipe_14x2x16	9x9	1.000	2.5432	22	0.9600	1.0200	1.0200	0.8416	0.0010	0.8436

Output File Name	Fuel Assembly Type	Interspersed Moderator Density (g/cm^3)	Pitch (cm)	Fuel Rod (#)	Pellet OD (cm)	Clad Inner Diameter (cm)	Clad Outer Diameter (cm)	k_{eff}	σ	$k_{eff} + 2\sigma$
rajII_hac_10_worstcase_sspipe_14x2x16	10x10	1.000	1.0305	144	0.9	1.000	1.000	0.8666	0.0007	0.8680
"	10x10	1.000	1.3213	84	0.9	1.000	1.000	1.0070	0.0008	1.0086
"	10x10	1.000	1.6416	56	0.9	1.000	1.000	1.0310	0.0011	1.0332
"	10x10	1.000	2.0484	30	0.9	1.000	1.000	0.8863	0.0008	0.8879

Table 6-37 Data for Figure 6-46 RAJ-II Fuel Rod Single Package Under Normal Conditions of Transport

Output File Name	Fuel Assembly Type	Interspersed Moderator Density (g/cm^3)	Pitch (cm)	Fuel Rod Number (#)	Pellet OD (cm)	Clad Inner Diameter (cm)	Clad Outer Diameter (cm)	k_{eff}	σ	$k_{eff} + 2\sigma$
rajII_normal_8_worstcasefuel_fuelrodtransport_moderatordensitysensitivity_singlepackage	8x8	0.00	2.815	25	1.05	1.1000	1.1000	0.1675	0.0004	0.1683
"	8x8	0.01	2.815	25	1.05	1.1000	1.1000	0.1675	0.0004	0.1683
"	8x8	0.02	2.815	25	1.05	1.1000	1.1000	0.1672	0.0004	0.1680
"	8x8	0.04	2.815	25	1.05	1.1000	1.1000	0.1702	0.0004	0.1710
"	8x8	0.06	2.815	25	1.05	1.1000	1.1000	0.1757	0.0005	0.1767
"	8x8	0.08	2.815	25	1.05	1.1000	1.1000	0.1845	0.0005	0.1855
"	8x8	0.10	2.815	25	1.05	1.1000	1.1000	0.1949	0.0004	0.1957
"	8x8	0.20	2.815	25	1.05	1.1000	1.1000	0.2567	0.0005	0.2577
"	8x8	0.40	2.815	25	1.05	1.1000	1.1000	0.3890	0.0007	0.3904
"	8x8	0.60	2.815	25	1.05	1.1000	1.1000	0.4967	0.0007	0.4981
"	8x8	0.80	2.815	25	1.05	1.1000	1.1000	0.5783	0.0009	0.5801
"	8x8	1.00	2.815	25	1.05	1.1000	1.1000	0.6365	0.0008	0.6381

Table 6-38 Data for Figure 6-47 RAJ-II Fuel Rod Transport Single Package HAC

Output File Name	Fuel Assembly Type	Interspersed Moderator Density (g/cm^3)	Pitch (cm)	Fuel Rod Number (#)	Pellet OD (cm)	Clad Inner Diameter (cm)	Clad Outer Diameter (cm)	k_{eff}	σ	$k_{eff} + 2\sigma$
rajII_hac_8_worstcase_fuelrodtransport_moderatordensitysensitivity_singlepackage	8x8	0.00	3.0056	25	1.05	1.1000	1.1000	0.1769	0.0004	0.1777
"	8x8	0.01	3.0056	25	1.05	1.1000	1.1000	0.1761	0.0004	0.1769
"	8x8	0.02	3.0056	25	1.05	1.1000	1.1000	0.1767	0.0004	0.1775
"	8x8	0.04	3.0056	25	1.05	1.1000	1.1000	0.1778	0.0005	0.1788
"	8x8	0.06	3.0056	25	1.05	1.1000	1.1000	0.1794	0.0004	0.1802
"	8x8	0.08	3.0056	25	1.05	1.1000	1.1000	0.1829	0.0004	0.1837
"	8x8	0.10	3.0056	25	1.05	1.1000	1.1000	0.1876	0.0004	0.1884
"	8x8	0.20	3.0056	25	1.05	1.1000	1.1000	0.2306	0.0005	0.2316
"	8x8	0.40	3.0056	25	1.05	1.1000	1.1000	0.3718	0.0007	0.3732
"	8x8	0.60	3.0056	25	1.05	1.1000	1.1000	0.5062	0.0007	0.5076
"	8x8	0.80	3.0056	25	1.05	1.1000	1.1000	0.5980	0.0008	0.5996
"	8x8	1.00	3.0056	25	1.05	1.1000	1.1000	0.6532	0.0008	0.6548

Table 6-39 Data for Figure 6-48 RAJ-II Package Array Under Normal Conditions of Transport with Loose Fuel Rods

Output File Name	Fuel Assembly Type	Interspersed Moderator Density (g/cm^3)	Pitch (cm)	Fuel Rod Number (#)	Pellet OD (cm)	Clad Inner Diameter (cm)	Clad Outer Diameter (cm)	k_{eff}	σ	$k_{eff} + 2\sigma$
rajII_normal_8_worstcasefuel_fuelrodtransport_moderatordensitysensitivity_21X3X24	8x8	0.00	2.815	25	1.05	1.1000	1.1000	0.5055	0.0006	0.5067
"	8x8	0.01	2.815	25	1.05	1.1000	1.1000	0.5827	0.0006	0.5839
"	8x8	0.02	2.815	25	1.05	1.1000	1.1000	0.5931	0.0007	0.5945
"	8x8	0.04	2.815	25	1.05	1.1000	1.1000	0.5891	0.0007	0.5905
"	8x8	0.06	2.815	25	1.05	1.1000	1.1000	0.5719	0.0007	0.5733
"	8x8	0.08	2.815	25	1.05	1.1000	1.1000	0.5523	0.0009	0.5541
"	8x8	0.10	2.815	25	1.05	1.1000	1.1000	0.5291	0.0007	0.5305
"	8x8	0.20	2.815	25	1.05	1.1000	1.1000	0.4383	0.0006	0.4395
"	8x8	0.40	2.815	25	1.05	1.1000	1.1000	0.4300	0.0007	0.4314
"	8x8	0.60	2.815	25	1.05	1.1000	1.1000	0.5079	0.0008	0.5095
"	8x8	0.80	2.815	25	1.05	1.1000	1.1000	0.5817	0.0008	0.5833
"	8x8	1.00	2.815	25	1.05	1.1000	1.1000	0.6365	0.0008	0.6381

Table 6-40 Data for

Figure 6-49 RAJ-II Fuel Rod Transport Under HAC

Output File Name	Fuel Assembly Type	Interspersed Moderator Density (g/cm^3)	Pitch (cm)	Fuel Rod Number (#)	Pellet OD (cm)	Clad Inner Diameter (cm)	Clad Outer Diameter (cm)	k_{eff}	σ	$k_{eff} + 2\sigma$
rajII_hac_8_worstcase_fuelrodtransport_100pcth2odensity_10x1x10	8x8	0.00	3.0056	25	1.05	1.1000	1.1000	0.3230	0.0005	0.3240
"	8x8	0.01	3.0056	25	1.05	1.1000	1.1000	0.3479	0.0005	0.3489
"	8x8	0.02	3.0056	25	1.05	1.1000	1.1000	0.3752	0.0007	0.3766
"	8x8	0.04	3.0056	25	1.05	1.1000	1.1000	0.4007	0.0006	0.4019
"	8x8	0.06	3.0056	25	1.05	1.1000	1.1000	0.4287	0.0006	0.4299
"	8x8	0.08	3.0056	25	1.05	1.1000	1.1000	0.4556	0.0006	0.4568
"	8x8	0.10	3.0056	25	1.05	1.1000	1.1000	0.5743	0.0009	0.5761
"	8x8	0.20	3.0056	25	1.05	1.1000	1.1000	0.7416	0.0009	0.7434
"	8x8	0.40	3.0056	25	1.05	1.1000	1.1000	0.8264	0.0008	0.8280
"	8x8	0.60	3.0056	25	1.05	1.1000	1.1000	0.8660	0.0008	0.8676
"	8x8	0.80	3.0056	25	1.05	1.1000	1.1000	0.8731	0.0007	0.8745
"	8x8	1.00	3.0056	25	1.05	1.1000	1.1000	0.3752	0.0007	0.3766

6.11.10 Summary of Experiments

This document provides a summary of the experiments used in Reference 3 to determine the SCALE 4.4a bias. Trending data is either from the original experiments or calculated herein, i.e., H/U values, have been added to the data. Note that in most cases the experimental $k_{eff} \pm \sigma$ from Reference 3 do not have a reference. If data from the original experiment and/or data from the International Handbook of Evaluated Criticality Safety Benchmark Experiments (see Reference 4) provided these values, it was so noted or additional values provided.

The USL method of NUREG/CR-6361 (Reference 7) has the tacit assumption that the experimental k is 1.0000. Likewise, it does not account for the uncertainty in the experimental values. It is recommended that the procedure discussed in NUREG/CR-6698, "Guide for Validation of Nuclear Criticality Safety Calculational Methodology," be considered. The document has the following definitions for the calculated' values used for the bias evaluation:

$$k_{norm} = k_{calc}/k_{exp} \text{ and}$$

$$\sigma_{norm} = [(\sigma_{calc})^2 + (\sigma_{exp})^2]^{1/2}$$

This will normalize the calculated to experimental to account for uncertainties in the experimental values.

Note: The reference numbers quoted in the following sections are references listed in each section, rather than those listed in Section 6.11.

6.11.10.1 Critical Configurations

6.11.10.1.1 Water-Moderated U(4.31)O2 Fuel Rods in 2.54-cm Square-Pitched Arrays

References:

1. "Critical Separation Between Subcritical Clusters of 4.29 Wt% U-235 Enriched UO_2 Rods in Water With Fixed Neutron Poisons," S.R. Bierman, B. M. Durst, E.D. Clayton, Battelle Pacific Northwest Laboratories, NUREG/CR-0073(PNL-2695).
2. "Water-Moderated U(4.31)O_2 Fuel Rods in 2.54-cm Square-Pitched Arrays," V.F. Dean, Evaluator, International Handbook of Evaluated Criticality Safety Benchmark Experiments," NEA/NSC/DOC(95)03, Sept 2001, Nuclear Energy Agency.
3. "Software Validation Document, EMF-2670, PC-SCALE 4.4a V&V", C.D. Manning, EMF-2670, Rev. 1, 11/26/2002, Framatome ANP.

Reference 3 uses the data from this set of experiments as part of a heterogeneous uranium oxide set of benchmark calculations. Table 6 of that reference provides some information on the experimental configuration and Tables 7 and 9 provide results for the 238 and 44 group Scale

4.4a cross-sections, respectively. Table 6-41 Summary of Information for Experiment below provides a summary of the benchmark information from References 1 and 2. The rod and oxide dimensional and material information came from Reference 1. The enrichment quoted in Reference 1 was changed in Reference 2 due to a later chemical analysis of the fuel rods used in the experiment. Thus, the table uses the 4.31 value from Reference 2 rather than 4.29 quoted in Reference 1. The temperatures of the experiments were not included in Reference 1 and were not explicitly noted at the time of the experiment. The authors of Reference 2 obtained log books from similar experiments at PNL that showed temperatures ranging from ~18°C to ~25°C. From these data Reference 2 inferred an average value of ~22°C which is listed here. The value used in the calculations of Reference 3 is not currently known. The temperature value is used to calculate the hydrogen atom density and a deviation of a few degrees will not significantly change the results. The U and H atom densities used a value of Avogadro's number of 0.6022142E-24. The H/U value applies only to the fuel cluster. Table 6-44 Urania Gadolinia Experiment Summary[a] contains cases using cell-weighted models, 'x' added to case ID. These are included for completeness and should not be included in the normal benchmarking trending.

Table 6-41 Summary of Information for Experiment

Pellet OD, cm	1.2649	Enrichment, wt%	4.31[a]	V_{H2O}/V_{oxide}	3.883228
Rod OD, cm	1.2827	Oxide Density, g/cm^3	94.9	U-235 Atom Density	1.0125E-03
Rod OD, cm	1.4147	Temperature, °C	22[b]	H Atom Density	0.066724
Rod Pitch, cm	2.54	Water Density, g/cm^3	0.9978	H/U	255.92
Clad Material	Aluminum	Boron, ppm	0.0		

a) Redefined from 4.29 in Reference 2 due to fuel evaluation after publication of Reference 1.
b) Not defined in Reference 1, assumed in Reference 2 based upon inference from data notebooks of experiments.

Table 6-42 Parameters for Benchmark Cases for SCALE 4.4a 44 Group Cross-Section Set

Case ID[c]	Lattice[a]	Spacing[a] between clusters, cm		Experimental k_{eff} and σ				SCALE 4.4a 44 Group Cross-Section Calculated k_{eff} and σ				Absorber Plates in Water Gap
		Rod-rod	Cell-cell	k_{eff}[b]	σ[b]	k_{eff}[c]	σ[c]	k_{eff}[d]	σ[d]	AFG[d]	EALF[d] (ev)	
c004.out	15x8	11.72	10.62	1.0000	0.0020	0.9997	0.0020	0.9971	0.0008	35.772	0.112667	None
c005b.out	15x8	10.77	9.64	1.0000	0.0180	0.9997	0.0020	0.9960	0.0008	35.763	0.112942	0.625 cm Al plates
c006b.out	15x8	10.72	9.59	1.0000	0.0019	0.9997	0.0020	0.9960	0.0008	35.768	0.112841	0.625 cm Al plates
c007a.out	15x8	9.76	8.63	1.0000	0.0021	0.9997	0.0020	0.9966	0.0008	35.768	0.112705	0.302 cm SS 304L plates
c008b.out	15x8	9.22	8.09	1.0000	0.0021	0.9997	0.0020	0.9948	0.0008	35.755	0.113485	0.302 cm SS 304L plates
c009b.out	15x8	8.08	6.95	1.0000	0.0021	0.9997	0.0020	0.9963	0.0008	35.748	0.113698	0.298 cm 304L plates with 1.05 wt% B
c010b.out	15x8	6.60	5.47	1.0000	0.0021	0.9997	0.0020	0.9980	0.0008	35.728	0.114519	0.298 cm 304L plates with 1.05 wt% B
c011b.out	15x8	7.90	6.77	1.0000	0.0021	0.9997	0.0020	0.9983	0.0009	35.750	0.113450	0.298 cm 304L plates with 1.62 wt% B
c012b.out	15x8	5.76	4.63	1.0000	0.0021	0.9997	0.0020	0.9975	0.0007	35.729	0.114508	0.298 cm 304L plates with 1.62 wt% B
c013b.out	15x8	9.65	8.52	1.0000	0.0021	0.9997	0.0020	0.9956	0.001	35.768	0.112832	0.485 cm, SS 304L plates
c014b.out	15x8	8.58	7.45	1.0000	0.0021	0.9997	0.0020	0.9970	0.0009	35.745	0.113819	0.485 cm, SS 304L plates
c029b.out	15x8	10.90	9.77	1.0000	0.0021	0.9997	0.0020	0.9967	0.0008	35.770	0.112874	0.652 cm, Zircaloy-4 plates
c030b.out	15x8	10.86	9.73	1.0000	0.0021	0.9997	0.0020	0.9977	0.0009	35.767	0.112860	0.652 cm, Zircaloy-4 plates
c031b.out	15x8	7.672	6.55	1.0000	0.0021	0.9997	0.0020	0.9975	0.0008	35.727	0.114536	0.723 cm, Boral plates, 28.7 wt% B

a) From Reference 1. The 'rod surface-to-rod' surface spacing is reported in Reference 1. Reference 2 (p. 9) provides the cell-to-cell spacing for selected experiments from Reference 1 as: (rod-rod) – (pitch) + (rod diameter). This formula was applied to all above values even though some 'rod-rod' may be 'array plate-to-plate'.

b) Values from Reference 3, Table 6, p. 42. Source of σ values is not listed in this reference.

c) Values from Reference 2, p. 23 based upon calculational uncertainties in parameters and assumptions in the benchmark models of the reference. Note that Reference 2 only includes 4 of the cases from Reference 1 listed above. Here it is assumed that the values listed above apply to all cases.

d) From Reference 3, Table 9, p. 61 for 44 group cross-sections. Table 7 in this reference has values for 238 group cross-sections.

Table 6-43 Parameters for Benchmark Cases for SCALE 4.4a 238 Group Cross-Section Set

Case ID[c]	Lattice[a]	Cluster Spacing[a], cm		Experimental k_{eff} and σ				SCALE 4.4a 238 Group Cross-Section Calculated k_{eff} and σ				Absorber Plates in Water Gap
		Rod-rod	Cell-cell	k_{eff}[b]	σ[b]	k_{eff}[c]	σ[c]	k_{eff}[d]	σ[d]	AFG[d]	EALF[d] (ev)	
c001x.out[e]	10x11.51	0.0	0.0	1.0000	0.0021	0.9997	0.0020	0.9987	0.0008	208.112	0.108721	--
c002x.out	8x16.37	0.0	0.0	1.0000	0.0021	0.9997	0.0020	0.9993	0.0008	208.157	0.108277	--
c003x.out	9x13.35	0.0	0.0	1.0000	0.0021	0.9997	0.0020	1.0015	0.0010	208.136	0.108496	--
c004.out	15x8	11.72	10.62	1.0000	0.0020	0.9997	0.0020	0.9930	0.0010	207.568	0.114058	None
c005b.out	15x8	10.77	9.64	1.0000	0.0180	0.9997	0.0020	0.9931	0.0008	207.550	0.114504	0.625 cm Al plates
c006b.out	15x8	10.72	9.59	1.0000	0.0019	0.9997	0.0020	0.9941	0.0009	207.508	0.114748	0.625 cm Al plates
c007a.out	15x8	9.76	8.63	1.0000	0.0021	0.9997	0.0020	0.9944	0.0008	207.547	0.114468	0.302 cm SS 304L plates
c007x.out	15x8	9.76	8.63	1.0000	0.0021	0.9997	0.0020	1.0010	0.0008	208.273	0.107285	0.302 cm SS 304L plates
c008b.out	15x8	9.22	8.09	1.0000	0.0021	0.9997	0.0020	0.9931	0.0007	207.487	0.114939	0.302 cm SS 304L plates
c008x.out	15x8	9.22	8.09	1.0000	0.0021	0.9997	0.0020	0.9981	0.0008	208.220	0.107758	0.302 cm SS 304L plates
c009b.out	15x8	8.08	6.95	1.0000	0.0021	0.9997	0.0020	0.9928	0.0008	207.472	0.114907	0.298 cm 304L plates with 1.05 wt% B
c010b.out	15x8	6.60	5.47	1.0000	0.0021	0.9997	0.0020	0.9952	0.0009	207.373	0.115896	0.298 cm 304L plates with 1.05 wt% B
c011b.out	15x8	7.90	6.77	1.0000	0.0021	0.9997	0.0020	0.9964	0.0008	207.507	0.114703	0.298 cm 304L plates with 1.62 wt% B
c012b.out	15x8	5.76	4.63	1.0000	0.0021	0.9997	0.0020	0.9938	0.0009	207.364	0.116224	0.298 cm 304L plates with 1.62 wt% B
c013b.out	15x8	9.65	8.52	1.0000	0.0021	0.9997	0.0020	0.9953	0.0008	207.495	0.114944	0.485 cm, SS 304L plates
c013x.out	15x8	9.65	8.52	1.0000	0.0021	0.9997	0.0020	1.0002	0.0009	208.270	0.107272	0.485 cm, SS 304L plates
c014b.out	15x8	8.58	7.45	1.0000	0.0021	0.9997	0.0020	0.9942	0.0009	207.484	0.115038	0.485 cm, SS 304L plates
c014x.out	15x8	8.580	7.45	1.0000	0.0021	0.9997	0.0020	1.0018	0.0008	208.211	0.107849	0.485 cm, SS 304L plates
c029b.out	15x8	10.90	9.77	1.0000	0.0021	0.9997	0.0020	0.9942	0.0008	207.549	0.114428	0.652 cm, Zircaloy-4 plates
c030b.out	15x8	10.86	9.73	1.0000	0.0021	0.9997	0.0020	0.9946	0.0008	207.508	0.114783	0.652 cm, Zircaloy-4 plates
c031b.out	15x8	7.672	6.55	1.0000	0.0021	0.9997	0.0020	0.9951	0.0008	207.387	0.115885	0.723 cm, Boral plates, 28.7 wt% B

a) From Reference 1. The 'rod surface-to-rod' surface spacing is reported in Reference 1. Reference 2 (p. 9) provides the cell-to-cell spacing for selected experiments from Reference 1 as: (rod-rod) – (pitch) + (rod diameter). This formula was applied to all above values even though some 'rod-rod' may be 'array plate-to-plate'.
b) Values from Reference 3, Table 6, p. 42. Source of σ values is not listed in this reference.
c) Values from Reference 2, p. 23 based upon calculational uncertainties in parameters and assumptions in the benchmark models of the reference. Note that Reference 2 only includes 4 of the cases from Reference 1 listed above. Here it is assumed that the values listed above apply to all cases.
d) From Reference 3, Table 9, p. 61 for 44 group cross-sections. Table 7 in this reference has values for 238 group cross-sections.
e) From Reference 3, Table 6. The 'x' before '.out' means the case is a cell weighted model.

6.11.10.1.2 Urania Gadolinia Experiments

References:

4. FANP Doc: 32-5012895-00, "Validation Report – SCALEPC-44A Urania-Gadolinia Experiments," R.S. Harding.
5. "Urania Gadolinia: Nuclear Model Development and Critical Experiment Benchmark," L.W. Newman, Babcock & Wilcox for DOE, DOE/ET/34212-41, BAW-1910, April 1984.
6. "Development and Demonstration of An Advanced Extended-Burnup Fuel Assembly Design Incorporating Urania-Gadolinia," L.W. Newman, Babcock & Wilcox for DOE, DOE/ET/34212-41, BAW-1681-2, August 1982.

Reference 4 uses the experimental data from References 5 and 6 to construct benchmark cases for SCALE 4.4a. Table 6-44 Urania Gadolinia Experiment Summary[a] summarizes the experimental configuration data that form the basis for the KENO V.a models. Table 6-46 Urania Gadolinia Critical Experiment Trending Data provides trending parameters for this set of experiments. Table 6-45 Experimental Parameters for Calculating U-235 and H Atom Densities lists the basis for the H/U values tabulated in Table 6-46 Urania Gadolinia Critical Experiment Trending Data. Table 6-47 Urania Gadolinia Benchmark k_{eff} Data provides the experimental and calculated results for the 44 and 238 group SCALE 4.4a cross-section sets from Reference 3.

Table 6-44 Urania Gadolinia Experiment Summary[a]

Parameter	Rod 1	Rod 2	Rod 3
U-235 wt%	4.02	2.459	1.944
Gadolinia Wt%	-	-	4
Pellet density[b], g/cm^3	9.46	10.218	10.328
Pellet OD, cm	1.1265	1.03	1.0296
Rod OD, cm	1.1265	1.044	1.0439
Rod OD, cm	1.2078	1.206	1.2065
Rod Pitch, cm	1.6358	1.6358	1.6358
Clad Material	SS	Al	Al
$V_{fuel/cell}$	0.996654	0.833229	0.832582
$V_{H2O/cell}$	1.530044	1.533399	1.532452
Water boron factor[c]		0.99928	
Temperature[d], ^oC		22	
Water density, g/cm^3		0.99777	

a) From Reference 4.
b) Based upon rod mass and fuel volume in rod.
c) A factor to correct water density from 25 ^oC to 20 ^oC. Boron ppm is based upon 25 ^oC measurements. See Reference 4, p. 9.
d) Not specified explicitly for this set of experiments. This value is inferred from temperature data in Reference 7.

Table 6-45 Experimental Parameters for Calculating U-235 and H Atom Densities

Case ID	Number of Different Type Rods in each Critical Configuration(Reference 1 Table 1))						Core Volume[a]		Atom Density[a]	
	2.46 Wt%	4.02 Wt%	1.94 Wt% (Gd)	Water	Misc	Core Total	Fuel	Water	U-235	H
core01.out	4808	-	-	153	-	4961	4006.16	7765.83	5.67711E-04	0.066676
core03.out	4788	-	-	137	16	4941	3989.50	7692.42	5.67711E-04	0.066676
core05.out	4780	-	28	153	-	4961	4006.15	7765.90	5.67061E-04	0.066676
core5a.out	4776	-	32	153	-	4961	4006.14	7765.91	5.66968E-04	0.066676
core5b.out	4780	-	28	153	-	4961	4006.15	7765.90	5.67061E-04	0.066676
core08.out	4772	-	36	153	-	4961	4006.14	7765.92	5.66875E-04	0.066676
core10.out	4772	-	36	137	16	4961	4006.14	7723.11	5.66875E-04	0.066676
core12a.out	3920	888	-	153	-	4961	4151.29	7768.81	6.21492E-04	0.066676
core14.out	3920	860	28	153	-	4961	4146.69	7768.79	6.19146E-04	0.066676
core16.out	3920	852	36	153	-	4961	4145.38	7768.78	6.18475E-04	0.066676
core18.out	3676	944	-	180	-	4800	4003.79	7553.60	6.27210E-04	0.066676
core19.out	3676	928	16	180	-	4800	4001.17	7553.58	6.25815E-04	0.066676
core20.out	3676	912	32	180	-	4800	3998.54	7553.57	6.24420E-04	0.066676

a) Calculated values. Atom densities based upon Avogadro's number of 0.6022142E-24

Table 6-46 Urania Gadolinia Critical Experiment Trending Data

Case Name	Clad[a]	Lattice[a]	wt% 235[a]	Boron, ppm[a]	Vh2o/Vfuel[b]	H/U[b]	k_{eff}[c]	Sigma[c]	Rod Configurations[a]
core01.out	Al	15x15	2.46	1337.9	1.9385	227.67	1.0002	0.0005	0
core03.out	Al	15x15	2.46/1.94	1239.3	1.9282	226.46	1.0000	0.0006	20-4%Gd
core05.out	Al	15x15	2.46/1.94	1208.0	1.9385	227.93	0.9999	0.0006	28-4%Gd
core5a.out	Al	15x15	2.46/1.94	1191.3	1.9385	227.97	0.9999	0.0006	32-4%Gd
core5b.out	Al	15x15	2.46/1.94	1207.1	1.9385	227.93	0.9999	0.0006	28-4%Gd
core08.out	Al	15x15	2.46/1.94	1170.7	1.9385	228.01	1.0083	0.0012	36-4%Gd
core10.out	Al	15x15	2.46/1.94	1177.1	1.9278	226.75	1.0001	0.0009	36-4%Gd+3 void rods
core12a.out	SS/Al	15x15	4.02/2.46	1899.3	1.8714	200.77	1.0000	0.0007	4.02 inner/2.456 outer
core14.out	SS/Al	15x15	4.02/2.46/1.94	1653.8	1.8735	201.76	1.0030	0.0009	28-4%Gd
core16.out	SS/Al	15x15	4.02/2.46/1.94	1579.4	1.8741	202.04	1.0001	0.0010	36-4%Gd
core18.out	SS/Al	16x16	4.02/2.46	1776.8	1.8866	200.56	1.0002	0.0011	CE Large Guide Tubes
core19.out	SS/Al	16x16	4.02/2.46/1.94	1628.3	1.8878	201.14	1.0002	0.0010	16-4%Gd
core20.out	SS/Al	16x16	4.02/2.46/1.94	1499.0	1.8891	201.72	1.0002	0.0010	Zone + 32-4%

a) Reference 4.
b) Calculated values from Table 5.
c) Reference 3, Table 6. The source of these values is not documented in the reference.

Table 6-47 Urania Gadolinia Benchmark k_{eff} Data

Case ID	Experimental k_{eff} and σ		SCALE 4.4a 44 Group Cross-Section Calculated k_{eff} and σ				SCALE 4.4a 238 Group Cross-Section Calculated k_{eff} and σ			
	k_{eff}[a]	σ[a]	k_{eff}[b]	σ[b]	AFG[b]	EALF[b] (ev)	k_{eff}[b]	σ[b]	AFG[b]	EALF[b] (ev)
core01.out	1.0002	0.0005	0.9955	0.0006	33.8930	0.2530	0.9952	0.0007	197.6190	0.2567
core03.out	1.0000	0.0006	0.9963	0.0006	33.9190	0.2499	0.9943	0.0006	197.6810	0.2547
core05.out	0.9999	0.0006	0.9968	0.0006	33.9280	0.2493	0.9935	0.0006	197.6840	0.2543
core5a.out	0.9999	0.0006	0.9963	0.0005	33.9270	0.2494	0.9940	0.0006	197.6850	0.2547
core5b.out	0.9999	0.0006	0.9959	0.0006	33.9160	0.2504	0.9941	0.0007	197.6280	0.2558
core08.out	1.0083	0.0012	0.9958	0.0006	33.9200	0.2503	0.9928	0.0005	197.7470	0.2534
core10.out	1.0001	0.0009	0.9956	0.0006	33.9130	0.2512	0.9922	0.0007	197.6080	0.2562
core12a.out	1.0000	0.0007	0.9982	0.0006	32.8910	0.3644	0.9950	0.0006	193.1960	0.3697
core14.out	1.0030	0.0009	0.9976	0.0007	33.0670	0.3421	0.9942	0.0007	193.8910	0.3488
core16.out	1.0001	0.0010	0.9969	0.0007	33.1010	0.3376	0.9941	0.0007	194.1570	0.3412
core18.out	1.0002	0.0011	0.9975	0.0007	32.8960	0.3645	0.9950	0.0007	193.2390	0.3684
core19.out	1.0002	0.0010	0.9973	0.0006	33.0140	0.3489	0.9941	0.0007	193.6610	0.3553
core20.out	1.0002	0.0010	0.9969	0.0007	33.1050	0.3382	0.9950	0.0006	194.0850	0.3425

a) Values from Reference 3, Table 6, p. 42. Source of σ values is not documented in this reference.
b) From Reference 3, Table 9, p. 61 for 44 group cross-sections. Table 7 in this reference has values for 238 group cross-sections.

6.11.10.1.3 Critical Experiments Supporting Close Proximity Water Storage of Power Reactor Fuel

References:

7. FANP Doc. 32-5012896-00, "Validation Report – SCALEPC-44A Close Proximity Experiments," R.S. Harding.
8. "Critical Experiments Supporting Close Proximity Water Storage of Power Reactor Fuel," M.N. Baldwin, etal., BAW-1484-7, July 1979.

Reference 7 uses the experimental data from Reference 8 to construct benchmark cases for SCALE 4.4a. Table 6-48 Close Proximity Experiment Summary[a] summarizes the experimental configuration data that form the basis for the KENO V.a models. Table 6-49 Close Proximity Experiment Trending Data provides trending parameters for this set of experiments. Table 6-50 Close Proximity Experiment k_{eff} Data provides the experimental and calculated results for the 44 and 238 group SCALE 4.4a cross-section sets from Reference 3.

Table 6-48 Close Proximity Experiment Summary[a]

U-235 wt%	2.459	Fuel Lattice	14x14
Pellet Density[b], g/cm^3	10.218	Clad Material	Al
Pellet OD, cm	1.030	Vfuel/cell	0.8332
Rod OD, cm	1.044	Vh2o/cell	1.5342
Rod OD, cm	1.206	Vh2o/Vf	1.8413
Rod Pitch, cm	1.636		

a) From Reference 7.
b) Based upon rod mass and fuel volume in rod.

Table 6-49 Close Proximity Experiment Trending Data

Case ID	Cluster Spacing[a], cm	Temp[a], °C	Boron[a], ppm	Boron Factors[b]	Water density[b], g/cm^3	Atom Density[c]		H/U[c]	Absorbers[a]
						U-235	H		
aclp1.out	--	21	0	0.999788	0.99799	5.6991E-04	0.066725	215.57	--
aclp2.out	0.000	18.5	1037	1.000298	0.99850	5.6991E-04	0.066793	215.79	--
aclp3.out	1.636	18	764	1.000392	0.99860	5.6991E-04	0.066806	215.83	H2O
aclp4.out	1.636	17	0	1.000572	0.99878	5.6991E-04	0.066830	215.91	84 B4C pins/H2O
aclp5.out	3.272	17.5	0	1.000483	0.99869	5.6991E-04	0.066818	215.87	64 B4C pins/H2O
aclp6.out	3.272	17.5	0	1.000483	0.99869	5.6991E-04	0.066818	215.87	64 B4C pins/H2O
aclp7.out	4.908	17.5	0	1.000483	0.99869	5.6991E-04	0.066818	215.87	34 B4C pins/H2O
aclp8.out	4.908	17.5	0	1.000483	0.99869	5.6991E-04	0.066818	215.87	34 B4C pins/H2O
aclp9.out	6.544	17.5	0	1.000483	0.99869	5.6991E-04	0.066818	215.87	H2O
aclp10.out	6.544	24.5	143	0.998967	0.99718	5.6991E-04	0.066616	215.22	H2O
acp11a.out	1.636	25.5	510	0.999712	0.99692	5.6991E-04	0.066648	215.32	0.462 cm, SS 304/H2O
acp11b.out	1.636	26	514	0.998578	0.99992	5.6991E-04	0.066773	215.73	0.462 cm, SS 304/H2O
acp11c.out	1.636	25.5	501	0.999712	0.99692	5.6991E-04	0.066648	215.32	0.462 cm, SS 304/H2O
acp11d.out	1.636	25.5	493	0.998840	0.99692	5.6991E-04	0.066590	215.14	0.462 cm, SS 304/H2O
acp11e.out	1.636	25	474	0.999712	0.99404	5.6991E-04	0.066456	214.70	0.462 cm, SS 304/H2O
acp11f.out	1.636	25	462	0.998840	0.99404	5.6991E-04	0.066398	214.52	0.462 cm, SS 304/H2O
acp11g.out	1.636	25.5	432	0.999712	0.99992	5.6991E-04	0.066849	215.97	0.462 cm, SS 304/H2O
aclp12.out	3.272	26	217	0.998578	0.99679	5.6991E-04	0.066564	215.05	0.462 cm, SS 304/H2O
aclp13.out	1.636	20	15	1.000000	0.99821	5.6991E-04	0.066754	215.67	0.645 cm, BAl 1.614 wt% B/H2O
acp13a.out	1.636	17	28	1.000572	0.99878	5.6991E-04	0.066830	215.91	0.645 cm, BAl 1.614 wt% B/H2O
aclp14.out	1.636	18	92	1.000392	0.99860	5.6991E-04	0.066806	215.83	0.645 cm, BAl 1.614 wt% B/H2O
aclp15.out	1.636	18	395	1.000392	0.99860	5.6991E-04	0.066806	215.83	0.645 cm, BAl 1.614 wt% B/H2O
aclp16.out	3.272	17.5	121	1.000483	0.99878	5.6991E-04	0.066824	215.89	0.645 cm, BAl 1.614 wt% B/H2O
aclp17.out	1.636	17.5	487	1.000483	0.99878	5.6991E-04	0.066824	215.89	0.645 cm, BAl 1.614 wt% B/H2O
aclp18.out	3.272	18	197	1.000392	0.99860	5.6991E-04	0.066806	215.83	0.645 cm, BAl 1.614 wt% B/H2O
aclp19.out	1.636	17.5	634	1.000483	0.99878	5.6991E-04	0.066824	215.89	0.645 cm, BAl 1.614 wt% B/H2O
aclp20.out	3.272	17.5	320	1.000483	0.99878	5.6991E-04	0.066824	215.89	0.645 cm, BAl 1.614 wt% B/H2O
aclp21.out	6.544	16.5	72	1.000740	0.99992	5.6991E-04	0.066918	216.19	0.645 cm, BAl 1.614 wt% B/H2O

a) Reference 8.
b) Boron factors to correct water density from 25°C to 20°C. Boron ppm is based upon 25°C measurements. See Reference 7, Table 3.0-1, p. 46. Water density from standard tables.
c) Calculated values based upon Avogadro's number of 0.6022142E-24

Table 6-50 Close Proximity Experiment k_{eff} Data

Case ID	Experimental k_{eff} and σ		SCALE 4.4a 44 Group Cross-Section Calculated k_{eff} and σ				SCALE 4.4a 238 Group Cross-Section Calculated k_{eff} and σ			
	k_{eff}[a]	σ[a]	k_{eff}[b]	σ[b]	AFG[b]	EALF[b] (ev)	k_{eff}[b]	σ[b]	AFG[b]	EALF[b] (ev)
aclp1.out	1.0002	0.0005	0.9931	0.0008	34.8710	0.1712	0.9889	0.0009	201.9510	0.1761
aclp2.out	1.0001	0.0005	0.9956	0.0008	33.9420	0.2484	0.9939	0.0008	197.6580	0.2540
aclp3.out	1.0000	0.0006	0.9963	0.0006	34.5210	0.1960	0.9934	0.0007	200.5280	0.2002
aclp4.out	0.9999	0.0006	0.9897	0.0008	34.6110	0.1910	0.9875	0.0008	200.7350	0.1946
aclp5.out	1.0000	0.0007	0.9883	0.0008	34.9500	0.1662	0.9873	0.0008	202.4670	0.1689
aclp6.out	1.0097	0.0012	0.9884	0.0007	34.8840	0.1716	0.9872	0.0007	201.9760	0.1760
aclp7.out	0.9998	0.0009	0.9900	0.0007	35.2100	0.1496	0.9867	0.0008	203.6900	0.1527
aclp8.out	1.0083	0.0012	0.9906	0.0008	35.1720	0.1526	0.9874	0.0007	203.3420	0.1573
aclp9.out	1.0030	0.0009	0.9906	0.0006	35.3620	0.1411	0.9879	0.0007	204.4120	0.1438
aclp10.out	1.0001	0.0009	0.9913	0.0007	35.2090	0.1494	0.9883	0.0008	203.7410	0.1528
acp11a.out	1.0000	0.0006	0.9955	0.0007	34.4600	0.2001	0.9919	0.0006	200.2820	0.2046
acp11b.out	1.0007	0.0007	0.9942	0.0007	34.4640	0.1997	0.9916	0.0009	200.2900	0.2043
acp11c.out	1.0007	0.0006	0.9943	0.0008	34.4550	0.2007	0.9915	0.0008	200.1800	0.2060
acp11d.out	1.0007	0.0006	0.9939	0.0006	34.4290	0.2035	0.9920	0.0009	200.1670	0.2063
acp11e.out	1.0007	0.0006	0.9952	0.0007	34.4350	0.2030	0.9918	0.0006	200.0830	0.2078
acp11f.out	1.0007	0.0006	0.9947	0.0008	34.4360	0.2033	0.9916	0.0006	200.0020	0.2089
acp11g.out	1.0007	0.0006	0.9941	0.0007	34.4200	0.2054	0.9908	0.0007	199.9760	0.2096
aclp12.out	1.0000	0.0007	0.9911	0.0007	34.8740	0.1702	0.9889	0.0008	202.2960	0.1727
aclp13.out	1.0000	0.0010	0.9922	0.0007	34.5220	0.1963	0.9906	0.0009	200.3490	0.2013
acp13a.out	1.0000	0.0010	0.9901	0.0008	34.5020	0.1979	0.9884	0.0007	200.2550	0.2031
aclp14.out	1.0001	0.0010	0.9905	0.0007	34.4720	0.2005	0.9891	0.0009	200.1840	0.2045
aclp15.out	0.9998	0.0016	0.9881	0.0008	34.4020	0.2057	0.9823	0.0007	199.8980	0.2102
aclp16.out	1.0001	0.0006	0.9860	0.0007	34.8250	0.1737	0.9841	0.0007	202.0010	0.1769
aclp17.out	1.0007	0.0019	0.9897	0.0007	34.3970	0.2061	0.9874	0.0007	199.9490	0.2097
aclp18.out	1.0002	0.0011	0.9869	0.0007	34.8410	0.1728	0.9859	0.0008	202.0310	0.1759
aclp19.out	1.0002	0.0010	0.9910	0.0007	34.4010	0.2052	0.9888	0.0006	199.9530	0.2096
aclp20.out	1.0003	0.0011	0.9889	0.0006	34.8410	0.1726	0.9869	0.0008	202.0440	0.1758
aclp21.out	0.9997	0.0013	0.9868	0.0008	35.1290	0.1544	0.9854	0.0007	203.3850	0.1570

a) Values from Reference 3, Table 6, p. 42. Generally obtained from Tables 8 and 9 of Reference 8; acp11 series of values not documented in Reference 3.
b) From Reference 3, Table 9, p. 61 for 44 group cross-sections. Table 7 in this reference has values for 238 group cross-sections.

6.11.10.1.4 Critical Experiments Supporting Underwater Storage of Tightly Packed Configurations of Spent Fuel Pins

References:

9. FANP Doc. 32-5012897-00, "Validation Report – SCALEPC-44A Consolidation Experiments," R.S. Harding
10. "Critical Experiments Supporting Underwater Storage of Tightly Packed Configurations of Spent Fuel Pins," G.S. Hoovler, etal., BAW-1645-4, November, 1981.

Reference 9 uses the experimental data from Reference 10 to construct benchmark cases for SCALE 4.4a. Table 6-51 Tightly Packed Configuration Experiment Summary[a] summarizes the experimental configuration data that form the basis for the KENO V.a models. Table 6-52 Tightly Packed Configuration Experiment Trending Data provides trending parameters for this set of experiments. Table 6-53 Tightly Packed Configuration Experiment k_{eff} Data provides the experimental and calculated results for the 44 and 238 group SCALE 4.4a cross-section sets from Reference 3.

Table 6-51 Tightly Packed Configuration Experiment Summary[a]

U-235 wt%	2.459	Fuel Volume, cm^3	0.833229
Pellet Density[b], g/cm^3	10.233	Pitch, cm	Vh20/Ffuel
U-235 atom density[c]	5.7075E-04	1.2093	0.149022
Pellet OD, cm	1.0300	1.2090	0.383292
Rod OD, cm	1.0440	1.4097	1.014058
Rod OD, cm	1.2060		
Clad Material	Al		

a) From Reference 9.
b) Based upon rod mass and fuel volume in rod, note this is the same 2.459 wt% fuel used in the previous 2 benchmark cases. The difference in densities has not been discussed.
c) Calculated values based upon Avogadro's number of 0.6022142E-24.

Table 6-52 Tightly Packed Configuration Experiment Trending Data

Case ID	Rod Pitch[a], cm	Lattice[a]	Cluster Spacing[a], cm	Temp[a], °C	Boron[a], ppm	Boron Factor[b]	Water density[b]	V_{h2o}/V_{fuel}[c]	H atom density$_l$[c]	H/U$_l$[c]
rcon01.out	1.2093	15x17 tria[d]	1.778x1.945	22.5	435	0.999451	0.99767	0.1490	0.066681	17.41
rcon02.out	1.2093	15x17 tria	1.778x1.945	23.5	426	0.999214	0.99742	0.1490	0.066648	17.40
rcon03.out	1.2093	15x17 tria	1.778x1.945	24.0	406	0.999091	0.99730	0.1490	0.066632	17.40
rcon04.out	1.2093	15x17 tria	1.778x1.945	22.5	383	0.999451	0.99767	0.1490	0.066681	17.41
rcon05.out	1.2093	15x17 tria	1.778x1.945	23.0	354	0.999334	0.99754	0.1490	0.066665	17.41
rcon06.out	1.2093	15x17 tria	1.778x1.945	23.0	335	0.999334	0.99754	0.1490	0.066665	17.41
rcon07.out	1.2093	15x17 tria	2.539x2.709	20.0	361	1.000000	0.99821	0.1490	0.066754	17.43
rcon09.out	1.2090	15x15 sq	1.7780	21.0	886	0.999788	0.99799	0.3833	0.066725	44.81
rcon10.out	1.2090	15x15 sq	1.7780	21.0	871	0.999788	0.99799	0.3833	0.066725	44.81
rcon11.out	1.2090	15x15 sq	1.7780	22.0	852	0.999566	0.99777	0.3833	0.066695	44.79
rcon12.out	1.2090	15x15 sq	1.7780	21.0	834	0.999788	0.99799	0.3833	0.066725	44.81
rcon13.out	1.2090	15x15 sq	1.7780	21.0	815	0.999788	0.99799	0.3833	0.066725	44.81
rcon14.out	1.2090	15x15 sq	1.7780	22.0	781	0.999566	0.99777	0.3833	0.066695	44.79
rcon15.out	1.2090	15x15 sq	1.7780	22.0	746	0.999566	0.99777	0.3833	0.066695	44.79
rcon16.out	1.4097	13x13 sq	1.7920	22.5	1156	0.999451	0.99767	1.0141	0.066681	118.47
rcon17.out	1.4097	13x13 sq	1.7920	22.5	1141	0.999451	0.99767	1.0141	0.066681	118.47
rcon18.out	1.4097	13x13 sq	1.7920	23.0	1123	0.999334	0.99754	1.0141	0.066665	118.44
rcon19.out	1.4097	13x13 sq	1.7920	23.0	1107	0.999334	0.99754	1.0141	0.066665	118.44
rcon20.out	1.4097	13x13 sq	1.7920	23.0	1093	0.999334	0.99754	1.0141	0.066665	118.44
rcon21.out	1.4097	13x13 sq	1.7920	23.0	1068	0.999334	0.99754	1.0141	0.066665	118.44
rcon28.out	1.4097	15x17 tria	3.807x2.976	18.5	121	1.000298	0.99850	1.0141	0.066793	17.44

a) Reference 9.
b) Boron factors to correct water density from 25°C to 20°C. Boron ppm is based upon 25 °C measurements. See Reference 10, Table 3.0-1, p. 46. Water density from standard tables.
c) Calculated values based upon Avogadro's number of 0.6022142E-24.
d) Triangular pitch for array.

Table 6-53 Tightly Packed Configuration Experiment k_{eff} Data

Case ID	Experimental k_{eff} and σ		SCALE 4.4a 44 Group Cross-Section Calculated k_{eff} and σ				SCALE 4.4a 238 Group Cross-Section Calculated k_{eff} and σ			
	k_{eff}[a]	σ[a]	k_{eff}[b]	σ[b]	AFG[b]	EALF[b] (ev)	k_{eff}[b]	σ[b]	AFG[b]	EALF[b] (ev)
rcon01.out	1.0007	0.0006	0.9999	0.0008	28.9400	2.4011	0.9910	0.0007	170.1330	2.4368
rcon02.out	1.0007	0.0006	1.0009	0.0007	28.9020	2.4444	0.9909	0.0008	169.9770	2.4688
rcon03.out	1.0007	0.0006	0.9973	0.0008	28.8680	2.4872	0.9882	0.0007	169.6020	2.5454
rcon04.out	1.0007	0.0006	1.0008	0.0007	28.8990	2.4644	0.9899	0.0007	169.6960	2.5284
rcon05.out	1.0007	0.0006	0.9995	0.0008	28.8970	2.4706	0.9899	0.0008	169.6200	2.5435
rcon06.out	1.0007	0.0006	0.9980	0.0007	28.8900	2.4915	0.9906	0.0008	169.5520	2.5553
rcon07.out	1.0007	0.0006	0.9982	0.0008	29.8910	1.6259	0.9904	0.0008	175.2760	1.6431
rcon09.out	1.0007	0.0006	0.9977	0.0006	29.8930	1.4607	1.0092	0.0007	180.0400	1.1271
rcon10.out	1.0007	0.0006	0.9966	0.0008	29.8760	1.4759	0.9884	0.0006	176.1470	1.4891
rcon11.out	1.0007	0.0006	0.9959	0.0007	29.8450	1.4982	0.9909	0.0008	176.1150	1.4922
rcon12.out	1.0007	0.0006	0.9980	0.0008	29.8490	1.4979	0.9876	0.0007	175.8550	1.5240
rcon13.out	1.0007	0.0006	0.9969	0.0007	29.8430	1.5074	0.9897	0.0007	175.8220	1.5280
rcon14.out	1.0007	0.0006	0.9963	0.0007	29.8310	1.5207	0.9894	0.0007	175.7230	1.5402
rcon15.out	1.0007	0.0006	0.9975	0.0008	29.8450	1.5180	0.9915	0.0007	175.7200	1.5399
rcon16.out	1.0007	0.0006	0.9948	0.0007	32.7100	0.4216	0.9892	0.0007	175.7140	1.5415
rcon17.out	1.0007	0.0006	0.9952	0.0006	32.6820	0.4276	0.9894	0.0006	191.3680	0.4309
rcon18.out	1.0007	0.0006	0.9939	0.0006	32.6400	0.4370	0.9909	0.0007	191.2180	0.4360
rcon19.out	1.0007	0.0006	0.9965	0.0006	32.6540	0.4344	0.9897	0.0007	191.0430	0.4426
rcon20.out	1.0007	0.0006	0.9967	0.0007	32.6370	0.4391	0.9915	0.0007	190.9880	0.4447
rcon21.out	1.0007	0.0006	0.9959	0.0008	32.6220	0.4427	0.9903	0.0007	190.8780	0.4485
rcon28.out	1.0007	0.0006	0.9968	0.0008	31.0790	1.0062	0.9915	0.0008	190.7670	0.4529

a) Values from Reference 3, Table 6, p. 42. Source of value not documented in this reference.
b) From Reference 3, Table 9, p. 61 for 44 group cross-sections. Table 7 in this reference has values for 238 group cross-sections

6.11.10.1.5 Reduced Density Moderation Between Fuel Clusters with 4.738 Wt% Fuel

References:

11. FANP Doc. 32-5012894-00, "Validation Report – SCALEPC-44A Dissolution Experiments," R.S. Harding.
12. "Dissolution and Storage Experimental Program with U[4.75]O_2 Rods," Transactions of the American Nuclear Society, Vol. 33, pg. 362.

Reference 11 uses the experimental data from Reference 12 to construct benchmark cases for SCALE 4.4a. Table 6-54 Reduced Density Moderation Experiments Summary and Trending Parameters[a] summarizes the experimental configuration data that form the basis for the KENO V.a models and provides trending parameters that are constant for the series of experiments. Table 6-55 Reduced Density Moderation Experiments Trending Data and k_{eff} Data provides trending parameters for this set of experiments. It also provides the experimental and calculated results for the 44 and 238 group SCALE 4.4a cross-section sets from Reference 3.

Table 6-54 Reduced Density Moderation Experiments Summary and Trending Parameters[a]

U-235 wt%	4.738	Temperature, ^oC	22
Pellet Density, g/cm^3	10.38	Water density, g/cm^3	0.99777
Pellet OD, cm	0.7900	Fuel Volume, cm^3	0.49017
Rod OD, cm	0.8200	Water Volume, cm^3	1.12852
Rod OD, cm	0.9400	V_{h2o}/V_{fuel}	2.30232
Rod Pitch, cm	1.3500	U-235 atom density[b]	1.1155E-03
Clad Material	Al alloy	H atom density[b]	0.066676
Lattice	18x18	H/U	1.3761E+02

a) From Reference 11.
b) Calculated values based upon Avogadro's number of 0.6022142E-24.

Table 6-55 Reduced Density Moderation Experiments Trending Data and k_{eff} Data

Case ID	Cluster Spacing[a], cm	Spacing Material[a] [Material (density)]	Experimental k_{eff} and σ		SCALE 4.4a 44 Group Cross-Section Calculated k_{eff} and σ				SCALE 4.4a 238 Group Cross-Section Calculated k_{eff} and σ			
			k_{eff}[b]	σ[b]	k_{eff}[c]	σ[c]	AFG[c]	EALF[c] (ev)	k_{eff}[c]	σ[c]	AFG[c]	EALF[c] (ev)
mdis01.out	0.0	-	1.0000	0.0014	0.9914	0.0008	33.5390	0.2824	0.9885	0.0010	195.994	0.2879
mdis02.out	2.5	H2O	1.0000	0.0014	0.9871	0.0009	33.6720	0.2644	0.9862	0.0008	196.836	0.2685
mdis03.out	2.5	Air/Box	1.0000	0.0014	0.9841	0.0011	33.6720	0.2647	0.9805	0.0008	196.750	0.2702
mdis04.out	2.5	Polystr(0.0323)/Box	1.0000	0.0014	0.9902	0.0008	33.8040	0.2514	0.9884	0.0008	197.439	0.2559
mdis05.out	2.5	Polyeth(0.2879)/Box	1.0000	0.0014	0.9908	0.0010	33.9160	0.2407	0.9891	0.0009	198.001	0.2442
mdis06.out	2.5	Polyeth(0.5540)/Box	1.0000	0.0014	1.0008	0.0010	34.0370	0.2295	0.9963	0.0008	198.539	0.2344
mdis07.out	2.5	H2O/Box	1.0000	0.0014	0.9917	0.0009	34.1100	0.2242	0.9886	0.0008	198.827	0.2288
mdis08.out	5.0	H2O	1.0000	0.0014	0.9873	0.0010	33.8000	0.2497	0.9840	0.0009	197.504	0.2545
mdis09.out	5.0	Air/Box	1.0000	0.0014	0.9869	0.0010	33.8110	0.2485	0.9861	0.0009	197.586	0.2524
mdis10.out	5.0	Polystr(0.0323)/Box	1.0000	0.0014	0.9938	0.0008	34.0940	0.2225	0.9912	0.0008	198.934	0.2267
mdis11.out	5.0	Polyeth(0.2879)/Box	1.0000	0.0014	1.0031	0.0010	34.3010	0.2048	0.9997	0.0008	200.018	0.2076
mdis12.out	5.0	Polyeth(0.0.5540)/Box	1.0000	0.0014	-	-	-	-	1.0027	0.0009	200.577	0.1984
mdis13.out	5.0	H2O/Box	1.0000	0.0014	0.9907	0.0008	34.4280	0.1951	0.9878	0.0008	200.547	0.1988
mdis14.out	10.0	H2O	1.0000	0.0014	0.9890	0.0008	33.9850	0.2294	0.9854	0.0009	198.552	0.2333
mdis15.out	10.0	Air/Box	1.0000	0.0014	0.9894	0.0009	34.0150	0.2266	0.9842	0.0008	198.647	0.2315
mdis16.out	10.0	Polystr(0.0323)/Box	1.0000	0.0014	1.0013	0.0008	34.4450	0.1907	0.9970	0.0009	200.792	0.1948
mdis17.out	10.0	Polyeth(0.2879)/Box	1.0000	0.0014	0.9985	0.0008	34.5970	0.1788	0.9951	0.0009	201.537	0.1831
mdis18.out	10.0	Polyeth(0.0.5540)/Box	1.0000	0.0014	0.9965	0.0008	34.6430	0.1740	0.9923	0.0009	201.894	0.1774
mdis19.out	10.0	H2O/Box	1.0000	0.0014	0.9931	0.0009	34.6530	0.1737	0.9888	0.0008	201.908	0.1772

a) References 11 and 12.
b) Values from Reference 3, Table 6, p. 42. Source of value not documented in this reference.
c) From Reference 3, Table 9, p. 61 for 44 group cross-sections. Table 7 in this reference has values for 238 group cross-sections.

6.12 References

1. Davis, J. K., "RAJ-II Shipping Container Test", Document Identifier 51-5032941-00, September 10, 2003.
2. Bierman, S.R., Durst, B. M., Clayton, E.D., "Critical Separation Between Subcritical Clusters of 4.29 Wt% U-235 Enriched UO_2 Rods in Water With Fixed Neutron Poisons," Battelle Pacific Northwest Laboratories, NUREG/CR-0073(PNL-2695).
3. Dean, V.F., Evaluator, "Water-Moderated U(4.31)O_2 Fuel Rods in 2.54-cm Square-Pitched Arrays," International Handbook of Evaluated Criticality Safety Benchmark Experiments," NEA/NSC/DOC(95)03, Sept 2001, Nuclear Energy Agency.
4. Newman, L.W., "Urania Gadolinia: Nuclear Model Development and Critical Experiment Benchmark," Babcock & Wilcox for DOE, DOE/ET/34212-41, BAW-1910, April 1984.
5. Newman, L.W., "Development and Demonstration of An Advanced Extended-Burnup Fuel Assembly Design Incorporating Urania-Gadolinia," Babcock & Wilcox for DOE, DOE/ET/34212-41, BAW-1681-2, August 1982.
6. American National Standard for Nuclear Criticality Safety in Operations with Fissionable Materials Outside Reactors, ANSI/ANS-8.1-1998.
7. Lichtenwalter, J. J., Bowman, S. M., DeHart, M. D., and Hopper, C. M., Criticality Benchmark Guide for Light-Water-Reactor Fuel in Transportation and Storage Packages, NUREG/CR-6361, ORNL/TM-13211, U. S. Nuclear Regulatory Commission.
8. SCALE Standardized Computer Analyses for Licensing Evaluation, NUREG/CR-2000 ORNL/NUREG/CSD-2, Volumes 1, 2, and 3.
9. Baldwin, M.N. et al., Critical Experiments Supporting Close Proximity Water Storage of Power Reactor Fuel, BAW-1484-7, July 1979.
10. Hovler, G.S. et al., Critical Experiments Supporting Underwater Storage of Tightly Packed Configurations of Spent Fuel Pins, BAW-1645-4, November, 1981.
11. Transactions of the American Nuclear Society, Dissolution and Storage Experimental Program with U[4.75]O_2 Rods, Vol. 33, pg. 362.
12. Harding, R.S., Validation Report – SCALEPC-44A Consolidation Experiments, FANP Doc. 32-5012897-00
13. Ao, Qi., GEH Criticality Safety Analysis – Shipment of Loose Rods in RAJ-II Shipping Container, Rev. 01, Doc, November 1, 2007
14. GEMER Monte Carlo Validation Report: RA-3/RAJ-II Shipping Containers, rev. 0, Qi Ao, November, 2007

TABLE OF CONTENTS

LIST OF FIGURES

LIST OF TABLES

Glossary of Terms and Acronyms

ASME – American Society of Mechanical Engineers
ASME B&PVC – ASME Boiler and Pressure Vessel Code
ASNT – American Society for Non-destructive Testing
CG – Center of Gravity
CTU – Certification Test Unit
BWR – Boiling Water Reactor
HAC – Hypothetical Accident Condition
IC – Inner Container
IC Inner Thermal Insulator (Aluminum Silicate) – The Alumina Silicate thermal insulation between the inner and outer walls of IC container to provide added margin to criteria set forth for HAC fire condition in 10 CFR 71.73(c)(4)
IC Lid – The lid of the inner container
IC Body – The body of the inner container consisting of the outer wall the thermal insulation, the inner wall, the polyethylene liner and the shock absorbing system along with the fuel securement system
JIS – Japanese Industrial Standards
JSNDI – Japanese Society for Non-destructive Inspection
LDPE – Low Density Polyethylene
NCT – Normal Conditions of Transport
NDIS – Non-destructive Inspection Society
OC – Outer Container
OC Body – The assembly consisting of the OC lower wall, and the internal shock absorbing material
OC Lid – The lid for the outer container.
Packaging – The assembly of components necessary to ensure compliance with packaging requirements as defined in 10 CFR 71.4. Within this SAR, the packaging is denoted as the RAJ-II packaging
Package – The packaging with its radioactive contents, as presented for transportation as defined in 10 CFR 71.4. Within this SAR, the package is denoted as the RAJ-II package.
Payload – Unirradiated fuel assemblies and fuel rods.
RAM – Radioactive Material
SAR – Safety Analysis Report (this document)
TI – Transport Index
USL – Upper Safety Limit

7.0 PACKAGE OPERATIONS

This chapter provides general instructions for loading and unloading and operation of the RAJ-II package. Specific detailed procedures based on and consistent with this application are used for the operation of the package. These procedures are maintained by the user of the package and may provide additional detail regarding the handling and operation of the package. Due to the low specific activity and low abundance of gamma emitting radionuclides, dose rates from the contents of the package when used as a Type A or Type B package are minimal. As a result of the low dose rates, there are no special handling requirements for radiation protection.

7.1 PACKAGE LOADING

This section delineates the procedures for loading a payload into the RAJ-II packaging. Hereafter, reference to specific RAJ-II packaging components may be found in Appendix 1.4.1.

7.1.1 Preparation for Loading

Prior to loading the RAJ-II with fuel, the packaging is inspected to ensure that it is in unimpaired physical condition. The inspection looks for damage, dents, corrosion, and missing hardware. Acceptable conditions are defined by the drawings in Section 1.4.1 as described in Section 8.2.5. Acceptance criteria and detailed loading procedures derived from this application are specified in user written procedures. These user procedures are specific to the authorized content of the package. Since the primary containment is the sealed fuel rod, radiation and contamination surveys are not required prior to loading. There is no required moderator, neutron absorbers or gaskets that require testing or inspection.

Defects that require repair will be fixed prior to shipping in accordance with approved procedures consistent with the quality program.

When used as a Type B package, verification that the primary containment (i.e., fuel rods have been leak checked) will be performed prior to shipping.

7.1.2 Loading of Contents

7.1.2.1 Outer Container Lid Removal

1. Remove the lid bolts.
2. Attach slings to the four lid lift attachment points on the lid.
3. Remove the outer lid.

7.1.2.2 Inner Container Removal

1. Release the inner clamp by removing the eight clamp bolts.
2. Remove the inner container from the outer container, and move it onto the packing table. Ensure that the inner container is lifted using the inner container handles and not the inner container lid handles.

3. Remove the bolts of the inner container lid and take the lid off.

7.1.2.3 Loading Fuel Assemblies into the RAJ-II

1. Clamp the inner container body to the packing table or up righting device, and remove the end lid.
2. Ensure that the following preparation work for packing has been completed if required.
    a. The separators have been inserted.
    b. The finger spring protectors have been attached.
    c. The foam has been put in place.
    d. The fuel assemblies have been covered with poly bags.
3. Stand the packing table upright. (The inner container body is fixed with clamps.)
4. Lift one fuel assembly and pack it in the inner container.
5. After packing one fuel assembly into the inner container, fit the securing fixtures of the fuel assembly. Then pack the other fuel assembly in the inner container
6. Lower the packing table back to the horizontal position from the upright position.
7. Attach the end lid of the inner container.
8. Check to ensure that the fuel assemblies are packaged in the container properly.
9. Attach the inner container lid and tighten the bolts securely (wrench tight or as defined in user procedures).
10. Place the inner container into the outer container.
11. Put on hold down clamps and tighten bolts.
12. Place the outer container lid on the package, and tighten the bolts securely (wrench tight or as defined in user procedures).
13. Install tamper-indicating devices on the outer container ends.

7.1.2.4 Loading Loose Rods in the Protective Case into the RAJ-II

1. Insert poly endcap spacers over each end or the fuel rod endcap (optional).
2. Sleeve (optional) each rod to be packed with a maximum of 5 mil polyethylene sleeve/tubing.
3. Insert up to 30, 10x10 design rods, 26, 9x9 design rods or 22, 8x8 design rods into the protective case and fill any empty space with empty tubing.
4. Place cushioning foam pads in protective case as needed to prevent sliding during shipment (optional).
5. Close the protective case and tighten bolts wrench tight.

7.1.2.5 Loading the Protective Case into the RAJ-II

1. Loose rods may be loaded in the protective case while either in the inner container or while removed from the inner container.

2. After packing the protective case(s) into the inner container, fit the securing fixtures for the case.
3. Check to ensure that the protective cases are packaged in the container properly.
4. Attach the inner container lid and tighten the bolts securely (wrench tight or as defined in user procedures).
5. Put on hold down clamps and tighten bolts.
6. Place the outer container lid on the package, and tighten the bolts securely (wrench tight or as defined in user procedures).
7. Install tamper-indicating devices on the outer container ends.
8. It is allowable to ship only one protective case in an RAJ-II inner.

7.1.2.6 Loading Loose Rods in the 5-Inch Stainless Steel Pipe into the RAJ-II

1. Sleeve (optional) each rod to be packed with a maximum of 5 mil polyethylene sleeve/tubing. The ends of the sleeves should be closed in a manner such as knotting or taping with the excess polyethylene trimmed away.
2. Place a cushioning foam pad in the capped end of the pipe (optional).
3. Insert up to 30, 10x10 design rods, 26, 9x9 design rods or 22, 8x8 design rods into the pipe and fill the empty space with empty zircaloy tubing with welded end plugs on both ends.
4. Place cushioning foam pads against the rod ends to block the rods from sliding during shipment (optional).
5. Close pipe with end cap.
6. Lift each 5-inch stainless steel pipe and pack it in the inner container.
7. Check to ensure that the 5-inch stainless steel pipe(s) is packaged in the container properly.
8. Attach the inner container lid and tighten the bolts securely (wrench tight or as defined in user procedures).
9. Place the outer container lid on the package, and tighten the bolts securely (wrench tight or as defined in user procedures).
10. Install tamper-indicating devices on the outer container ends.
11. It is allowable to ship one or two 5-inch pipes containing rods in an RAJ-II inner.

7.1.2.7 Loading Loose Rods (25 Maximum Per Side) into the RAJ-II

1. Sleeve (optional) each rod to be packed with a maximum of 5 mil polyethylene sleeve/tubing. The ends of the sleeves should be closed in a manner such as knotting or taping with the excess polyethylene trimmed away.
2. When only one rod per side is to be packed, no clamps are required. Block the rod in the lower corner of the container by evenly spacing 10 or more notched foam pads the length of the rod.

3. When 2 rods up to a maximum of 25 rods are to be packed, banding with steel clamps is not required for criticality safety purposes. If banding is chosen, position 10 or more open steel clamps evenly in each side of the inner container in which loose rods are place.
4. Place foam pads on top of the open clamps, lay the rods on top of the foam.
5. Close and tighten the clamps so the foam surrounds the array of rods. Tighten each clamp until the foam collapses slightly.
6. Place foam pads against the ends of the rods, above the rods and beside the rods to block the rods from moving during shipment.
7. Repeat the above steps for the other side of the inner container, if required.
8. Fill each side (if used) with foam pads so as to minimize movement during shipment.
9. Attach the inner container lid and tighten the bolts securely (wrench tight or as defined by user procedure).
10. Place the outer container lid on the package, and tighten the bolts securely (wrench tight as defined by user procedure).
11. Install tamper-indicating devices on the outer container ends.

7.1.3 Preparation for Transport

When used as a type B package leak testing of the rods (primary containment) is performed during the manufacturing process. Verification of successful leak testing is done prior to shipment. There are no surface temperature measurements required for this package.

Procedure: (These steps may be performed in any sequence.)

1. Complete the necessary shipping papers in accordance with Subpart C of 49 CFR 172.
2. Ensure that the RAJ-II package markings are in accordance with 10 CFR 71.85(c) and Subpart D of 49 CFR 172. Package labeling shall be in accordance with Subpart E of 49CFR 172. Package placarding shall be in accordance with Subpart F of 49 CFR 172.
3. Survey the surface of the package for potential contamination and dose rates.
4. Transfer the package to the conveyance and secure using tie-downs secured to the package.

7.2 PACKAGE UNLOADING

7.2.1 Receipt of Package from Carrier

Radiation and contamination surveys are performed upon receipt of the package and the packages are inspected for significant damage. There are no fission gases, coolants or solid contaminants to be removed.

7.2.2 Removal of Contents

After freeing the tie downs, the RAJ-II package is lifted from the carrier either by fork lift or by the use of lifting slings placed around the package. If lifted by forklift, the forks are placed at the

designated lift locations and the package is lifted. If slings lift the package, a sling is placed under each end of the package at the lifting angles that prevent the sling from sliding. Care should be taken to ensure that the slings are placed in the correct location depending on whether the package is loaded or empty.

7.2.2.1 Outer Container Lid Removal

1. Remove the lid bolts.
2. Attach slings to the four sling fittings on the lid.
3. Remove the outer lid.

7.2.2.2 Inner Container Removal

1. Release the inner clamp by removing the eight clamp bolts.
2. Remove the inner container from the outer container, and move it onto the packing table. Ensure that the inner container is lifted using the appropriate inner container handles and not the inner container lid handles.
3. Remove the bolts of the inner container lid and take the lid off.

7.2.2.3 Unloading Fuel Assemblies from the RAJ-II

1. Clamp the inner container body to the packing table or up righting device, and remove the end lid.
2. Stand the packing table upright. (The inner container body is fixed with clamps.)
3. Attach the lifting device to the assembly and remove the securing fixture.
4. Lift one fuel assembly at a time from the package.
5. Repeat for other assembly.

7.2.2.4 Removing / Unloading Protective Case or 5-Inch Stainless Steel Pipe from the RAJ-II

1. Remove the outer container and inner container lids as described in Sections 7.2.2.1 and 7.2.2.2.
2. The inner container may be removed or left in place while removing the protective case or 5-inch pipe.
3. Remove the 5-inch stainless steel pipe with a sling or remove the cover from the protective case.
4. Remove the rods from the 5-inch pipe or protective case.

7.3 PREPARATION OF EMPTY PACKAGE FOR TRANSPORT

Empty RAJ-II's are prepared and transported per the requirements of 49 CFR 173.428. Prior to shipping as an empty RAJ-II, the packaging is surveyed to assure that contamination levels are less than the 49 CFR 173.433(a) limit. The RAJ-II is visually verified as being empty. The

packaging is inspected to assure that it is in an unimpaired condition and is securely closed so that there will be no leakage of material under conditions normally incident to transportation.

Any labels previously applied in conformance with subpart E of part 172 of this subchapter are removed, obliterated, or covered and the "Empty" label prescribed in 49 CFR 172.450 of this subchapter is affixed to the packaging.

7.4 OTHER OPERATIONS

The following are considered normal routine maintenance items and do not require QA or Engineering evaluation for replacement. Material must be of the same type as original equipment parts.

a. Wooden Bolster Assemblies
b. Bolster Bolting
c. Delrin Inserts
d. Polyethylene Container Guides
e. Gaskets
f. Shock Absorbers (Paper Honeycomb)
g. Fork Pocket Rubber Protective Pads
h. Outer Container Stopper #2 (Rubber Pad)
i. Safety Walk
j. Plastic Plugs
k. Lid Tightening Bolts (Outer, Inner and End Lid)
l. Inner Container End Face Lumber (Upper)
m. Inner Container End Face Lumber (Lower "Y" Block)
n. Inner Container Polyethylene Foam
o. Heliserts

When deviations to items other than those listed above are identified, the RAJ-II shall be removed from service, and the item(s) shall be identified as non-conforming material, and dispositioned in accordance with written procedures including the 10 CFR 71, Subpart H approved QA Plan.

7.5 APPENDIX

No additional information is required. Loading and unloading this package is a relatively simple and routine operation. The weights, contamination levels and radiation dose rates do not impose significant hazards or operations outside normal material handling.

Note: The regulatory references provided, such as 49 CFR and 10 CFR, are the current requirements. If regulatory references change, the new references are applicable. This applies throughout the SAR.

8.0 ACCEPTANCE TESTS AND MAINTENANCE PROGRAM

8.1 ACCEPTANCE TESTS

Per the requirements of subpart G of 10 CFR 71, this section discusses the inspections and tests to be performed prior to first use of the RAJ-II. The RAJ-II is manufactured under a Quality Assurance Program meeting the requirements of 10 CFR 71 subpart H.

8.1.1 Visual Inspections and Measurements

Prior to the first use of the RAJ-II for the shipment of licensed material, the RAJ-II will be inspected to ensure that it is conspicuously and durably marked with its model number, serial number, gross weight and package identification number assigned by NRC. Prior to applying the model number, it will be determined that the RAJ-II was fabricated in accordance with the drawings reference in the NRC Certificate of Compliance.

Critical dimensions related to quality are called out in the Appendix 1.4.1 drawings as Critical to Quality (CTQ). Data for these dimensions is recorded and verified in accordance with the quality plan. Documentation of these measurements is compiled in a data pack. This data pack will be checked for completeness for each RAJ-II as part of the acceptance program.

RAJ-II's are inspected to ensure that there are no missing parts (nuts, bolts, gaskets, plugs, etc.) or components and that there is no shipping damage on receipt.

8.1.2 Weld Examinations

RAJ-II packaging materials of construction and welds shall be examined in accordance with requirements delineated on the drawings in Appendix 1.4.1, per the requirements of 10 CFR 71.85(a). This includes 100% liquid penetrant examination of specified areas of the first ten (10) production units.

The non-destructive examination personnel qualification and certification shall be in accordance with either The American Society for Non-destructive Testing (ASNT) SNT-TC-1A (recommended practice) or Japanese Society for Non-destructive Inspection (JSND) Japanese Industrial Standard (JIS) JIS Z 2305 latest revision.

Subsequent production units will be tested as defined in the manufacturing quality plan.

8.1.3 Structural and Pressure Tests

The RAJ-II is not pressurized and is structurally the same to the test units. There are no additional structural or pressure tests required.

8.1.4 Leakage Tests

No leak tests of the packaging are required. The fuel rod weld joints are examined at the time of fuel fabrication and leak tested to ensure they are sealed. The welding and leak testing of fuel

rods is performed during manufacturing using a qualified process. This process assures that the fuel is acceptable for use in a nuclear reactor core and is tightly controlled. The acceptable leak rate is less than $1x10^{-7}$ atm-cc/s. The inner and outer container are not relied on for containment, and do not require leak testing.

8.1.5 Component and Material Tests

The RAJ-II packaging does not contain gaskets that perform a safety function or pressure boundary, and as such, do not require testing. The packaging does not contain neutron absorbers that would require testing. No component tests are required.

Material testing or certifications from the suppliers of material for this container must show compliance to the properties found in Tables 2-2 and 2-3, or to other properties that satisfactorily indicate compliance to the properties found in these tables and that are approved by the licensee.

8.1.6 Shielding Tests

The RAJ-II packaging does not contain shielding and therefore shielding tests are not required.

8.1.7 Thermal Tests

The alumina silicate thermal properties will be assured by procuring this material with a certified pedigree. This procurement is done consistent with the QA program.

8.1.8 Miscellaneous Tests

There are no additional or miscellaneous tests are required prior to the use of the RAJ-II packaging.

8.2 MAINTENANCE PROGRAM

8.2.1 Structural and Pressure Tests

Prior to each use of the RAJ-II, the packaging is visually inspected to assure that the packaging is not damaged and that the components parts are in place. The packagings are constructed primarily from stainless steel making it corrosion resistant. Since the packaging is not relied on for containment, there are no pressure test requirements for the inner or outer containers that comprise the packaging. When used as a Type B package, each fuel rod is leak checked and the successful results of the test are checked before shipment.

The RAJ-II packaging is maintained consistent with a 10 CFR 71 subpart H QA program. Packagings that do not conform to the license drawings are removed from service until they are brought back into compliance. Repairs are performed in accordance with the approved procedures and consistent with the quality assurance program.

8.2.2 Leakage Tests

Containment is provided by the fuel rod for Type B shipments. Each loaded fuel rod is leak checked to assure that the rod is leak tight. Neither the inner or outer container is credited with providing leak protection. Therefore, no leak test of the packaging is required.

8.2.3 Component and Material Tests

There are no prescribed component tests or replacement requirements for this packaging. The packaging does not use neutron absorbers or shielding that would require testing or maintenance.

8.2.4 Thermal Tests

The alumina silicate thermal material is sealed within the stainless steel plates of the container wall. The packaging is visually inspected prior to use to assure that the alumina silicate is contained.

8.2.5 Miscellaneous Tests

There are no additional or miscellaneous tests are required for the use of this packaging. The RAJ-II packaging is inspected prior to each use and maintained consistent with the license drawings. The package is inspected to verify that the package remains within the tolerances specified on the drawings in Section 1.4.1. As noted on the drawings localized deformation in the shell is permitted up to 25mm if the internal structure of the package remains within tolerance. The packaging is repaired in accordance with drawings found in Section 1.4.1.

Foam cushioning material may have up to 2% of the total volume removed for packing purposes, handling or as a result of tears or punctures to the foam.

Small dents, tears and rounding of corners on paper honeycomb are acceptable providing the area is less than 2%. The corners of the individual pieces of paper honeycomb may be rounded to approximately a radius of 3 inches.

8.3 APPENDIX

No appendix for this section